

SYNTHESIS, PROPERTIES AND APPLICATIONS OF BIO-BASED MATERIALS

By

Madhusudhan Srinivasan

A DISSERTATION

Submitted to
Michigan State University
In partial fulfillment of the requirements
for the degree of

DOCTOR OF PHILOSOPHY

Materials Science and Engineering

2010

ABSTRACT

SYNTHESIS, PROPERTIES AND APPLICATIONS OF BIO-BASED MATERIALS

By

Madhusudhan Srinivasan

Bio-based feedstock have become very significant as they offer a value proposition in terms of carbon balance and also in terms of endowing biodegradability where needed. Thus a lot of attention is being given to the modification such feedstock for different applications. Soybean oil is one such feedstock. The oil is a triglyceride ester composed of different fatty acids, which are common to other plant oils. Thus soybean oil serves as a platform for plant oils, as modifications of this oil, can in theory be extended to cover other plant oils.

Methyl oleate was used as a model fatty acid ester, to synthesize hydroxyesters with ethylene glycol via a two stage oxidative cleavage of the double bonds. Ozone was chosen as the oxidant due to its many advantages. The first stage involved oxidation of the double bond to aldehydes, ozonides and acetals, which were subsequently converted to hydroxyesters (hydroxy values of 220 – 270) in near quantitative yield by treatment with Oxone. This method could be extended to soybean oil to make “polyols” which could find applications in resin syntheses.

Silylation was employed as another platform to functionalize soybean oil and fatty acid methyl esters with a reactive silane (vinyltrimethoxy silane). This simple modification produced materials that are cured by atmospheric moisture and are useful

as coatings. The silylation was controlled by varying the grafting time, cure temperature and the concentration of the silane. Products with gel content as high as 90% could be achieved. The coating exhibited good adhesion to metal, glass, concrete and paper. Steel panels coated with these coatings exhibited good stability against corrosion in high humidity conditions and moderate stability against a salt spray.

The silylation was also successfully utilized to improve the tensile strength of the blend of biodegradable polyester, poly (butylene adipate-co-terephthalate) with talc. A reactive extrusion process was employed to graft vinyl silanes on the polyester in short reaction times of 5 minutes. This improved the compatibility with the talc filler. This biodegradable polyester product was characterized by high tensile strength and moderate elongation. The modification method is simple is applicable to a variety of aliphatic biodegradable polyesters.

Finally a rapid polymerization of 1, 4-dioxan-2-one in very short times was accomplished with titanium alkoxides as initiators. At low [monomer]/ [initiator] ratios (100:1), nearly all the alkoxide groups initiated polymerization. High conversions up to 90% were achieved even at high ratios (2400:1). The activation energy for polymerization for titanium tetraisopropoxide is the lowest reported (33.7 kJ/mol) for this monomer system.

Dedicated to

Bhagawaan Shree Ramana Maharishi

Acknowledgments

I would like to thank Dr. Ramani Narayan for having spent a great deal of his time towards guiding me in my research work. I am also indebted to him deeply for providing me the freedom to work in a variety of areas. Dr. Daniel Graiver has been supportive throughout and a special thanks to him for involving me in work related to silicones and Ken Farminer, for his valuable inputs and encouragement and the frequent chats about cricket. I am deeply thankful for the advice and support offered by my Ph.D. committee: Dr. Gregory Baker, Dr. Andre Lee and Dr. Krishnamurthy Jayaraman, during the course of my work. I am also thankful to Dr. Jian-bing Zeng, Dr. Yogaraj Nabar and Dr. Jean-Marie Raquez and (Late) Dr. Phuong Tran for allowing me to be a part of their research work and acknowledging me in their publications. Laura Patrick , Dr. Dana Miloaga and Dr. Baradhwaj have been very supportive and encouraging throughout this endeavor and more than anything else have been great friends.

I am grateful for all the help and support from my family: my parents, my sister Anuradha and my brothers Narayanan and Vivek. Vivek has been a good friend with whom I could converse with on the technical aspects of my work. In that regard my thanks also to Dr. Jagadis Sankaranarayan and Dr. Shishir Chundawat. To name all is impossible in this tiny space. Many people I have come across during my work have taught me one thing or the other. To all those people who have in some way enriched my intellect, my heartfelt thanks.

TABLE OF CONTENTS

List of Tables.....	x
List of Figures.....	xii
List of Abbreviations.....	xvii
CHAPTER 1.....	1
1.1 Introduction	1
1.1.1 Industrialization and its environmental impact	1
1.1.2 Global warming	2
1.1.3 Sustainable development – biobased products.....	4
1.1.4 Is bio-based sustainable?	6
1.1.5 Reduce, Reuse, Recycle.....	7
1.2 Proposed goals of the work	8
1.3 Specific goals	10
1.4 Specific research objectives	10
1.5 Organization of thesis.....	12
1.6 References	17
CHAPTER 2: INTRODUCTION TO VEGETABLE OILS AND SOYBEAN OIL.....	18
2.1 Vegetable oils.....	18
2.2 Soybean oil as a feedstock.....	19
2.3 Triglyceride distribution in soybean oil	21
2.4 References	26
CHAPTER 3: OZONOLYSIS: SYNTHESIS OF HYDROXYESTERS (“POLYOLS”) FROM SOYBEAN OIL.....	27
Abstract	27
3.1 Introduction	29
3.1 Introduction	29
3.1.1 Vegetable oils in polymers	29
3.1.2 Ozonolysis	30
3.3 Materials	35
3.4 Experimental	36
3.4.1 Synthesis of azelaic acid.....	36
3.4.2 Synthesis of 2 – hydroxyethyl esters from methyl oleate	37
3.4.3 Synthesis of soybean oil polyols	37
3.5 Characterization	38

3.6 Results and Discussion.....	39
3.6.1 Hydroxy ethyl esters from methyl oleate	39
3.6.2 “Polyols” from soybean oil.....	48
3.6.3 Effect of excess alcohol and solvent.....	56
3.7 Conclusion.....	58
3.8 References	61
CHAPTER 4: SYNTHESIS OF SOYBEAN OIL BASED UNSATURATED POLYESTER RESINS.....	63
Abstract	63
4.1 Introduction	65
4.2 Synthesis of Soybean oil based polyols	65
4.3 Synthesis of Resins	66
4.4 Characterization	67
4.5 Results and Discussion.....	68
4.6 Conclusions	73
CHAPTER 5: SYNTHESIS OF 2-HYDROXYETHYL ESTERS FROM METHYL OLEATE VIA OZONOLYSIS	74
Abstract	74
5.1 Introduction	76
5.2 Materials	79
5.3 Experimental	81
5.3.1 Synthesis of 2-hydroxyethyl oleate	81
5.3.2 Ozonolysis of 2-hydroxyethyl oleate	81
5.3.3 Oxone™ treatment.....	82
5.4 Results and discussion	83
5.4.1 Transesterification	83
5.4.2 Ozonolysis	86
5.4.3 Oxone treatment	97
5.4.4 A note on Baeyer – Villiger oxidation	103
5.5 Conclusions	104
5.6 References	107
CHAPTER 6: SYNTHESIS AND PROPERTIES OF SOYBEAN OIL – VINYLTRIMETHOXY SILANE ADDUCTS.....	109
Abstract	109
6.1 Introduction	112
6.2 Materials	115
6.3 Experimental	117
6.3.1 Synthesis of soybean oil – silane adducts.....	117
6.3.2 Gel content.....	118
6.3.3 Cure kinetics	118
6.3.4 Coating on wood.....	119

6.3.5 Coating on metal panels	120
6.4 Characterization	121
6.5 Results and Discussion.....	124
6.5.1 Kinetics of silylation	124
6.5.2 Mechanism of silane incorporation.....	129
6.5.3 Gel content and cross – link density.....	139
6.5.4 Cure kinetics	144
6.5.4.1 Effect of catalyst	146
6.5.4.2 Effect of water	148
6.5.4.3 Effect of temperature	149
6.6 Corrosion testing on coated metal panels	150
6.6.1 Formulation of coating	150
6.7 Water uptake of wood	157
6.8 Conclusions	158
6.9 References	161
 CHAPTER 7: SYNTHESIS AND PROPERTIES OF FATTY ACID METHYL ESTER – VINYLTRIMETHOXY SILANE ADDUCTS	 164
Abstract	164
7.1 Materials	166
7.2 Experimental	166
7.3 Characterization	168
7.4 Results and Discussion.....	170
7.4.1 Kinetics of silylation	171
7.4.2 Mechanism of silylation	176
7.4.2.1 NMR Spectra	181
7.5 Conclusions	188
7.6 References	190
 CHAPTER 8: RAPID RING-OPENING POLYMERIZATION OF 1, 4-DIOXAN-2-ONE INITIATED BY TITANIUM ALKOXIDES	 192
Abstract	193
8.1 Introduction	194
8.2 Experimental	197
8.2.1 Materials	197
8.2.2 Polymerization of PDO	198
8.2.3 Characterization and Measurement.....	198
8.3 Results and Discussion.....	199
8.3.1 Polymerization of PDO initiated by Titanium Alkoxides	199
8.3.2 Polymerization Mechanism.....	202
8.3.3 ROP of PDO initiated by Ti(OiPr) ₄	206
8.3.4 Polymerization Kinetics.....	210
8.4 Conclusions	214

8.5 References	216
CHAPTER 9: CONCLUSIONS AND FUTURE DIRECTION	220
9.1 Ozonolysis	220
9.2 Silylation of soybean oil/fatty acid esters	222
9.3 Transesterification chemistry	225
9.4 Ring opening polymerization of PDO	226
CHAPTER 10: OTHER PRELIMINARY STUDIES AND FUTURE RECOMMENDATIONS	227
Abstract	227
SYNTHESIS OF ALPHA OLEFIN LIKE ESTERS FROM SOYBEAN OIL	229
10.1 Introduction	229
10.2 Materials	231
10.3 Experimental	231
10.3.1 Synthesis of allyl ester	231
10.3.2 Hydrosilylation of allyl esters	232
10.4 Characterization	234
10.5 Results and discussion	234
10.6 Future work.....	241
PBAT – VINYLSILANE– TALC BLENDS	244
10.7 Introduction	244
10.8 Materials	246
10.9 Experimental	246
10.9.1 One-Step (In Situ) Reactive Extrusion Process	246
10.10 Results and Discussion.....	248
10.10.1 Mechanical properties of PBAT-silane-talc composites	248
10.11 Recommendations for the PBAT-silane-talc composites	250
10.12 References	253

LIST OF TABLES

Table 2.1 Percentage composition of some common plant oils (Adapted from (2))	19
Table 3.1 Titrimetric results of ozonated samples of methyl oleate. (Percent change in parentheses)	40
Table 3.2 Integral ratios of functional groups (relative to CH ₃ area =3) from NMR spectra; proton of interest is italicized. ¹³ C shifts reported for carbon bearing proton of interest (Sample: methyl oleate with ethylene glycol)	46
Table 3.3 Titrimetric results of ozonated samples of soybean oil. (Percent change in parentheses)	49
Table 3.4 Theoretical estimation of hydroxyl values for soybean oil polyols	50
Table 3.5 Integral ratios of functional groups (relative to CH ₃ area =9) from NMR spectra; proton of interest is italicized. ¹³ C shifts reported for carbon bearing proton of interest (Sample: soybean oil with ethylene glycol)	54
Table 4.1 Acid and Hydroxyl values of polyols synthesized with varying ozonolysis time	66
Table 4.2 Hydroxyl and Acid values of resins obtained from soy polyols	70
Table 4.3 Properties of resins based on soy polyol.....	72
Table 5.1 Fatty acid composition of methyl oleate *	84
Table 5.2 Integral ratios of functional groups (relative to CH ₃ area =3) from NMR spectra; proton of interest is italicized. ¹³ C shifts reported for carbon bearing proton of interest (Sample: transesterified oleate ester) N.D – Not determined	93
Table 5.3 Integral ratios of functional groups (relative to CH ₃ area =3) from NMR spectra; proton of interest is italicized. ¹³ C shifts reported for carbon bearing proton of interest (Sample: methyl oleate).....	96

Table 5.4 Titrimetric data for transesterified methyl oleate samples (percent change in parentheses)	99
Table 5.5 Titrimetric data for methyl oleate samples (percent change in parentheses)99	
Table 5.6 Representative peak data from Mass spectra	101
Table 6.1. Conversion, Iodine value and double bond reduction for silylated soybean oils	128
Table 6.2 Gel content and solvent uptake ratio for cured silylated oils (Cure temperature: 75° C) after extraction with chloroform (72 hours)	141
Table 7.1 Fatty acid composition of methyl oleate *	170
Table 7.2 Conversion, Iodine value and double bond reduction for silylated fatty acid methyl esters; methyl ester: silane molar ratio of 1:5, reaction time: 8 hours, 1 wt% L 101 used (except Entry 6)	179
Table 7.3 Gel content and solvent uptake ratio for cured silylated methyl esters (Cure Temperature : 75 °C) after extraction with chloroform (72 hours); NMR data is for the extracted portion or “Sol”	180
Table 8.1 Polymerization of PDO initiated by titanium alkoxides	201
Table 8.2 Polymerization of 1,4-dioxan-2-one initiated by Ti(OiPr) ₄	207
Table 8.3 The effect of reaction temperature on the polymerization of 1,4-dioxan-2-one initiated by Ti(OiPr) ₄	210
Table 10.1 Temperature profile used for blown films	247
Table 10.2 Tensile Properties (Machine Direction) of blown films derived from the PBAT-silane-talc blends	249
Table 10.3 Tensile Properties (Transverse Direction) of blown films derived from the PBAT-silane-talc blends	250

LIST OF FIGURES

Figure 2.1 Fatty acid composition of soybean oil	20
Figure 2.2 Frequency distribution (theoretical) of triglycerides in Lowsat™ oil	23
Figure 3.2 Initial attack of ozone on double bond leading to formation of secondary ozonide.....	32
Figure 3.3 Formation of ester from intermediates in ozonolysis (Note: 1 mole of water is formed) – The structures and arrows do not necessarily mean a concerted mechanism.	33
Figure 3.4 Formation of dimeric peroxide (tetraoxanes) and polymeric peroxides (Structures do not imply concerted mechanism)	34
Figure 3.5 Ozonolytic scheme showing formation of esters	35
Figure 3.6 FTIR spectra of Ozonated methyl oleate – EG sample (Top) and methyl oleate (Bottom).....	41
Figure 3.7 IR spectra (Carbonyl region) of Ozonated methyl oleate – EG sample (Top) and methyl oleate (Bottom).....	42
Figure 3.8 ^1H NMR spectrum of methyl oleate with assignments	43
Figure 3.9 ^{13}C NMR spectrum of methyl oleate with assignments	44
Figure 3.10 ^1H NMR of methyl oleate ozonated with EG with peak assignments; inset shows region between 4 – 5ppm	47
Figure 3.11 ^{13}C NMR of methyl oleate ozonated with EG with peak assignments.....	48
Figure 3.12 IR Spectrum of soybean oil ozonated with ethylene glycol (Top); pure soy oil (Bottom).....	51
Figure 3.13 ^1H NMR spectrum of neat soybean oil with peak assignments	52
Figure 3.14 ^{13}C NMR spectrum of neat soybean oil with peak assignments.....	53

Figure 3.15 ^1H NMR spectrum of soybean oil ozonated with ethylene glycol with assignments; inset shows region from 4.7 – 5.6 ppm.....	55
Figure 3.16 ^{13}C NMR spectrum of soybean oil ozonated with ethylene glycol; inset shows region from 100 – 134 ppm.....	56
Figure 3.17 ^1H NMR spectrum of soybean oil ozonated with ethylene glycol in dichloromethane; inset shows region from 3.8 – 4.4 ppm	57
Figure 5.1 ^1H -NMR spectrum of transesterified methyl oleate	85
Figure 5.2 Products of transesterification of methyl oleate with ethylene glycol	86
Figure 5.3 Ozone uptake of transesterified methyl oleate sample	87
Figure 5.4 ^1H - NMR spectrum of ozonated transesterified oleate ester	90
Figure 5.5 ^1H - NMR spectrum of ozonated methyl oleate; inset shows expanded spectrum in the region 3.8 – 5.6 ppm	91
Figure 5.6 ^{13}C NMR spectrum of ozonated methyl oleate showing aldehydes @ 203 ppm, ozonides and acetals @ 100 - 110 ppm.....	92
Figure 5.7 Products of ozonolysis of oleate fragment	97
Figure 5.8 & 5.9 NMR spectra of Oxone treated samples: ^1H (Top); ^{13}C (Bottom)	100
Figure 5.10 IR spectra of transesterified methyl oleate samples : Carbonyl region.....	102
Figure 5.11 IR spectra of transesterified methyl oleate samples: Hydroxyl region	103
Figure 6.1 TGA plots of neat soy oil and soy oil - silane mixture (T = 160 °C)	122
Figure 6.2 Conversion of silane with time - as determined by TGA (soy: silane ratio = 1:5 mole, 1 wt% peroxide).....	125
Figure 6.3 First order plot for the consumption of silane (soy: silane ratio = 1:5, 1 wt% peroxide)	126

Figure 6.4 Arrhenius plot of Log k Vs 1/T	127
Figure 6.5 Diels – Alder reaction between conjugated linoleate fragment and vinyl silane	130
Figure 6.7 Peroxide mediated grafting of vinyl silane to linoleate fragment.....	132
Figure 6.8 ^1H - NMR spectrum of silylated oil (Table 6.1 Entry 5) with peak assignments	134
Figure 6.9 ^{13}C - NMR spectrum of silylated oil (Table 6.1 Entry 5).....	135
Figure 6.10 Stacked ^1H - NMR spectra of samples (Table 6.1: Entries 6 – 10)	136
Figure 6.11 Stacked ^{13}C – NMR of distilled samples (Table 6.1: Entries 6 – 10)	137
Figure 6.12 Postulated mechanism for the origin of peaks at 39 ppm and 65 ppm (Adapted from (19)).....	139
Figure 6.14 ^1H – NMR spectra of soluble fractions (Entries 6 -10)	142
Figure 6.15 ^{13}C – NMR of soluble fractions (Entries 6 – 10)	143
Figure 6.16 Effect of DBTDL catalyst on cure rate (4 phr water, T= 65 °C)	147
Figure 6.17 Effect of water on cure rate (4 phr DBTDL, T= 65 °C)	148
Figure 6.18 Effect of temperature on cure rate (4 phr water & DBTDL)	150
Figure 6.19 Initial cracking (Top) and complete cracking (bottom) of panel coated with 1:15 silylated oil, 0.5 phr DBTDL	152
Figure 6.20 Panels before testing (filiform corrosion); No corrosion inhibitor (Top), 3% Corrosion inhibitor "93" (Bottom).....	154
Figure 6.21 Panels after 144 hours in humidity chamber. Blank (Top), Coated - no corrosion inhibitor (middle), Coated - 3% corrosion inhibitor (bottom).....	155
Figure 6.22 Panels after 91 hours in salt spray. Blank (Top), Coated -no corrosion inhibitor (middle) and Coated - 3% corrosion inhibitor (bottom)	156

Figure 6.23 Water uptake of wood. Uncoated wood (Top), soy oil coated (middle), silylated oil (1:5 ratio, 240 °C) coated (bottom)	158
Figure 7.1 Conversion of silane with time - as determined by GC (methyl oleate: silane ratio = 1:5 mole, 1 wt% peroxide)	172
Figure 7.2 First order plot for the consumption of silane (methyl oleate: silane ratio = 1:5, 1 wt% peroxide)	173
Figure 7.3 Arrhenius plot of Log k Vs 1/T	174
Figure 7.4 ^1H NMR spectrum of silylated methyl oleate with assignments (Table 7.2, Entry 5) – after distillation	182
Figure 7.5 ^{13}C NMR of silylated methyl oleate with assignments (Table 2, Entry 5) after distillation.....	184
Figure 7.6 Stacked ^1H NMR spectra of soluble fractions (Table 7.2, Entries 1-5)	185
Figure 7.7 Stacked ^{13}C NMR spectra of soluble fractions (Table 7.2, Entries 1-5)	186
Figure 7.8 ^{13}C NMR spectrum of methyl stearate – soluble fraction	188
Figure 8.1 ^1H NMR of PPDO with titanium alkoxide initiators	203
Figure 8.2 The effects of reaction time and temperature on the conversion of 1,4-dioxan-2-one, $[\text{M}]/[\text{I}]=2400:1$; initiator $\text{Ti}(\text{OiPr})_4$	208
Figure 8.3 Plots of $\ln[\text{M}]_0 - \ln[\text{M}]_t$ versus time for different reaction temperatures	212
Figure 8.4 Plot of $\ln k_{\text{app}}$ versus $1/\text{RT}$	213
Figure 10.1 Reaction set up for hydrosilylation	233
Figure 10.2 Transesterification of vegetable oil with different olefinic alcohols	235
Figure 10.3 Hydrosilylation of a terminal olefin	235

Figure 10.4 ^1H NMR spectrum of allyl fatty ester (from soybean oil) showing assignments.....	236
Figure 10.5 ^1H NMR spectrum of allyl ester from vegetable shortening.....	237
Figure 10.6 ^{13}C NMR of allyl fatty ester (from soybean oil) with assignments.....	237
Figure 10.7 ^1H NMR of Hydrosilylated product (allyl soyate with DMS –H11) (Top); product with MCSiH (Bottom).....	239
Figure 10.8 ^{13}C NMR of hydrosilylated product (allyl soyate with DMS – H11)	240
Figure 10.9 Sulfitation of alpha olefin from soybean oil	242
Figure 10.10 Copolymerization of alpha olefin with ethylenic monomer	243

LIST OF ABBREVIATIONS

Chapter 1

LCA	Life Cycle Assessment/Analysis
RTV	Room Temperature Vulcanizate
MO	Methyl Oleate
SO	Soybean Oil
PDO	1, 4 – dioxan – 2 – one or Para dioxanone
REX	Reactive Extrusion
PCL	Poly (ϵ – caprolactone)

Chapter 2

MMT	Million Metric Tonnes
-----	-----------------------

Chapter 3

FTIR	Fourier Transform Infra Red
NMR	Nuclear Magnetic Resonance
UV	UltraViolet
ATR	Attenuated Total Reflectance
ppm	Parts per million
EG	Ethylene glycol
IR	Infra Red

Chapter 4

MA	Maleic Anhydride
DSC	Differential Scanning Calorimetry
TGA	Thermogravimetric analysis

Chapter 5

DBTDL	Dibutyltin dilaurate
scfm	Standard cubic feet per minute
LPM	Liters per minute
FAME	Fatty acid methyl ester
GC	Gas Chromatograph (y)

Chapter 6

Luperox 101/ L101	2,5-Bis(<i>tert</i> -butylperoxy)-2,5-dimethylhexane
UPR	Unsaturated polyester resin
FRC	Fiber reinforced composites
TAG	Triacylglycerol
RIS	Radical Initiation sequence
M.W	Molecular weight
RH	Relative humidity

Chapter 8

PPDO	Poly (para dioxanone)
LA	Lactide (dilactide of lactic acid)
TMS	Tetramethyl silane

Chapter 10

XLPE	Cross – linked polyethylene
LLDPE	Linear low density polyethylene
LAB	Linear alkyl benzene
PBAT	Poly(butylene adipate –co – terephthalate)
VTMOS	Vinyltrimethoxy silane
VMDMOS	Vinylmethyldimethoxy silane

CHAPTER 1

1.1 INTRODUCTION

1.1.1 Industrialization and its environmental impact

The last three centuries of human civilization, has seen tremendous technological growth. This is attributable mainly to the Industrial Revolution that had its origins in the mid eighteenth century. While the Industrial Revolution had its origins in the harnessing of steam, the rapid industrialization that the world has seen in the last century had its origins in the petrochemical industry. The one thing underlying the growth in both cases was the availability and the ability to harness fossil fuels. While the mid eighteenth century saw the use of coal, the late nineteenth century saw of the use of petroleum crude.

The ability to refine crude petroleum was crucial in the development of the modern chemical industry. This has led to the introduction of one of most ubiquitous materials on the planet “plastics”, in addition to advancements in other industries like construction, transportation, healthcare and many more.

However a lack of awareness of the consequences of indiscriminate industrialization, coupled with an anthropocentric view of the world has led to the emergence of several problems. Pollution of the air, water and soil, widespread

deforestation and a catastrophic extinction of many species of plants and animals are just a few of the consequences of mankind's "growth". The rapid growth of population has only complicated existing problems, with more people battling for a share of the very limited resources available on the planet.

It can be safely stated that while industrial growth has largely improved the material life of the human species, its unpleasant effects have been borne more by the rest of species and the planet as a whole. With the list of problems virtually unending, the battle is on to manage the earth's resources in a way that ensures a harmony between the technological growth and the environment.

1.1.2 Global warming

"Global warming" has become one of most discussed topics in the last decade. One of the problems associated with the use of fossil resources to drive industrialization is the effect it has on the global carbon cycle. Fossil resources – coal and petroleum are derived from dead and decayed plant and animal life, over a period of millions of years by a process of slow cooking under immense pressure and heat. The organic carbon contained in such life forms in the form of proteins, fats and carbohydrates is slowly converted to hydrocarbons, which becomes the petroleum crude or coal that is mined for. In essence, some of the very essential chemicals needed for fueling cars to making plastics are present in this crude, albeit as a mixture. It has been easy to separate the components of this mixture by refining and thus drive economic and industrial growth.

The downside of such a model is the limited availability of the above resources on the planet surface. Moreover, the rapid utilization of such a resource in quantities of millions of tons every year, poses a problem for the global carbon balance. Carbon dioxide is one of the main products of combustion of fossil resources and gets released at a rate much higher than the rate at which it is fixed (converted to organic carbon) by the flora on the planet. Since carbon dioxide is a good absorber of infra red radiation, which is radiated by the earth surface, it becomes an effective heat trap for radiated heat and raises atmospheric temperature. This is in essence the “Greenhouse or Glass house” effect that has led to debate and discussion across the globe on reducing greenhouse gas emissions.

One solution seems to be a more efficient use of fossil resources, thereby reducing their usage, but that would at best have a mitigatory effect on the problem and never be a solution. Additionally the currently existing excess of carbon dioxide would have to be sequestered in a way that reduces the levels of this gas back to an acceptable state. However, given the current population growth and the endless demand for more products, the demand for fossil resources would be expected to increase and so would the problems associated with their use.

In addition to the above, the issue of “Global warming” still remains today a contentious issue, not necessarily in its veracity, but its implications for a majority of the world population. The consequences of accepting this theory, especially for the developing nations – where most of the growth is projected to occur in the next few

decades, is especially disastrous. The reduction in the use of fossil resources is tantamount to a slowdown in their economic growth. This has serious repercussions for the vast majority of the world population (nearly two thirds) residing in such geographical areas, whose quality of life is much lower than the average resident in a developed country. Thus the idea of greenhouse gas emissions reductions, which have been widely proposed, is an unpleasant one for these countries. Thus a solution to this problem would have to take into account the socio-economic impacts that the solution is likely to have across different countries.

1.1.3 Sustainable development – biobased products

The idea of biodegradable products was born out of the need to eliminate persistent wastes in the environment. This would include products like plastic packaging and a myriad other plastic products. Unlike metals, most of which are recycled, not all plastics find their way into recycling streams. Also the intrinsic nature of some plastics (polyethylene, polypropylene etc.) precludes them from assimilation into their environment (decomposition in soil and water). The amount of such waste eventually flowing into the oceans has created garbage dumps in mid ocean thousands of miles away from landmasses, due to ocean currents. Environmental degradation of plastics may not necessarily be beneficial, as the products of degradation could also be toxic to life forms. Of particular concern are “single use” items, especially plastic packaging, because of their higher volume.

These concepts are being incorporated into the design of many products and thus a product's biodegradability has become one of the selling points. While these products would be environmentally responsible, by virtue of not being persistent and degrading to harmless products, their production could still involve petrochemical feedstock, which would make them unattractive from a greenhouse emissions perspective. However, if the feedstock for the manufacture of these products (biodegradable or not) is an annually renewable biomass, a new class of carbon – conscious products would emerge (1-3). These materials would still require the use of energy to convert them to their requisite form and shape, but the carbon present in them would be fixed carbon (derived from atmospheric CO₂ by photosynthesis) and not fossil – carbon. For example Braskem – a Brazilian petrochemical company plans to make polyethylene from ethanol. This ethanol would be obtained by fermentation of sugarcane. This example illustrates how atmospheric carbon can actually be sequestered as a polymer. The ethanol could also be used as a fuel, and in this case, the energy derived from this ethanol would add no new carbon to the atmosphere. It is thus not difficult to envision a biomass based feedstock which would strike a balance between carbon fixation and its release due to consumption (4,5).

Thus an environmentally responsible product should have a biobased feedstock (carbon – conscious) and whenever possible, should biodegrade at the end of its use. Since all products from biobased feedstock, cannot necessarily be made biodegradable (due to service requirements), recyclability or recycling should also form part of the

product life cycle and must be conceived right at the time of design. In the absence of proper recycling, even chemically inert plastics can become potential pollutants.

1.1.4 Is bio-based sustainable?

With the increasing attention given to agricultural feedstock as alternatives to petrochemical feedstock, blindness to the true sustainability of such feedstock is likely to develop and it is dangerous. It should be noted our agriculture itself has deviated much from its civilizational roots and is more modern and energy and chemical intensive. Thus even to make a pound of corn or soybean oil, so much of petrochemical input is required in the form of fertilizers, energy to drive irrigation, harvesting and transportation systems. This is prior to any chemical modifications on the feedstock, which would add more energy requirements as well as material requirements.

Thus the true sustainability of any feedstock would need to be ascertained by methods such as LCA (Life Cycle Assessment or Analysis), keeping in mind also the long term impact as dictated by ecological and environmental concerns. Relying solely on agricultural feedstock to drive the increasing demands of an increasing population, would mean increased land requirements, which ultimately would lead to deforestation and reclaiming land, which would be part of various ecosystems. It should also be remembered; land often taken for granted, is itself a resource which takes long times to get replenished naturally (complex nutrient cycles and mineral cycles involved). Thus the simplistic assumption of “anything bio-based is sustainable” should be avoided and replaced with a refined definition of what true sustainability is.

1.1.5 Reduce, Reuse, Recycle

With the rapid growth of human population and increased life expectancy, the population is projected to reach 12 billion within the next 50 years. There is some apprehension (6-8), about the limitation of the earth's resources to sustain such a vast population, especially with its sophisticated lifestyle. Thus in such a scenario even a bio – based economy may be unsustainable, since non – food uses would compete for food uses of many bio – renewable resources like starch, vegetable oils etc.

In such a scenario, there might be a need for a change in lifestyle – which unfortunately might be hard to achieve. As much as the advancements in science and technology have been remarkable, our record of material balance has abysmal. Year after year, millions of tons of waste get buried under land and tons of materials, on making which a huge amount of energy was expended are being dumped, without exploring the possibility of reuse or recycling – all in the name of economics and logistics. As such any talk of sustainable or environmentally responsible development, sounds hypocritical at best.

The drive should be to reduce consumption and reduce wastage. Especially in the area of plastics – the second “R” – reuse, should be explored. Many packages are capable of perfectly serving a secondary purpose other than their primary purpose, but still are either getting recycled or discarded. Examples of such cases, are milk cans, juice containers etc. For such items recycling would still be energy intensive, as compared to just a reuse for a secondary purpose.

Recycling needs to be pushed for almost all materials that enter and exit our lives. Where materials are not recyclable, as in certain plastics – every effort should be made to derive energy from those materials. Profitability while still important can never be an excuse for pollution or not recycling. As we realize more and more that we live in times where energy is more important, conserving materials also reduces energy expenditure.

1.2 PROPOSED GOALS OF THE WORK

Pursuant to the discussion outlined in the previous sections, the purpose of this work was to investigate various chemical routes for modification of soybean oil for industrial applications. Soybean oil serves as a particular example for vegetable oils in general. If the result of such modifications results in the applicability of the oil as a feedstock for various industrial applications, such modifications may be subsequently tailored to cover a whole family of other oils. Thus the logical extension of this work is to perform value addition to vegetable oils in general, while working with soybean oil as an easily and widely available substrate.

It is also essential to remember that all vegetable oils, owing to the climes in which cultivation occurs, seed type, maturity, soil conditions etc. and have intrinsic variability. Thus any method that attempts to functionalize the oils needs to account for this variability or at least be able to predict the outcome based on the composition of

the oils. Since the present work was an attempt at value addition by chemical modification, no particular applications were targeted. Rather the objective was to synthesize and characterize these modified oils and determine their applicability in certain broad areas.

Cleavage of double bonds (unsaturation) – Ozonolysis was chosen as the platform to accomplish this goal. Ozonolysis carried out with participating alcohols like ethylene glycol, glycerol - to explore the possibility of generating polyols (via oxidation of the double bonds), which could find use in polyester, polyurethane synthesis.

Grafting of reactive groups on the oil – this does not break the double bonds in the molecule. Silylation of soybean oil, to graft the reactive, readily hydrolysable siloxane groups on the oil backbone. The method would yield room temperature curable materials that could find applications as coatings, sealants etc.

The triglyceride/methyl ester structure of vegetable oils or their fatty acids can be transesterified using reactive alcohols like allyl, propargyl and cinnamyl alcohol, to yield functionalized fatty acid derivatives. The allyl and propargyl derivatives could find use as co monomers in ethylenic polymerizations. The allyl, cinnamyl and propargyl derivatives can also be sulfonated selectively or totally to yield sulfonated products which could find use in surfactants. Hydrosilylation of allyl and propargyl derivatives could yield products suitable for lubricant and personal care applications.

1.3 SPECIFIC GOALS

In the context of the discussion in the previous sections of this work, this work was undertaken to functionalize soybean oil and/or its derivatives to create a new family of products that could find applications as starting materials for polyesters, polyurethanes, room temperature vulcanizates (RTVs), personal care products, lubricants etc. It was also the goal to understand the chemistry of such modifications and establish how and why deviations from what was proposed were observed in the formation of products. While this work would never carry a guarantee of sustainability, it would at least be a first step in the harnessing of agricultural feedstock to substitute or complement, petrochemical derived materials.

1.4 SPECIFIC RESEARCH OBJECTIVES

1. Ozonation of soybean oil for the synthesis of “polyols” from soybean oil.
 - a. Investigate the bulk ozonolysis (single step) of methyl oleate (MO) as a model compound.
 - b. Determine product distribution (acetals, ozonides, peroxides, and “polyols”) in such a process and reasons for their formation.
 - c. Extend the observations to the soybean oil (SO) system with different alcohols (Ethylene glycol and glycerol).

- d. "Proof of concept" synthesis of unsaturated polyesters – to determine applicability of such "polyols" (even as a mixture of products) in synthesis.
- e. Propose a two step Ozonolytic process for methyl oleate (MO) model compound involving a solid oxidant (Oxone) to overcome the limitations of the single step bulk ozonolysis strategy.

2. Silylation of soybean oil (SO) and methyl oleate (MO)

- a. Develop a simple process to attach reactive siloxanes on to soybean oil and one of its methyl esters – this would confer room temperature curing abilities on the otherwise unreactive oil.
- b. Kinetics of silylation – effect of time, temperature and peroxide, activation energies for the reaction
- c. Determine the mechanistic aspects of the reaction (ENE reaction vs. Diels – Alder vs. peroxide grafting)
- d. Cure kinetics of the system – effect of water, catalyst and temperature on the curing rate.
- e. Evaluate the gel and sol contents and determine the composition of the extract.
- f. Applicability of the material as a water repellant coating and corrosion protective coating (from soybean oil).

3. Transesterification of soybean oil with olefinic alcohol
 - a. Transesterify soybean oil with allyl alcohol to get allyl soyate (allyl ester of soybean oil).
 - b. “Proof of concept” hydrosilylation of the allyl end group with two different hydrosilane compounds – to derive soybean oil – silicone hybrids for potential application as lubricant and in personal care products.

1.5 ORGANIZATION OF THESIS

The thesis is divided into three main segments and consists of 10 Chapters. The first chapter (Chapter 1) gives a general introduction to the concept of bio-based products and sustainability. Chapter 2 gives a brief introduction to soybean oil, its production, typical fatty acid composition and structure and how that is likely to influence the direction of any functionalizing chemistry.

The first segment (Chapter 3 – 5) deals with the extension of work previously reported in our group on Ozonolysis. Chapter 3 covers the key points of ozonolysis in bulk (conventional ozonolysis is done in solvents/solution). It expands on the simplistic treatment given in previous work, to account for the intrinsic immiscibility of the reactants (soybean oil /methyl ester with ethylene glycol and glycerol) and how it influences product formation. It also addresses the drawbacks of the catalyst system previously employed and proposes an alternative.

Chapter 4 discusses the applicability of such products (mixture of products termed “polyols”) in polymer synthesis (unsaturated polyesters). Some physical properties of the resulting resins have been tabulated, with the general conclusion that the applicability is present, but control of gelation and other properties is difficult. Chapter 5 proposes a two step oxidation for obtaining “polyols” or hydroxyesters using Oxone as a second stage solid oxidant to ensure higher conversion to products of the unwanted side products that are formed in Chapter 3.

The second segment (Chapter 6 and 7) discuss the work done on the synthesis and properties of silylated derivatives of soybean oil and methyl ester (methyl oleate). Chapter 6 deals with silylated soybean oil products, with an emphasis on the kinetics of the reaction, the activation energy and mechanism of the silylation. The effect of time, temperature and the ratio of the silane on the conversion are explored. Physical properties like gel content and chemical composition of the “sol” are explored. The influence of catalyst, added water and temperature on the rate of cure is briefly explored. The applicability of the material as a “water repellant” coating and corrosion protective coating is also briefly explored.

Chapter 7 deals with the silylation of one particular methyl ester (methyl oleate) to understand the mechanistic differences between the ester and soybean oil. As in Chapter 6, the effect of time and temperature on silylation and activation energy is determined. Gel content and composition of the “sol” are also determined. The work also deals briefly with one saturated ester (methyl stearate). This discussion thus

completes the mechanism of silane addition to polyunsaturated, monounsaturated and saturated fatty acids, which then allows us to decide the silylation strategy for any vegetable oil or its derivative.

Chapter 8 deals with the use of titanium alkoxides as highly active catalysts for the ring opening polymerization of 1, 4-dioxan-2-one (PDO). The mechanism of polymerization was confirmed as a co-ordination insertion type and at low [monomer]/[initiator] concentrations, initiation was observed on alkoxide sites of the catalysts. The activation energy reported is the lowest of any system reported till date for PDO. The catalysts could find use in reactive extrusion polymerization (REX) and in solid state post – polymerization molecular weight build up of polyesters. Also the multiple initiations could imply synthesis of branched polymer structures with better melt strength.

Chapter 9 summarizes the work done in Chapters 3 – 8 and suggests future directions for work in the project areas.

Chapter 10 deals with preliminary studies undertaken in the transesterification of soybean oil to its allyl esters. Hydrosilylation of these esters is also proved with two different hydrosilane containing silicone compounds. Extension to synthesize the propargyl and cinnamyl esters is proposed as future work for applications ranging from co -monomers in polymerizations to surfactants to personal care products and lubricants.

The second portion of Chapter 10 deals with an extension of silylation of soybean oil to biodegradable polyester (EcoflexTM), to impart better compatibility with inorganic fillers. The method is very simple and the silane is required in small amounts. The method is extensible to cover other polyesters with aliphatic chains in them, like PCL or PPDO and can increase mechanical strength at the expense of elongation.

REFERENCES

1.6 REFERENCES

1. R. Narayan, *Polymeric Materials from Agricultural Feedstocks*, In: *Polymers from Agricultural Coproducts*, Ed., Fishman, M.L., Friedman, R.B. and Huang, S.J. American Chemical Society Symposium Series, American Chemical Society, Washington, DC, **575**, 2 (1994).
2. R. Narayan, *Paradigm for Successful Utilization of Renewable Resources*, 78 (1998).
3. R. Narayan, *Biomass (Renewable) Resources for Production of Materials, Chemicals, and Fuels -- A Paradigm Shift*. Rowell, R. M., Schultz, T. P., Narayan, R., Eds; American Chemical Society Symposium Series, American Chemical Society, Washington, DC, 476, 1, 1992.
4. R. Narayan, *Biobased & Biodegradable Polymer Materials: Rationale, Drivers, and Technology Exemplars*; ACS (an American Chemical Society publication) Symposium Ser. 939, **Chapter 18**, p. 282, (2006).
5. R. Narayan, *Biobased & Biodegradable Polymer Materials: Rationale, Drivers, and Technology Exemplars*, Polymer Preprints (American Chemical Society, Division of Polymer Chemistry), **46**(1), p.319-320, (ACS Publications, 2005).
6. D. Pimentel *et al.*, *Environment, Development and Sustainability* **1**, 19 (1999).
7. D. Pimentel, R. Harman, M. Pacenza, J. Pecarsky, M. Pimentel, *Population & Environment* **15**, 347 (1994).
8. D. Pimentel, M. Pimentel, *American Journal of Clinical Nutrition* **78**, 660S (2003).

CHAPTER 2

INTRODUCTION TO VEGETABLE OILS AND SOYBEAN OIL

2.1 VEGETABLE OILS

Vegetable oils are triglyceride esters which have their source in plants. Thus they are different from animal fats based on source mainly. Chemically they are best described as esters of the triol glycerol with long chain fatty acids having carbons as low as 14 and as high as 22 or more in some cases. The fatty acids can be saturated or unsaturated (possess double bonds).

The world vegetable oil supply stood at 137 MMT (million metric tons) in 2009 (1). The consumption was around 131 MMT leaving a surplus of 6 MMT of oil. This accounts only for the major vegetable oils whose primary use is in food applications. The surplus oil thus can be tapped into as a feedstock, if value addition can be done to the oils. Also value addition to the oil would ensure that demand for the oil itself would increase, which would lead to benefits for the farmers directly.

The fatty acid composition of some common plant oils are provided in Table 2.1. It can be seen that for the most part, three main fatty acids make up a significant portion of the composition. The unsaturated fats are listed and typically the remainder is made of saturated fats. The structure of these fatty acids is provided in Figure 2.1.

Table 2.1 Percentage composition of some common plant oils (Adapted from (2))

Oil	Linolenic	Linoleic	Oleic
Soybean oil	8.0	53.0	21.0
Sunflower oil	<0.5	63.0	23.0
Corn oil	1	52.0	32.5
Olive oil	1	7.5	75.5
Peanut oil	0	25.0	55.0
Linseed oil	58.0	14.0	18.0

2.2 SOYBEAN OIL AS A FEEDSTOCK

Soybean oil, like other vegetable oils is a triglyceride ester composed of long chain fatty acids. It is the second most widely produced and used oil in the world, next only to palm oil. As of January 2009 the world production stood at 37 MMT. The surplus stood at 0.2 million tons. Value addition to soybean oil (or vegetable oils) is thus attractive economically and environmentally. However, consideration should be given to the fact, the nature and composition of soybean oil and in general all vegetable oils, depends on seed variety, climate and geography. Thus any process of value addition should take into account this intrinsic variability in the starting material. It should also be noted that genetic modifications now allow for changing the composition of the oil to a certain degree. Thus oils high in certain fatty acids or low in saturates can be produced.

The structures of the five major fatty acids constituting the triglyceride are shown in Figure 2.1. The variable percentages indicate the variability in composition depending on the type of seed used. Higher numbers for the linoleic and lower numbers for the Stearic and Palmitic acids are for the Lowsat™ soybean oil.

It can be seen that on average, a molecule of triglyceride can possess anywhere from **4.3 - 5.1** double bonds or unsaturation. Mathematically there are **35** possible triglycerides resulting from placement of fatty acid chains along the triglyceride, creating a complex mixture of triglycerides. From the composition it is also clear that the major fatty acids are likely to occur more than once in the triglyceride structure.

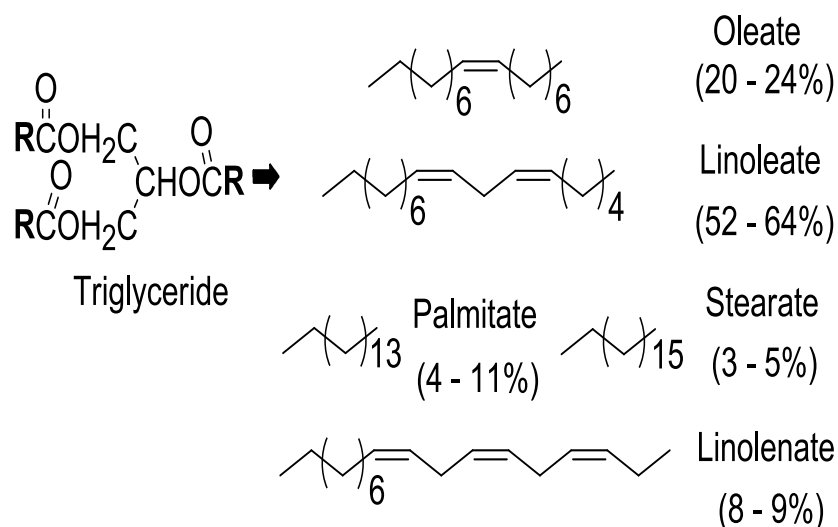


Figure 2.1 Fatty acid composition of soybean oil

The degree of unsaturation and their nature decide the reactivity of the oil. It is well known that oils with higher proportion of polyunsaturated fatty acids are more reactive (Linseed oil, Tall oil). Oils with lower unsaturation tend to be less reactive.

Linseed oil (a drying oil) is capable of oxidative polymerization in air to yield a cross-linked network, mainly due to its higher **linolenic** and **linoleic** content as seen from Table 2.1. Soybean oil even though high in linoleic content is stable in air and does not polymerize. Also conjugated fatty acids are more reactive than the unconjugated fatty acids.

From the structure, it is evident that the oil offers three locations for functionalization:

1. The double bonds – which can be oxidized (3-6), hydroformylated (7), epoxidized (8) etc.
2. The remaining methylenic sites, which can be subjected to radical chemistry to graft reactive groups on the oil
3. The ester linkage with glycerol – which can be replaced by other alcohols to yield functional esters.

The current work focuses on the above three and the chapters are arranged in that order.

2.3 TRIGLYCERIDE DISTRIBUTION IN SOYBEAN OIL

Each molecule of glycerol has three – OH groups which can be esterified. From Figure 2.1, it can be seen that the five fatty acids make up for the total composition in

soybean oil. Using the lower numbers for the saturates (LowsatTM), we can arrive at a theoretical distribution of triglycerides for the oil.

In mathematical terms, the three positions of the glycerol can be filled in by any of the five acids (unique – each fatty acid occurs once) for a total of 60 triglycerides. Based on the symmetry of the molecule, the 1 and 3 positions will yield identical structures, thus reducing the number by two to 30. Also five triglycerides can have all the fatty acids identical. Thus the total possibility would be given by $30+5 = 35$ triglycerides. Also the presence of each fatty acid in the triglyceride in the molecule will be directly proportional to its mole fraction.

Based on the above assumptions, it is possible to theoretically compute a frequency distribution for the triglycerides. This is important since the functionality of the molecule after chemical modification (epoxidation, ozonolysis etc.) can be directly estimated using this distribution. Without even the detailed frequency distribution, it can be seen that roughly 2/3 of all triglycerides are likely to have 3 or more double bonds (due to linoleic acid). Thus any modification, will introduce a difunctional entity at least on the triglyceride. From Figure 2.2 it can be seen that theoretically a significant portion of the triglycerides have more than 4 double bonds/per molecule.

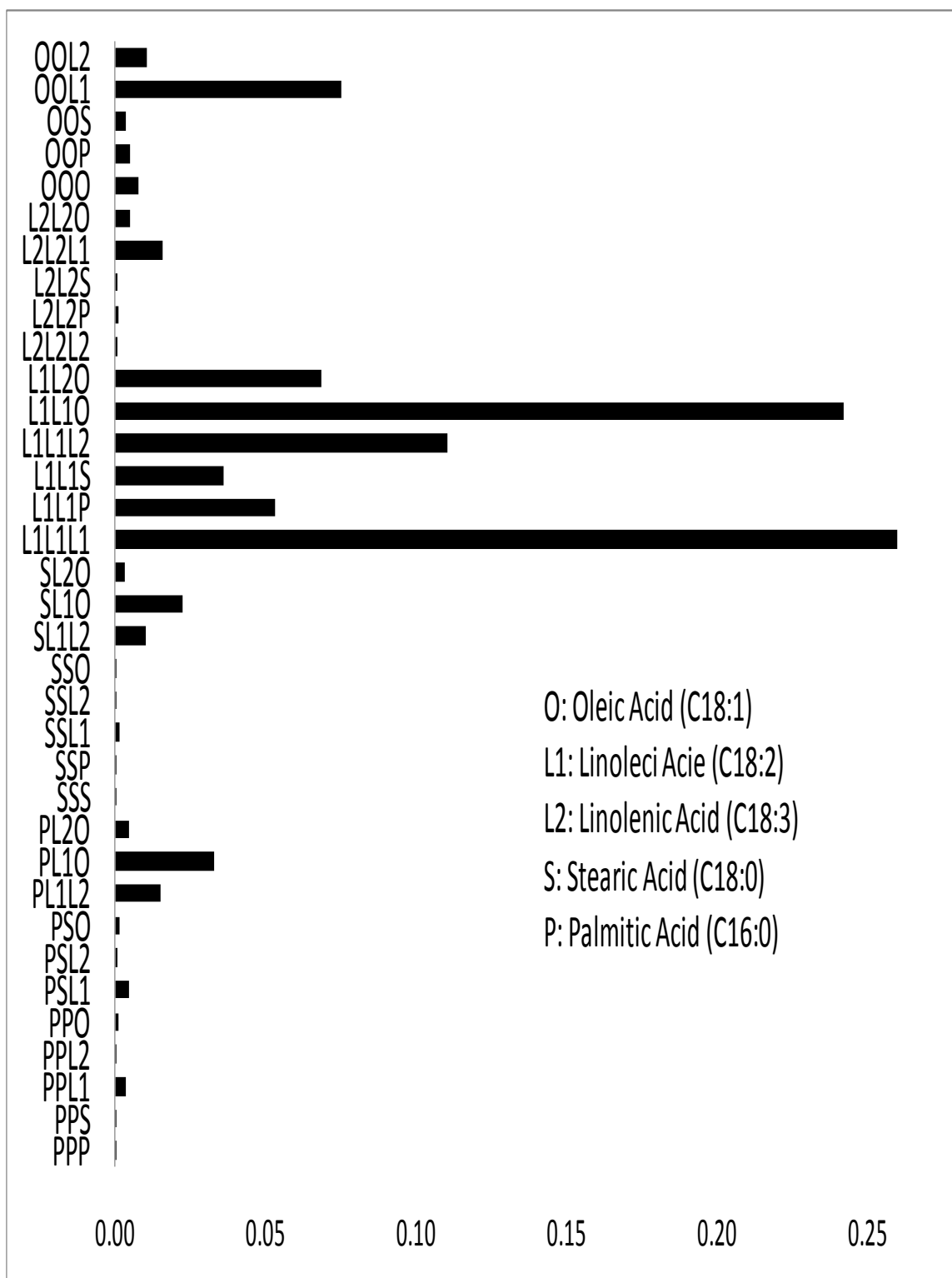


Figure 2.2 Frequency distribution (theoretical) of triglycerides in Lowsat™ oil

Thus any cleavage of the double bonds is likely to leave at least two functional groups on the triglyceride. The other fragments would typically then consist of molecules with one or two functional groups depending on the fatty acid.

The same argument would hold for other oils as well and in their case the proportion of saturated vs. unsaturated fatty acids and monounsaturated vs. polyunsaturated fatty acids is likely to dictate product distribution. However, this is not a concern when modification is done via grafting on the backbone or on the ester portion of the triglyceride.

REFERENCES

2.4 REFERENCES

1. Oil seeds: World Market and Trade;United States Department of Agirculture, 2009, pp. 35.
2. M. Guillén, A. Ruiz, *European Journal of Lipid Science and Technology* **105**, 688 (2003).
3. R. Ackman, *Lipids* **12**, 293 (1977).
4. J. Marshall, A. Garofalo, *The Journal of Organic Chemistry* **58**, 3675 (1993).
5. J. Sebedio, R. Ackman, *Canadian Journal of Chemistry* **56**, 2480 (1978).
6. J. Neumeister, H. Keul, M. Saxena, K. Griesbaum, *Angewandte Chemie International Edition in English* **17**, 939 (1978).
7. U. Biermann, J. O. Metzger, *Topics in Catalysis* **27**, 119 (2004).
8. S. Khot *et al.*, *Journal of Applied Polymer Science* **82**, 703 (2001).

CHAPTER 3

OZONOLYSIS: SYNTHESIS OF HYDROXYESTERS (“POLYOLS”) FROM SOYBEAN OIL

ABSTRACT

Oleic acid was ozonated (as a test compound) in acidified water and the oxidation to azelaic acid was accomplished successfully (yield 75%, purity 98%, m.p 108 °C – 110 °C). Thus ozone was verified to be a good oxidant for the unsaturation present in fatty acids.

Methyl oleate was employed as model compound to characterize the ozonolysis with participating alcohols (ethylene glycol, glycerol). Methyl oleate was chosen since only two products were expected from the ozonolysis, leading to easier characterization. Methyl oleate was ozonated with stoichiometric amounts of the alcohols (1 double bond: 2 moles alcohol) for predetermined amount of time with calcium carbonate as a basic catalyst. The products were characterized by FTIR, NMR and titrimetry. While titrations indicated increase in hydroxyl values (amounting to ester formation), NMR spectra seem to indicate that acetals, ozonides, ethers and aldehydes are the major products.

The procedure was extended to soybean oil and under identical conditions, similar products were observed. Use of excess alcohol did not change the product profile significantly. However, conducting the same reaction in a solvent (dichloromethane) yielded the hydroxyester in small quantities. The soybean oil samples were also extensively characterized by NMR, FTIR and titrimetry. It is concluded that the intrinsic immiscibility of the oil with the alcohols used, coupled with their low reactivity and the weakly basic nature of the catalyst, prevent the oxidation of the double bond to the ester. The products however do exhibit hydroxyl values and it was proposed that they can be used in a trial polyester synthesis. The products also exhibit acid values, which implies that aldehydes formed during ozonolysis get converted to acids.

3.1 INTRODUCTION

3.1.1 Vegetable oils in polymers

One of the earliest uses for vegetable oils can be traced back to the synthesis of alkyd resins for coating type applications. Ozonolysis has been utilized as a platform to functionalize soybean oil. A reaction of ozone with olefins is extremely rapid. Polyols have been made by ozonolysis of vegetable oil followed by a simple borohydride reduction (1) or hydrogenation to yield primary hydroxyls on the triglyceride. Ozonolysis of methyl esters of fatty acids has also been reported in acidic (2-4) and basic media (5-6) to form methanol capped esters. Functionalization of vegetable oils has been studied using a variety of chemistries including epoxidation (7-9), hydroformylation (10) and simple alcohol interchange (11) which involves reacting triglycerides with other polyhydric alcohols like glycerol, pentaerythritol and also via ozonolysis catalyzed by acid (12) and base (13). With the development of metathesis chemistries, it has also become possible to perform metathesis on the double bonds of fatty acid esters.

However there are some drawbacks to these techniques. Epoxidation yields secondary hydroxyls (upon acid hydrolysis of epoxides), which are less reactive than primary hydroxyls. Borohydride and hydrogenation reductions are often expensive and also use flammable reagents. Hydroformylation requires a multi-step process and it often involves expensive catalysts, which are difficult to recover.

Thus, there is a need for improvement of the chemistry and technology in functionalizing vegetable oils for substituting the various petrochemical polyols currently in use in applications like polyurethane foams, unsaturated and saturated polyesters etc. The procedure outlined in this work offers an attractive way of functionalizing vegetable oils, especially soybean oil for value added applications and more specifically for synthesizing polyols that can further be used in the production of polyurethanes, and polyester resins. It should be noted that unlike conventional ozonolysis that is run at very low temperatures ($-70\text{ }^{\circ}\text{C}$) and in dilute solutions, the present procedure is run close to room temperature and with no additional solvents. Furthermore, heterogeneous catalyst is used, which is easily separated from the product after the reaction is complete.

3.1.2 Ozonolysis

Ozone is a powerful oxidant, occurring naturally in the upper atmosphere, by the action of ultraviolet (UV) radiation on molecular oxygen. It is synthesized on a laboratory scale by a high voltage electric discharge and also by the action of middle or far UV radiation (170 – 200 nm). Being an allotrope of oxygen, it exhibits much stronger oxidizing power than molecular oxygen. The formation of ozone and its resonant structures are given in Figure 3.1.

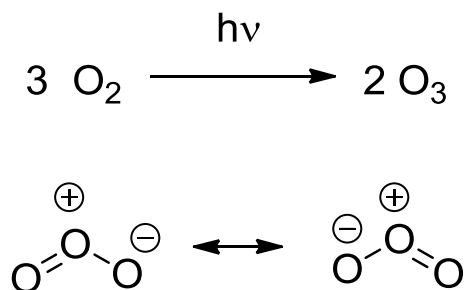


Figure 3.1 Photochemical formation of Ozone and its resonant structures

Because of the intrinsic instability, ozone is typically manufactured “at site” and is never stored. Compressing ozone promotes its decomposition to oxygen. Ozone also can be explosive at high concentrations. Thus industrially, ozone is typically produced at 14 wt%. Ozone has limited solubility in water and this enables it to be used widely as a sterilizing agent. However, ozone exhibits good solubility in halogenated hydrocarbons (typically chlorinated and fluorinated).

For purposes of ozonolysis of disubstituted ethylenes (as is the case with fatty acids), the mechanism of ozone addition to the double bond is a two center, 1, 3 – dipolar addition across the double bond (14). The primary product of this addition is a “molozonide” or “primary ozonide”. At normal temperatures, the primary ozonide is short lived and immediately dissociates to a “carbonyl oxide” and an aldehyde. These two fragments rearrange to form the secondary ozonide. This happens in the absence of any protic molecules in the mixture. The reaction scheme is provided in Figure 3.2.

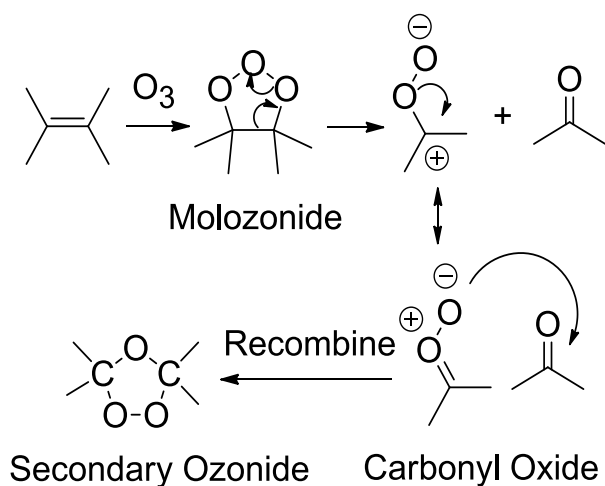


Figure 3.2 Initial attack of ozone on double bond leading to formation of secondary ozonide

However, in the presence of protic species (like alcohols), this rearrangement to the secondary ozonide is interrupted and the reaction pathway can be changed. This has been exploited in the direct conversion of double bonds to esters as mentioned earlier. The carbonyl oxide is immediately attacked by the alcohol to form hydroperoxy ether. In the presence of acid catalysts, the aldehyde can also react with the alcohol forming acetals. In the case of base catalysis, hemi – acetals can be formed; in addition to the hydroperoxy ether. The postulated mechanism is shown in Figure 3.3.

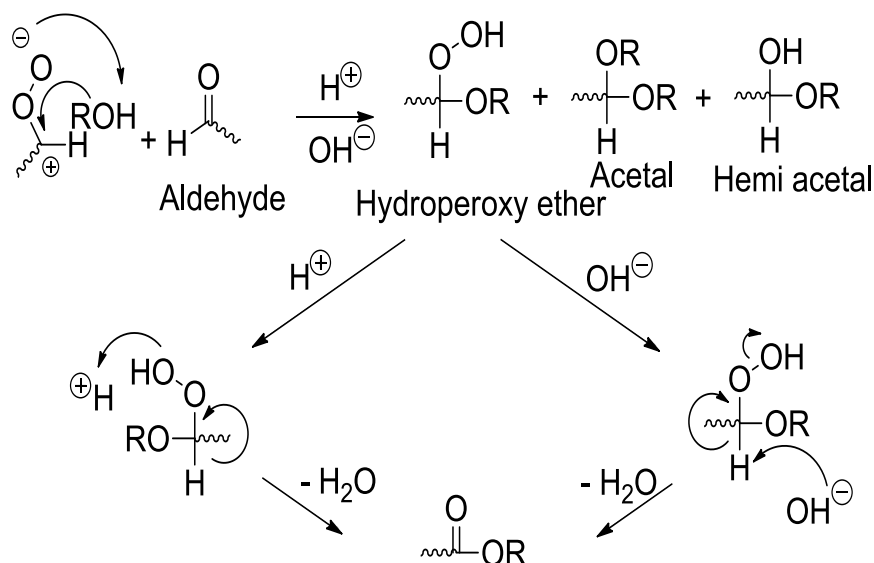


Figure 3.3 Formation of ester from intermediates in ozonolysis (Note: 1 mole of water is formed) – The structures and arrows do not necessarily mean a concerted mechanism

From the above it can be seen that a mole of water is formed for each ester linkage that is formed from the double bond. The catalyst is regenerated at the end of the process. Since two carbonyl groups are formed at the end of ozonolysis, there is a net liberation of two moles of water. This second step of ozonolysis is much slower than the initial attack on the double bond. The formation of water is very important and this can be seen easily from the above figure. Replacing the “R” group of the alcohol with “H” to determine the product, it is easily seen that the product is carboxylic acid. The potential formation of acids can be a disadvantage, since the acids would need to be esterified again to yield the hydroxy ester.

The secondary ozonide formed in the process is fairly stable and has been reported so in literature (15-18). Also in the absence of any protic species as detailed

above, rearrangements other than the one shown in Figure 3.2 can occur. The carbonyl oxide can basically dimerize to form tetraoxanes (ozonides are 1, 2, 4 – trioxolanes). They can also polymerize to form polymeric peroxides (14). The formation of these species would be detrimental to the objective of ozonolysis in the present case. The reactions are shown in Figure 3.4.

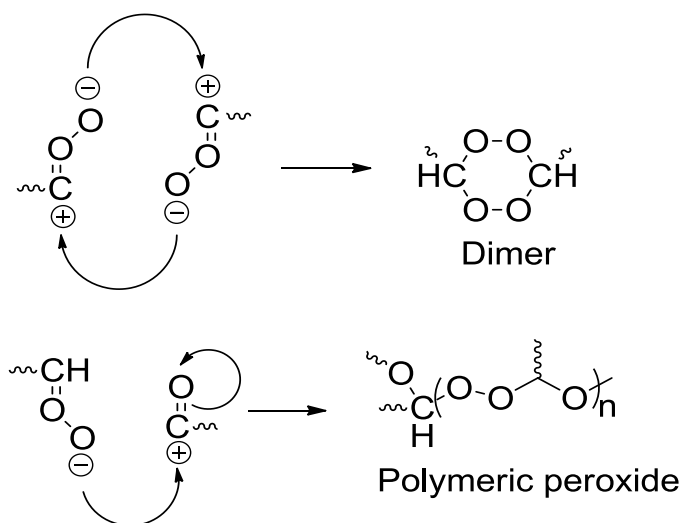


Figure 3.4 Formation of dimeric peroxide (tetraoxanes) and polymeric peroxides (Structures do not imply concerted mechanism)

Although secondary ozonides are known to decompose in alcoholic media (19) to give their respective carboxylic acids and aldehydes (for this case), the reaction has been shown for methanol solvent, it is still acids and aldehydes that are the products of the reaction and not the required esters. Thus, even though ozone can act as an efficient oxidant, side reactions happening are quite common.

received. Ozone was made in the lab from dry oxygen (from AGA gas) in a Praxair Trailgaz OZOBLOC OZC 1001 ozone generator (Cincinnati, OH). Deuterated Chloroform for NMR spectroscopy was obtained from Sigma Aldrich and used as received.

3.4 EXPERIMENTAL

Ozone (4 – 6 wt %) in oxygen was obtained by passing oxygen through the ozone generator at 0.25 cu.ft/min. The ozone exiting the ozone generator was fed into a 500 ml wash bottle fitted with a sandstone fritted disc at the bottom to ensure uniform sparging of the gas. The reactants were added to this glass vessel and residual ozone and oxygen were taken out to a glass vessel with a 10 wt % solution of potassium iodide (KI) in water to destroy any residual, unreacted ozone. The reaction vessel was maintained at constant temperature using a water bath.

3.4.1 Synthesis of azelaic acid

To confirm the oxidation of double bonds in the present set up. 100 gm of oleic acid was ozonated with 200 ml of water acidified with 1 ml of conc. HCl. The time of reaction was 200 minutes. The mixture was then transferred to a beaker, heated to 85 °C to dissolve all solids formed. The mixture was then allowed to cool to 60° C and filtered. Ozonolysis of oleic acid with water as a reactant is expected to produce Azelaic acid (C9 - diacid) and pelargonic acid (C9 mono acid). Pelargonic acid is a liquid and

azelaic acid is insoluble in water at 60 °C and is precipitated out. The crude azelaic acid was then recrystallized from boiling water. The purity of the acid (75% yield) was determined to be 98% based on its acid value and the observed melting point was determined to be 108° C – 110 °C, in good agreement with literature.

3.4.2 Synthesis of 2 – hydroxyethyl esters from methyl oleate

118.6 gm (approx.0.4 mol) methyl oleate and 34.7 gm ethylene glycol (51.5 gm for glycerol) that has been reacted previously with 0.12 gm NaOH were added with 11.86 gm coarse CaCO₃ catalyst to a wash bottle fitted with a fritted disc. The reaction mixture was cooled to 0 °C in an ice bath and ozone (4-6 wt% in oxygen) was bubbled through a fine fritted glass at a rate of 0.25 cu.ft/min for 2 minutes per gram (21) (p.51) of the methyl ester used. The product mixture was filtered to remove the catalyst, excess alcohol was removed by water wash and the product was then dried over anhydrous CaSO₄.

3.4.3 Synthesis of soybean oil polyols

88gm (~0.1 mol) of soy oil was mixed well with 0.92 moles of the polyhydric alcohol (ethylene glycol (57.04gm) + 0.88 gm NaOH, glycerol (84.64gm) + 0.88 gm NaOH) and CaCO₃ catalyst (8.8 gm – 10 wt % of soybean oil). Ozone was bubble through the resultant homogenized mixture for 176 minutes (2 minutes/gm of oil (21)).The

resultant soy based polyol was centrifuged to remove the CaCO_3 catalyst and excess alcohol was removed by washing the product with distilled water five times. The product was then dried over anhydrous CaSO_4 and used for all further experiments.

3.5 CHARACTERIZATION

The polyols were characterized for their acid value, hydroxyl value, and saponification value and iodine numbers. The acid value was determined by titrimetry according to ASTM D1980. Hydroxyl values were determined by titrimetry according to ASTM D1957 using the pyridine – acetic anhydride method and saponification value by ASTM 1962. Iodine numbers were determined according to ASTM D1959. In accordance with the above standards, acid and hydroxyl values were expressed as milligrams of potassium hydroxide (KOH) per gram of sample used. The iodine numbers were expressed as centigrams of Iodine per gram of sample.

Fourier Transform Infra Red spectra (FTIR) were run on a Perkin Elmer Spectrum One spectrometer with an ATR diamond top cell using air as the background. For each sample analyzed, four scans were used at a resolution of 4 cm^{-1} . The spectra were also subjected to an ATR correction prior to analysis.

Nuclear Magnetic Resonance spectra (NMR) were run on a Varian Unity Plus spectrometer operating at 500 MHz. CDCl_3 was used as the solvent for all experiments with its proton resonance at 7.24 ppm and carbon resonance at 77.0 ppm used as the reference. Samples were obtained by dissolving about 0.2 gm of the polyol in about 0.7 ml of CDCl_3 . A standard 5mm tube was used for all experiments. Standard acquisition parameters were used for all samples except for carbon spectra, where a recycle delay of 2 seconds was employed.

3.6 RESULTS AND DISCUSSION

3.6.1 Hydroxy ethyl esters from methyl oleate

The results of the titrimetric analysis are given in Table 3.1. From the data, it can be seen that ozonolysis proceeds smoothly and the double bonds are consumed as expected. From the values it can be seen that, there is a reduction of the double bonds by about 75%. There is a concurrent increase in hydroxyl values and saponification value correlating with an increase in ester groups. While the hydroxyl value shows a significant increase, the saponification values do not increase that significantly. This indicates that although ozonolysis proceeds, with cleavage of double bonds, the conversion of the intermediates to the ester groups is not occurring as expected (Figure 3.5).

Table 3.1 Titrimetric results of ozonated samples of methyl oleate. (Percent change in parentheses)

Attribute	Methyl oleate (MO)	Ozonated with EG	Ozonated with glycerol
Acid Value (mg KOH/gm)	1	28	31
Hydroxyl value (mg KOH/gm)	1	174	137
Saponification value (mg KOH/gm)	276	364 (32%)	-
Iodine value (gm/100gm)	60	15 (-75%)	14 (-76%)

The IR spectra (Figures 3.6 and 3.7) indicate a reduction in double bonds. They also show –OH groups at 3500 cm^{-1} . These could be from the formation of ethers and acetals as indicated earlier. They could also be from the formed hydroxyesters, which NMR spectroscopy should confirm. The – OH groups can also be from the acids, which are confirmed from the acid value titration. The carbonyl region is broadened with a hump at 1750 cm^{-1} . . It is also observed that most of the double bonds have been cleaved since the C=C–H stretching vibration at 3008 cm^{-1} has mostly disappeared. Furthermore, expansion of the FTIR spectra around the ester region ($1700\text{-}1800\text{ cm}^{-1}$) shows that the original peak of methyl oleate is much broader after the ozonation reaction and appears as multiple overlapping peaks.

Some residual glycol cannot be ruled out, but the amount is likely to be minimal due to the extensive water washing given to the sample. Overall, the IR spectra confirm the inference from the titrimetric data, but do not offer any clue as to the reduced saponification values obtained. The NMR spectra of the sample (Figures 3.8 – 3.11) provide detailed structural information on the products of ozonolysis.

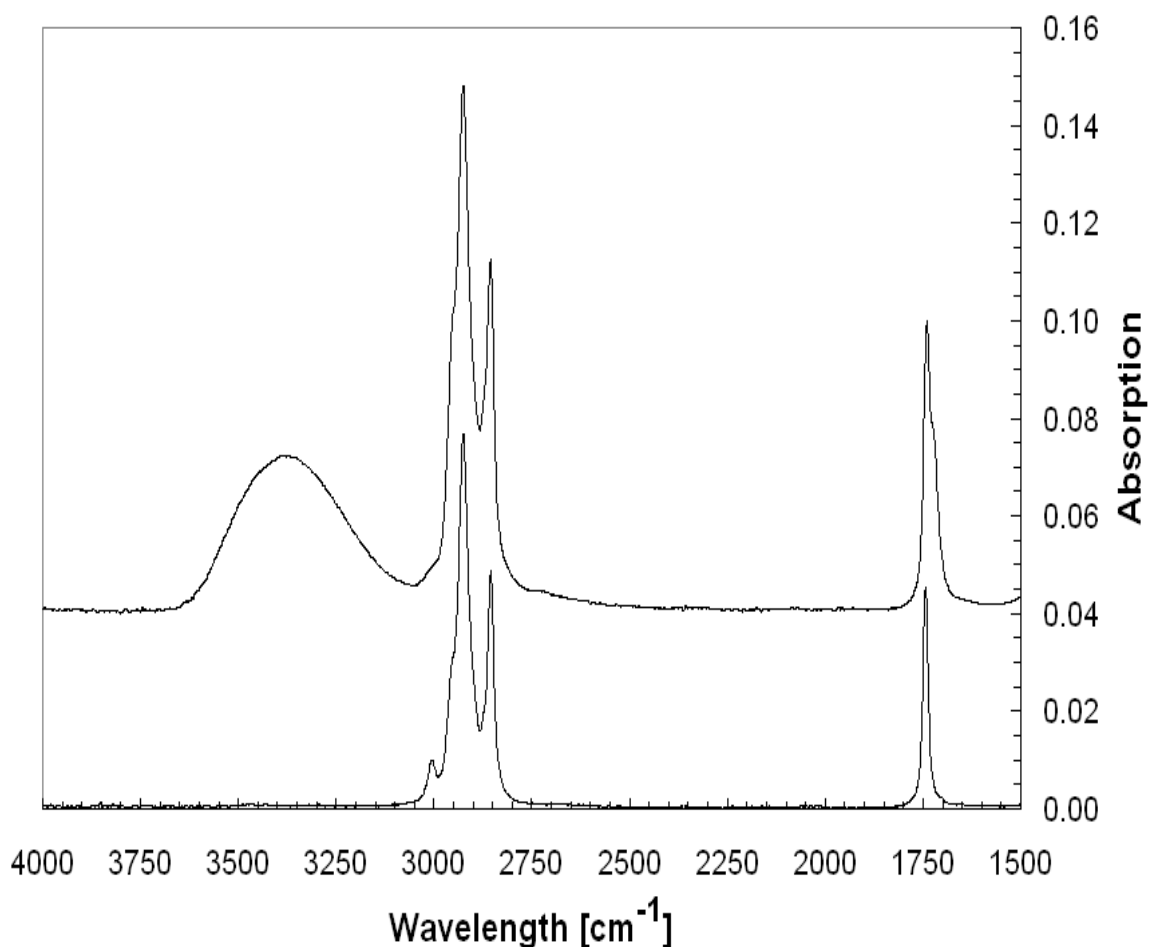


Figure 3.6 FTIR spectra of Ozonated methyl oleate – EG sample (Top) and methyl oleate (Bottom)

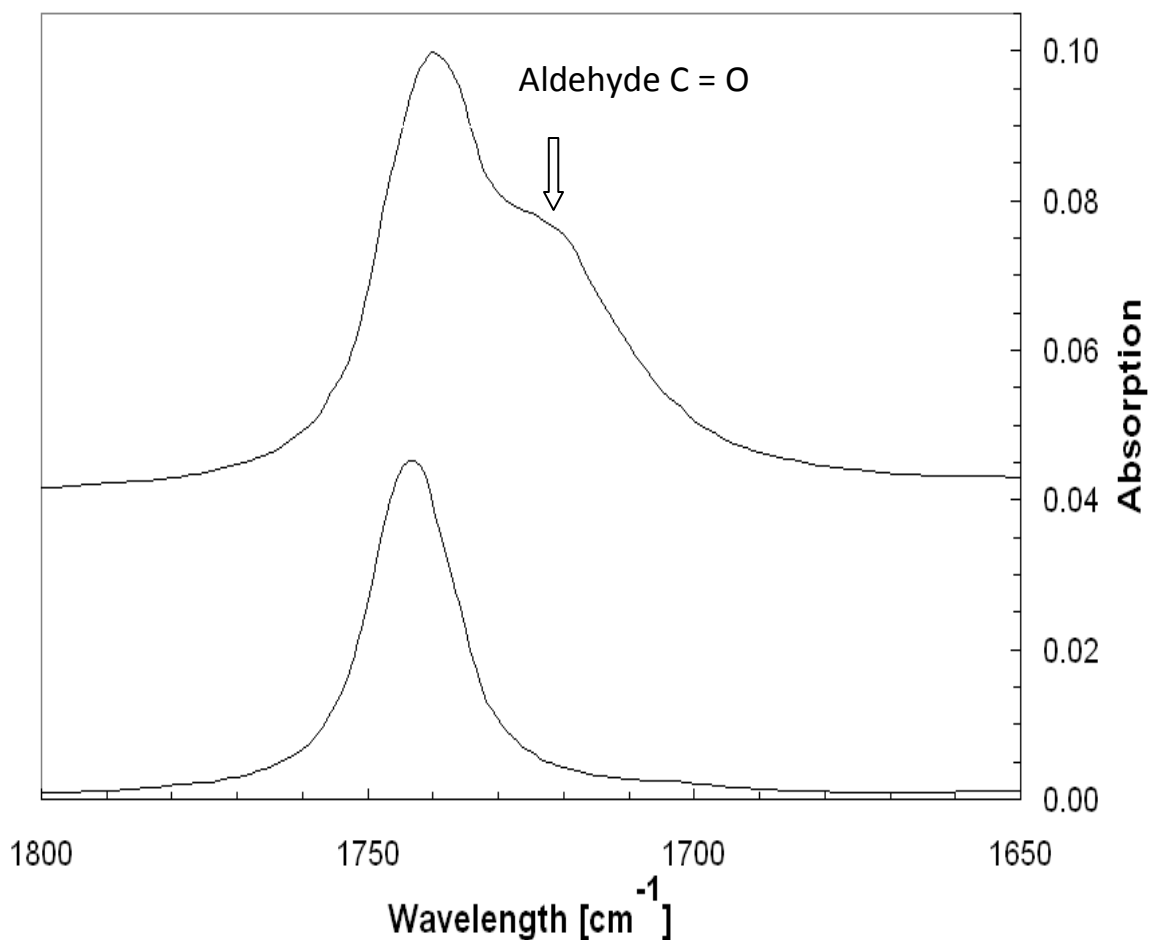


Figure 3.7 IR spectra (Carbonyl region) of Ozonated methyl oleate – EG sample (Top) and methyl oleate (Bottom)

The IR spectra for the methyl oleate – glycerol runs are similar except for the reduced intensity of the – OH peak. This is also visible from the titrimetric results. Since glycerol is trifunctional, the hydroxyl values for the glycerol based ester, should be nearly 75% higher than that of the ethylene glycol ester for the same conversion. Since the hydroxyl values are lower, it can be inferred that the reaction with glycerol does not proceed at the same rate due to probably the higher viscosity of glycerol.

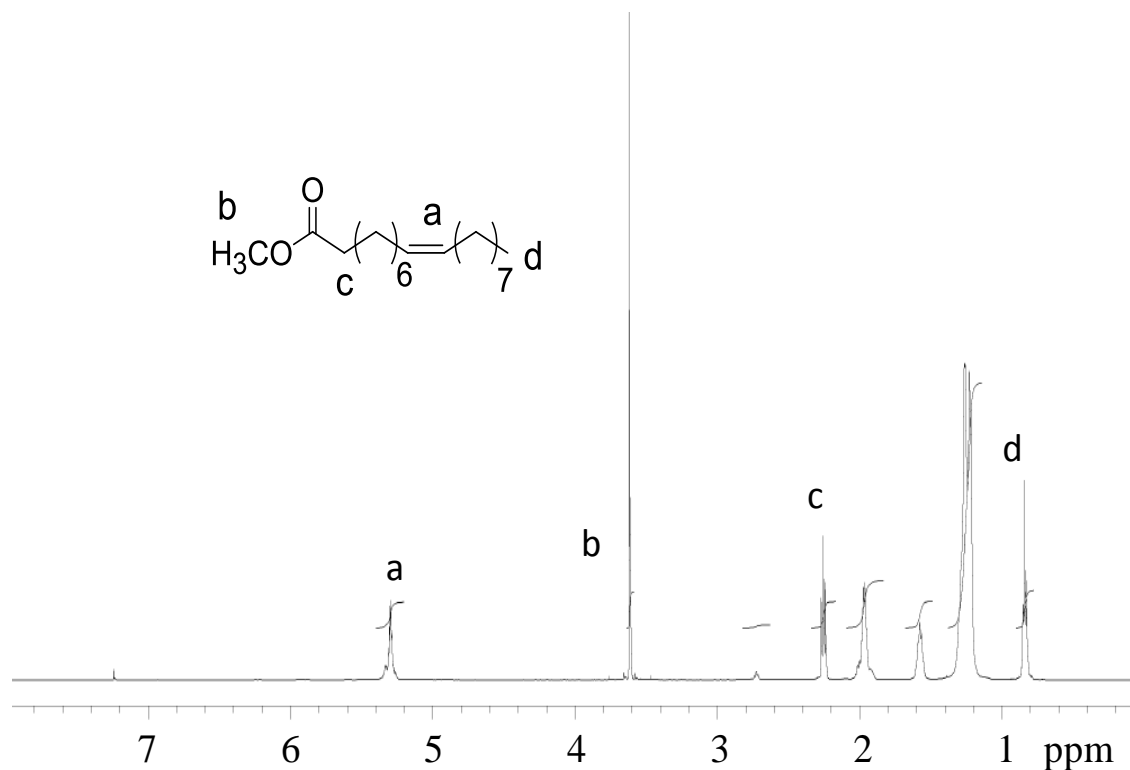


Figure 3.8 ^1H NMR spectrum of methyl oleate with assignments

NMR spectra can also be used for quantitative estimates of functional groups relative to a standard peak in the sample. ^1H NMR is amenable to this kind of calculation. The calculations based on NMR for the different functional groups are tabulated in Table 3.2. The peak assignments for the fatty acid residues of soybean oil and methyl ester have been drawn from literature (22-24). The assignment of the ozonide has been made from reported literature (15, 25) and the cyclic acetals from known chemical shifts of 1, 3 – dioxolanes. It should be noted that the term “acetals” has been used generically to account for cyclic, linear acetals, hemi – acetals and hydroperoxy acetals. No specific assignments to one particular species have been made

due to the complex nature of the mixture. The ratios give an estimate of products formed in terms of mole percent relative to the methyl group (0.88 ppm). For example, if methyl oleate is completely converted to its secondary ozonide, the ratio of the methyl group (0.88 ppm) to the two protons on the ring (5.2 ppm) should be 3:2. In Table 3.2, the ratio is 3: 0.54, indicating that 27% by mole of the double bonds are converted to ozonide. It should be remembered that the double bonds have been reduced only by 75% from the original.

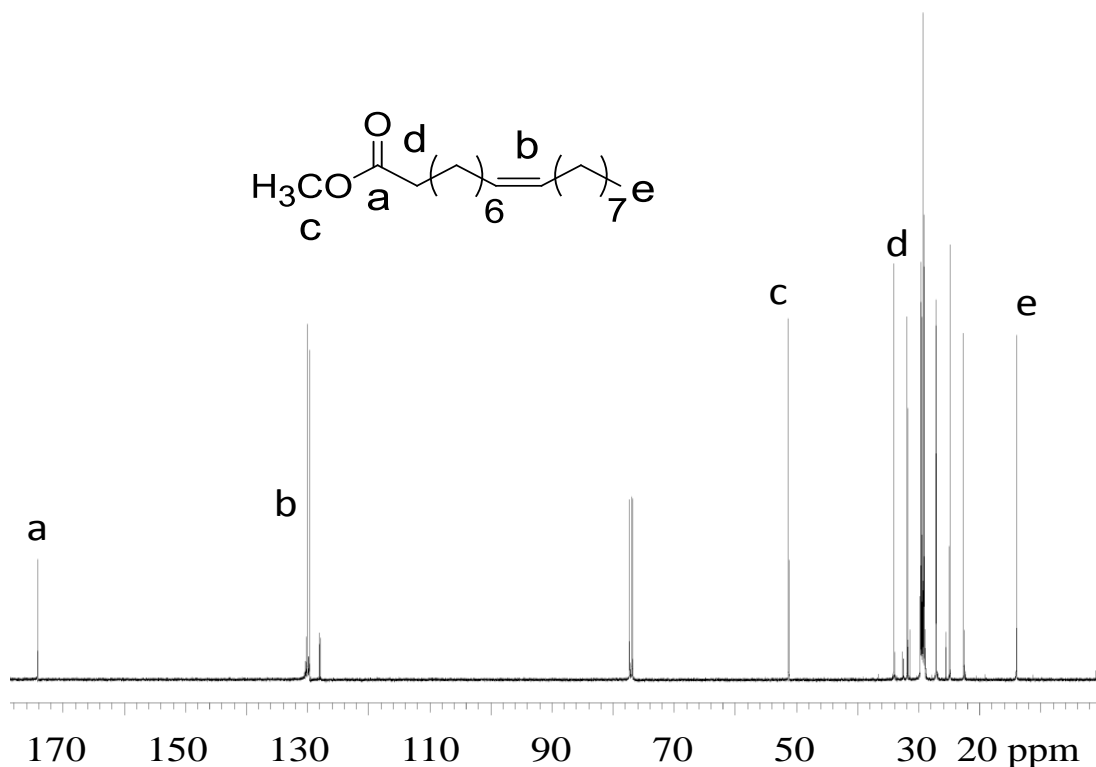


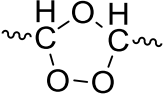
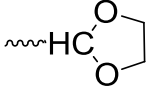
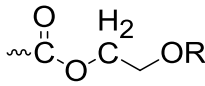
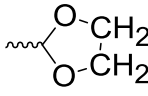
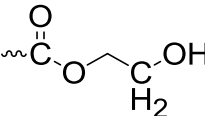
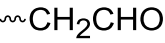
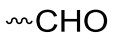
Figure 3.9 ^{13}C NMR spectrum of methyl oleate with assignments

Similarly, the aldehydes account for around 15% by mole and the ether or acetals account for another 45%. This total however does not add up to 75%. The reason for this is that the acetals have not been accurately estimated due to a broad baseline,

which causes errors in the integration. It is important to note, the objective of the ozonolysis, formation of hydroxyesters is not accomplished at all. There are no peaks in the 4.0 – 4.2 ppm region that would indicate so. As discussed earlier, to redirect the primary ozonide decomposition, to the products, intimate contact needs to exist between the alcohol and the primary ozonide.

In this case, the only energy for mixing comes from the gas being bubbled. Thus it might not ensure a high degree of mixing. The two stage oxidation discussed in Chapter 5, the methyl oleate in that case is not successfully oxidized to the hydroxyester in any significant amount. The reason could also be lack of sufficient base to drive to reaction forward and/or the poor reactivity of glycol and glycerol in comparison to alcohols like methanol.

Table 3.2 Integral ratios of functional groups (relative to CH₃ area =3) from NMR spectra; proton of interest is italicized. ¹³C shifts reported for carbon bearing proton of interest (Sample: methyl oleate with ethylene glycol)

¹ H (ppm)	¹³ C (ppm)	Functional group	Methyl Oleate	Ozonated with EG
5.0 – 5.2	105		0	0.54
4.6 – 4.9	108	 , other ether	0	0.62
4.1 (R = H)	66		0	0
4.2 (R = COR ₂)	62	R = H, COR ₂	0	0
3.9	65	 , ether		
3.8	61		0	1.80
2.4	44		0	0.62
9.72	202.8		0	0.21

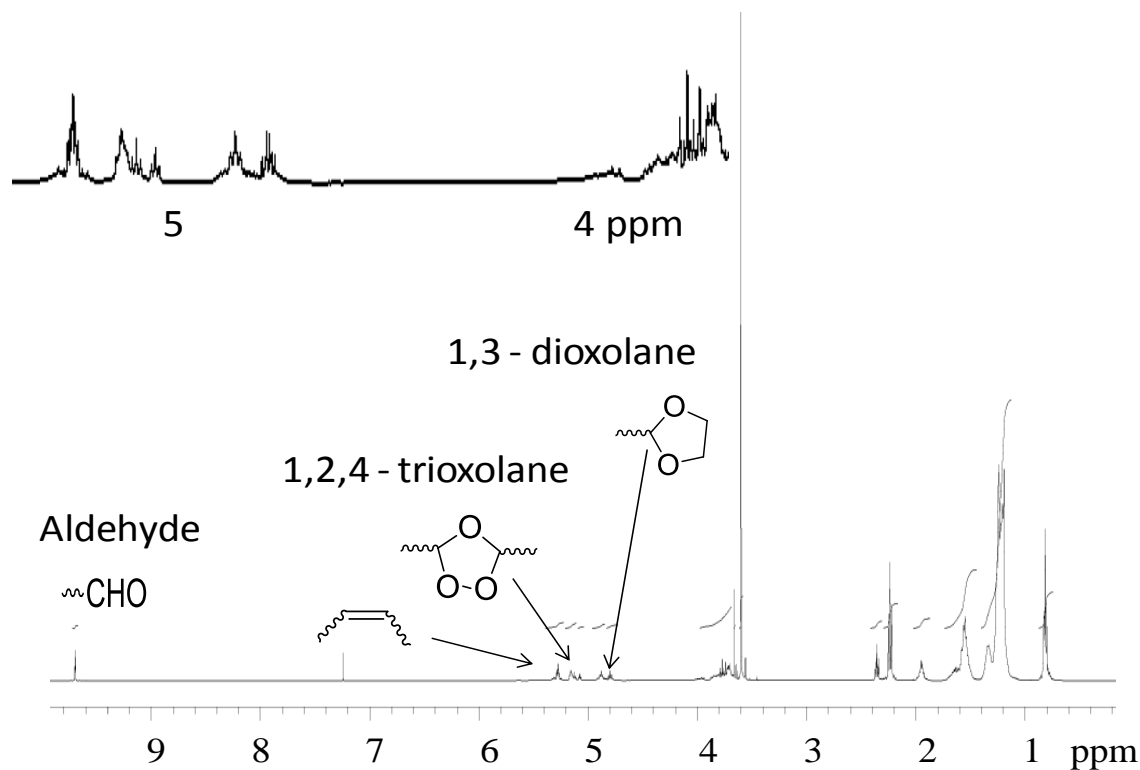


Figure 3.10 ^1H NMR of methyl oleate ozonated with EG with peak assignments; inset shows region between 4 – 5ppm

As seen from Figure 3.3, formation of the hydroperoxy ether or acetal requires that the alcohol be a good nucleophile, in order to attack the carbon of the carbonyl oxide. Also the proton of the carbonyl oxide needs to be either eliminated or abstracted by a base to take the oxidation to the ester stage. Since the base used in the reaction is a solid, the reaction might be limited to the surface. Thus the reaction is static at the acetal and ozonide stage without progressing.

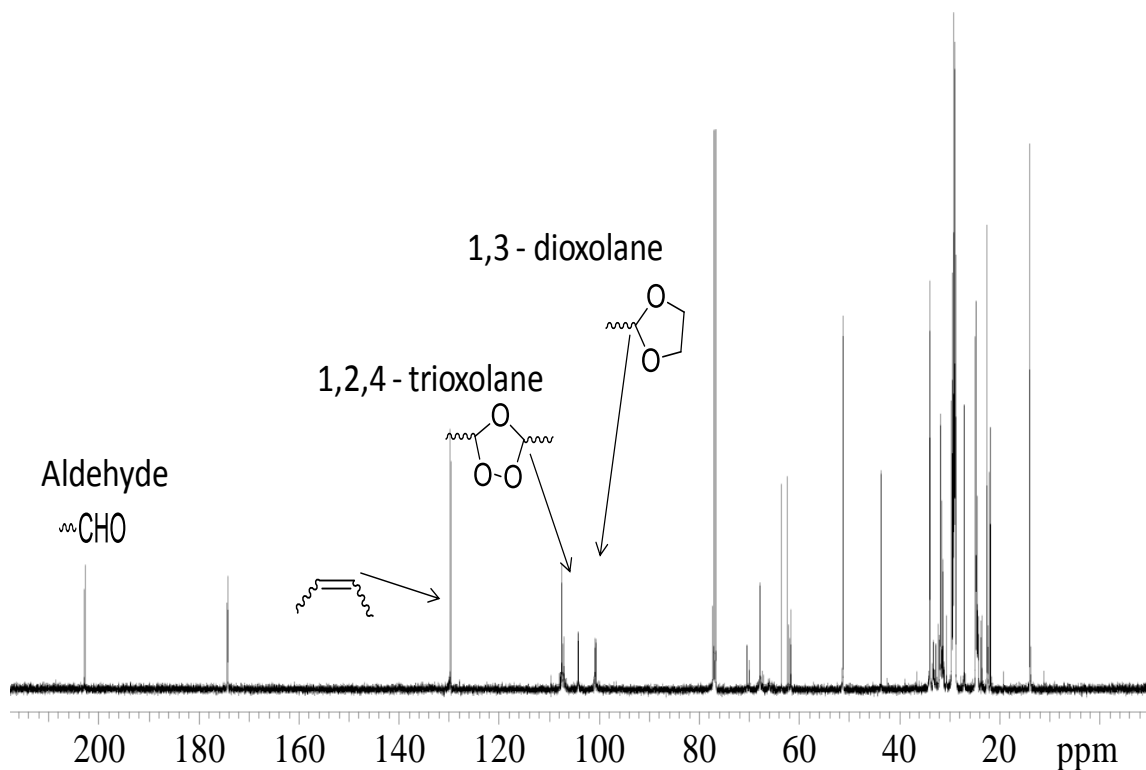


Figure 3.11 ^{13}C NMR of methyl oleate ozonated with EG with peak assignments

3.6.2 “Polyols” from soybean oil

The results from the titrimetric analysis are provided in Table 3.3. It can be seen that there is an 80% reduction in double bonds. It should also be noted that peroxides in the sample can positively interfere in iodine value estimation, by liberating iodine. Thus the double bonds would show up higher. As is seen from Table 3.3 the hydroxyl values are not very high and they are comparable to methyl oleate. Soybean oil has for the same mass, about 50% more double bonds than methyl oleate. Hence the values are

Table 3.3 Titrimetric results of ozonated samples of soybean oil. (Percent change in parentheses)

Attribute	Soybean oil (SO)	Ozonated with EG	Ozonated with glycerol
Acid Value (mg KOH/gm)	1	10	15
Hydroxyl value (mg KOH/gm)	1	185	180
Iodine value (gm/100gm)	132	22 (-84%)	30 (-78%)

expected to be higher. But this is not the case, implying the same problems as with methyl oleate. Also for soybean oil the theoretical triglyceride distribution is known. Hence the theoretical hydroxyl values can easily be derived. The values are listed in Table 3.4. The calculations are based on the distribution discussed in Chapter 2. From the calculations it can be seen the hydroxyl values to be 285 for ethylene glycol and 494 for glycerol. The actual value is much lower for glycerol, which indicates the conversion to ester is not happening.

The IR spectrum for the ethylene glycol sample is given in Figure 3.12. It can be seen that the features are similar to methyl oleate sample. The carbonyl group at 1750 cm^{-1} is broadened and the $\text{C}=\text{C}-\text{H}$ stretch at 3010 cm^{-1} is diminished. The $-\text{OH}$ peak

Table 3.4 Theoretical estimation of hydroxyl values for soybean oil polyols

Symbol	Mole Fraction	-OH	Contribution to functionality	Mass
NNN	0.29249	3	0.87747	214.69
NNP	0.03774	2	0.07548	28.61
NNS	0.02831	2	0.05662	22.25
NPS	0.00002	1	0.00002	0.02
PPN	0.00005	1	0.00005	0.04
PPP	0.00162	0	0	1.31
PPS	0.00001	0	0	0.01
SSN	0.00004	1	0.00004	0.03
SSP	0.00091	0	0	0.78
SSS	0.00243	0	0	2.14
EE	0.29818	2	0.59636	57.25
E1	0.07273	1	0.07273	14.69
E2	0.23273	1	0.23273	37.24
E3	0.03273	1	0.03273	3.86
1.00			1.944	382.9
Hydroxyl value for Ethylene glycol = 284.85 mg KOH/gm				
Hydroxyl value for Glycerol = 494.38 mg KOH/gm				

N – Nonanoate fragment (on triglyceride); P – Palmitate fragment; S – Stearate fragment

EE – Bis (2-hydroxyethyl) malonate; E1– (2-hydroxyethyl) nonanoate;

E2 – (2-hydroxyethyl) hexanoate; E3 – (2-hydroxyethyl) propionate;

These are fragments formed on complete ozonolysis of different fatty acid residues according to Figure 3.5, with the alcohol as ethylene glycol.

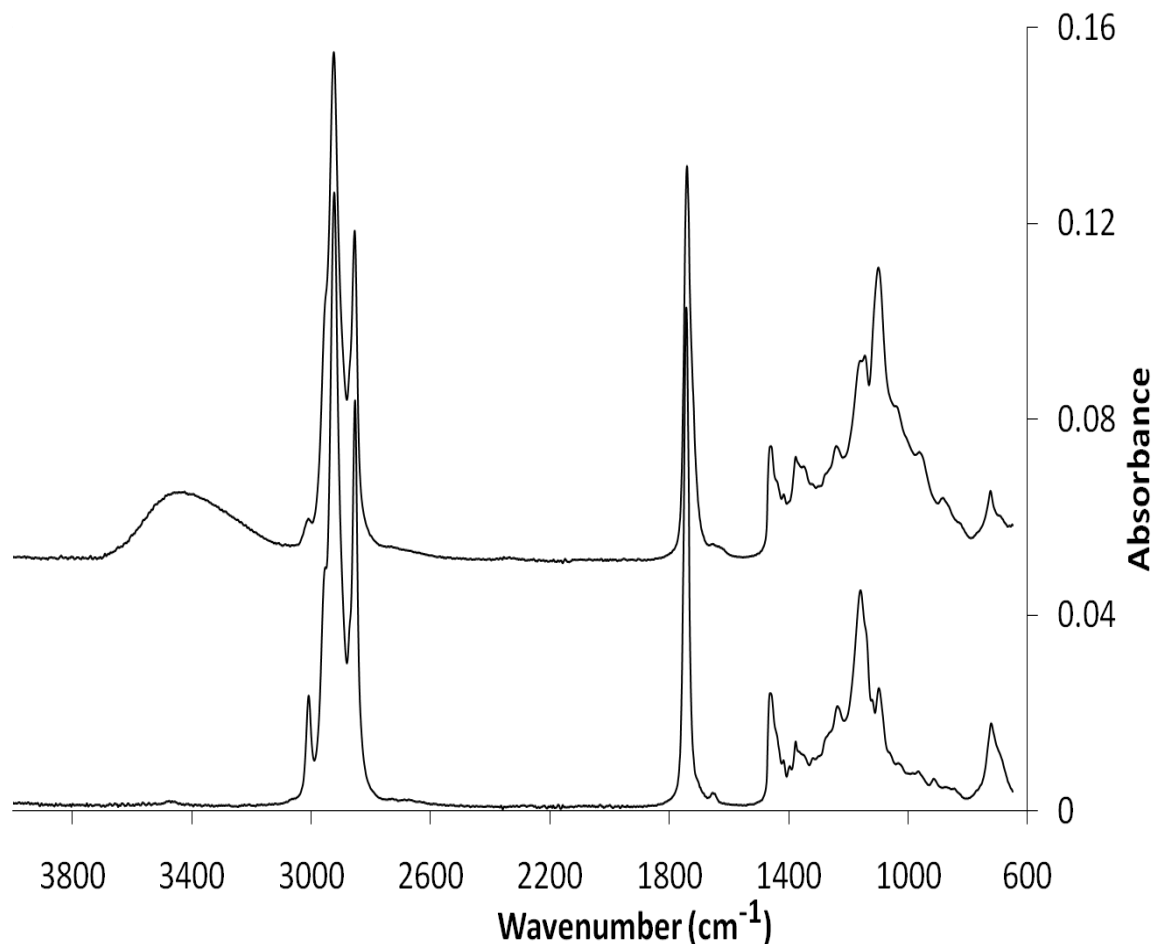


Figure 3.12 IR Spectrum of soybean oil ozonated with ethylene glycol (Top); pure soy oil (Bottom)

is also visible at 3500 cm^{-1} though it is not as intense, due to the reasons mentioned in the previous paragraph. One other reason for the reduced hydroxyl values for both methyl oleate and the soybean oil samples is the fact that water washing can also remove some of the lower molecular weight hydroxyesters. This is bound to happen more for the glycerol case, since the hydroxyesters will possess two – OH groups (one

reacts to form the ester) which will provide increased solubility in water. Thus using a short path distillation to remove excess unreacted alcohol might be a better option.

The NMR spectra for the soybean oil samples are given in Figures 3.13 – 3.16.

The integration results are also summarized in a table similar to the methyl oleate case.

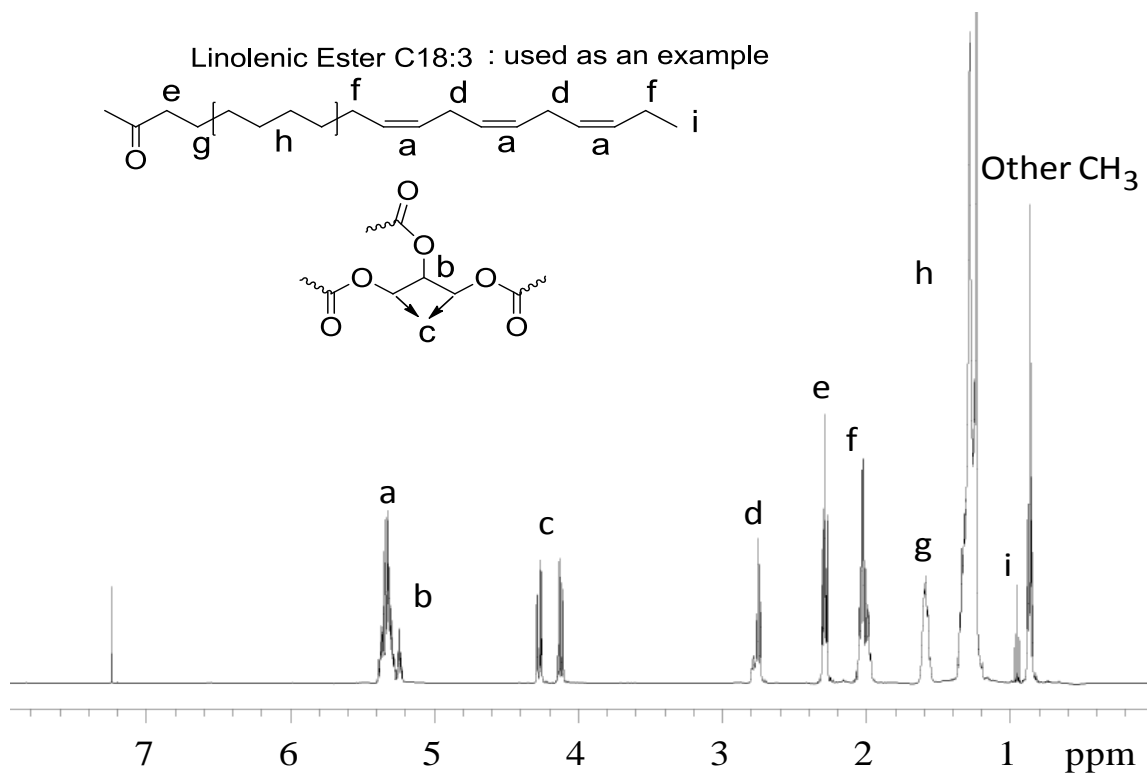


Figure 3.13 ^1H NMR spectrum of neat soybean oil with peak assignments

The peak ratios for the above spectrum are detailed in this paragraph. The total of peaks at 0.8 – 0.9 ppm is set to 9 to account for three – CH₃ groups of fatty acids. If this peak is used as a reference peak “r”, then a: r = 9.6: 9; b: r = 1: 9; c: r = 4: 9 or each peak is 2: 9; d: r = 4.6: 9; e: r = 6: 9; f: r = 9.7: 9 and g: r = 6: 9.

From the NMR spectrum of the ozonated sample, it can be seen that, in the case of soybean oil, even acetals are not formed in significant amounts. The only main component is the ozonide and aldehyde. In the case of soybean oil, the triglyceride structure probably leads to higher viscosity and thus lesser mixing with the alcohol. Also because of the branched nature of the triglyceride, formation of oligomeric peroxides or ozonides is probably facile. Thus the NMR confirms the results from titrations, that ozonolysis does not proceed to the ester stage.

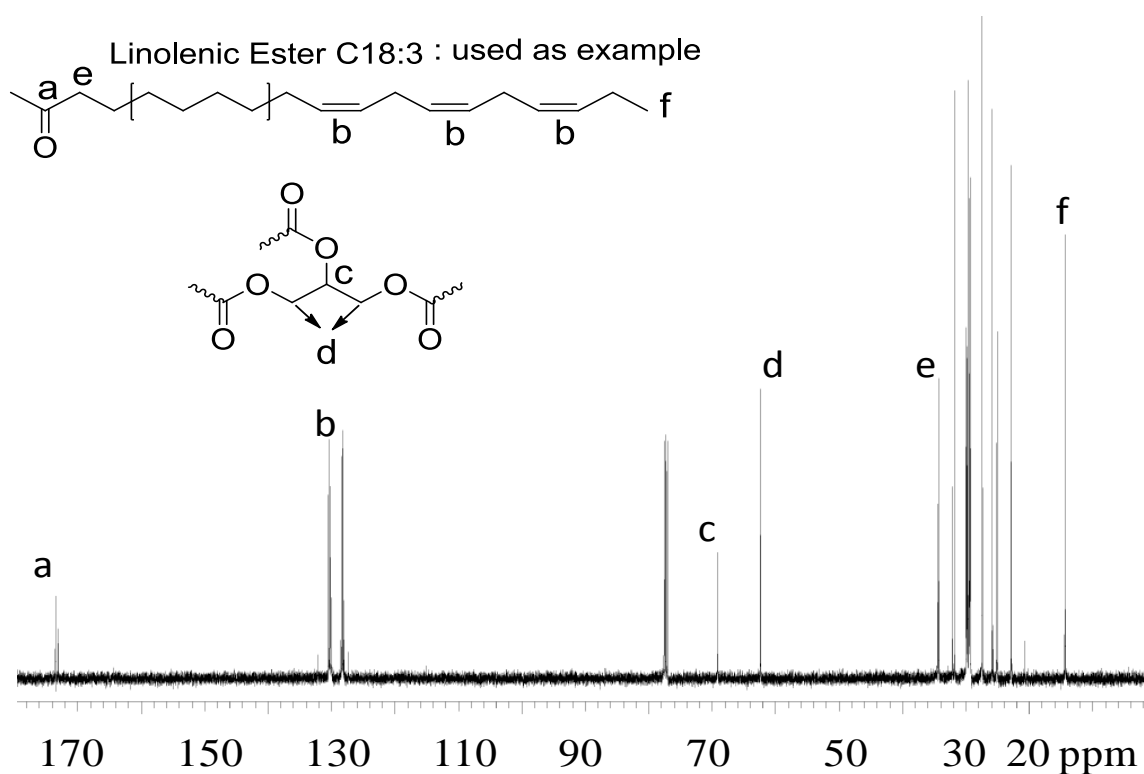
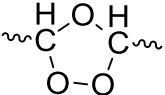
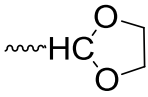
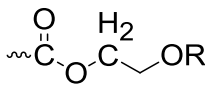
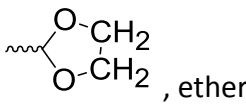
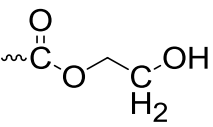
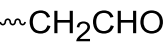
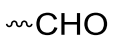


Figure 3.14 ^{13}C NMR spectrum of neat soybean oil with peak assignments

The carbon spectrum for the ozonated sample also shows the aldehyde carbon (aldehyde was not captured but is indirectly verified by peak at 44 ppm) and ozonides and acetals in the 100 – 110 ppm region. The alkoxy groups of esterified glycol, which

should appear at 64 ppm, are not present. This again confirms the results from the proton NMR and titrimetry.

Table 3.5 Integral ratios of functional groups (relative to CH₃ area =9) from NMR spectra; proton of interest is italicized. ¹³C shifts reported for carbon bearing proton of interest (Sample: soybean oil with ethylene glycol)

¹ H (ppm)	¹³ C (ppm)	Functional group	Soybean oil	Ozonated with EG
5.0 – 5.2	105		0	0.34
4.6 – 4.9	108	 , other ether	0	0.02
4.1 (R = H)	66		0	0
4.2 (R = COR ₂)	62	R = H, COR ₂	0	0
3.9	65	 , ether		
3.8	61		0	0.07
2.4	44		0	0.23
9.72	202.8		0	0.21

Note: Soybean oil has its glyceryl methylenic protons at 4.1 and 4.3. Thus the monoester can be difficult to estimate if present. But the diester with ethylene glycol should appear in between the peaks of the glyceryl protons. Also soybean oil can have protons downfield of 5.2 at 5.5 ppm – these would represent olefinic protons beta to ozonide. The glyceryl – CH appears at 5.2 ppm.

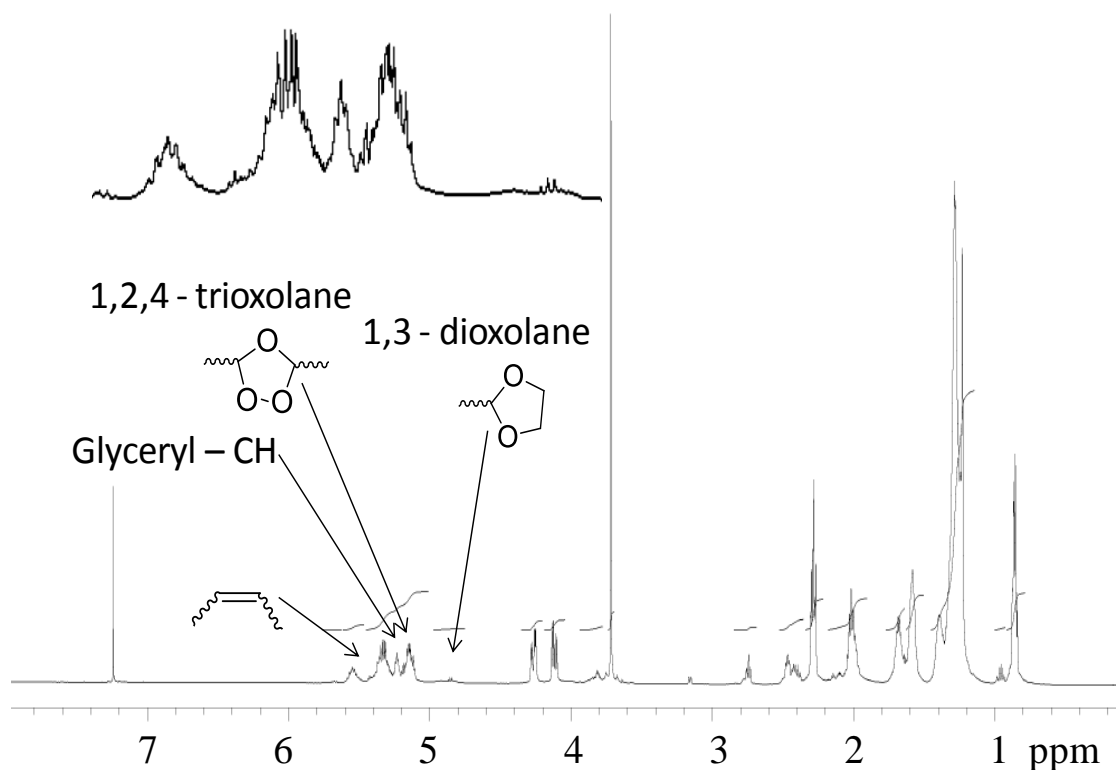


Figure 3.15 ^1H NMR spectrum of soybean oil ozonated with ethylene glycol with assignments; inset shows region from 4.7 – 5.6 ppm

Thus from the above experiments, it is seen that ozonolysis of a fatty ester with an immiscible co-reactant alcohol, always leads to the formation of a mixture of ozonides, aldehydes and acetals. This is not unexpected, since the direct esterification of the double bond has always been reported at low temperatures (-80°C to -25°C) and in the presence of non – participating solvents. The catalysts used have also been much stronger acids or bases (NaOH , HCl , H_2SO_4 etc.)

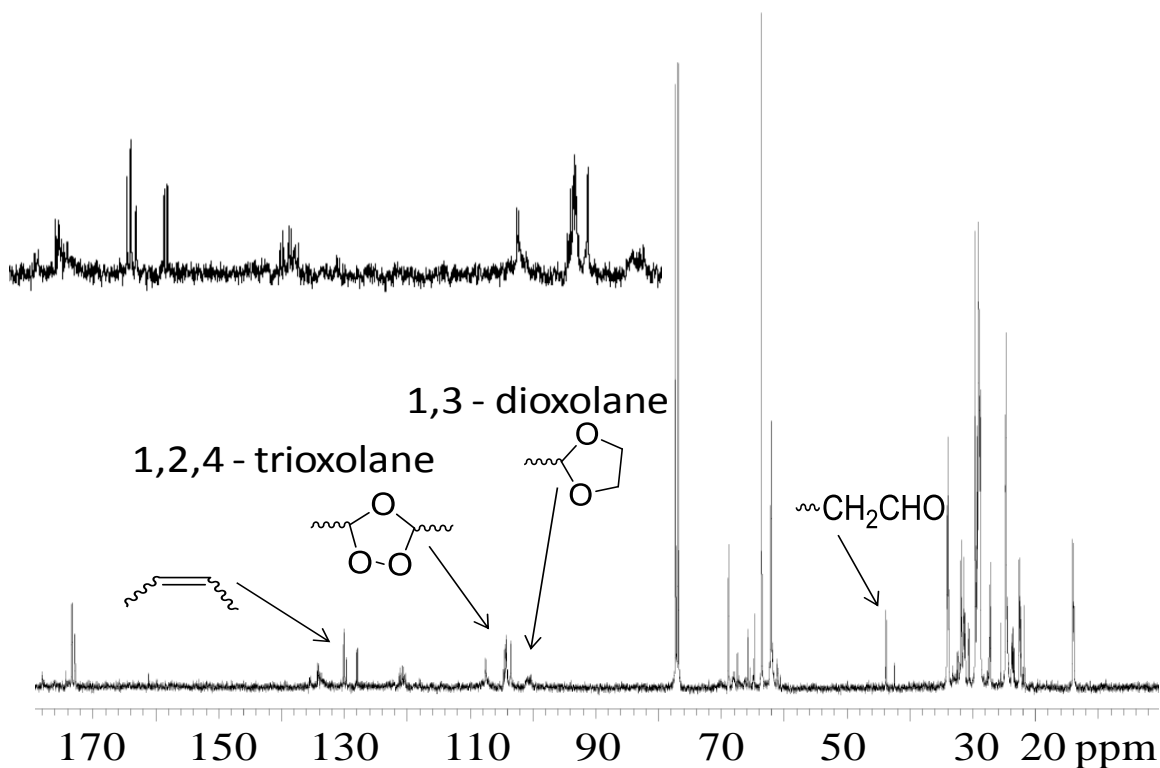


Figure 3.16 ^{13}C NMR spectrum of soybean oil ozonated with ethylene glycol; inset shows region from 100 – 134 ppm

3.6.3 Effect of excess alcohol and solvent

A single run was made with 50% molar excess of the alcohol over the stoichiometry. The samples did not show any significant difference from the regular samples of soybean oil with ethylene glycol. The acetals were formed in slightly higher amounts.

Since past work on ozonolysis was invariably done in solution, similar conditions were adopted for a trial run. Soybean oil and ethylene glycol were mixed with the catalyst as described earlier. The entire mixture (scaled down to about 50 gm) was dissolved in 250 ml of dichloromethane and the reaction run in an ice – water bath. Due

to the high flow rates of the gas, dichloromethane was evaporated (even with a condenser), so it was replenished from time to time. The resulting mixture was subjected to the same work up and the proton NMR is presented in Figure 3.17.

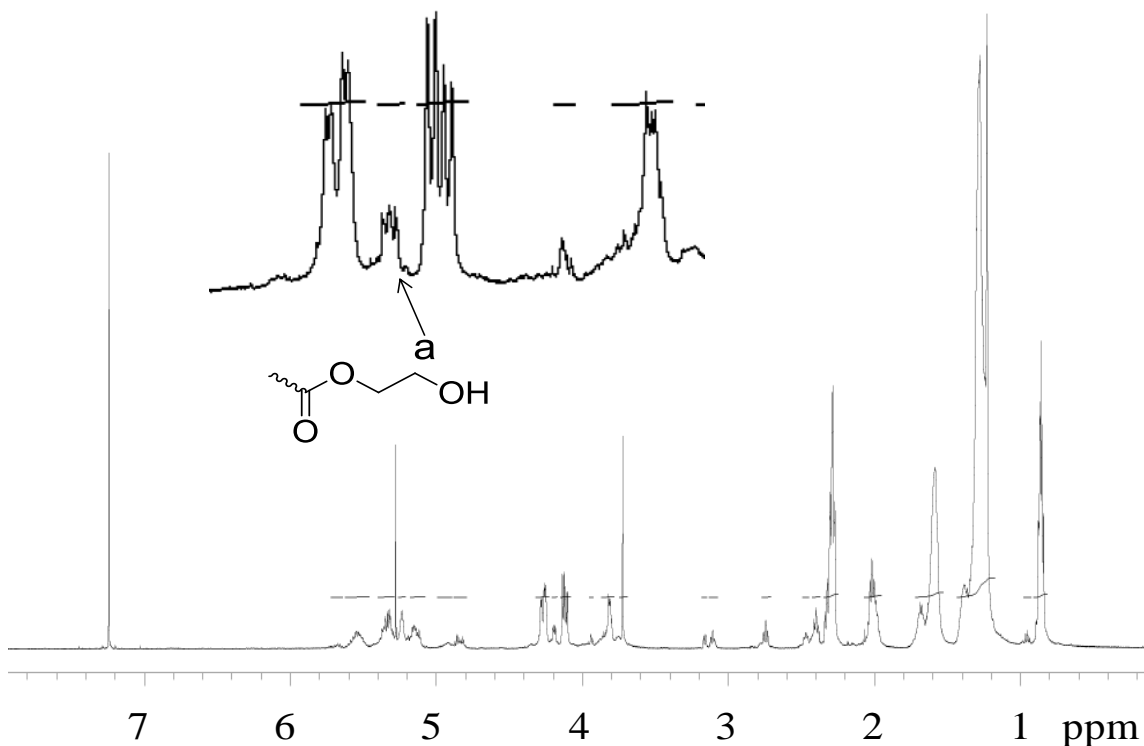


Figure 3.17 ^1H NMR spectrum of soybean oil ozonated with ethylene glycol in dichloromethane; inset shows region from 3.8 – 4.4 ppm

It can be seen that in this case, the double bonds have been reduced more and the amount of ozonides and aldehydes is reduced at the cost of increased formation of acetals. It is also seen that the peak labeled “a” corresponding to esterified ethylene glycol appears. Its ratio relative to the terminal methyl group was calculated as 0.66: 9. It should be noted the glyceryl protons at 4.1 and 4.3 together have a ratio of 4: 9. This implies that 15% by mole of glycol has been esterified.

From this it is clearly established that for the two phase ozonolysis of fatty acid methyl ester or vegetable oil in an immiscible alcohol, better miscibility is likely to provide increase yield of hydroxyesters and less of the undesirable ozonides or acetals.

3.7 CONCLUSION

Ozonolysis of model compound methyl oleate and soybean oil were conducted under conditions prescribed by earlier work. It was found that while double bonds were effectively cleaved in a reasonably short time with two alcohols (ethylene glycol and glycerol); the dominant products were the ozonides and acetals rather than the hydroxyesters. The reason for this is attributed to the intrinsic immiscibility of the two reactants, the weak nature of the base employed and the lack of any additional mixing other than the kinetic energy of the gas.

While hydroxyl values were obtained from the ozonated products, acid formation was also seen to happen though in relatively small amounts. The effect of solvent was examined and it was seen that solvent promotes not just the trapping of the Criegee intermediate but also leads to further oxidation to form the hydroxyesters, albeit not in high yields.

The merit of the present process is the bulk nature of ozonolysis without any solvent and a solid catalyst that is easy to separate. However, considering the product formation, the process would need to be modified to allow for better contact between

the two phases in order to minimize the formation of undesirable products. Also more alkaline catalysts like MgO (magnesium oxide) can be explored as alternatives to effect conversion to products.

REFERENCES

3.8 REFERENCES

1. Z. Petrovic , W. Zhang, I. Javni, *Biomacromolecules* **6**, 713 (2005).
2. R. Ackman, *Lipids* **12**, 293 (1977).
3. J. Sebedio, R. Ackman, *Canadian Journal of Chemistry* **56**, 2480 (1978).
4. J. Neumeister, H. Keul, M. Saxena, K. Griesbaum, *Angewandte Chemie International Edition in English* **17**, 939 (1978).
5. J. Marshall, A. Garofalo, *The Journal of Organic Chemistry* **58**, 3675 (1993).
6. J. Marshall, A. Garofalo, R. Sedrani, *Synlett* **1992**, 16 (1992).
7. B. Gruber, R. Hoefer, H. Kluth, A. Meffert, *Fett Wiss. Technol* **89**, 147 (1987).
8. J. A. Sherringham, A.J. Clark, B.R.T. Keene, *Lipid Technology* **12**, 129 (2000).
9. A. Heidbreder, R. Höfer, R. Grützmacher, A. Westfechtel, C. W. Blewett, *Lipid - Fett* **101**, 418 (1999).
10. A. Guo, I. Javni, Z. Petrovic, *Journal of Applied Polymer Science* **77**, 467 (2000).
11. J. Stanton, *Journal of the American Oil Chemists' Society* **36**, 503 (1959).
12. H. Benecke, B. Vijayendran, D. Garbark, K. Mitchell, *CLEAN-Soil, Air, Water* **36**, 694 (2008).
13. P. Tran, D. Graiver, R. Narayan, *Journal of the American Oil Chemists' Society* **82**, 653 (2005).
14. P. S. Bailey, *Ozonation in Organic Chemistry*. (Academic Press, New York, 1978), vol. I.

15. N. U. Soriano, V. P. Migo, M. Matsumura, *Chemistry and Physics of Lipids* **126**, 133 (2003).
16. O. Ledea *et al.*, *Revista CENIC Ciencias Quimicas* **34**, (2003).
17. J. N. U. Soriano, V. P. Migo, M. Matsumura, *Fuel* **85**, 25 (2006).
18. L. Rebrovic, *Journal of the American Oil Chemists' Society* **69**, 159 (1992).
19. R. Criegee, H. Korber, *Adv. Chem. Ser* **112**, 22 (1972).
20. T. M. Baber, PhD Thesis, Michigan State University (2005).
21. P. T. Tran, PhD Thesis, Michigan State University (2005).
22. G. Knothe, J. A. Kenar, *European Journal of Lipid Science and Technology* **106**, 88 (2004).
23. M. Guillén, A. Ruiz, *European Journal of Lipid Science and Technology* **105**, 688 (2003).
24. L. Mannina, C. Luchinat, M. Emanuele, A. Segre, *Chemistry and Physics of Lipids* **103**, 47 (1999).
25. M. Wu, D. Church, T. Mahier, S. Barker, W. Pryor, *Lipids* **27**, 129 (1992).

CHAPTER 4

SYNTHESIS OF SOYBEAN OIL BASED UNSATURATED POLYESTER RESINS

ABSTRACT

Three different “polyols” were synthesized from soybean oil and ethylene glycol, using an Ozonolytic process described in Chapter 3. The “polyols” were synthesized by varying the time of ozonolysis from 2 min. / gm of oil to 3 and 4 min. /gm of oil. It was seen that increasing the time of ozonolysis gave rise to increasing acid values for the polyols. At 4 min. / gm, the acid value was nearly equal to the hydroxyl value. As discussed in the previous chapter, even though these are not true polyols, in the sense that they are mixtures of ozonides, acetals etc.; the hydroxyl value, which is determined by reacting with an acid anhydride shows, that these were capable of reacting like alcohols.

Thus to test the properties of unsaturated polyester resins made from such materials, these polyols were employed at 10%, 50% and 90% of the total diol content of a polyester resin formulation with maleic anhydride and ethylene glycol. The polymerization was conducted in two stages. At the end of the polymerizations, pale yellow to reddish brown resins with good viscosity were obtained. With increasing

“polyol” content, the resins exhibit lesser solubility in toluene and also start cross – linking after being cooled down.

Good gel contents up to 45% were obtained by using 90% of polyol in the formulation. The resins generally exhibited glass transitions between -5 °C and -20 °C and were malleable. However, shear viscosity could be determined only for the 10% polyol resins and rheometry on higher polyol content resins was impossible due to the inability to mold the resins to bubble free disks required for such analysis.

4.1 INTRODUCTION

Vegetable oils have long been used in the synthesis and formulation of alkyd resins for coating applications. Alkyd resins are the earliest examples of unsaturated polyester resins. However in alkyd resins, the fatty acid portion of the oil serves little purpose as the unsaturation in the acid is usually slow to cure and often causes yellowing during the service life of the resin. In fact the major useful component in alkyd resins is the glyceryl backbone of the oil which is reacted with anhydrides to form the polyester resin with the fatty acid chains serving as dangling ends with unsaturations that can be cross – linked. In this work we propose a new strategy for incorporating bio – based content in such unsaturated polyester resin systems, by use of soybean oil based polyols, in a synthetic scheme with maleic anhydride as the anhydride species and ethylene glycol as the second polyol. While patents outline the addition of soybean oil up to 35 wt% in such resin formulations, we believe our proposed strategy could lead to higher incorporation (> 50 wt% of bio – based content) of oil based polyols in such systems.

4.2 SYNTHESIS OF SOYBEAN OIL BASED POLYOLS

Soybean oil based polyols (Refer to Chapter 3 for materials and procedure) were synthesized using novel ozone based chemistry. The Lowsat oil is reacted with an excess of ethylene glycol (50% molar excess) in the presence of ozone, with CaCO_3 (10 wt% of

the oil) and NaOH (0.2 wt% of the oil) serving as catalysts. Typical ozonolysis times employed were 2, 3 and 4 minutes per gram of the oil used. The polyols were then separated using centrifugation from the catalyst and excess alcohol and then characterized for their acid and hydroxyl values. The values are summarized below.

Table 4.1 Acid and Hydroxyl values of polyols synthesized with varying ozonolysis time

Polyol	Alcohol	Acid Value		Hydroxyl Value	
		Theoretical	Actual	Theoretical	Actual
SPEG-2	EG	0	7.5	284.85	75
SPEG-3	EG	0	92	284.85	110
SPEG-4	EG	0	105	284.85	135

4.3 SYNTHESIS OF RESINS

For the unsaturated polyester resins, three different formulations were identified for each polyol synthesized using different ozonolysis times. The soybean oil based polyols were used in 10 %, 50 % and 90 % by weight of the total alcohol content in the resin system. Such a formulation results in the soy polyol being incorporated in the resin from ~5 wt% (in the case of 10 wt %) to 28 wt% (in the case of 50 wt% polyol) and more than 50 wt % (in the case of 90 wt%).

The resin synthesis was performed in two stages. In the first stage the soy polyol was reacted with all the maleic anhydride required for the polyester synthesis at 70 °C

for 3 hours. The resultant product was then characterized for its acid value and iodine value according to ASTM standards (D1980 and D1959 respectively). Since acid values do not accurately measure maleic anhydride content and measures only the free acid in the system, the iodine numbers were used to decide the amount of ethylene glycol needed to neutralize the anhydride in the second stage.

The second stage of the synthesis was done with the product from stage 1 and ethylene glycol. The reaction was carried out at temperatures of 175 °C – 180 °C for 2 hours. All synthesis was done under a blanket of nitrogen and the water of the reaction was collected using a Dean – Stark trap.

It was observed that the resins tend to become dark during the second stage of the synthesis. In particular, the reaction mixture assumes a dark brown color upon heating which is discharged to produce a dark yellow to reddish yellow final product. This is seen to occur at temperature of 145 °C – 165 °C. The lower soy polyol content resin (10 wt %) is liquid at room temperature while the 50 wt% resins are semi solid at room temperature. Also the lower polyol content resins are much lighter in color than the higher soy polyol content resins.

4.4 CHARACTERIZATION

Acid, hydroxyl and iodine values were determined according to ASTM standards D1980, D1957 and D1959 respectively. Gel contents were determined by weighing

around 1 gm of the resin sample into filter paper pouches. The resins were then extracted with dichloromethane for 24 hours in a Soxhlet extractor and then dried to a constant weight at 60 °C to determine the gel content.

Differential scanning calorimetry (DSC) was run on the samples using a DSC 2920 from TA Instruments. The experiment was conducted in an inert atmosphere of nitrogen with the nitrogen flow rate at 50 ml/min. The sample was quickly heated to 200 °C at heating rate of 20 °C/min to erase thermal history. It was cooled to -50 °C at 3 °C /min and heated back at the same rate to 200 °C. Thermogravimetric analysis (TGA) was conducted using a high resolution Thermal Gravimetric Analyzer (TGA) 2950 from TA Instruments to determine the degradation temperature.

Viscosity measurements were conducted using a Brookfield Digital viscometer (Model. HBDV II) equipped with a Thermosel arrangement. A small sample holder was used with an SC – 27 spindle.

4.5 RESULTS AND DISCUSSION

The exact structure or the functionality of the ozonated materials was not known in this case. Thus synthesis was done by matching the hydroxyl values of the sample to the theoretical acid value of maleic anhydride. Similarly after the first stage, iodine and matched to the amount of MA present in the system and thus to the ethylene glycol required for the second stage of the polymerization.

Overall goal of this exercise was to see if such ozonated products could be directly used in resin synthesis. It should be noted, that ozonated products in general should not be handled without adequate care. In this care all the precautions were taken, and sample sizes were kept very small. Also prior to polymerization, all the “polyols” were separately heated to 120 °C in small vials and temperature was measured to determine if any exotherm resulted due to decomposition of peroxygenic species.

All the three polyols used in this study, polymerize well to yield viscous resinous material. At lower concentrations, the material is pliable and at higher concentrations it was found that the resins tend to get harder and rubber like with time. The final acid and hydroxyl values for the resins are tabulated in Table 4.2. For higher polyol content resins, insolubility in toluene necessitated warming of the solution and addition of carbon tetrachloride to dissolve the resin.

The 10 wt% polyol batches all lead to pale yellow resins with good viscosity and solubility in toluene. This indirectly indicates good miscibility with styrene, which is a typical reactive diluent used in UPRs. The 50 wt% batches however dissolve only after heating in toluene, which implies that they are going to dissolve in styrene only after refluxing for a while. The 50 wt% resins are also darker as compared to the 10 wt% ones. A chemical change occurs during the second stage of heating – because there is a classic discoloration of the dark brown resin to a translucent reddish yellow resin.

The 50 wt% polyol batches – give an impression that they are gels. However they are liquid at 165 °C when poured out of the reaction vessel but become gel like when cold. One of the reasons could be a transesterification of the glyceryl backbone with ethylene glycol in the latter stages of the reaction that leads to release of the latent trifunctional glycerol which can lead to gellation. Also peroxide residues in the polyol, can promote cross – linking of the MA residues on the backbone leading to gellation.

Table 4.2 Hydroxyl and Acid values of resins obtained from soy polyols

Entry	Ozonolysis time ^a (min./gm)	Percent used in resin ^b	Acid value (mg KOH/gm)	Hydroxyl value (mg KOH/gm)
1	2	10	94	115
2	2	50	85	110
3	2	90	75	95
4	3	10	93	102
5	3	50	82	109
6	3	90	72	93
7	4	10	95	102
8	4	50	87	105
9	4	90	79	91

a – Time of ozonolysis (refer to Table 4.1)

b – Percent used in the total alcohol content (glycol + polyol)

The acid and hydroxyl values are on the higher side. Typical UPR formulations require resins with acid and hydroxyl values in the range of 50 mg/gm. The reason for the higher acid and hydroxyl values (almost as high as the polyol), is probably the lack of

reaction between MA and polyol in the first stage and with ethylene glycol in the second stage. The partially reacted MA and EG could contribute to these high numbers

Secondly it could also mean that the polymer formed is a highly branched structure, with many acid and hydroxyl groups pendant, which could give rise to the high values. It is difficult to explain the high viscosity of the resins in the absence of any reaction between the MA and the polyol or EG. Thus the polymerization probably leads to highly branched structures.

The peak degradation temperature and gel content of the resins along with the shear viscosity are provided in Table 4.3. The glass transition temperatures for these resins are below zero; the transitions are not very noticeable and hence have not been reported. The resins are likely to be rubbery gel like at room temperature with increasing polyol content. No crystallization was observed indicating a random polyester formation.

The degradation temperature (maximum derivative weight loss), is indicative of the effect of ozonolysis. As can be seen from the viscosity, the highest ozonation time produces the highest shear viscosity. It also has the lowest degradation temperatures and gel content. The reason for this could be excessive fragmentation of the fatty acid chain on prolonged exposure to ozone. This is likely to create small fragments, which

Table 4.3 Properties of resins based on soy polyol

Entry	T _d (°C)	Viscosity (cPs) @ 70° C, 0.1 s ⁻¹	Gel content (%)
1	443	1800	<1
2	437	-	26
3	445	-	38
4	445	2000	~1
5	446	-	35
6	448	-	45
7	439	2500	~1
8	418	-	11
9	456	-	16

would decompose at lower temperatures, thereby reducing the degradation temperatures. This would also explain the lower gel content for the 4 min. / gm samples. It can be seen that at 10% all the samples have negligible gel content. The highest gel content is for the 3 min. / gm sample, which would be explained by the optimum number of functional groups generated. This polyol has a good hydroxyl and acid value and is probably not too fragmented.

The gravimetric analysis shows the importance of polyol structure as opposed to the polyol content in the polyester resins. The higher ozonolysis times, give polyols of higher functionality and shorter chain lengths. Thus the degradation temperatures are lower for the higher ozonolysis times. Longer ozonolysis times lead to greater fragmentation of the soybean oil, thus creating acid groups and also mono functional groups. These can effectively reduce the overall functionality of the polyol and can cause loose ends to be present in the resin.

4.6 CONCLUSIONS

Three different polyols were synthesized by varying the ozonolysis time. They were successfully used at different weight percentages in formulating a very simple unsaturated polyester resin system. The polyols gave resins of good viscosity at all proportions. However, cross – linking is observed even at ambient conditions in the resins at higher polyol loading.

This has been attributed to the cross – linking from peroxide residues on the polyols. It is also known, that maleic anhydride containing resins, tend to photopolymerize to a certain extent and that could explain the cross – linking also. The resins have high degradation temperatures, owing to their cross – linked structure and also due to the stable nature of the fatty acids at relatively high temperatures.

The simple study proves that even partially ozonated derivatives of soybean oil and ethylene glycol can participate in polymerization and give resins with good gel contents; however, the control on gellation is poor, limiting the applications of such a system.

CHAPTER 5

SYNTHESIS OF 2-HYDROXYETHYL ESTERS FROM METHYL OLEATE VIA OZONOLYSIS

ABSTRACT

2- hydroxyethyl esters were obtained in good yields via a two step procedure from methyl oleate. Firstly methyl oleate was transesterified with a 20 fold excess of ethylene glycol, using dibutyltin dilaurate (DBTDL) as a catalyst. The procedure yields a mixture of 2 – hydroxyethyl oleate (63%) and 1, 2 – ethanediyl oleate (31%) in molar quantities. To this mixture sodium hydroxide was added as a catalyst for ozonolysis. The mixture was ozonated to yield the corresponding hydroxyesters, aldehydes and their acetals with ethylene glycol. The consumption of double bonds was nearly 90%. The reaction was monitored by measuring the ozone concentration at the outlet. The acetals and aldehydes were subsequently converted to the hydroxyesters by treating with OxoneTM at a temperature of 50 °C for a period of 72 hours. The process yields 2-hydroxyethyl esters in high yields and selectivity. Infrared spectroscopy, nuclear magnetic resonance and titrimetry (hydroxyl values, acid values and iodine values) were employed to characterize the products at each step. It was seen that the hydroxyl values of the samples increased significantly after Oxone treatment and NMR revealed that

aldehydes and acetals formed after ozonolysis had been almost completely converted to the hydroxy esters. The procedure was repeated with methyl oleate as the starting material without any transesterification and similar results were obtained and hydroxy esters were formed after the Oxone treatment.

5.1 INTRODUCTION

Chemical modifications of vegetable oils are essential to produce value-added chemicals from biobased feedstock. One such example is the preparation of polyols from vegetable oils that can be used instead of petroleum-based polyols in polyurethanes and polyesters (1-2). Methyl oleate (cis-9-octadecenoic methyl ester) has been used as a model compound for studying various reaction schemes of fatty acids, lipids and their derivatives including their reactions with ozone. These model compounds were used in studying the effects of ozone in different disciplines varying from reaction of organic aerosols in the atmosphere (3) to pour point depression in biodiesel (4).

Methyl oleate and oleic acid were chosen as model compounds in the ozonation studies instead of triglycerides and other fats as these monounsaturated species are susceptible to oxidation through addition of oxygen to the double bonds as other more complex fatty acids, yet, they provide a simpler system to determine the reaction pathways, possible intermediates and the reaction products. It is not surprising that in all cases, the initial attack of ozone is directed toward the double bond. However, the reaction pathway and the reaction products depend on the temperature and other conditions.

The ozonolysis reaction pathway is different when protic solvents (e.g. alcohols, water, acids) are used. In this case the Criegee intermediates can react with the solvent more efficiently than undergoing 1, 3-dipolar cycloaddition with the carbonyl containing

product that is formed from the decomposition of the primary ozonides. As a result, this route leads to the formation hydroperoxides as the major products (5).

The fate of the carbonyl oxides, which are formed in the ozonolysis of alkenes by cycloreversion of the primary ozonides, determines the distribution of the reaction products. When the carbonyl oxides are trapped by unhindered alcohols (6) and other related nucleophiles generates hydroperoxyacetals and similar addition products (7). When neither addition nor cycloaddition pathways are available, the carbonyl oxides undergo dimerization or oligomerization to yield 1, 2, 4, 5-tetraoxanes or polymeric peroxides (8). It has been reported that ozonolysis of olefins with alcohols (typically primary monohydric alcohols) under acid or base catalysis yields directly the corresponding alkyl esters of the carboxylic acids (9-12). While the acid and base catalysis have been reported to work for polyhydric alcohols also (13-14) recently, the product contains significant amount of acetals in the case of the acid catalysis. Further, the acid catalysis employs solvent which has implications for large scale production. It should also be emphasized that ozonolysis in bulk has rarely been employed for synthesis of bulk chemicals, and even in those cases, temperatures used have been low. It is our intent to employ this facile oxidation route in bulk and at room temperature to synthesize polyols from vegetable oils or their derivatives.

While ozone itself would act as a benign oxidant for the double bond (ozone is intrinsically toxic by inhalation, but the byproduct of ozonolysis is oxygen), the acetals and/or aldehydes, can be oxidized to their corresponding esters by using Oxone. Oxone

is a potassium monopersulfate compound, and has been shown to be a benign oxidant (15), with non – toxic byproducts (potassium bisulfate) for the oxidation of aldehydes to their alkyl esters in the presence of monohydric alcohols. It has been proposed (15) that oxidation by Oxone proceeds via a Baeyer – Villiger scheme. There is reason to believe this oxidation by Oxone can be extended to cover polyhydric alcohols also. This basically would then open up a route for synthesis of polyols from vegetable oils, employing a two step procedure of ozonolysis, followed by Oxone oxidation to yield hydroxy esters (polyols).

It should be noted that, the Ozonolytic procedures outlined above, typically are run at low temperatures (-70 °C to 0 °C) and also employ a solvent at some stage of the product formation. Here in we propose a method, unlike conventional ozonolysis is, run close to room temperature and with no additional solvents. This method offers several advantages over the procedures outlined above. The reaction of ozone is spontaneous with double bonds, leading to a rapid primary oxidation to a mixture of products. The process is run in an excess of the participating alcohol (1:20 mole ratio per double bond), thus eliminating the need for solvents. This also effectively traps the reactive intermediates and offers stability in terms of dissipating the exothermic nature of the oxidation.

The second stage oxidation is slower and converts the said mixture of products with good selectivity to hydroxyesters and diesters. The catalyst is a solid and the byproduct of the oxidation is potassium bisulfate (KHSO_4) which can be easily filtered

off and presents no toxicity problems unlike transition metals used in hydroformylation or hydrogenation or in other oxidation chemistry involving transition metal oxides (KMnO_4 , OsO_4 , V_2O_5 etc.). Due to the rapid nature of ozonolysis, the first stage oxidation is amenable to operation in continuous mode and the second stage oxidation can be deployed in batch mode.

The hydroxyesters obtained were typically immiscible in the bulk glycol and can separate as a distinct physical layer. Thus recycling of the alcohol can be done, without the need for an expensive distillation step. Thus this process is novel, although it employs a two stage process to obtain the hydroxyesters like some of the procedures outlined above. However, the absence of any solvent in the entire process is a key advantage of this process. We believe the same procedure can be extended to soybean oil or other vegetable oils, due to the similarity in reactivity of other fatty acids (in addition to oleate) which constitute these oils.

5.2 MATERIALS

Methyl oleate [CAS 112-62-9, 70%] was procured from Sigma Aldrich (St.Louis, Missouri) and used as received. Ethylene glycol [CAS 107-21-1, 99%] reagent grade, sodium hydroxide, dibutyltin dilaurate [CAS 77-58-7, 95%] were procured from Sigma Aldrich and used as received. Oxone [70693-62-8] was obtained from Sigma Aldrich. The

salt contains 47% by weight of potassium monopersulfate (KHSO_5) and it was used as received. Deuterated chloroform (CDCl_3) for NMR spectroscopy was obtained from Cambridge Isotope laboratories and used as received.

Ozone was produced by passing oxygen gas at a flow rate of 0.2 scfm (standard cu.ft/min.)/ 5.6 liter/min. through a TS-60 model ozone generator from Ozone solutions Inc. (Hull, Iowa). Ozone concentrations (in weight percent) were measured using a Mini Hi-con ozone analyzer from InUSA Corp. (Norwood, MA).

Mass Spectra were recorded using a HP 5890 Series II gas chromatograph coupled to a 5972 series Mass Selective Detector. Samples were ionized using EI mode at 70 eV. The column employed was an Agilent DB-5MS column (30 X 0.25 mm) with a film thickness of 0.25 μm .

NMR spectra were recorded on Varian Unity plus spectrometer operating at 500 MHz. The solvent used was CDCl_3 (^1H @ 7.24 ppm, ^{13}C @ 77 ppm). Standard parameters were used in acquisition except in carbon spectra where a d1 of 2 seconds was employed. Infra red spectra were recorded on a Perkin Elmer Spectrum One spectrometer with a diamond top ATR fixture. A minimum of 4 scans were acquired for each sample with a resolution of 4 cm^{-1} . Hydroxyl values, Acid values and Iodine values of the samples were determined in accordance with ASTM D1957, D1980 and D1959 respectively.

5.3 EXPERIMENTAL

5.3.1 Synthesis of 2-hydroxyethyl oleate

Methyl oleate (250 gm) was mixed with 2.5 gm of DBTDL and ethylene glycol (1054 gm) in a 2L flask fitted with a mechanical stirrer. The mixture was heated to 135 °C for a period of 4.5 hours and the distillate containing methanol was collected using a mild vacuum. About 23 ml of distillate was collected. The mixture was allowed to cool to room temperature. Phase separation occurred upon standing and the top layer consisting of the product was sampled. The sample was gently washed 4 – 5 times with distilled water to remove any excess glycol and the sample was dried over molecular sieves prior to analyses. It is worth noting that phase separation occurs only upon standing for long periods of time and a turbid solution is obtained by mechanical agitation. For NMR spectroscopy the samples were centrifuged to perform a density separation of ethylene glycol and used.

5.3.2 Ozonolysis of 2-hydroxyethyl oleate

The reaction mixture from the transesterification reaction, was mixed with sodium hydroxide (1wt% of the oleate), till the sodium hydroxide was completely dissolved in the glycol phase. The contents of the flask were cooled in an ice bath and a mixture of ozone and oxygen (4.7% - 5% by weight ozone) was introduced into the mixture at a flow rate of 5.6 LPM. The ozone exiting the reaction was monitored through the ozone analyzer and the reaction mixture was kept agitated using a

mechanical stirrer. The ozone flow was stopped when the ozone at the outlet reached a steady value close to the inlet concentration. Care was taken to ensure that the reaction mixture was always at a temperature of 15 °C to 21 °C.

The reaction mixture was allowed to warm up to room temperature. Two distinct phases are formed (pale yellow translucent top layer and transparent colorless bottom layer). The top layer containing the products was carefully sampled. The sample was washed 4 – 5 times with distilled water and dried over molecular sieves prior to analysis. For NMR spectroscopy samples were centrifuged as in the previous case.

A similar procedure was employed for methyl oleate also and the reaction conditions were maintained the same.

5.3.3 OxoneTM treatment

The products from the ozonolysis were reacted with 2 equivalents of Oxone. Oxone (powder form) was mixed well with the product mixture using a mechanical stirrer, till slurry of Oxone resulted. This mixture was allowed to warm up to a temperature of 50 °C and maintained at that temperature for a period of 72 hours. The system was isolated from atmospheric air to prevent any oxidation of products to carboxylic acids. After the set time period, the mixture was allowed to cool to room temperature.

Two distinct phases resulted (translucent top layer and transparent bottom layer) and the top layer was again carefully sampled out and water washed 4 -5 times

with distilled water and dried over molecular sieves prior to analysis. As in the above cases samples for NMR spectroscopy were obtained by centrifugation. In all the cases, the bottom layer was found to contain predominantly unreacted ethylene glycol and thus was not characterized further.

5.4 RESULTS AND DISCUSSION

5.4.1 Transesterification

The methyl oleate used in the experiments was 70% pure and in order to determine the composition of the sample, the starting material was subjected to a GC analysis. The percent composition of the starting methyl oleate (MO) is given in Table 5.1. The Linoleic acid content of ~9% from GC is also confirmed from NMR spectroscopy (~10%). Thus the sample approximately has 1 double bond/mole. Thus two carbonyl groups on average are expected to be formed after ozonolysis.

Thus transesterification of the starting methyl oleate with ethylene glycol (EG) would lead to a mixture of 2-hydroxyethyl esters of the above fatty acids. Also the formation of 1, 2 – ethanediyl diacylates cannot be ruled out (Figure 5.2). The H-NMR spectrum of the transesterified product is shown in Figure 5.1. The assignments for the fatty acid have been made from reported literature (16-17) and esters from known chemical shifts of glycol esters. From the spectrum it can be clearly seen that both the

mono (*t*, 4.15 ppm) and diester (*s*, 4.2 ppm) of ethylene glycol are formed. The relative area of the two peaks gives the quantity of these two esters to be 63% and 31% by mole respectively. Further confirmation of the transesterification is obtained from titrimetry (Table 5.2). The hydroxyl values give an indication of the transesterification. The hydroxyl values obtained for the product (83 mg KOH/gm) is half of what would be expected (~172 mg KOH/gm). This is supportive of the NMR data that significant diesterification of ethylene glycol occurs.

Table 5.1 Fatty acid composition of methyl oleate^{*}

Fatty Acid	Carbon	Weight %	FAME (Mol. Wt)
Myristic	14:0	2.83	242.38
Palmitic	16:0	4.37	270.43
Palmitoleic	16:1	4.64	268.42
Heptadecenoic	17:1	1.1	282.45
Stearic	18:0	0.86	298.49
Oleic	18:1	69.96	296.47
Linoleic	18:2	8.85	294.46
Other	-	7.39	-

* - samples analyzed on a Varian 3900 GC equipped with a WCOT fused silica column (100m X 0.25 mm) with a CP-Sil 88 (CP7489) coating. Injection temperature of 250 °C and isothermal run at 180 °C was used. An FID detector was employed at a flow rate of 1 mL/min.

The formation of 2-hydroxyethyl esters was also confirmed from mass spectrometry. Unreacted methyl oleate was also present, which indicates the transesterification to be incomplete. This however is difficult to discern from NMR since there is some ethylene glycol left, which overlaps the OCH_3 peak of the methyl ester. The IR spectrum confirms formation of the hydroxyethyl esters (broad OH at 3050 cm^{-1} to 3500 cm^{-1}). The $\text{C}=\text{O}$ region of the spectrum (1750 cm^{-1}) is also broadened indicating formation of new ester linkages.

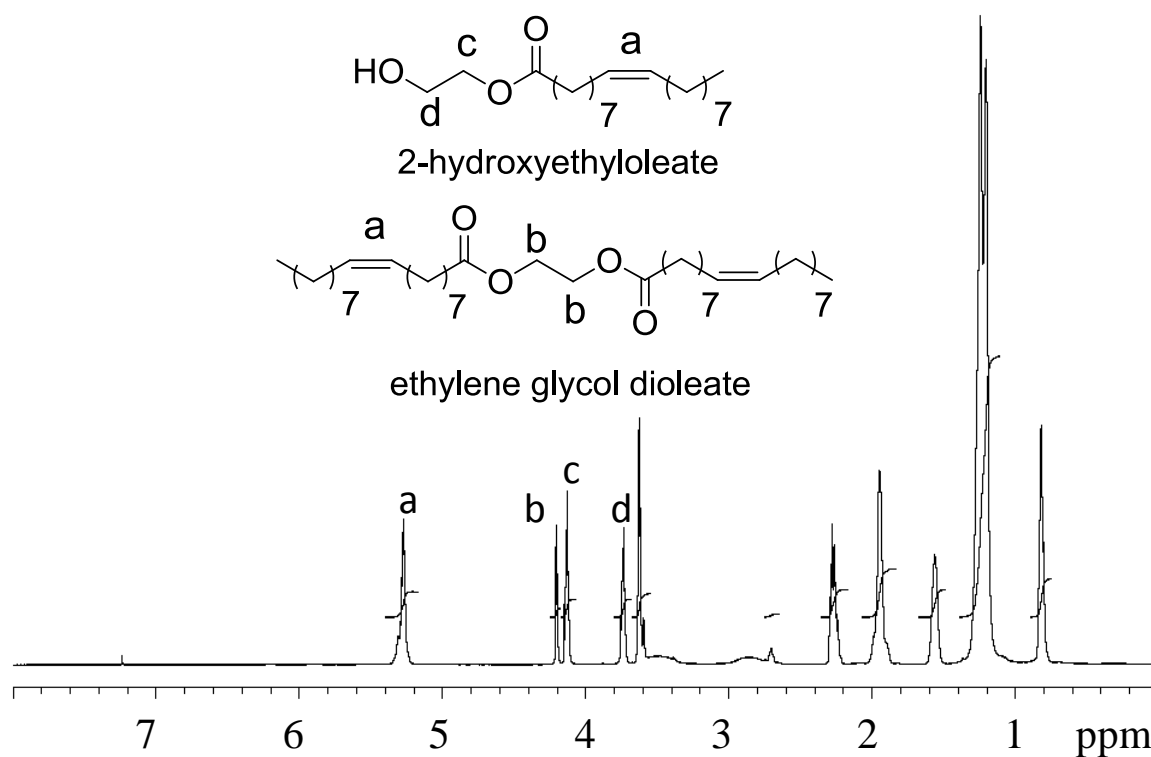


Figure 5.1 ¹H-NMR spectrum of transesterified methyl oleate

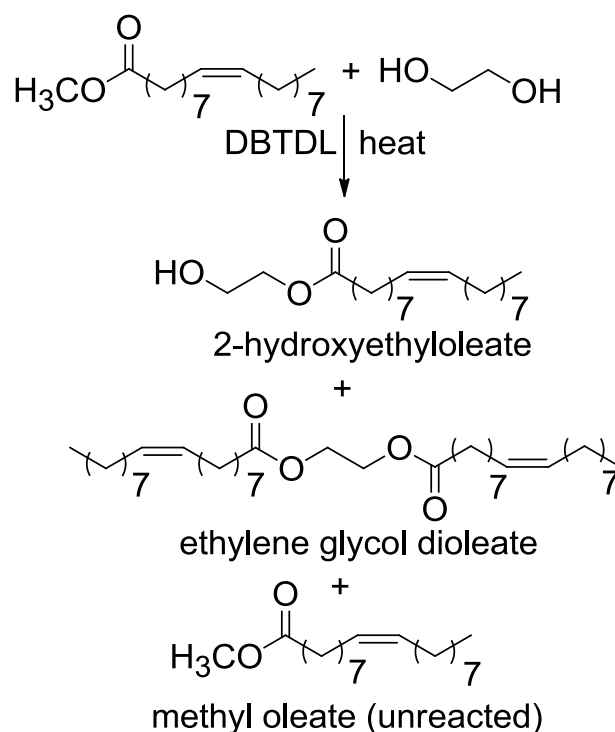


Figure 5.2 Products of transesterification of methyl oleate with ethylene glycol

5.4.2 Ozonolysis

Ozonolysis of the above mixture was carried out and ozone at the exit was monitored. The plot of the exit concentration of ozone is given in Figure 5.3. It can be seen that there is virtually no ozone at the outlet for the first 30 minutes of the reaction. The current system is ozone limited (semi-batch mode) and thus the reaction essentially consumes all the ozone in the initial stages. Since the activation energy for ozonolysis is low (5), all of the ozone is readily consumed by the unsaturation present in the sample. The moles of ozone reacted in this time can be calculated using the flow rate and concentration of ozone (inlet concentration) as ~0.25 mole.

At a time of 140 minutes, the ozone uptake by the sample was essentially zero and from the flow rate and concentration of ozone, the amount of ozone utilized was determined to be ~42 gm (0.88 mol). This agrees very well with the amount of unsaturation in the methyl oleate used for ozonolysis. It can be seen that ozone uptake does not happen beyond this point. Similar behavior is also observed for methyl oleate run under identical conditions.

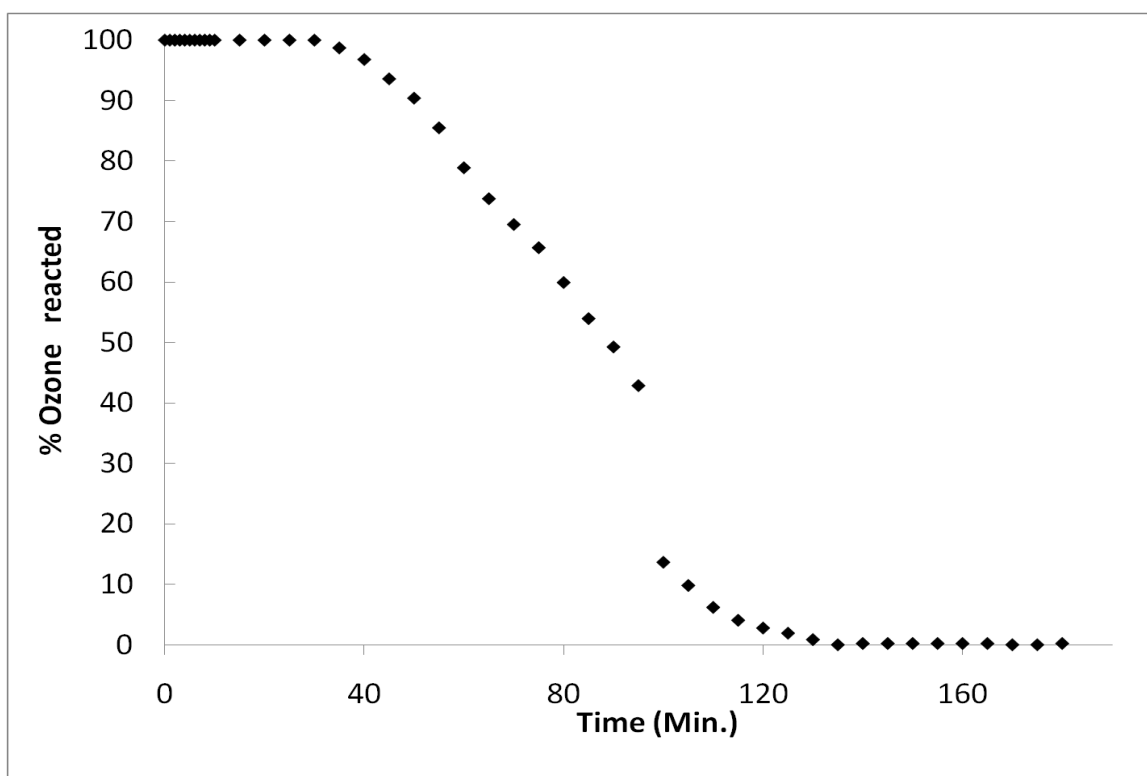


Figure 5.3 Ozone uptake of transesterified methyl oleate sample

The ^1H – NMR spectrum for the ozonated samples is presented in Figure 5.4 & 5.5. A summary of pertinent functional groups and their integral areas relative to the

terminal CH₃ area (referenced to 3 units) have been presented in Table 5.2 & 5.3. The terminal CH₃ was chosen since it was far upfield of any other proton and essentially does not change during ozonolysis in the present case. As can be seen from the NMR spectrum and Table 5.3, ozonolysis proceeds smoothly and all the double bonds have been consumed within the time of the reaction. The assignment of the ozonide has been made from reported literature (18-19) and the cyclic acetals from known chemical shifts of 1, 3 – dioxolanes. It should be noted that the term “acetals” has been used generically to account for cyclic, linear acetals, hemi – acetals and hydroperoxy acetals. No specific assignments to one particular species have been made due to the complex nature of the mixture.

It can also be seen that aldehydes are formed in relatively small quantities (10 mole %) and predominantly ozonides and acetals are formed. This is consistent with earlier reports that in the presence of protic reactants, aldehydes are minimally formed. Also it can be seen that the amount of free hydroxy ester (resulting from transesterification) has been reduced, implying that these groups also acetalize with the intermediates formed during ozonolysis. The presence of ozonide species even in the presence of the protic ethylene glycol could be explained by the fact that there still exists some immiscibility of both the transesterified product and methyl ester with the bulk glycol. This would basically allow the rearrangement of the primary ozonide to the secondary ozonide (inside the oil phase). It is reasonable to assume that this would be minimized if

enough mechanical energy is provided to disperse the oil phase better into the glycol phase.

The existence of acetals in the ozonated product and the absence of ozone absorption, beyond the 1 mole ozone/double bond requirement are interesting. There are reports (20-21), that cyclic acetals or 1, 3 – dioxolanes, which would be one of the expected products, (Figure 5.6) spontaneously react with ozone to form hydroxy esters. Of note is the fact that they do so faster than linear acetals, which can also form in this case. This however is not seen in this case. Whether or not the absence of this oxidation in the present system is due to ozone limitations (from the generator) or mass transfer limitations is yet to be determined. The formation of acetals is confirmed from both NMR and Mass spectrometry (formation of $[M - H]^+$, $[M - R]^+$ ions – peak data presented in Table 5.7).

The ^{13}C NMR spectrum also confirms the presence of aldehydes ($\delta = 203$ ppm), ester carbonyl ($\delta = 174$ ppm), trioxolane ($\delta = 104$ ppm) and dioxolane ($\delta = 100$ ppm). Also seen are peaks corresponding to the glycol ether carbon ($\delta = 65$ ppm) and glycol ester carbon ($\delta = 61, 62$ ppm). Residual double bonds are also seen ($\delta = 128$ ppm).

From the titrimetric data, it can be seen that the iodine values have been reduced by about 90% from the starting value. This is consistent with what is observed from NMR data. Also the hydroxyl values for the ozonated samples are seen to increase. While the NMR would suggest that no significant hydroxy ester formation occurred on

ozonolysis, the acetals formed could very well interfere, along with the aldehydes in the titrimetric determination of hydroxyl value.

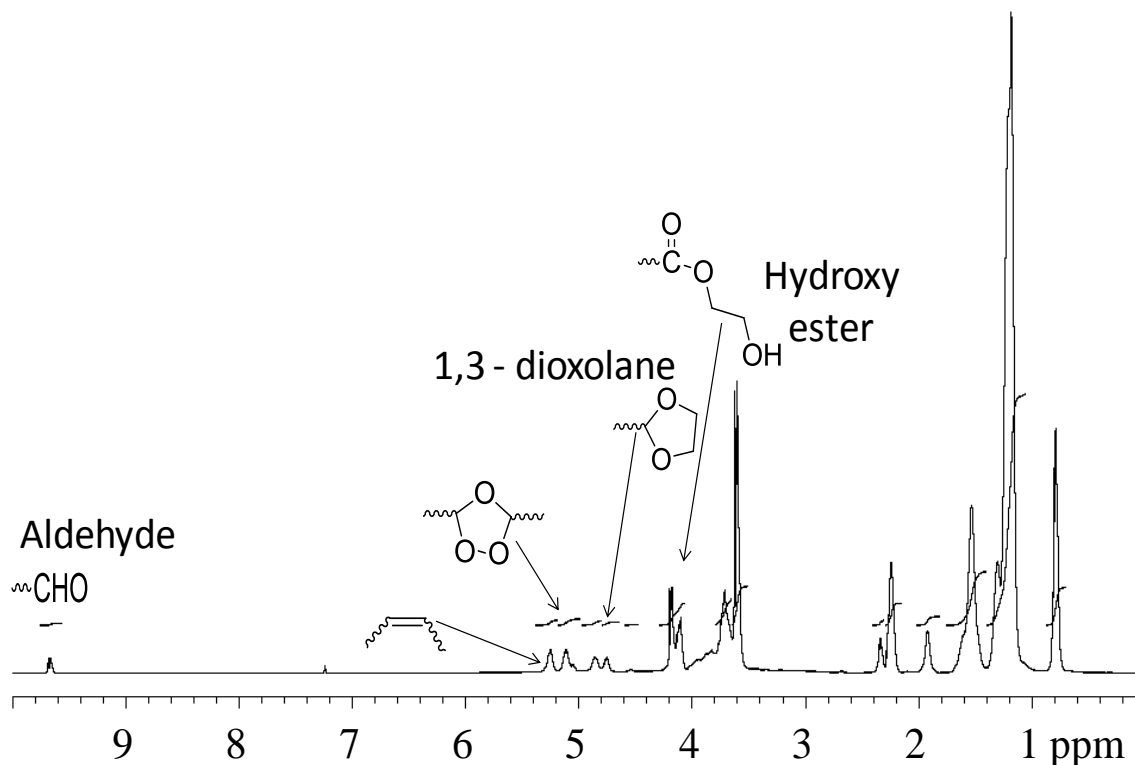


Figure 5.4 ^1H - NMR spectrum of ozonated transesterified oleate ester

As mentioned previously, mass spectra reveal the formation of acetals (dioxolanes). Also seen are nonanal and small amounts of nonanoic acid. This is not unexpected since aliphatic aldehydes are susceptible to oxidation by oxygen or ozone to the carboxylic acid. The fact that this does not happen significantly is inferred from the low acid values of the samples. Nonanal is the significant component seen in the mass spectrum and the 9 – oxomethylnonanoate ester (methyl or 2 – hydroxyethyl derivative) is not seen in significant amounts. This implies, that disproportionation of the ozonide occurs preferentially forming the nonanal.

The expected and possible products from the ozonolysis are provided in Figure 5.7 . It can be seen that while hydroxy esters are the expected products, acetals, peroxides, acids and aldehydes are all possible products and the characterization reveals that side products do form and in some cases in significant quantities.

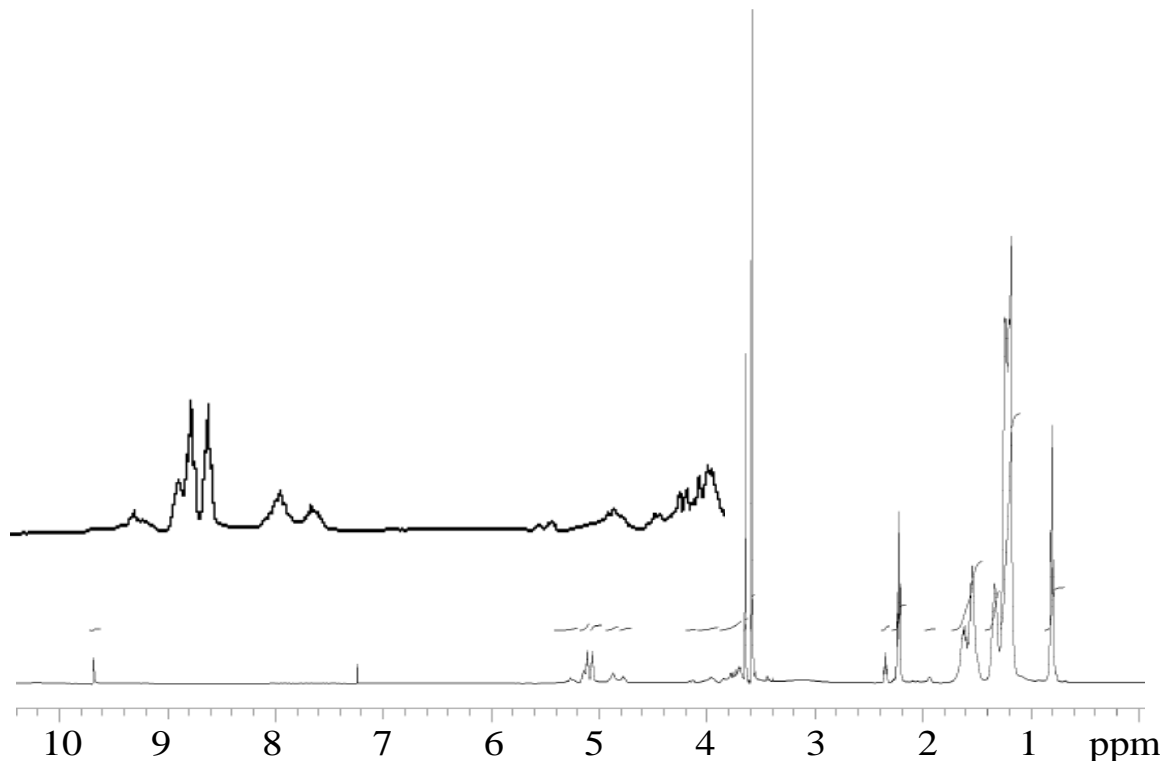


Figure 5.5 ¹H - NMR spectrum of ozonated methyl oleate; inset shows expanded spectrum in the region 3.8 – 5.6 ppm

The IR spectrum for the ozonated sample shows no discernible unsaturation peak ($C = C - H$ at 3005 cm^{-1}). This confirms the consumption of most of the double bonds in the sample. The OH peak has also not changed in intensity with regard to the starting transesterified sample. This is consistent with the NMR result that ozonolysis

mainly leads to formation of acetals and ozonides and not new hydroxy esters. The C=O region of the spectrum is also broadened, with a shoulder like feature appearing near 1700 cm^{-1} . This is characteristic of aldehydes forming during ozonolysis. The methyl oleate sample (spectra not shown), displays the same characteristics, with some residual glycol appearing in the –OH region at 3500 cm^{-1} .

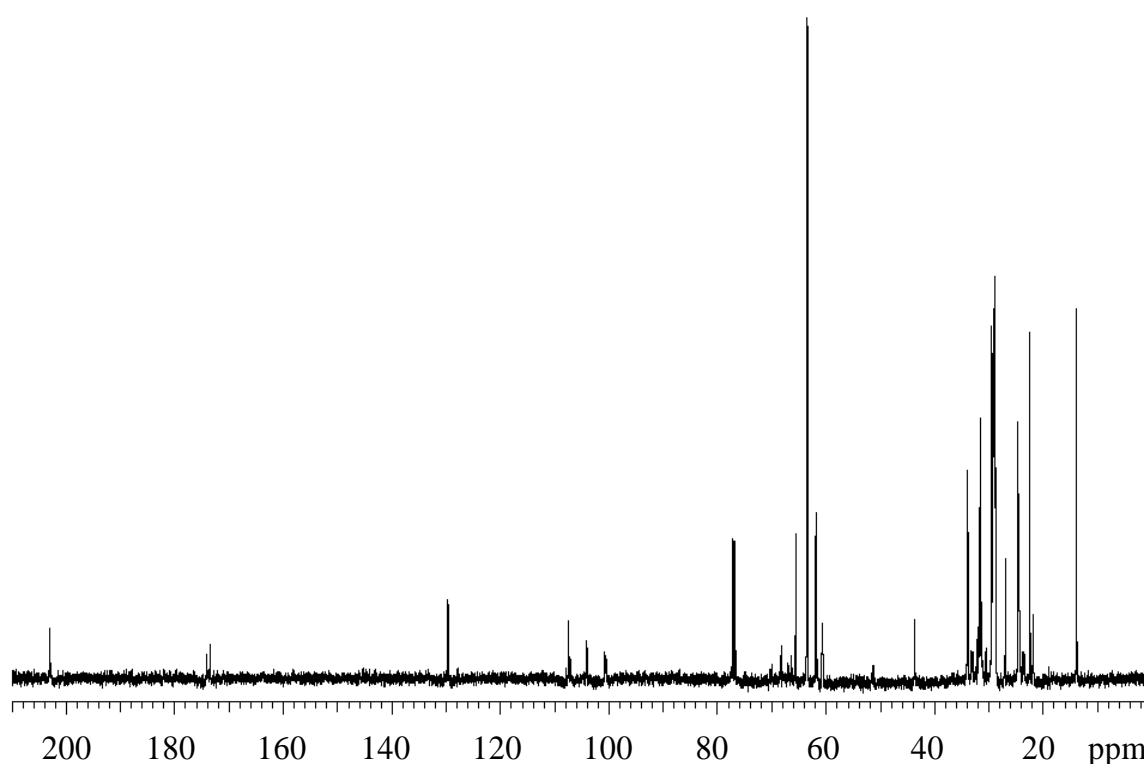


Figure 5.6 ^{13}C NMR spectrum of ozonated methyl oleate showing aldehydes @ 203 ppm, ozonides and acetals @ 100 - 110 ppm

**Table 5.2 Integral ratios of functional groups (relative to CH₃ area =3) from NMR spectra; proton of interest is italicized.
¹³C shifts reported for carbon bearing proton of interest (Sample: transesterified oleate ester) N.D – Not determined**

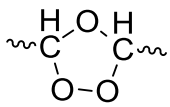
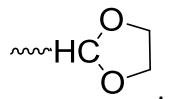
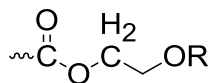
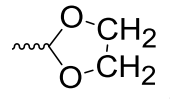
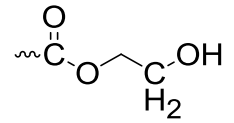
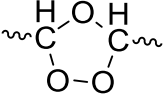
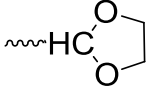
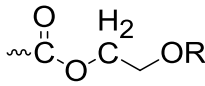
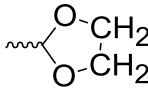
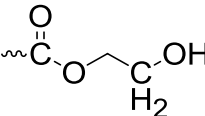
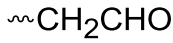
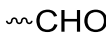
¹ H (ppm)	¹³ C (ppm)	Functional group	Transesterified	Ozonated	Oxone treated
5.0 – 5.2	105		-	0.78	0.09
4.6 – 4.9	108	 , other ether	-	0.65	0.07
4.1 (R = H)	66		1.34	0.8	2.22
4.2 (R = COR ₂)	62	R = H, COR ₂	0.66	0.88	1.15
3.9	65	 , ether	-	N.D	N.D
3.8	61			N.D	2.69
2.4	44	$\sim\text{CH}_2\text{CHO}$	-	0.40	0.0
9.72	202.8	$\sim\text{CHO}$		0.11	0.0

Table 5.3 Integral ratios of functional groups (relative to CH₃ area =3) from NMR spectra; proton of interest is italicized. ¹³C shifts reported for carbon bearing proton of interest (Sample: methyl oleate)

¹ H (ppm)	¹³ C (ppm)	Functional group	Ozonated	Oxone treated
5.0 – 5.2	105		0.88	0.33
4.6 – 4.9	108	 , other ether	0.39	0.15
4.1 (R = H)	66		0	1.24
4.2 (R = COR ₂)	62	R = H, COR ₂	0.05	0.66
3.9	65	 , ether		N.D
3.8	61		0.70	1.52
2.4	44		0.30	0.0
9.72	202.8		0.10	0.0

during the oxidation. This is not unexpected since Oxone can oxidize aldehydes to the esters, with a 2 – hydroxyethyl ester itself acting as the alcohol. Similar results are also seen for the plain methyl oleate sample, ozonated and subjected to Oxone treatment.

The ^{13}C – NMR spectrum also clearly shows the absence of the aldehyde carbon at 203 ppm and complete absence of the peaks in the 100 – 110 ppm region. Thus the oxidation of these products is also well supported by the carbon NMR. The mass peaks for all the hydroxy esters and diesters are however difficult to see in the mass spectrum. This could be due to difficulty in volatilizing the samples for mass detection. However, the fragments of these compounds are seen (Table 5.6). The facile fragmentation of the esters, coupled with high boiling points is probably responsible for the increased visibility of fragment ions. The formation of these esters is however clearly seen from the NMR, IR and titrimetric results.

Table 5.4 Titrimetric data for transesterified methyl oleate samples (percent change in parentheses)

Attribute	Methyl oleate (MO)	Transesterified methyl oleate (MOEG)	Ozonated product	Oxone treated product
Acid Value(mg KOH/gm)	2	3	13	10
Hydroxyl value (mg KOH/gm)	3	83	170 (+105%)	256 (+208%)
Iodine value (gm/100gm)	79	73 (-7.5%)	9 (-88%)	8 (-90%)

Table 5.5 Titrimetric data for methyl oleate samples (percent change in parentheses)

Attribute	Methyl oleate (MO)	Ozonated product	Oxone treated product
Acid Value(mg KOH/gm)	2	16	12
Hydroxyl value (mg KOH/gm)	3	158	220 (139%)
Iodine value (gm/100gm)	79	10	8 (-90%)

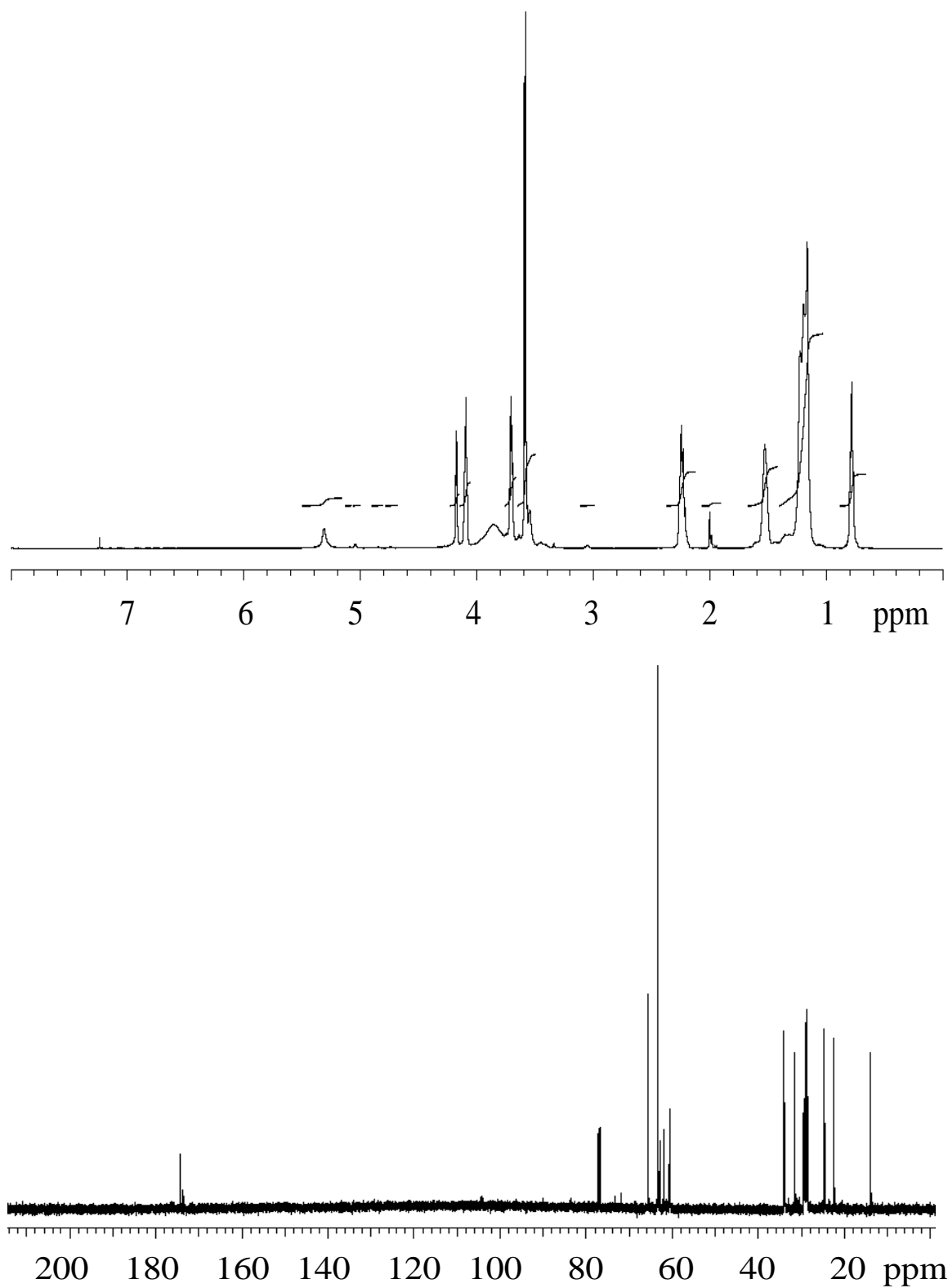
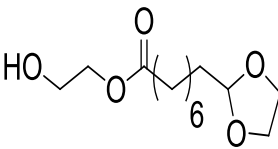
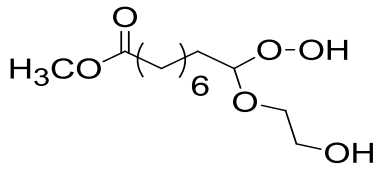
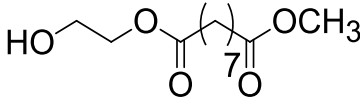
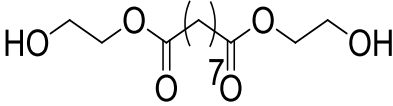


Figure 5.8 & 5.9 NMR spectra of Oxone treated samples: ^1H (Top); ^{13}C (Bottom)

Table 5.6 Representative peak data from Mass spectra

Compound	Parent Ion	Fragments
	244	73 ($\text{C}_3\text{H}_5\text{O}_2^+$) 243 $[\text{M} - \text{H}]^+$
	264	73 ($\text{C}_3\text{H}_5\text{O}_2^+$) 203 $[\text{M} - \text{OCH}_3]^+$
	N.D	215 $[\text{M} - \text{OCH}_3]^+$ 185 $[\text{M} - 61]^+$
	N.D	245 $[\text{M} - \text{OCH}_3]^+$ 215 $[\text{M} - 61]^+$
N.D – Not detected		

Further insight to the oxidation reaction can be obtained by normalizing the IR spectra and then expanding them around the hydroxyl and carbonyl regions (Figures 5.10 & 5.11). It can be seen that there is a progressive increase in the intensity of the OH peak from pure methyl oleate to the oxone treated sample. Similarly, the carbonyl region for these samples also shows broadening and increase in intensity, indicating that new carbonyls (esters) are formed during the course of ozonolysis and oxone treatment.

To the best of our knowledge, this is the first reported work on the use of a dihydric alcohol in an Oxone oxidation of an ozonated fatty acid ester to a hydroxyester derivative. This is significant since, ozonolysis to produce aldehydes is a lot simpler than the direct conversion to esters. Thus a wide variety of polyols can be synthesized, by appropriate use of alcohol and extent of ozonolysis. Earlier work by Sharghi et al. (22) on the synthesis of hydroxyesters, have dealt with aromatic compounds. Other oxidations of acetals and aldehydes to hydroxyesters have employed hydrogen peroxide (23-24), oxygen (25) (with cobalt catalysts). The hydrogen peroxide route employs concentrated HCl while the latter employs a solvent with long reaction times.

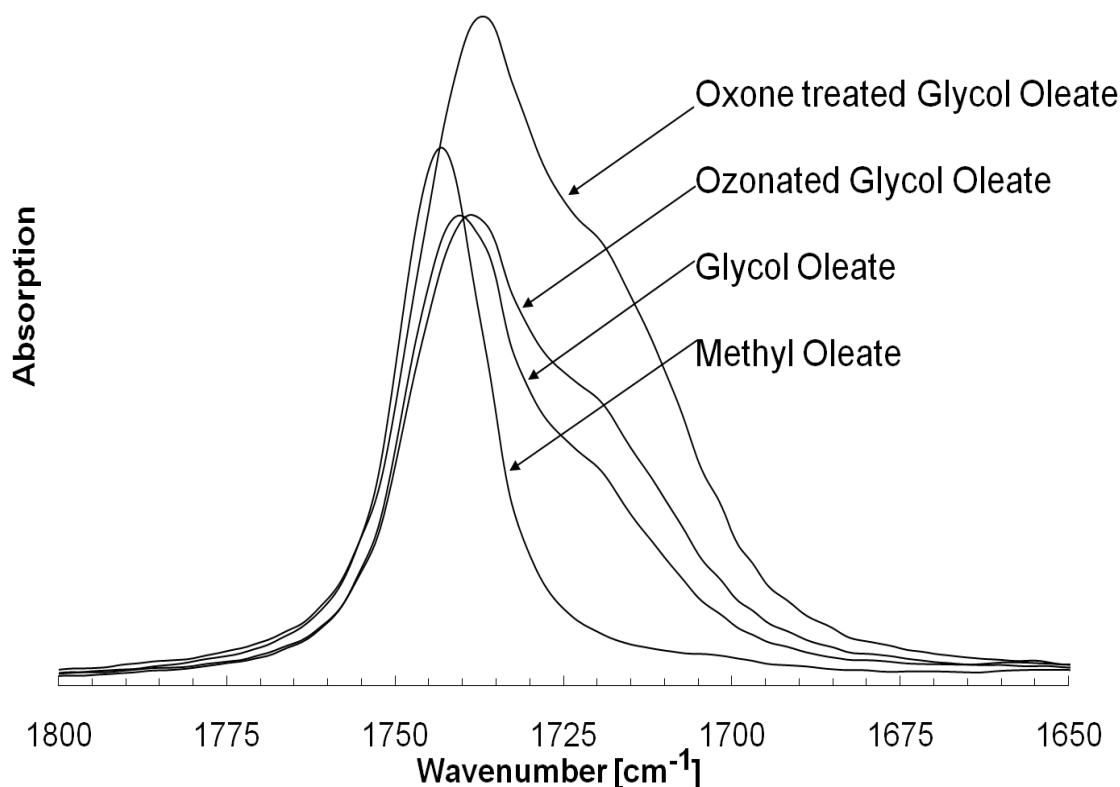


Figure 5.10 IR spectra of transesterified methyl oleate samples : Carbonyl region

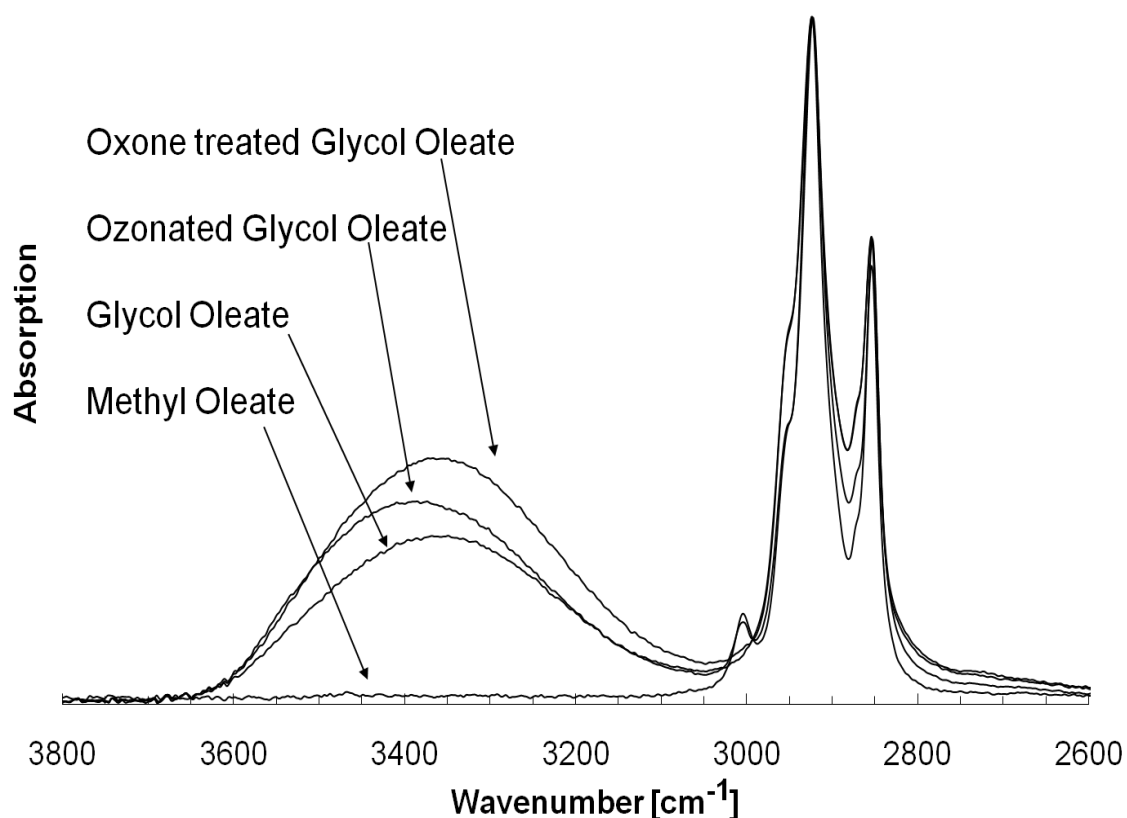


Figure 5.11 IR spectra of transesterified methyl oleate samples: Hydroxyl region

5.4.4 A note on Baeyer – Villiger oxidation

It was mentioned earlier in the work that oxidation by Oxone is often postulated to proceed via a Baeyer – Villiger route. It should be noted that small amounts of 2 – hydroxyethyl formate and 1, 2 – ethanediyl formate were seen in the mass spectrum of the sample after Oxone treatment. These are most likely from the transesterification of formate esters of the aldehydes with ethylene glycol. However, the corresponding peaks in the ^1H NMR (s, 8.1 ppm & s, 4.42 ppm) and ^{13}C NMR (C=O, 161 ppm) are not seen.

This implies that it is a very minor product. This is not unexpected, since alkyl group migration during such oxidations depends to a large extent on stabilization of the carbocation, which is minimal for a primary cation that would be generated with the C₉ fragment.

5.5 CONCLUSIONS

Methyl oleate was used as a model compound to study the oxidation reaction of vegetable oils to primary polyols. Accordingly, it was transesterified with ethylene glycol and the product was oxidized by ozone in the presence of ethylene glycol under basic conditions followed by treatment with Oxone. The transesterification proceeded smoothly to yield the corresponding 2-hydroxy esters. Ozonolysis of these esters in ethylene glycol was effective and reduced essentially all the double bonds. However, in addition to the desired hydroxy esters, some aldehydes, acetals and ozonide were also produced.

These species were subsequent oxidized to the desired hydroxy esters by Oxone treatment in good yield. However, oligomerization of the hydroxy esters during the Oxone treatment is still an issue that needs to be resolved. While it reduces the hydroxyl value, it also increases the molecular weight of hydroxy esters, which could be useful in the synthesis of polymeric polyols for use in flexible polyurethane foams for example. Similar results could also be obtained for methyl oleate without transesterification.

The process can possibly be extended to cover vegetable oils and thus would enable production of polyols by controlling the extent of ozonolysis and the reacting alcohol to get a wide range of hydroxyl values and molecular weights.

REFERENCES

5.6 REFERENCES

1. A. Guo, I. Javni, Z. Petrovic, *Journal of Applied Polymer Science* **77**, 467 (2000).
2. S. Khot *et al.*, *Journal of Applied Polymer Science* **82**, 703 (2001).
3. J. Zahardis, G. Petrucci, *Atmospheric Chemistry and Physics* **7**, 1237 (2007).
4. J. N. U. Soriano, V. P. Migo, M. Matsumura, *Fuel* **85**, 25 (2006).
5. P. S. Bailey, *Ozonation in Organic Chemistry*. (Academic Press, New York, 1978), vol. I.
6. E. Niki *et al.*, *Journal of Biological Chemistry* **260**, 2191 (1985).
7. W. Bunnelle, *Chemical Reviews* **91**, 335 (1991).
8. M. Barton, J. Ebdon, A. Foster, S. Rimmer, *Organic & Biomolecular Chemistry* **3**, 1323 (2005).
9. J. Marshall, A. Garofalo, *The Journal of Organic Chemistry* **58**, 3675 (1993).
10. R. Ackman, *Lipids* **12**, 293 (1977).
11. J. Sebedio, R. Ackman, *Canadian Journal of Chemistry* **56**, 2480 (1978).
12. J. Neumeister, H. Keul, M. Saxena, K. Griesbaum, *Angewandte Chemie International Edition in English* **17**, 939 (1978).
13. H. Benecke, B. Vijayendran, D. Garbark, K. Mitchell, *CLEAN-Soil, Air, Water* **36**, 694 (2008).
14. P. Tran, D. Graiver, R. Narayan, *Journal of the American Oil Chemists' Society* **82**, 653 (2005).

15. B. Travis, M. Sivakumar, G. Hollist, B. Borhan, *Org. Lett* **5**, 1031 (2003).
16. G. Knothe, J. A. Kenar, *European Journal of Lipid Science and Technology* **106**, 88 (2004).
17. M. Guillén, A. Ruiz, *European Journal of Lipid Science and Technology* **105**, 688 (2003).
18. M. Wu, D. Church, T. Mahier, S. Barker, W. Pryor, *Lipids* **27**, 129 (1992).
19. N. U. Soriano, V. P. Migo, M. Matsumura, *Chemistry and Physics of Lipids* **126**, 133 (2003).
20. W. J. Baumann, T. H. Madson, *J. Lipid Res.* **15**, 528 (September 1, 1974, 1974).
21. P. Deslongchamps, P. Atlani, D. Fréhel, A. Malaval, C. Moreau, *Canadian Journal of Chemistry* **52**, 3651 (1974).
22. H. Sharghi, M. H. Sarvari, *The Journal of Organic Chemistry* **68**, 4096 (2003).
23. T. Takeda, H. Watanabe, T. Kitahara, *Synlett* **1997**, 1149 (1997).
24. R. Gopinath, B. Barkakaty, B. Talukdar, B. Patel, *J. Org. Chem* **68**, 2944 (2003).
25. B. Karimi, J. Rajabi, *Synthesis* **2003**, 2373 (2003).

CHAPTER 6

SYNTHESIS AND PROPERTIES OF SOYBEAN OIL – VINYLTRIMETHOXY SILANE ADDUCTS

ABSTRACT

Adducts of soybean oil and vinyltrimethoxy silane were synthesized using an organic peroxide initiator (Luperox 101) in a high pressure Parr reactor. The reactions were carried out at five different temperatures (160 °C to 240 °C in 20 °C increments). In all the cases, the molar ratio of the soybean oil to silane was kept constant (1:5) and the peroxide was kept at 1 wt% of the oil. The grafting reaction of the silane to the fatty acid ester was followed by thermo gravimetric analysis, NMR and iodine values. It was found that the silylation rate and the overall conversion were directly proportional to the reaction time and the temperature when the reactions were run above a temperature of 200 °C. The data allowed us to define experimental conditions to achieve predetermined grafting and good conversions. There was a good agreement between the different methods used to determine the conversion. In addition, soybean oil was also reacted with the silane at 260 °C with the peroxide at different ratios of oil to silane (1:3 mol, 1:5, 1:7, 1:11 and 1:15). It was seen that the silane ratio strongly influenced conversion, with higher silane ratios yielding higher conversions. In this case, conversions approached 50% (1:15 mole ratio, 260 °C, 6 hours) based on the initial

charge. Silylated oils of varying “silicone” content could thus be synthesized. The reaction mechanism was expected to follow an Alder – ENE type pathway based on the reaction conditions and reported literature; however, NMR spectra suggest a concurrent radical pathway for the grafting of silane onto the oil. Furthermore, the uncatalyzed reaction of the oil with the silane (1:15 mole ratio) at 260 °C produced grafting at about the same conversion as the peroxide catalyzed reaction. Apparently, the peroxide does not appear to influence this reaction significantly at high temperatures. The silylated oils were cured via moisture aided hydrolysis and subsequent condensation and gel contents as high as 90% were obtained.

The silylated oil was used to stain wood in order to test its water repellency. Plain soybean oil was used as a control. It was observed that the silylated oil acted as excellent water repellent, cutting down the absorption by 75% of that of untreated wood and was twice as effective as plain soybean oil.

The cure kinetics of one particular silylated oil was evaluated (1:5 mole ratio, 240 °C, 10 hours) using a Brookfield viscometer. The effect of temperature, moisture and catalyst (Dibutyltin dilaurate) were evaluated. It was observed that moisture and catalyst had a marked effect on the cure rate while the temperature had only a minor effect on the cure rate. Onset of cure was accomplished in under 5 minutes at high catalyst and water content (4 phr each).

The silylated oils also had good spread ability on metal. The oils in their original form could be applied as thin coatings to steel panels as coatings as thin as 2

mils. They were also formulated with commercially available corrosion inhibitors to form pale yellow, transparent coatings on metal substrates. The coatings in general had good resistance towards humidity and resisted cracking for longer than 300 hours in our test chambers. The unformulated oil itself exhibited excellent corrosion protection and samples stored in laboratory conditions with minimal physical wear resisted corrosion for more than 9 months.

The oil could also be mixed with fumed silica, to yield rubbery gels which could serve as caulks. The material looks promising as a corrosion protection coating, paper coatings and as a sealant.

6.1 INTRODUCTION

The growing need for renewable materials has spawned tremendous research in the area of bio – renewable feedstock. Vegetable oils thus have received increasing attention as potential feedstock; notable examples being the use of alkyl esters vegetable oil fatty acids as fuel or fuel additives, polyols and other derivatives produced by various chemical modifications of oils – for use in resin syntheses. Most of the vegetable oils are fairly unreactive and thus several strategies have been used to functionalize vegetable oils with reactive groups or to make the oil more reactive. Historically vegetable oils have been used in alkyd resin formulations, primarily for coating applications. Soybean oil is readily available and relatively inexpensive vegetable oil. As such it has been used as a major source of oil in a number of industrial applications; most notably, soy oil has been incorporated into unsaturated polyesters (1) (UPRs) though not in high amounts, for manufacture of fiber reinforced composites (FRCs). One of the most common techniques for functionalizing has been the generation of polyols from vegetable oils – via alcoholysis, transesterification, epoxidation and ozonolysis. Such polyols could then be reacted with isocyanates or acids to yield polyurethanes (2) and polyesters. Thus, functionalizing the vegetable oils, which is typically accomplished via the double bonds (unsaturation) on their fatty acids, requires the use of strong oxidizers like ozone, hydrogen peroxide and other metal oxides – for cleaving the double bond for synthesis of polyols or other modified derivatives. Alternatively, complex metal catalysts are also used as in the case of hydroformylation

and metathesis (3-4). Peroxides are commonly used in maleation (5) or polymerization of the oils.

As mentioned above the common vegetable oils that find applications as cooking media are composed of fairly unreactive fatty acids. This is a rather important criterion for their use as a cooking medium. This also makes utilization of such oils in certain applications difficult; for example Linseed oil, which is a “drying oil”, is capable of polymerizing by an air oxidation mechanism, by which it has found use in varnishes and lacquers. Soybean oil on the other hand, is a major edible oil that unlike linseed oil lacks the “air drying” capacity. Thus any resin (unsaturated polyesters) that employs soybean oil as the bio-based component typically will have to use co monomers like styrene (6) or acrylate esters to copolymerize with the unsaturation of the oil.

Room temperature vulcanization (RTV) of vegetable oils or their fatty esters has not pursued with great success thus far. Silicones are one example of RTV systems having wide ranging applications. Adding a hydrolysable silane group to vegetable oils or their alkyl esters could potentially enable them to form networks by an RTV process. This has been accomplished by end capping vegetable oil derived polyols with isocyanates, which were then reacted with amino silane and small amount of methanol (7). The method however is still a multi step process involving synthesis of the polyol, reaction with isocyanates and finally reaction of excess isocyanate moieties with amino groups. Hydrosilylation of the double bond in vegetable oils has also been carried out with trichlorohydrosilane, under UV light to functionalize the oil for reducing moisture

absorption in concrete (8). Hydrosilylation of fatty acid methyl esters (FAMES) (9-10) and triacylglycerols (TAGs) (11) and other derivatives (12-13) have been reported in the presence of platinum catalysts and radical initiators. The common hydrosilanes employed are triethoxy and trichlorosilane. The triethoxy derivative has been shown to work only with terminal olefins (undecenoic acid derivatives are mostly used) while the trichloro derivative has been reported to work even for non – terminal double bonds under suitable conditions. But in all the above cases, where internal double bonds are involved, the silane invariably has been a chlorosilane and either a radical initial sequence (RIS) with a mixture of peroxides or platinum based catalysts (Speier's or Karstedt's catalyst) have been employed and the triethoxy derivative has been reported to be ineffective in such cases. There has been one report of a high temperature process involving only vinylsilanes (alkoxy and acyloxy), chlorosilanes and vegetable oils and/or their esters (14). Temperatures as high as 320 °C were used and gel contents as high as 92% were obtained. However, the method does not discuss the mechanism of silane addition or the nature of the products formed. Also the work does not report the same reaction for saturated fats. This is essential since saturated fatty acids are important constituents, which are often present at 10% or higher concentrations in vegetable oils.

Although hydrosilylations as the ones mentioned above are novel techniques for simple functionalization of unreactive fatty acid chains, they involve highly corrosive chlorosilanes and in some cases expensive catalysts – which may or may not be recoverable. The purity constraints on the starting material are also likely to be higher, since platinum catalysts are poisoned easily by sulfur and phosphorous compounds. The

involvement of chlorosilanes mandates their hydrolysis (a separate unit process) before it can be used in applications, due to high corrosivity of the hydrochloric acid that would evolve upon hydrolysis. Even when the hydrosilylating agent is an alkoxyhydrosilane, their sensitivity to moisture, and other impurities (acids, hydroxyls etc.) would impose additional constraints.

In this following work, we report a simple peroxide mediated silylation process that is accomplished in a relatively short time frame (6 – 12 hours), with minimal constraints on the starting materials used. The silane (vinyltrimethoxy silane) is one of the most common and inexpensive alkoxy silanes available. The vegetable oil also just represents one of the commonly used vegetable oils. Alternatively, the method can also be simply extended to cover non – essential oils and oils from waste streams (post cooking). The only post reaction processing involves removal of unreacted silane, which might be done according to the end use requirements.

6.2 MATERIALS

Low saturates Soybean oil (refined and bleached – Select OilTM) was obtained from Zeeland Farm Services Inc. (Zeeland, MI). Vinyltrimethoxy silane [CAS 2768-02-7] was obtained from Gelest Inc. (Morrisville, PA) and had a purity of 97%. Luperox 101 [CAS 78-63-7] - 2, 5-Bis (*tert*-butylperoxy)-2, 5-dimethylhexane (90% technical grade), Chloroform [CAS 67-66-3] used for swelling studies and Dibutyltin dilaurate [CAS 201-

039-8] used as the cure catalyst were obtained from Sigma Aldrich (St.Louis, MO). All the reagents were used as received without any further purification. However the reagents (except Luperox 101) were dried prior to use. Soybean oil was dried over molecular sieves and the silane was kept dry by a nitrogen flush before and after the container was opened.

The corrosion inhibitors and a proprietary surface treating agent WARTM were supplied by Northern Technologies International Corporation (Circle Pines, MN) and were used as received. To increase the surface area of the panels, they were scrubbed with 320 grit abrasive paper from 3M Corporation.

Metal panels were procured from Q-Panel Inc. (Westlake, OH). The panels were of the type QD-24 (4 in. X 2 in. X 0.02 in) smooth finish, cold rolled steel. Prior to coating, they were scratched with abrasive paper.

Coatings on metal panels were obtained using two different applicators from BYK Instruments (Wallingford, CT). PA-5331 U-shaped applicator with 6, 10 mil clearance and PA-5358 multiple clearance square applicator (4 in. width) with clearances from 0.5 mil to 6 mil were used.

6.3 EXPERIMENTAL

6.3.1 Synthesis of soybean oil – silane adducts

Low saturate soybean oil has approximately 5 double bonds per mole and thus about 5 mole of silane (M.W. 148.23 g/mol) were mixed with soybean oil (M.W. ~871 g/mol) and the peroxide initiator (1 wt% of the oil, M.W. 290.44) in a closed flask. The mixture was pumped using a nitrogen blanket into a 2L Parr reactor (Parr Instrument Company, Moline, IL), equipped with a mechanical stirrer, pressure gauge, pressure relief device, inlet, sampling and vent ports and thermocouple well. The temperature of the reactor was controlled using an external controller (from 160 °C to 240 °C in 20 °C increments). The agitation was kept at 200 rpm to mix the reactants and distribute heat uniformly in the system. Before the start of reaction, the reactor was purged with nitrogen for about 5 minutes to ensure an inert atmosphere. The time for reaction was taken as the time from the reactor reaching set temperature till shut down.

Samples were withdrawn (for samples with 1:5 silane ratio only) at various time intervals using the sampling port into vials. The vials were then sealed tightly and refrigerated prior to analysis. To the extent possible, samples for thermo gravimetric analysis (TGA) were drawn from the cold vials, to minimize the silane migration the vapor phase. The heating rate was adjusted for each run to ensure that the reaction time for the different runs was nearly the same. In all cases, samples were withdrawn, before the heating was switched on, and then at regular intervals thereafter. The zero

time samples for the reaction kinetics were taken when the reactor reached the set temperature.

The effect of oil to silane mole ratio was evaluated at a temperature of 260 °C and a reaction time of 6 hours (1 wt% Luperox 101). Sampling was not done (no kinetics evaluated) and only the ultimate conversion was evaluated using reduced pressure distillation (0.3 Torr, 110 °C). The unreacted silane was collected in two dry ice traps and weighed.

6.3.2 Gel content

Samples were cured using the following procedure. A 60 X 15 glass petri dish was filled with 20 ml of water. Onto the surface of this water, about 12 ml of the silylated oil, was transferred drop wise, to form a liquid layer about 3-4 mm thick. The dishes were then transferred to an oven held at 70 °C and allowed to cure for a week. During this time humidity was also maintained inside, by means of a 2L trough of water. Samples were monitored to see the extent of cure. Once the oil had solidified (1 week), the cast sheet of oil was allowed to post cure at the same temperature for another week.

6.3.3 Cure kinetics

The silylated oil (1:5 ratio, 240 °C, 10 hours) was distilled as mentioned earlier and was used for all experiments. The oil had a silane content of ~ 1.8 mole/mole of oil. The effect of catalyst Dibutyltin dilaurate (DBTDL), moisture (as added water) and temperature were evaluated. The catalyst and water were varied as 3, 4, 5 and 6 phr

and the temperature was varied from 50 °C to 75 °C (5 °C increments). In each set of experiments two of the parameters (e.g. temperature, moisture content and catalyst concentration) were held constant while the other parameter was varied.

Viscosity measurements were conducted using a Brookfield Digital viscometer (Model. HBDV II) equipped with a Thermosel arrangement. A small sample holder was used with an SC – 21 spindle. All measurements were conducted at the speed of 50 RPM, to increase the observable viscosity range. A small amount of sample was premixed well with the predetermined amount of catalyst and water to form a fine dispersion. This was immediately transferred to the preheated sample holder and the speed was sequentially and quickly increased to 100 RPM. Measurements were made when the temperature reached set temperature (~2 min delay) and were stopped when the viscometer reached the preset viscosity limit for the spindle type used.

6.3.4 Coating on wood

A sample of untreated wood (~1 in. cube) was coated with the silylated oil (1:5 ratio, 240 °C, 10 hours) on all sides but one. The same procedure was followed for coating with soybean oil. The average mass of the wooden cubes was ~25 gm. After staining with the oil, the weights increased to ~30 gm indicating 5 gm of the oil had percolated the wood. The samples were allowed to cure at ambient temperature for a day followed by a post cure at 50 °C in an oven for a day.

The samples were immersed to half their height in a water bath with the uncoated side above the water. The weight increase was measured after wiping the water from the surface using a blotting paper.

6.3.5 Coating on metal panels

The metal panels were scoured with the abrasive paper, with the WARTM cleaner as the medium, till fine lather was generated. The panels were kept aside for 5 minutes and the procedure was repeated. The panels were then rinsed with de-ionized water and dried with a clean room grade lint free cloth. Additionally they were dried in an oven at 60° C prior to coating.

Samples of the oil were formulated with different loadings of corrosion inhibitors and different concentrations of the cure catalyst. The premixed formulation was introduced on top of the panels using a plastic pipette and a thin film was obtained using a single drawing motion of the applicator. After this, the panels were placed on glass plates and placed in an oven maintained at 65 °C for curing. Humidity was maintained using a container of water. When curing was done the samples were stored under ambient conditions on leveled surfaces in a dust free-environment.

6.4 CHARACTERIZATION

Thermo gravimetric analysis was done using a TA Instruments Q 2950 high resolution thermogravimetric analyzer. The samples ranging from 15 mg to 35 mg were added to a standard pan; the temperature was raised to 160 °C and held at that temperature for a period of 20 minutes to completely remove the volatile vinyltrimethoxy silane. The conversion of the silane was then calculated by subtracting the volatile fraction (e.g. unreacted silane) from the total amount of the silane in the sample. It should be noted that no weight change in the soy oil itself was observed under these conditions. Care was taken to ensure that there was minimal loss of silane by vaporization during the entire process. The method was validated by subjecting the starting material (1:5 soy oil: silane) to the analysis and determining the weight loss. This was compared to the theoretical weight loss expected and found to be in agreement. The representative plot is shown in Figure 6.1.

Gravimetric determination of conversion was done on the final product of the reaction. The product (pre – weighed) was distilled under reduced pressure (0.3 Torr, 110 °C) till no further distillate was obtained. The unreacted vinyltrimethoxy silane was collected using two dry ice traps and weighed to give the conversion. The distilled product was stored under nitrogen tightly sealed, to prevent any hydrolysis of the silane.

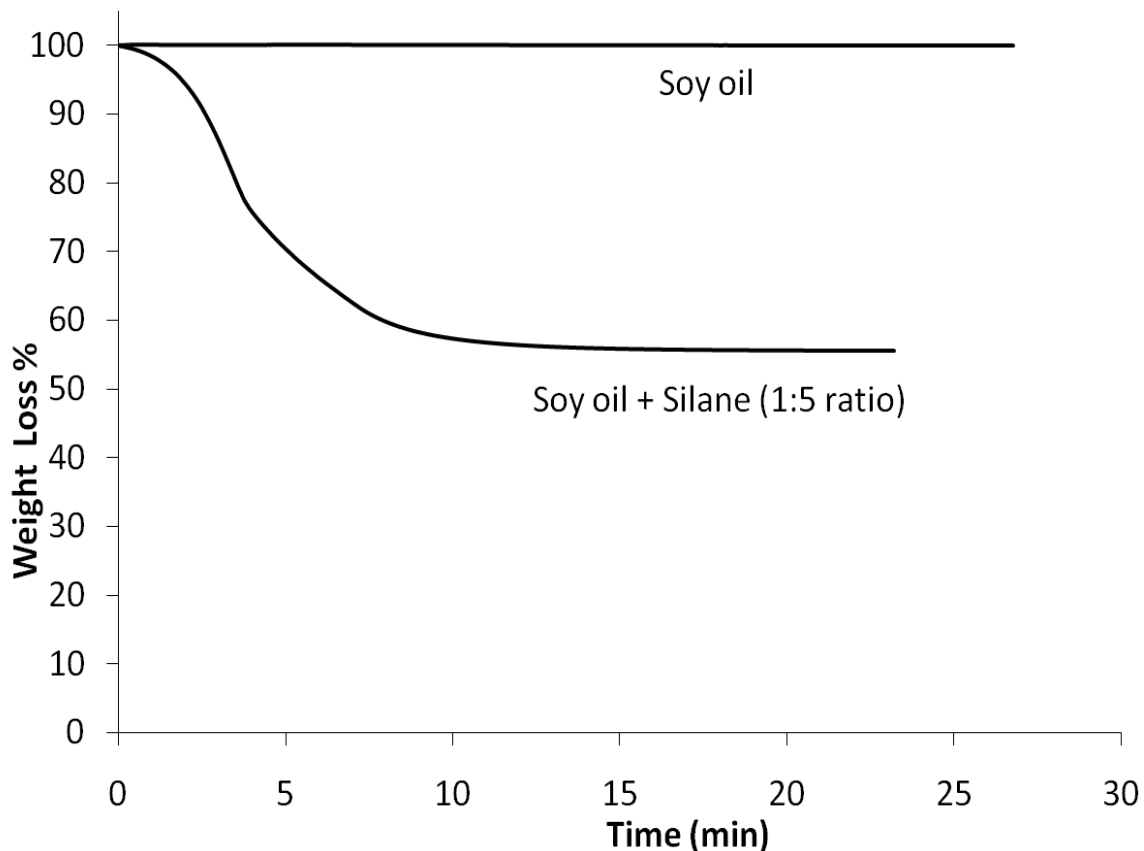


Figure 6.1 TGA plots of neat soy oil and soy oil - silane mixture (T = 160 °C)

Iodine values were measured according to ASTM D1959 on the samples after distillation. The sample mass was estimated using the conversion obtained earlier and assuming the double bonds of the oleate remained unchanged during the reaction. The titers were cross – checked against the recommended range in the standard to ensure accuracy of sample weights used.

NMR spectra were recorded on Varian Unity plus spectrometer operating at 500 MHz. The solvent used was CDCl_3 (^1H @ 7.24 ppm, ^{13}C @ 77 ppm). Standard

parameters were used in acquisition except in carbon spectra where a recycle delay of 2 seconds was employed.

The solvent uptake and gel content were measured using a modification of ASTM D2765. Small pieces of the cured sample were weighed (1.2 – 2 gm) and placed inside a pouch made of filter paper and allowed to soak in chloroform solvent for 72 hours at room temperature. The pouches were withdrawn and the solvent was completely squeezed out and the weight of the sample was immediately measured to give an estimate of the solvent uptake. The pouches were then dried in an oven at 80 °C till constant weight was reached. The gel content of the cured materials was then determined in the usual way from the difference in these weights. The soluble fraction was isolated by evaporation of the solvent and NMR spectra recorded on the samples.

The coated panels were subjected to elevated temperature and humidity on a continuous basis (100% RH and 44 °C per ASTM G60). In addition to this, they were also exposed to humidity at 95 °C, in a simple convection oven in the laboratory. Coated test specimens were also subjected to continuous 5 to 20% salt spray at 33 – 36 °C per ASTM B117 and ASTM G85. Filiform corrosion resistance was evaluated per ASTM D2830.

6.5 RESULTS AND DISCUSSION

6.5.1 Kinetics of silylation

It was observed that the silylation of soybean oil proceeded smoothly at all temperatures higher than 200 °C. Six samples were withdrawn for each temperature run and four samples were available for the isothermal region of the kinetics. The plot of conversion with time for different temperatures is presented in Figure 6.2.

The reaction data have also been fitted to a first order plot with respect to the silane. The data are presented in Figure 6.3. From the rate constants evaluated from these plots, the activation energy for the reaction was estimated at 24.9 kJ/mol (Figure 6.4). The value is very small when compared to the activation energy reported for grafting of vinyltrimethoxy silane on polyethylene (15).

In the present system we have used Luperox 101, whose estimated half – life is ~6 minutes at the lowest temperature of 160 °C. Thus any silylation that occurs due to radical decomposition would probably occur early on in the reaction. It should be noted that the non –isothermal region of the reaction has not been sampled well in our case.

There is no clear distinction between the kinetics at 160 °C and 180 °C. This could be due to the small conversion of silane and the errors associated with measurement of conversion. It should also be noted that the amount of silane in the vapor phase has been ignored, since vapor liquid equilibrium data for this system have not been

established. Also the sampling is done from the liquid phase. Thus at small conversion, the accuracy of the gravimetric method may be limited.

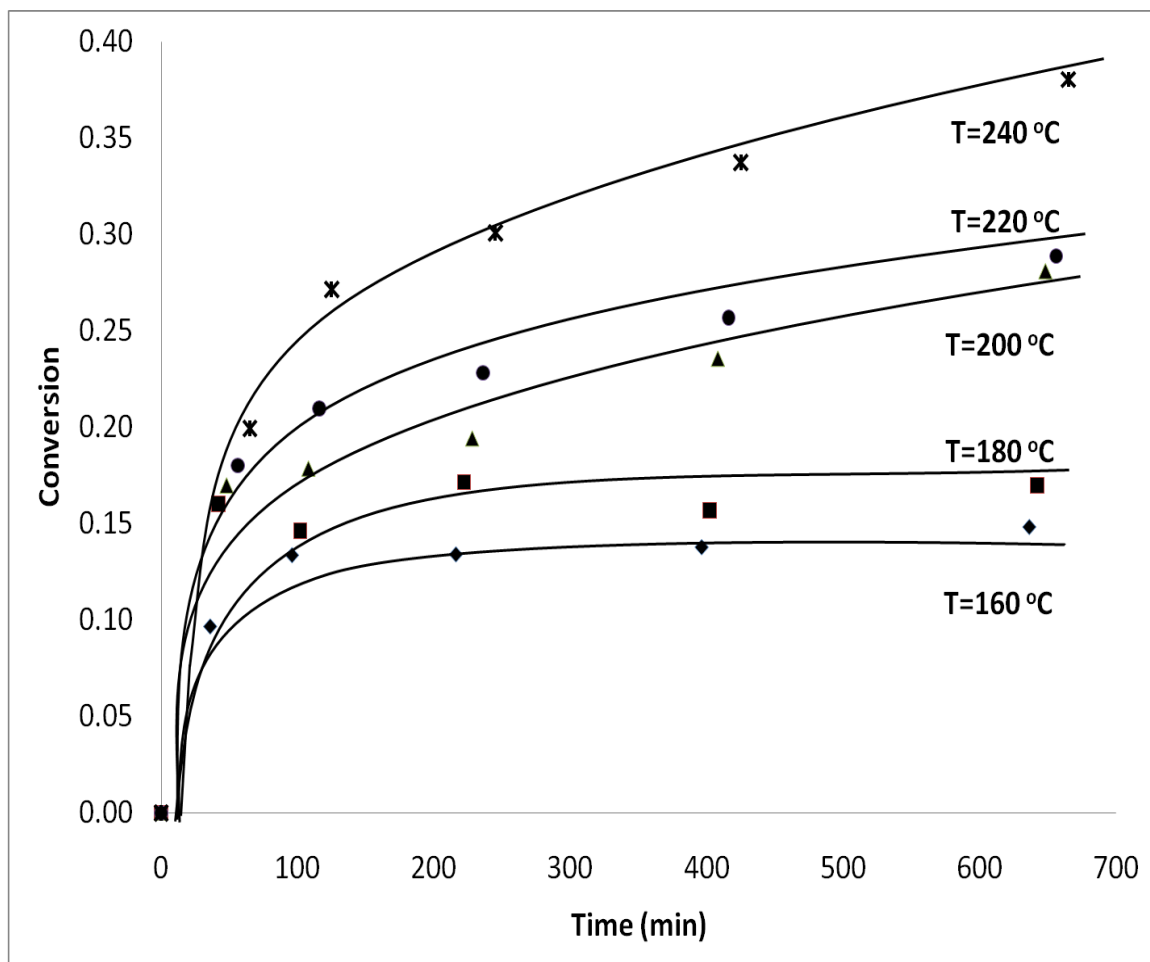


Figure 6.2 Conversion of silane with time - as determined by TGA (soy: silane ratio = 1:5 mole, 1 wt% peroxide)

From the plots however, it can be seen that a good control on the extent of silylation can be achieved by varying the time and temperature of the reaction.

The effect of silane ratio on the extent of silylation has been presented in Table 6.1. It can be seen that for the same amount of peroxide used, higher silane ratios yield higher silylated products. In the case of 1:15 ratio of silane, it can be seen that ~7.5 moles of silane has been incorporated into the product.

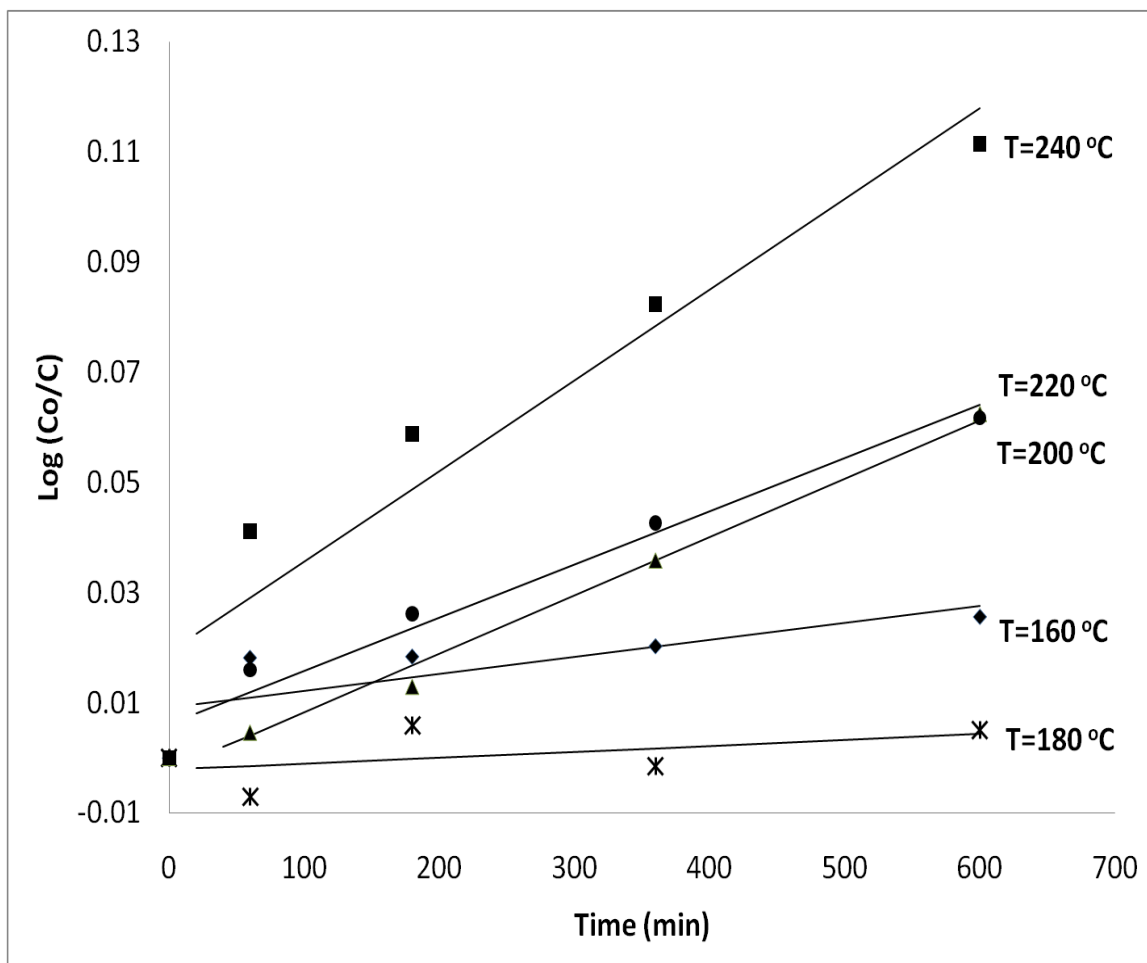


Figure 6.3 First order plot for the consumption of silane (soy: silane ratio = 1:5, 1 wt% peroxide)

It can thus be seen that the bio – based content of the product can be varied widely based on time, temperature and silane ratio employed. The effect of peroxide is

also summarized in the last entry of Table 6.1. The conversion does seem independent of the peroxide at least in the highest silane ratio employed. This is in stark contrast to the results we have obtained with methyl oleate as the starting fatty acid ester (Chapter 7), where the conversion was reduced by half. We postulate that the high reactivity of the bis allylic protons in linoleic and linolenic acid present in soybean oil lead to reactions with silane regardless of the use of peroxides.

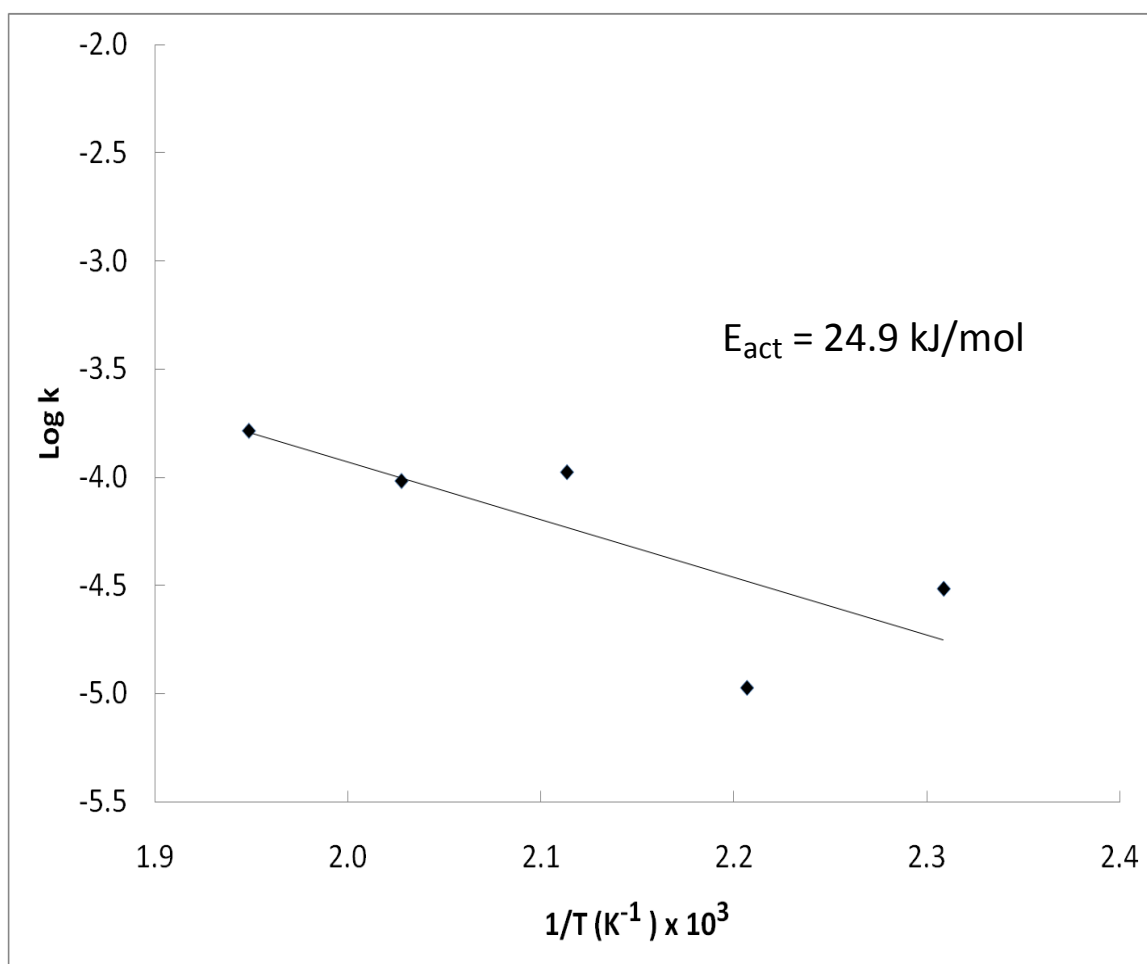


Figure 6.4 Arrhenius plot of $\text{Log } k$ Vs $1/T$

Table 6.1. Conversion, Iodine value and double bond reduction for silylated soybean oils

Entry	Ratio ^a	Temperature	Time (hrs)	Conversion (mol silane/mol oil)			Area ratio ^f	Iodine value ^g
				TGA ^b	Gravimetry ^c	NMR ^d		
1	1:5	160 °C	10	0.80	-	-	-	-
2	1:5	180 °C	10	0.90	-	-	-	-
3	1:5	200 °C	10	1.46	-	-	-	-
4	1:5	220 °C	10	1.50	-	-	-	-
5	1:5	240 °C	10	1.96	-	-	-	-
6	1:3	260 °C	6	-	1.33	1.31	1.15	128
7	1:5	260 °C	6	-	2.01	1.97	1.15	115
8	1:7	260 °C	6	-	2.36	2.31	1.13	108
9	1:11	260 °C	6	-	5.51	4.01	0.975	46
10	1:15	260 °C	6	-	6.93	6.25	0.850	65
11 ^e	1:15	260 °C	6	-	6.91	6.19	0.860	66

a – Soybean oil: Silane (mole: mole); b – Isothermal TGA run using ~ 30 mg sample at 160 °C for 20 minutes; c – Reduced pressure distillation of large sample (110 °C, 0.3 Torr); d – Ratio of –OCH₃ peak (3.55 ppm) to –CH₂C (=O) proton (1 mole silane/mole oil corresponds to a ratio 9:6); e – No peroxide catalyst; entries 1 – 10 use 1 wt% Luperox 101; f – ratio of –CH=CH– (5.4 ppm) to –CH₂C (=O) (Neat soybean oil has a ratio 10:6 or 1.67); g – determined according to ASTM D1959 on vacuum distilled samples

6.5.2 Mechanism of silane incorporation

Based on the structure of soybean oil and the vinyl silane employed, the following three mechanisms can be postulated for the reaction.

1. An Alder – ENE type reaction, where the unsaturated fatty acids of the triglyceride act as the ENE and the silane acts as the enophile (Figure 6.5).
2. A Diels – Alder type reaction where conjugation of the double bonds in the oil is brought about by the peroxide and the silane acts as the dienophile (Figure 6.6).
3. A peroxide mediated grafting of the silane onto the fatty acid backbone in the oil (Figure 6.7).

The three alkoxy (methoxy) groups attached to the silicone make it an enophile as reported in literature (16-17). It is also reasonable to suppose that the vinyl silane having electron withdrawing groups (Cl or OR) would also behave as a dienophile. Alternatively, the said silane can also react with radicals to give grafting reactions (15, 18-22) as has been demonstrated on a variety of substrates or it could polymerize or copolymerize to a limited extent as established in several works (23-25). Copolymerization has not been postulated since free radical copolymerization of vinyl silane has been reported with only reactive monomers and we have not encountered any previous literature on copolymerization of vinyl silanes with unreactive monomers like soybean oil. Homopolymerization of silane is also limited and reported to occur only under near perfect conditions, and has been reported only for the triethoxy derivative (23). Soybean oil or its conjugated variant have been shown to copolymerize with

monomers like acrylonitrile, styrene, divinyl benzene and cyclopentadiene (6, 26). However, strong cationic initiation for soybean oil seems essential, while the conjugated derivative works with peroxides.

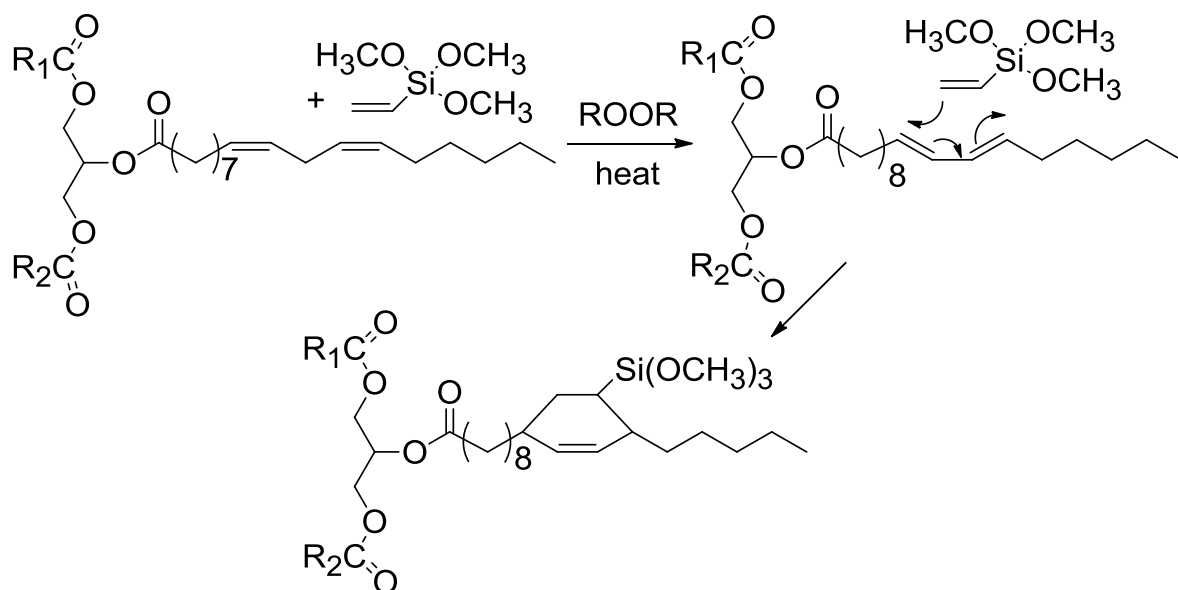


Figure 6.5 Diels – Alder reaction between conjugated linoleate fragment and vinyl silane

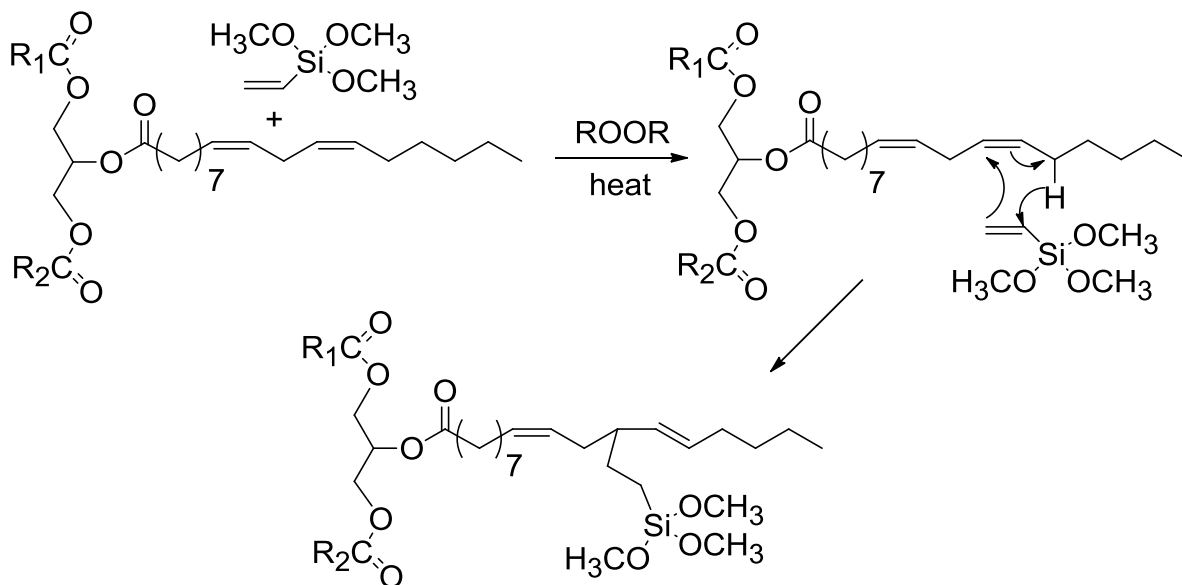


Figure 6.6 Alder – ENE reaction between linoleate fragment and vinyl silane

It can be noted from the schemes that the Alder – ENE pathway would yield a product with one double bond less than the starting materials (the vinyl group of the silane is reduced). However, the double bonds on the soybean oil are unaffected. From the Diels – Alder pathway, it can be seen that there is a net reduction of two double bonds and one double bond on the soybean oil is reduced. The Diels – Alder pathway also has an intrinsic limitation that conjugation needs to occur on the linoleic and linolenic fragments and the number of moles of silane that can react in that fashion is restricted to one per conjugated double bond.

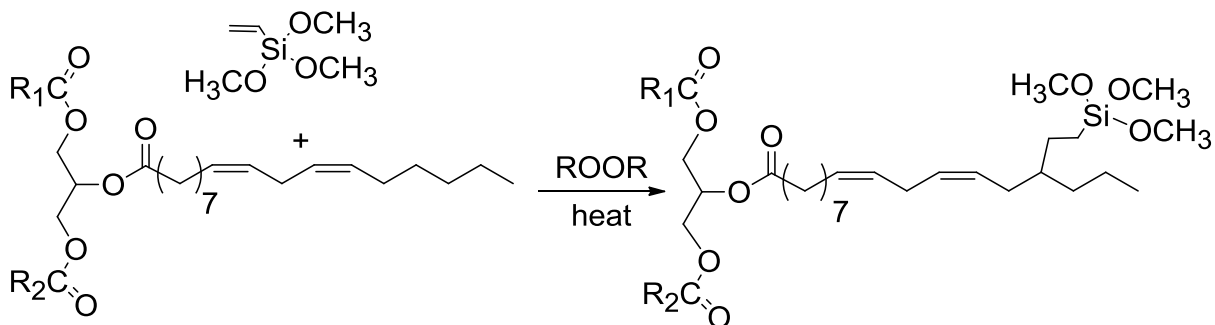


Figure 6.7 Peroxide mediated grafting of vinyl silane to linoleate fragment

The peroxide mediated grafting would lead to products similar to those obtained via an Alder – ENE pathway; the double bonds on soybean oil would remain unaffected. The structures formed by copolymerization of the oil with the vinyl silane, would result in products, where there is a loss of double bonds on soybean oil and vinyl silane, to the extent both are present in the copolymer. A homopolymerization of the silane alone would lead to a product where the oil exists in a mixture with the polymer.

The iodine values of the samples of silylated soybean oil (after removal of unreacted silane) are listed in Table 6.1. It is easily seen that iodine value (a measure of unsaturation) easily distinguishes between a Diels – Alder type product and other products. Since an additional double bond in soybean oil (assumed to conjugate at high temperature in the presence of peroxide) is consumed, the corresponding decrease in iodine value should be easy to observe. From the iodine values it can be easily established that the major products formed are either Alder-Ene or the peroxide mediated pathways.

The proton and carbon NMR spectra for the sample (Entry 5, Table 6.1) are provided in Figures 6.8 and 6.9. The assignments for the oil have been made from reported literature on fatty acid residues (27-29) and silylated hydrocarbons (19, 21). From these spectra it can be seen that very little cyclics indicative of a Diels – Alder product are found (expected at 5.9 ppm, 135ppm). While the proton spectrum shows broad resonances at 5.9 ppm, the carbon spectrum does not show the corresponding carbon, probably due to low concentration. A very small amount of residual silane is observed (e.g. vinyl group at 6 ppm in the proton spectrum and at 138 ppm in the carbon spectrum), most likely due to hydrolysis of the methoxy groups and subsequent condensation to yield high boiling point siloxane species that could not be removed by distillation. The amount of these siloxanes is however insignificant and their presence would not affect the property of the network after cure.

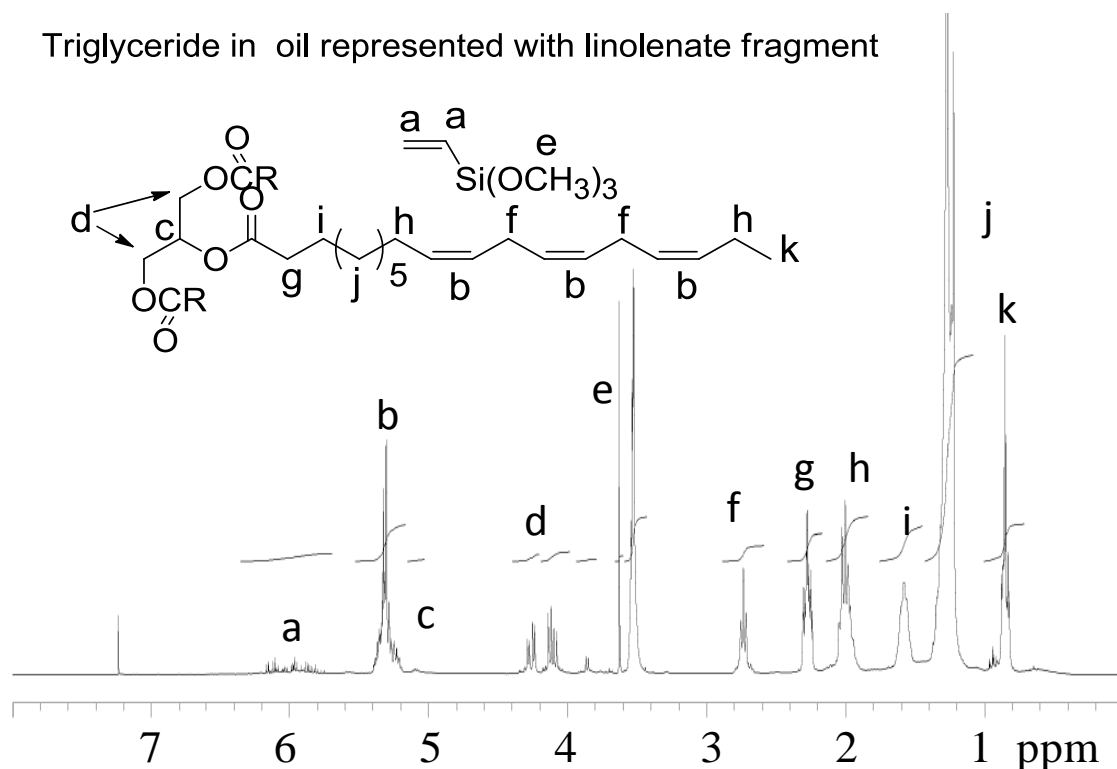


Figure 6.8 ^1H -NMR spectrum of silylated oil (Table 6.1 Entry 5) with peak assignments

While the iodine value data seem to point to an ENE mechanism, it is also seen from the carbon NMR that a new methane ($-\text{CH}$) group that would be expected to form at around 46 ppm is not seen at all. This would seem to indicate that whatever silylation happens predominantly happens through a peroxide mediated route. Since iodine values would be incapable of providing any distinction between the ENE product and grafted product, NMR helps in postulating the best possible mechanism. From the integration of the proton NMR spectra for the samples synthesized at 260 $^{\circ}\text{C}$, it was found that increasing silane ratios lead to a significant reduction of the olefinic protons at 5.4 ppm; their area relative to the protons alpha to carbonyl are reported in Table 6.1.

Triglyceride in oil represented with linolenate fragment

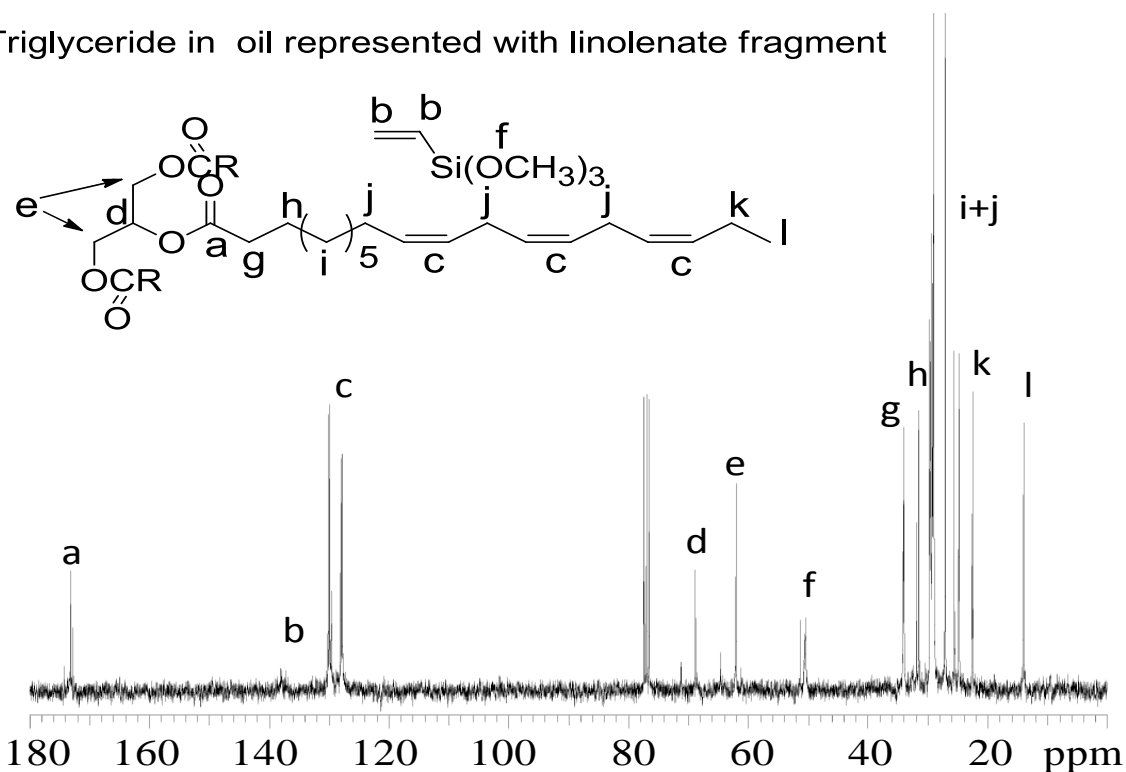


Figure 6.9 ^{13}C - NMR spectrum of silylated oil (Table 6.1 Entry 5)

It can be seen that for the highest silane ratio (1:15), the protons are reduced to half of their area in soybean oil. The stacked spectra for samples with increasing silane ratio are provided in Figure 6.10 and 6.11. This would not be expected for an ENE pathway or a peroxide grafting route. This reduction is not apparent from the iodine values of the samples listed in Table 6.1. The iodine values were close to what would be the case with an ENE product. We believe this to be a consequence of the residual vinyl groups of the silane and presence of moisture due to sensitivity of silane to moisture. An explanation for the above can be tendered as follows. There are three active proton sites in the triglyceride – proton alpha to carbonyl (on the acid side), the allylic and bis allylic protons. The radicals formed by peroxide decomposition, can theoretically

abstract protons from all three sites. However, the bis allylic sites are the most active followed by the allylic site. Thus proton abstraction occurs from these sites preferentially. Proton abstraction from the bis allylic site can lead to conjugation, which would explain the small amount of cyclics formed.

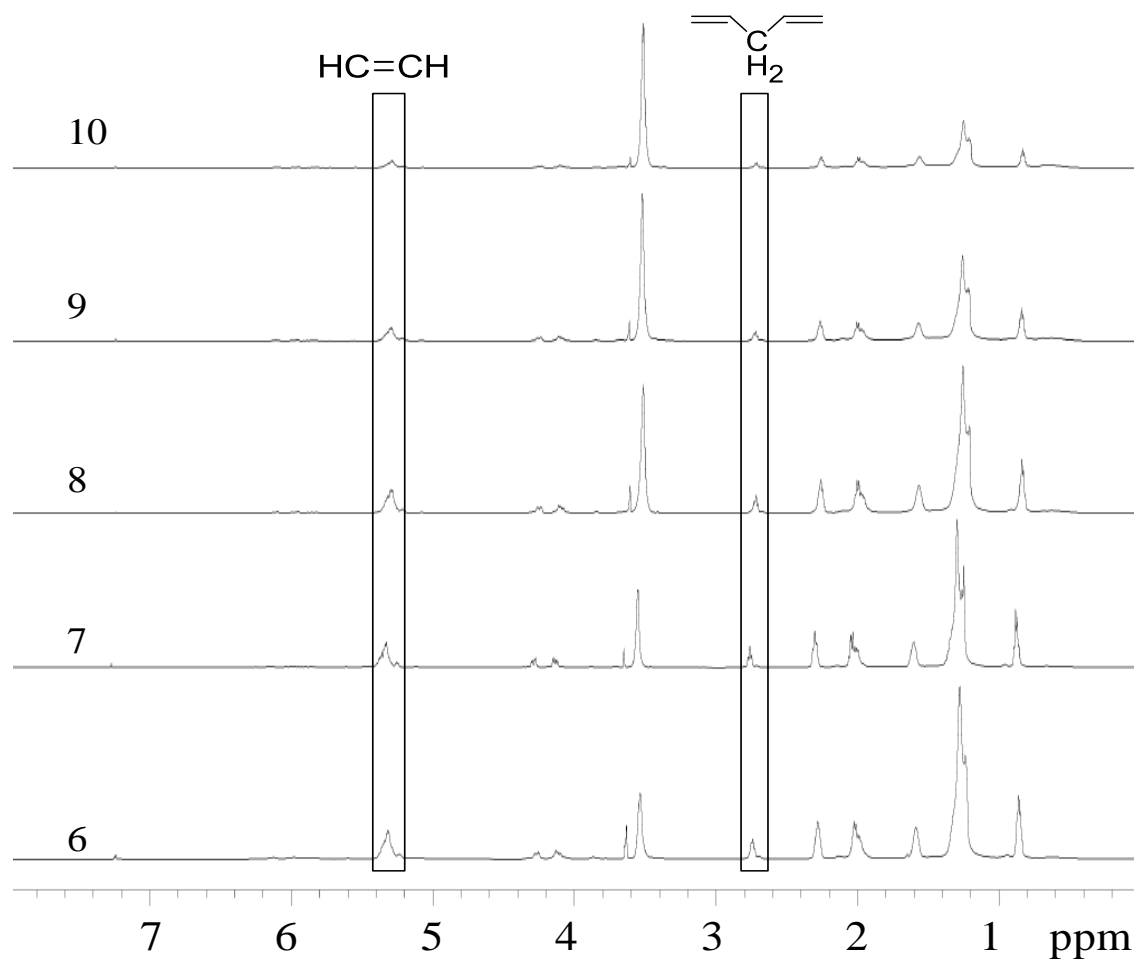


Figure 6.10 Stacked ^1H - NMR spectra of samples (Table 6.1: Entries 6 – 10)

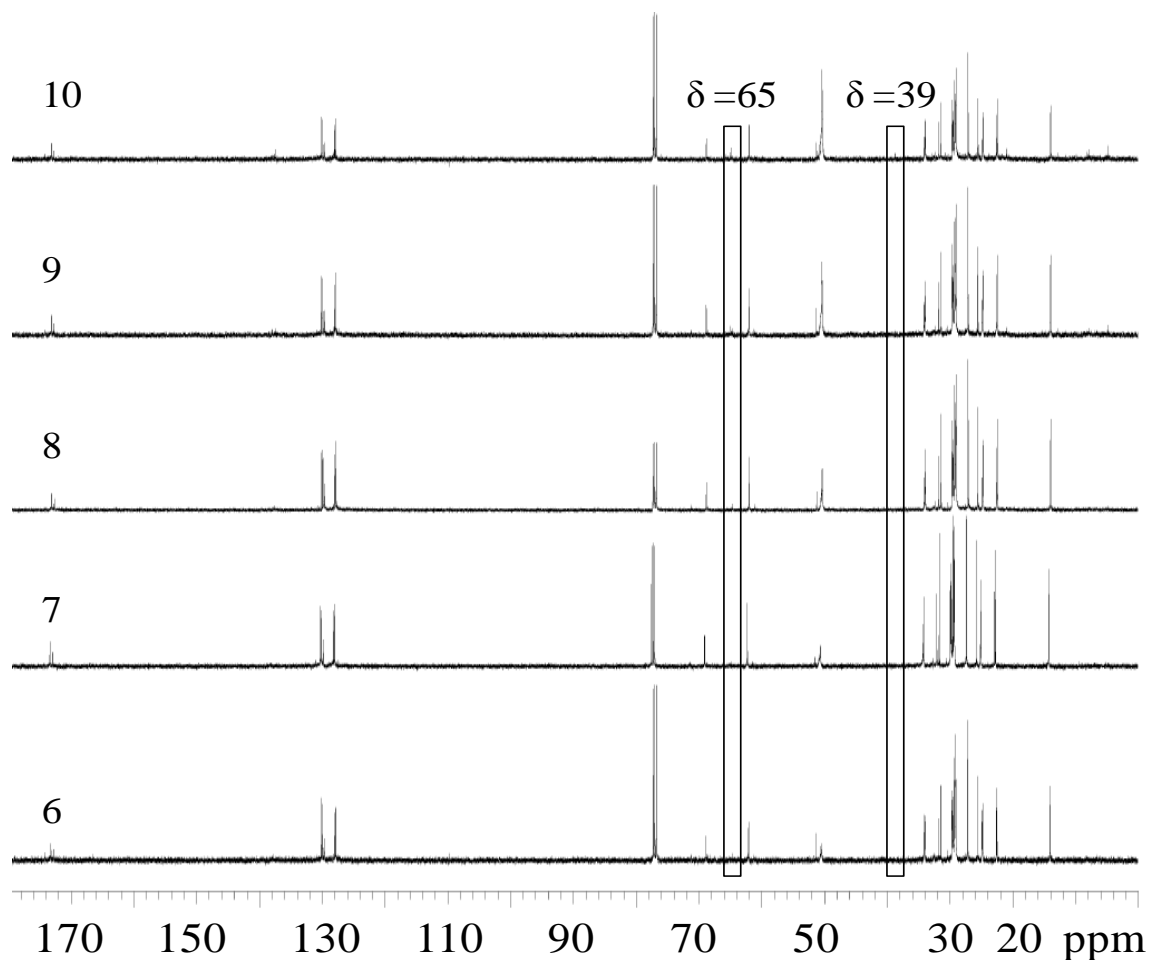


Figure 6.11 Stacked ^{13}C – NMR of distilled samples (Table 6.1: Entries 6 – 10)

Also polymerizations of vinyl monomers in fatty esters (30) and polymerization of vinyl and allyl fatty esters (31-32) leads to low conversions with increasing double bonds in the ester backbone. In the present case, the decrease in double bonds can be explained by a similar mechanism, where the double bonds of linoleate and linolenate fragments act as chain terminators for a growing chain of vinyltrimethoxy silane oligomer. Alternatively, because of the high reactivity of the allylic and bis allylic protons, radical formation by thermal means can also promote the silylation, especially

at high temperatures and higher silane ratios. This could also explain why the peroxide has little effect on the conversion for the case of 1:15 silane ratio.

However, a clear distinction between peroxide grafting and polymerization cannot be made, as the carbon shifts associated with both reactions would be the same ($\delta \leq 34$ ppm changes to 39 – 46 (21) ppm for methylenes; $\delta = 130$ ppm changes to 39 – 42 ppm for vinyl carbons). It has been reported that peroxide grafting often leads to multiple grafts of silane due to intramolecular radical transfers (19, 21). These should result in downfield shifts to beyond 40 ppm – however the NMR for the highest silane ratio shows peaks only at 38 ppm and 64 ppm, indicating multiple grafts do not occur in our system. However, the 64 ppm carbons should be a result of radical transfer to the methoxy group of the silane as mentioned in the work of Forsyth et al. (19). The postulated mechanism is outlined in Figure 6.12.

Also for the 1:15 ratio sample, the ^{13}C – NMR shows peaks at 4 and 8 ppm.

These indicate carbons adjacent to silicon. Grafting should not give rise to such low chemical shifts, since the point of attachment would be a deshielding methine. Such chemical shifts can be expected, when there is oligomerization of the silane. This would then fall along the chain termination by the double bonds mechanism.

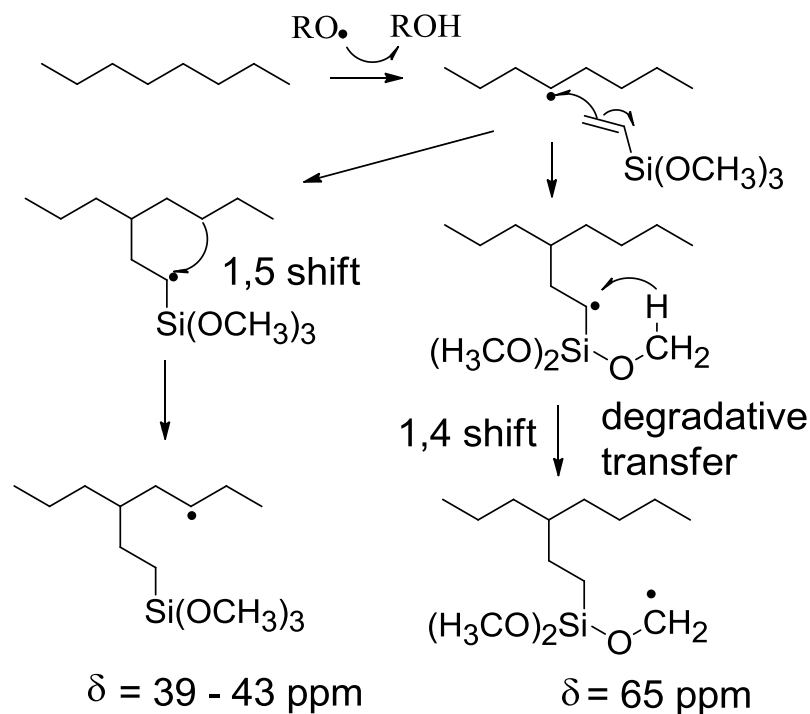


Figure 6.12 Postulated mechanism for the origin of peaks at 39 ppm and 65 ppm (Adapted from (19))

6.5.3 Gel content and cross – link density

The gel content and the solvent uptake ratio are provided in Table 6.2. The solvent uptake ratio is simply defined as “the amount of solvent taken up by a swollen gel” and was calculated using the following equation:

$$\text{Solvent uptake ratio} = \frac{W_s - W_{gel}}{W_{gel}}$$

Where W_s – Weight of swollen gel and W_{gel} – Weight of dry gel

The uptake factor is an indication of the cross – link density of the gel. Highly cross – linked gels do not swell in solvents and thus have low uptake factors. It is desirable to have high gel content and low solvent uptake factors. The mechanism by which network formation occurs is presented in Figure 6.13.

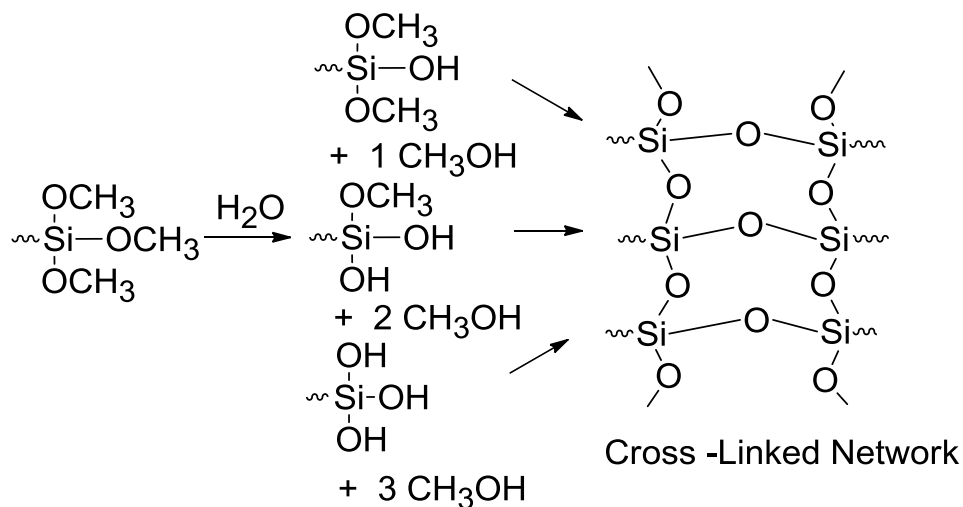


Figure 6.13 Moisture cross – linking of silylated oil

Table 6.2 Gel content and solvent uptake ratio for cured silylated oils (Cure temperature: 75 °C) after extraction with chloroform (72 hours)

Entry	Gel content (%)	Soy oil content ^a (%)	Solvent uptake ratio	Area ratio		
				$\delta = 3.6 \text{ ppm}^b$	$\delta = 4.3 \text{ ppm}^c$	$\delta = 5.4 \text{ ppm}^d$
6	70 ± 1.6	81.5	3.8	0.35	0.45	0.29
7	77 ± 4.9	74.5	2.9	0.29	0.46	0.32
8	84 ± 0.4	71.4	3.1	0.31	0.43	0.27
9	89 ± 1.8	51.6	1.8	0.40	0.42	0.21
10	90 ± 1.0	45.9	0.6	0.42	0.36	0.20
11 ^e	91 ± 0.6	46	0.9	0.29	0.43	0.21

a – theoretical oil content estimated from gravimetry

b – ratio of multiplet at 3.6 ppm to the $-CH_3$ peak at 0.8 ppm

c – ratio of glyceride protons at 4.1, 4.3 ppm to $-CH_3$ peak at 0.8 ppm (ratio in soy oil is 4:9 or 0.44)

d – ratio of vinyl protons at 5.4 ppm to $-CH_3$ peak at 0.8 ppm (ratio in soy oil is 10:9 or 1.11)

e – sample synthesized with 1:15 soy: silane ratio with no peroxide

From the scheme, it is evident that at least 1 mole of silane per mole of soybean oil is required to achieve gelation and network formation. It can be seen that the gel content is higher for samples synthesized at the highest temperature and silane ratios. The swelling of these gels is also minimal in the solvent. This is a direct consequence of increased silane incorporation in these materials. It should be noted however that all the samples after cure do not possess any free oil and generally cure into a transparent and pale yellow colored material. Thus, even in cases where the gel content is less, there is no exudate of oil that is seen when the materials are cast as films.

The cure conditions have not been optimized at least for evaluation of gel contents. Thus the 90% gel content may not represent the maximum achievable, in this system. In this regard, it is known that silicones cure rather slowly, when the cure is not catalyzed. Also for any cross – linkable system, the cure does not happen, once the T_g of the cured material reaches the temperature at which the curing is done.

The ^1H NMR spectra of the soluble fraction of all the samples (Figure 6.14), showed a mixture of protons of soybean oil and a resonance at 3.6 ppm. The ratio of the fatty acid methyl groups and this peak was nearly constant (3:1). This peak could result from the transesterification of the oil, during the curing (which was done over a layer of water). However, there is no free glycerol or glyceryl protons observed in the spectra. Also the ratio of the fatty acid methyl groups and glyceryl protons was nearly constant (9:4). This would mean that the 3.6 ppm resonance corresponds to the product

obtained by chain transfer to the $-\text{OCH}_3$ group of the silane. It is also seen that the vinyl protons at 5.4 ppm are greatly reduced in the extract (Table 6.2). This reduction can be attributed to the chain termination by the double bonds.

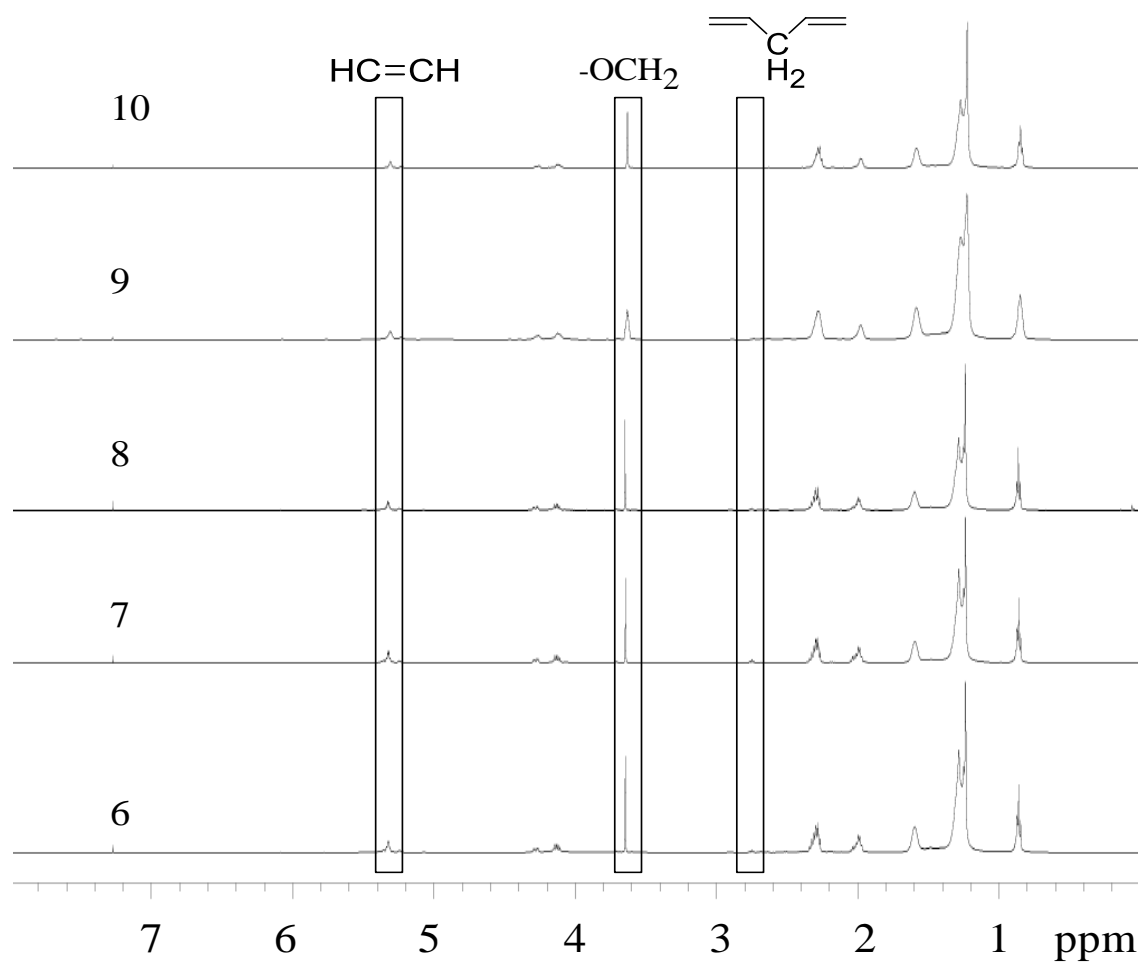


Figure 6.14 ^1H – NMR spectra of soluble fractions (Entries 6 -10)

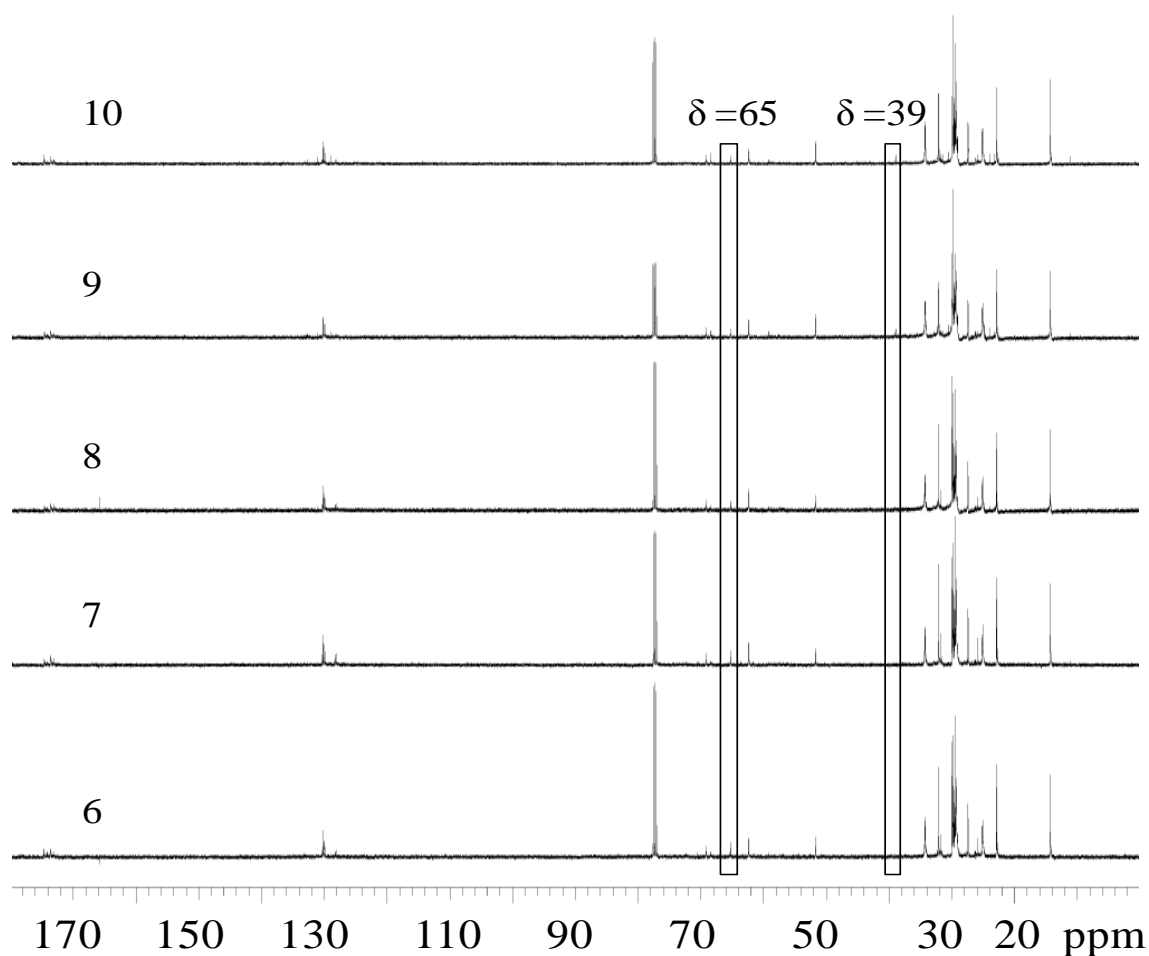


Figure 6.15 ^{13}C – NMR of soluble fractions (Entries 6 – 10)

The ^{13}C NMR spectra (Figure 6.15) also shows corresponding peaks ($-\text{OCH}_3$ at 51 ppm). It should be noted that ^{13}C NMR of the extract (sol) all show peaks at 65 ppm.

This can only be attributed to the product obtained by chain transfer to the $-\text{OCH}_3$ group, since from Table 6.2 and the NMR, it can be seen that there is no transesterification of the oil with the methanol by product. Also peaks corresponding to

glycerol or monoglycerides are absent (63 ppm, 72 ppm). Thus the NMR clearly shows that the extract is largely composed of unreacted soybean oil and chain termination products of VTMOs oligomers.

The extracts also show peaks at 39 ppm, 58 ppm in addition to the peak at 65 ppm. This would mean that some grafted material does not involve in network formation. The peak at 58 ppm is most likely due to epoxidation of the oil by air. Fractionation of the distilled oil and the extracts should provide additional information on the species that are formed during the silylation and curing process.

6.5.4 Cure kinetics

The curing mechanism of polyfunctional alkoxy silanes is illustrated in Figure 6.13. It is evident that moisture (water) is an important component of the curing process, since it is essential to hydrolyze the silane to silanols. It has also been established that catalysts can accelerate the curing process; tin catalysts particularly are favored. In addition, titanium compounds, amines also have been shown to catalyze the cross – linking reaction.

The cure kinetics of silane grafted polymer systems have been reported in literature. In particular Sen et al. (15) have reported moisture and catalyst concentration to influence the cross – linking as a first order process. Thus the curing rate is directly proportional to the amounts of these two components. Catalysts like dibutyltin dilaurate are postulated to accelerate the cure due to their strong Lewis acid

character. Since the cure kinetics was evaluated viscometrically, the effect of moisture was studied by using water directly in the formulation. Temperatures were also maintained in a range where the liquid would not display vigorous bubbling (due to elimination of volatiles) that could affect the viscosity measurements.

Typical catalyst loadings found in literature are of the order of 0.1 to 0.01 phr. However to observe the cure in a very short span of time, catalyst loading 100 times higher has been used in the experiments. The effects of moisture, catalyst and temperature have been presented in Figures 6.16 – 6.18. Conventional cure of silicones is often accomplished in a matter of hours or days. Since in our case, we wanted to test the utility of oil as a coating material, it was desirable to have rapid setting times and thus experiments were performed to see if the cure could be accelerated to satisfy time constraints involved in operations like paper coatings.

Accordingly, the effect of catalyst and added water were studied first. The temperature to study these effects was set at 65 °C. This temperature was close the boiling point of the methanol by product and cure times at this temperature were within a reasonable, observable range. Once an optimum catalyst and water concentration were determined, temperature effect was studied at this optimized catalyst and water concentration. It should be noted that all the measurements were conducted on one sample of oil (240 °C, 1:5 ratio). The effect of silane concentration has not been evaluated and it is postulated that samples with increased silane incorporation

would generally cure faster. The cure rate can generally be expressed as a slight modification from Sen et al. (15):

$$\frac{dX}{dt} = k C_w^a C_c^b C_s^c$$

where: C_w – concentration of water; C_c – concentration of catalyst; C_s – concentration of silane; k – Rate constant; a, b, c – order of cure reaction with respect to individual components

In the present case the last term of the equation is constant and hence can be incorporated into the rate constant. However, it is clear that for samples with different silane content, the curing rates are bound to differ due to the last term of the equation. It is expected that under similar conditions higher silane content oils would cure faster.

6.5.4.1 Effect of catalyst

The cure rate is directly proportional to the catalyst concentration as seen from the curve presented in Figure 6.16. It can be seen that onset of cure is reduced with increasing concentration. However, since the plot is exponential, in nature, rate of change of viscosity cannot be employed to see the effect of catalyst concentration on cure rate. Also the 3 phr catalyst concentration seems to cure at a rate slower than the rest. Sen et al. have reported a linear dependence on catalyst concentration; the regimes in which our experiments have been carried out are different. However, it can be seen from the curve that for the mixture to reach the same viscosity (“Isoviscous”

state) after the viscosity build up, the time required with each catalyst concentration (4, 5, 6 phr) linearly decreases. If this state of shear viscosity can be taken as a measure of cure or network formation, then a degree of linearity does exist with regard to catalyst concentration, with respect to the 4, 5 and 6 phr concentrations.

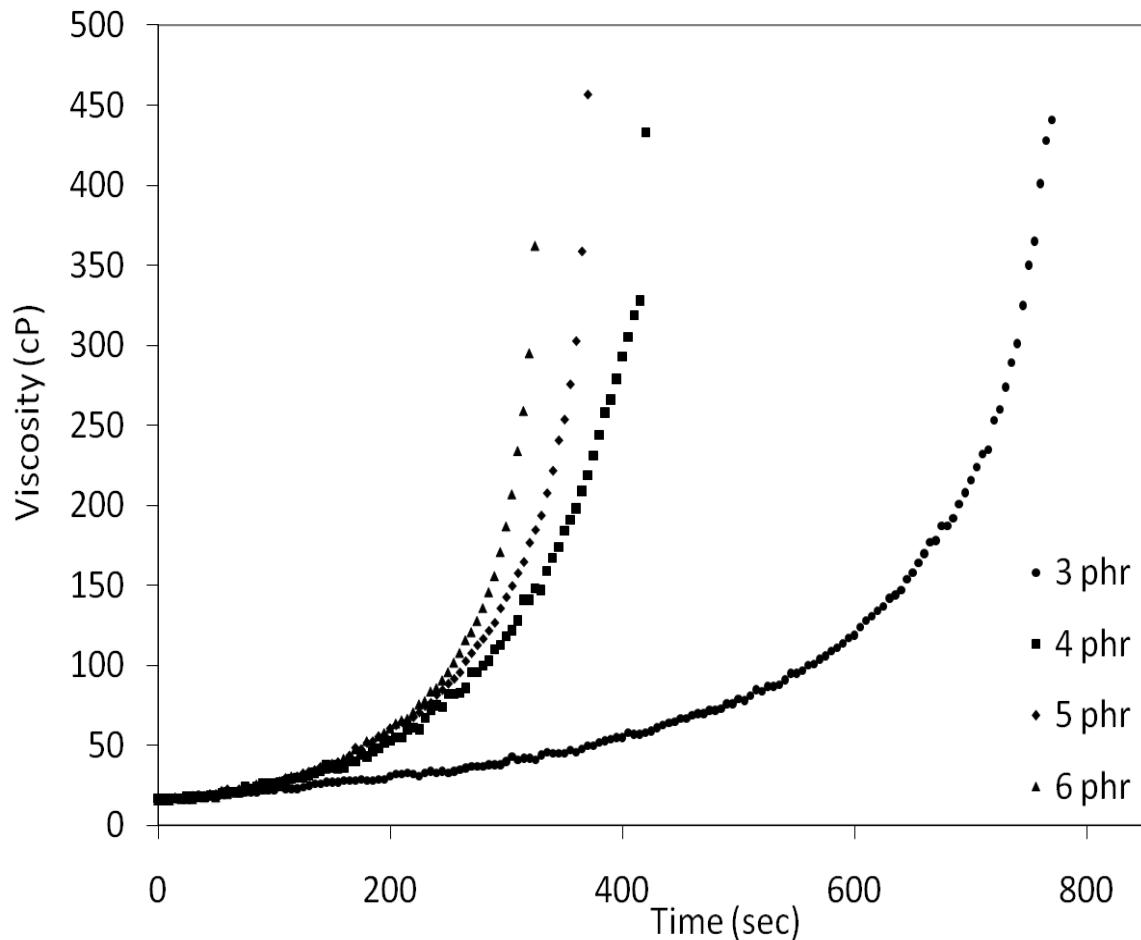


Figure 6.16 Effect of DBTDL catalyst on cure rate (4 phr water, T= 65 °C)

6.5.4.2 Effect of water

The presence of water has a similar impact on the cure rate (Figure 6.17). However, unlike the catalyst case, at 3 phr of water the cure seems to progress linearly within the time frame of measurement and we do not observe a viscosity build up. At higher concentrations, the onset of cure rapidly decreases and exhibits a behavior similar to the catalyst.

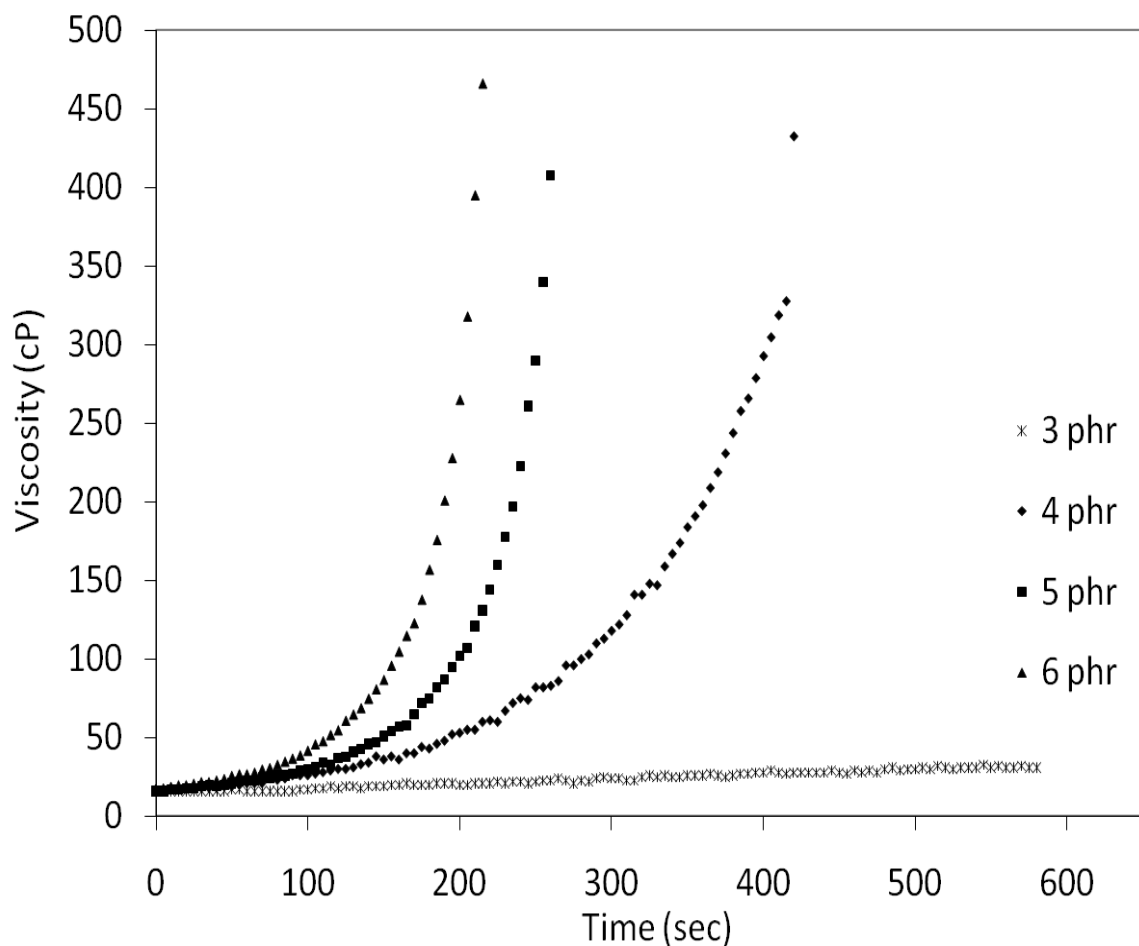


Figure 6.17 Effect of water on cure rate (4 phr DBTDL, T= 65 °C)

6.5.4.3 Effect of temperature

In comparison to the catalyst, the temperature plays a relatively significant role in the cure process (Figure 6.18). This can be attributed to the fact that the catalyst and water are in high enough concentrations that the perceivable effect from temperature decreases. The effect is still visible from the plots, but is rather small. It should however be emphasized that temperature would be critical for removal of the byproducts from the cure, namely water and methanol. Thus, even when the catalyst and water were added in optimum quantities at room temperature, the change in viscosity was not very high (not reported) and the material was a deformable viscous fluid, as opposed to the solids that resulted in a matter of minutes at high temperature.

The higher loading of catalyst and water results in rapid cure times, which can be exploited especially in paper coatings. Ideally to avoid the use of such high catalyst loadings, the material could be pre cured with water to a certain viscosity level and final cure accomplished post application on to a substrate.

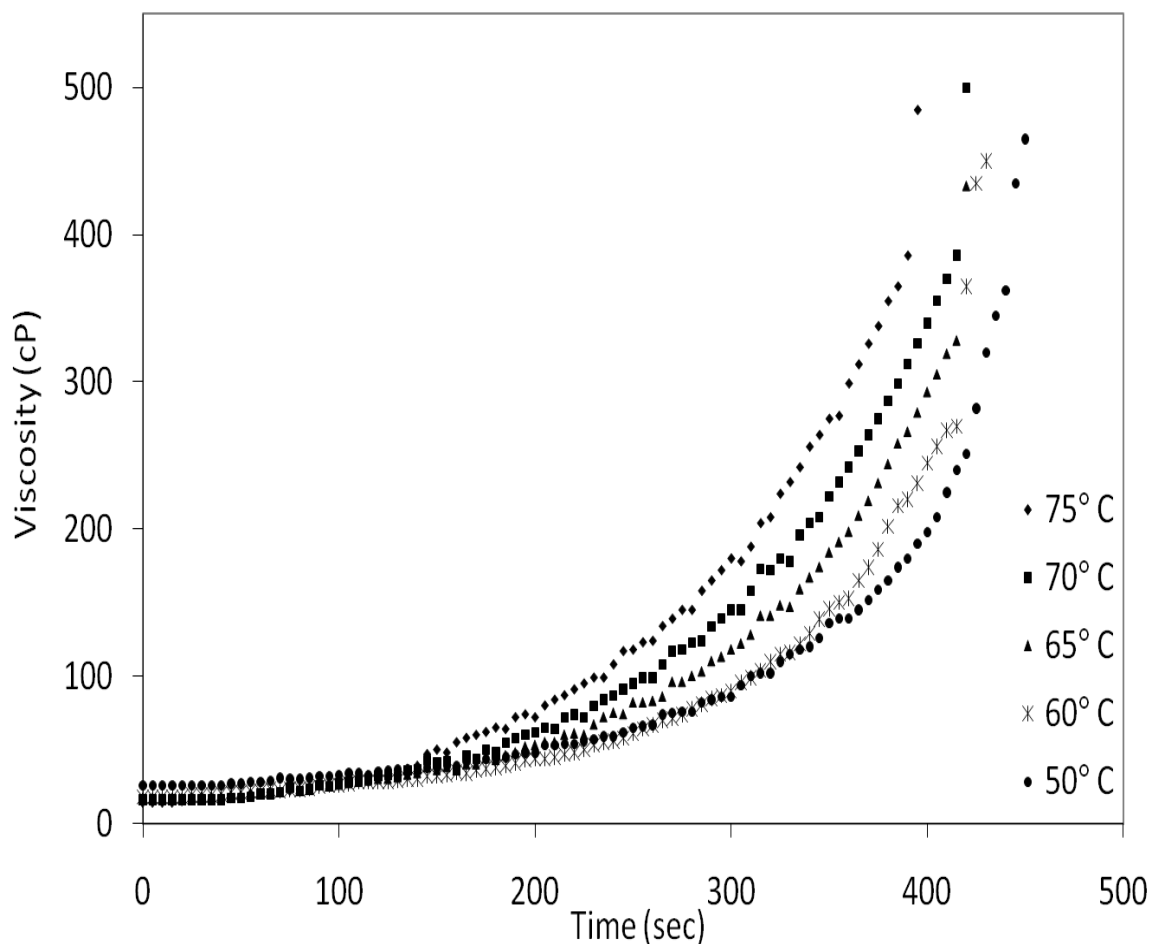


Figure 6.18 Effect of temperature on cure rate (4 phr water & DBTDL)

6.6 CORROSION TESTING ON COATED METAL PANELS

6.6.1 Formulation of coating

Five corrosion inhibitors (Armeen O: Dimer acid 1:1, THE, CIC, V and 93) were used to formulate the silylated oil. The corrosion inhibitors were used at 1, 2, 3 phr respectively. Additionally to effect the cure in a reasonable time frame, 2 phr of catalyst was used. The silylated oils selected for the coating formulation was the 1:15 ratio

product, since it had the highest silane content and hence was expected to cure into a hard coating. The oil, corrosion inhibitor and catalyst were mixed for 10 minutes in a vial using a magnetic stirrer at high speed, to yield a homogeneous mix. This mix was then drawn on to metal panels, treated using the procedure mentioned earlier and allowed to cure at ambient temperature.

It was found that all the panels cured to give transparent coatings of good gloss and hardness. However, cracks appeared in all the panels within a week of application and propagation of the cracks lead to peeling of the coating from the metal surface. A characteristic initial cracking pattern and the ultimate cracking are shown in Figure 6.19. Of the corrosion inhibitors used corrosion inhibitor “93” cracked last. This behavior was seen even when no corrosion inhibitor was used and when the catalyst was reduced to 0.5 phr. It was deemed that the cross – link density was too high and the shrinkage associated with the curing reaction caused excessive stresses on the coating leading to cracking. Also room temperature cure often lead to a thin film of moisture on the surface of all panels and in some cases small bubbles inside the coating. Since these bubbles could act as defects for cracks to initiate, it was decided that curing would be done at 65 °C which would eliminate volatiles more efficiently.



Figure 6.19 Initial cracking (Top) and complete cracking (bottom) of panel coated with 1:15 silylated oil, 0.5 phr DBTDL

Thus the silylated oil with 1:7 mole ratio was chosen as the coating material. Also since the structural details or composition of the corrosion inhibitors was unknown, it was decided that corrosion inhibitor “93” would be used at its highest concentration,

since cracking was observed last. Also since corrosion testing was involved, the catalyst which was tin based was also excluded and curing was done in the absence of catalyst. Cure was typically complete in 24 hours, but an additional 24 hours of time was provided to ensure the maximum extent of cure.

Since curing was done in a convection oven, there was some oxidation of the oil and the corrosion inhibitor. Thus the coatings look dark yellow, but transparency was still retained. The coated panels prior to testing are shown in Figure 6.20. Two sets of panels were made – for regular corrosion testing in a humidity chamber and filiform corrosion testing in a salt spray chamber. For each coated panel, an uncoated panel and panel coated with the neat oil (no corrosion inhibitor) were employed as controls.

The results of the test are provided in Figures 6.21 and 6.22. It can be seen that the salt spray chamber produces severe corrosion in as little as 91 hours. For a coating to qualify as a temporary protective coating, the time period to resist salt spray is typically counted as 168 hours (7 days). Thus in the present case, the coatings exhibit a little resistance to salt spray corrosion. It should be noted however that the panels with no corrosion inhibitor seem to perform marginally better. The cause for this could be the incompatibility between the inhibitor and the coating material, which leads to premature cracking of the coating under the salt spray.

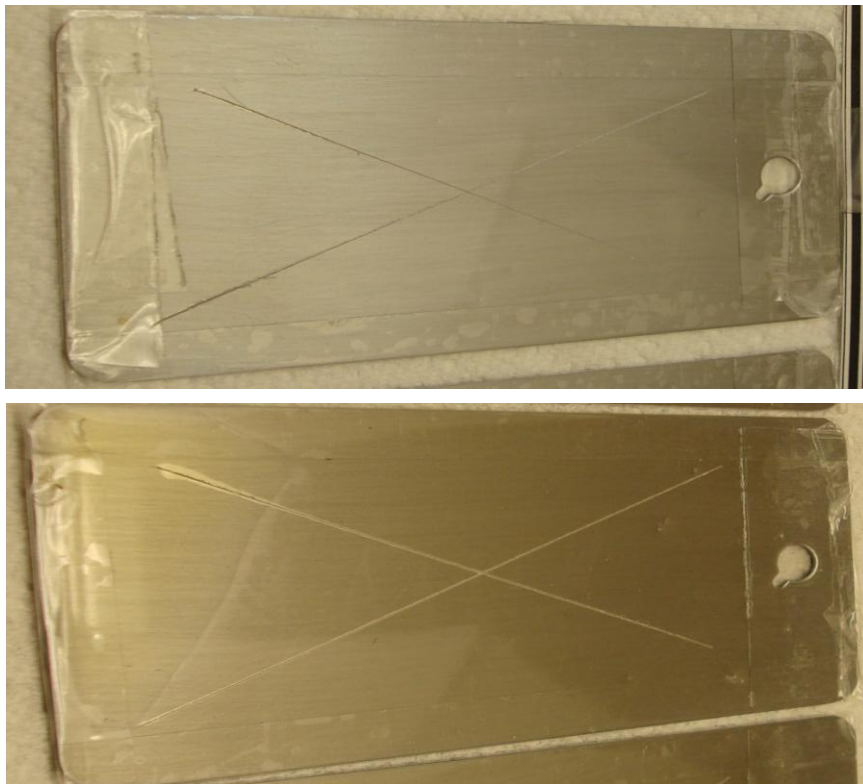


Figure 6.20 Panels before testing (filiform corrosion); No corrosion inhibitor (Top), 3% Corrosion inhibitor "93" (Bottom)

The humidity chambers yielded better results. In this case the coatings maintained their integrity for 144 hours in the chamber without significant corrosion. It can be seen that the blank panels also are marginally better than the panels with corrosion inhibitor. The coated panels with no corrosion inhibitor show no corrosion in the test area. In order to also test this under laboratory conditions, coated panels as stated above were left in an oven at 95 °C for a period of 300 hours. Humidity was maintained by a trough of water, which was refilled every 24 hours. The coatings showed no cracking or corrosion during this time.

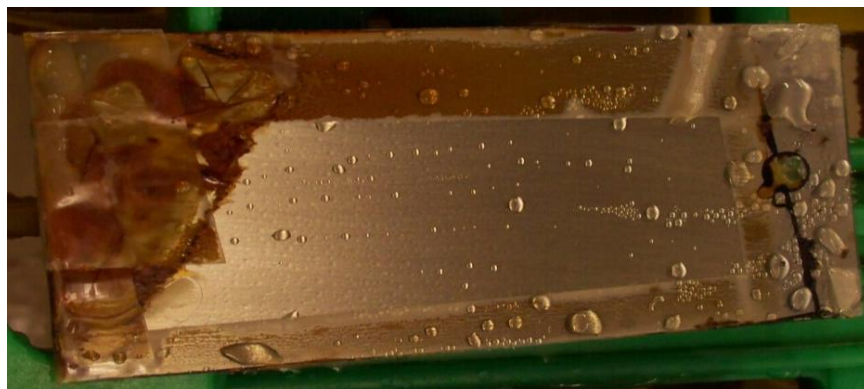
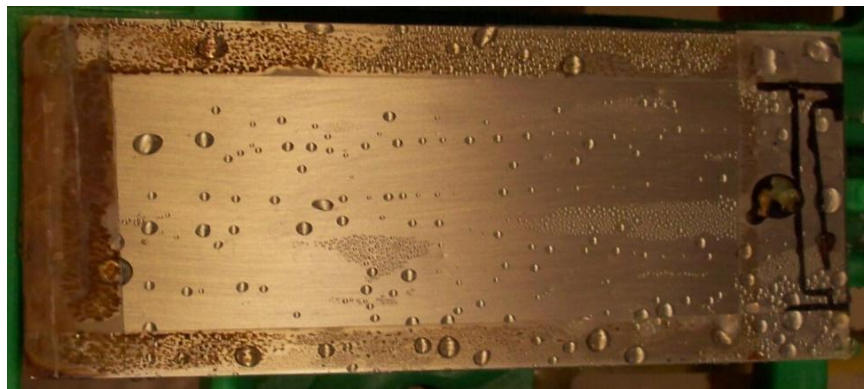


Figure 6.21 Panels after 144 hours in humidity chamber. Blank (Top), Coated - no corrosion inhibitor (middle), Coated - 3% corrosion inhibitor (bottom)



Figure 6.22 Panels after 91 hours in salt spray. Blank (Top), Coated -no corrosion inhibitor (middle) and Coated - 3% corrosion inhibitor (bottom)

It is known that silanes have good adhesion and more so for the case of metallic substrates due to strong M – O – Si type linkages. Thus the performance of the coatings seems to be related to their adhesion to the metal substrate. The WARTM procedure only creates organic functional groups on the surface, which may or may not be conducive to adhesion. Ideally the adhesion should be improved, if Metal – OH groups can be generated on the surface. This would lead to metal – silicate type bonds, which should improve adhesion.

6.7 WATER UPTAKE OF WOOD

The efficacy of the material to act as water repellant for wood is provided in Figure 6.23. It can be seen that porous untreated wood, absorbs about 1.2 times its weight of water in a span of 7 days. Soybean oil was used as a control. In comparison it can be seen that the absorption is cut down to 1/3rd by the silylated oil. While soybean oil also effectively cuts down the absorption, since the oil is not chemically bound to the wood, the effect is likely to temporary. Silanes have been used as coupling agents for wood based fillers. The same effect would operate in this case and the silylated oil would react with any hydroxyl or acid functionalities of wood and remain bound to the substrate, thereby providing a longer lasting effect.

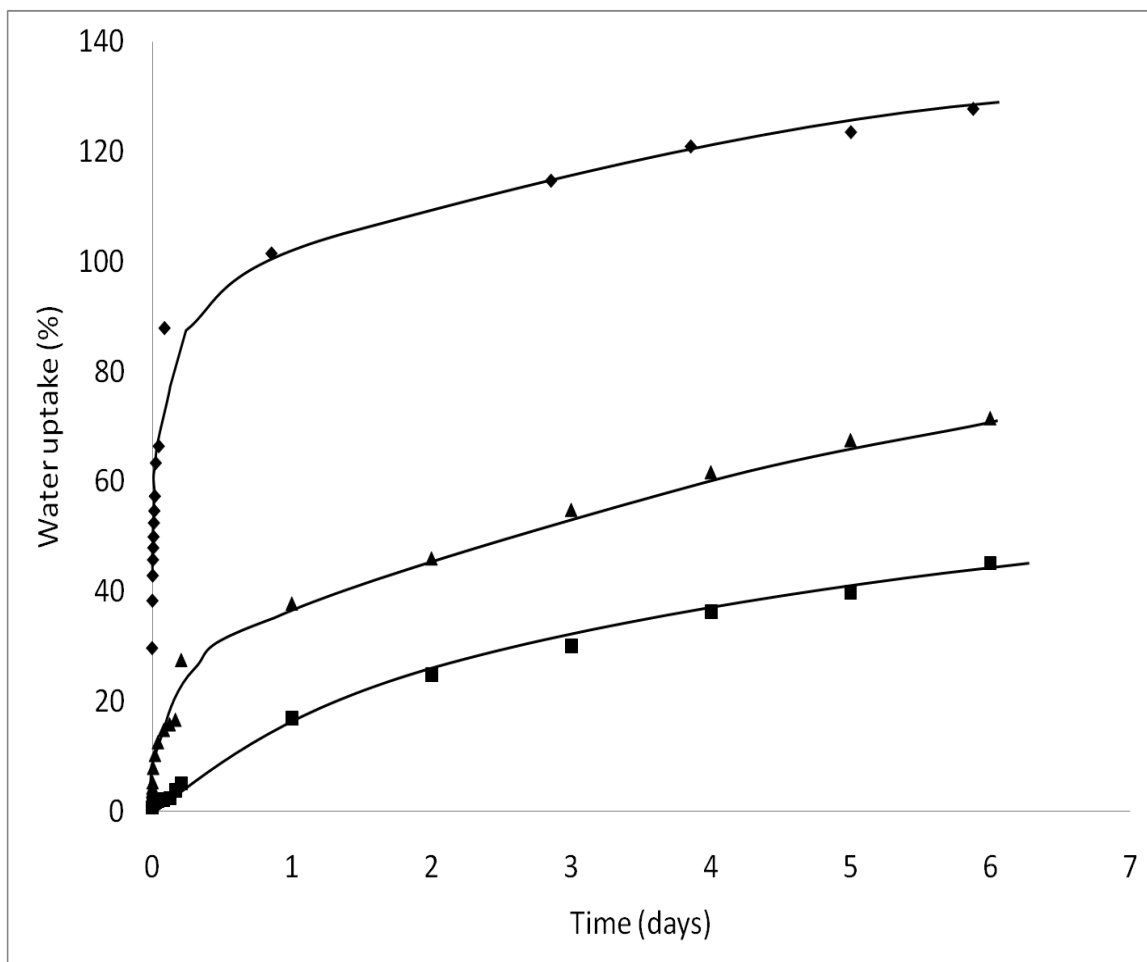


Figure 6.23 Water uptake of wood. Uncoated wood (Top), soy oil coated (middle), silylated oil (1:5 ratio, 240 °C) coated (bottom)

6.8 CONCLUSIONS

We have reported a simple method to react soybean oil with a vinyl silane. The reaction proceeds smoothly at high temperatures in reasonable time to yield silane modified vegetable oils. It is easy to control the extent of silane incorporation, by

varying the temperature, time and ratio of silane employed. The reaction seems to proceed via a radical route and at higher silane ratios, the double bonds of the oil are consumed, indicating a copolymerization of the silane with the oil. The peroxide catalyst does not seem to significantly influence the silane incorporation, especially when the ratio of the silane to the oil is high.

Downstream processing of the material is minimal, with excess silane removal an optional step, depending on end use requirements. The starting materials are fairly inexpensive, providing a low cost room temperature curable material. Also the product has viscosity similar to the starting vegetable oil, which makes the use of this material in coating applications solvent free. The cure rate of the material is strongly influenced by presence of water and catalyst. Temperature plays little role in the onset of cure, but is important in determining the extent of cure.

The silylated oils have good adhesion to paper, wood, glass and steel substrates. The oil when applied to wood improves the water repellency and reduces water uptake of porous wood. The material also acts as an excellent protective coating against corrosion at least under conditions of high humidity. Resistance to salt spray is not good, partly due to its relatively weak adhesion to metal. Proper choice of surface treatment could improve adhesion and lead to better salt spray resistance. Overall, the material in its current form looks promising as a temporary protective coating on metal substrates. We believe the method can be extended to a variety of vinyl functional silanes, enabling the synthesis of a new class of vegetable oil – silicone hybrids.

REFERENCES

6.9 REFERENCES

1. R. Loza, P. McDaniel. (WO Patent WO/2001/040,351, 2001).
2. A. Guo, I. Javni, Z. Petrovic, *Journal of Applied Polymer Science* **77**, 467 (2000).
3. U. Biermann *et al.*, *Angewandte Chemie International Edition* **39**, 2206 (2000).
4. U. Biermann, J. O. Metzger, *Topics in Catalysis* **27**, 119 (2004).
5. P. Tran, K. Seybold, D. Graiver, R. Narayan, *Journal of the American Oil Chemists' Society* **82**, 189 (2005).
6. F. Li, R. Larock, *Journal of Applied Polymer Science* **80**, 658 (2001).
7. J. Baghdachi, D. Li, J. LaForest, *Journal of Coatings Technology* **74**, 81 (2002).
8. M. J. Snyder;, E. S.Lipinsky;, J. E. Burch. (US Patent 3,424,598, 1969).
9. A. Behr, F. Naendrup, D. Obst, *Advanced Synthesis & Catalysis* **344**, 1142 (2002).
10. N. Saghian, D. Gertner, *Journal of the American Oil Chemists' Society* **51**, 363 (1974).
11. A. El Kadib, A. Castel, F. Delpech, P. Rivière, *Chemistry and Physics of Lipids* **148**, 112 (2007).
12. A. El Kadib, N. Katir, A. Castel, F. Delpech, P. Rivière, *Applied Organometallic Chemistry* **21**, 590 (2007).
13. G. Lligadas, L. Callau, J. C. Ronda, M. Galià, V. Cádiz, *Journal of Polymer Science Part A: Polymer Chemistry* **43**, 6295 (2005).
14. W. Kampf;, R. Streck;, H. G. Haag. (US Patent 4,512,926, 1985).

15. A. Sen, B. Mukherjee, A. Bhattacharyya, P. De, A. Bhowmick, *Journal of Applied Polymer Science* **44**, 1153 (1992).
16. A. Laporterie, J. Dubac, M. Lesbre, *Journal of Organometallic Chemistry* **101**, 187 (1975).
17. J. Dubac, A. Laporterie, *Chemical Reviews* **87**, 319 (1987).
18. M. Beltraán, C. Mijangos, *Polymer Engineering and Science* **40**, 1534 (2000).
19. J. Forsyth, W. Baker, K. Russell, R. Whitney, *Journal of Polymer Science Part A: Polymer Chemistry* **35**, 3517 (1997).
20. J. Parent, K. Geramita, S. Ranganathan, R. Whitney, *Journal of Applied Polymer Science* **76**, 1308 (2000).
21. J. Weaver *et al.*, *Journal of Polymer Science Part A: Polymer Chemistry* **46**, 4542 (2008).
22. C. Jiao, Z. Wang, Z. Gui, Y. Hu, *European Polymer Journal* **41**, 1204 (2005).
23. R. Mixer, D. Bailey, *Journal of Polymer Science* **18**, 573 (1955).
24. B. Thompson, *Journal of Polymer Science* **19**, 373 (1956).
25. M. Gorbunova, V. Surkov, M. Fedoseev, *Russian Journal of Applied Chemistry* **74**, 1608 (2001).
26. M. Valverde, D. Andjelkovic, P. Kundu, R. Larock, *Journal of Applied Polymer Science* **107**, 423 (2008).
27. M. Guillén, A. Ruiz, *European Journal of Lipid Science and Technology* **105**, 688 (2003).

28. G. Knothe, J. A. Kenar, *European Journal of Lipid Science and Technology* **106**, 88 (2004).
29. L. Mannina, C. Luchinat, M. Emanuele, A. Segre, *Chemistry and Physics of Lipids* **103**, 47 (1999).
30. S. Harrison, W. Tolberg, *Journal of the American Oil Chemists' Society* **30**, 114 (1953).
31. S. Harrison, D. Wheeler, *Journal of the American Chemical Society* **73**, 839 (1951).
32. H. Teeter, *Journal of the American Oil Chemists' Society* **40**, 143 (1963).

SYNTHESIS AND PROPERTIES OF FATTY ACID METHYL ESTER – VINYLTRIMETHOXY SILANE ADDUCTS

ABSTRACT

Adducts of methyl oleate and vinyltrimethoxy silane were synthesized using an organic peroxide initiator (Luperox 101) in a high pressure Parr reactor. The reactions were carried out at five different temperatures (180 °C to 260 °C in 20 °C increments). In addition, methyl stearate was also reacted with the silane at 260 °C with the peroxide to determine grafting efficiency on saturated fatty acid esters. In all the cases, the molar ratio of the fatty ester to silane was kept constant (1:5) and the peroxide was kept at 1 wt% of the fatty ester. The kinetics of silane addition to the fatty acid ester was followed by gas chromatography. It was found that at lower temperatures (180 °C and 200 °C), the reaction did not conform well to first order kinetics and at higher temperatures (220 °C, 240 °C and 260 °C) there was a good fit to the first order plot. The ultimate conversions were also determined by gravimetry (vacuum distillation of unreacted silane) and by NMR of the final distilled product. High conversions of the silane were obtained this way (68% for methyl oleate and 84% for methyl stearate). There was generally a good agreement between the methods used for determination of conversion. The order of the rate constants changed from 10^{-5} min^{-1} to 10^{-3} min^{-1} with

increasing temperature from 180 °C to 260 °C. The rate constants were used to determine the activation energy for the process (74.5 kJ/mol). Overall, the reaction was expected to follow an Alder – ENE type pathway; however NMR spectra seem to suggest a concurrent radical pathway for the grafting of silane onto the fatty ester. Reaction of methyl oleate with the silane at 260 °C without the peroxide still produced grafted material but the conversion of the silane was reduced by 50%, in comparison to the peroxide catalyzed run. Iodine values were also measured for the samples to determine the unsaturation present in the methyl oleate – silane adducts. The silylated fatty esters were cured via moisture aided hydrolysis and subsequent condensation and gel contents as high as 72% were obtained. The efficacy of this method was also tested on a saturated ester (methyl stearate) and in this case a gel content of 64% was obtained. The method offers a simple and efficient process for the synthesis of moisture curable oils/fatty esters, which can have applications as coatings and sealants.

[Note: No Introduction section is presented for this chapter, since it basically aims to extend the work done on soybean oil in Chapter 6. References mentioned in this chapter are also drawn from the references in Chapter 6. Thus discussion in this chapter is restricted largely to results. This chapter is best read and understood in the context of work presented in Chapter 6.]

7.1 MATERIALS

Vinyltrimethoxy silane [CAS 2768-02-7] was obtained from Gelest Inc. (Morrisville, PA) and had a purity of 97%. Methyl oleate [CAS112-62-9] – 70% pure technical grade, Luperox 101 [CAS 78-63-7] - 2, 5-Bis (*tert*-butylperoxy)-2, 5-dimethylhexane, Chloroform [CAS 67-66-3] used for swelling studies were obtained from Sigma Aldrich (St.Louis, MO). All the reagents were used as received without any further purification. However the reagents (except Luperox 101) were dried prior to use. Soybean oil was dried over molecular sieves and the silane was kept dry by a nitrogen flush before and after the container was opened.

7.2 EXPERIMENTAL

The methyl oleate used in the experiments was 70% pure. The composition of the methyl oleate analyzed was determined by gas chromatography. All the components are fatty acid methyl esters and there are no compounds that could potentially interfere in any of the reactions. The methyl oleate was also analyzed for its Iodine value and the value obtained was in good agreement with what was calculated from the percentage composition.

Methyl oleate (~266 gm, 0.9 mol) was mixed with vinyltrimethoxy silane (~667 gm, 4.5 mol) and Luperox 101 (2.66 gm, 9 mmol). A 2L Parr reactor (from Parr Instrument Company, Moline, IL, USA), equipped with a mechanical stirrer, an inlet port,

sampling port, vent port , pressure gauge and thermocouple well was used for the reactions. The temperature of the reactor was controlled using an external controller (from 180 °C to 260 °C in 20 °C increments). The agitation was kept at 200 rpm to mix the reactants and distribute heat uniformly in the system. Before the reactor was heated, it was purged with nitrogen for about 5 minutes to ensure an inert atmosphere. The time for reaction was taken as the time from the reactor reaching set temperature till shut down. The same procedure was used was for runs without the peroxide and runs with methyl stearate.

Samples were withdrawn at various time intervals using a sampling port into vials. The vials were then sealed tightly and refrigerated prior to analysis. To the extent possible, samples for gas chromatography were drawn from the cold vials, to minimize the silane migration the vapor phase. The heating rate was adjusted for each run to ensure that the reaction time for the different runs was nearly the same (30 – 45 minutes to set point temperature). Initial samples were withdrawn before the heating was switched on, however, the zero time sample for the reaction kinetics was taken when the reactor reached set temperature. Eight samples were withdrawn for analysis for each temperature run.

7.3 CHARACTERIZATION

Gas chromatograms were recorded using a HP 5890 Series II gas chromatograph equipped with a flame ionization detector. The column employed was a Supelco PTA-5 column (30 X 0.25 mm) with a film thickness of 1 μm . An injection temperature of 250 $^{\circ}\text{C}$ and a ramp of 20 $^{\circ}\text{C}$ was used (start: 50 $^{\circ}\text{C}$ end: 300 $^{\circ}\text{C}$) with a hold of 10 minutes at 300 $^{\circ}\text{C}$.

Gravimetric determination of conversion was done on the final product of the reaction. The product (pre – weighed) was distilled under reduced pressure (0.3 Torr, 110 $^{\circ}\text{C}$) till no further distillate was obtained. The unreacted vinyltrimethoxy silane was collected using two dry ice traps and weighed to give the conversion. The distilled product was stored under nitrogen tightly sealed, to prevent any hydrolysis of the silane.

Iodine values were measured according to ASTM D1959. The sample mass was estimated using the conversion obtained earlier and assuming the double bonds of the oleate remained unchanged during the reaction. The titers were cross – checked against the recommended range in the standard to ensure accuracy of sample weights used.

NMR spectra were recorded on Varian Unity plus spectrometer operating at 500 MHz. The solvent used was CDCl_3 (^1H @ 7.24 ppm, ^{13}C @ 77 ppm). Standard parameters were used in acquisition except in carbon spectra where a recycle delay of 2 seconds was employed.

Samples were cured using the following procedure. A 100 X 15 glass petri dish was filled with 20 ml of water. Onto the surface of this water, about 12 ml of the silylated oil, was transferred drop wise, to form a solid layer about 3-4 mm thick. The dishes were then transferred to a oven held at 70 °C and allowed to cure for a week. During this time humidity was also maintained inside, by means of a 2L trough of water. Samples were monitored to see the extent of cure. Once the oil had solidified (1 week), the cast sheet of oil was allowed to post cure at the same temperature for another week.

The solvent uptake and gel content were measured using a modification of ASTM D2765. Small pieces of the cured sample were weighed (1.2 – 2 gm) and placed inside a pouch made of filter paper and allowed to soak in chloroform solvent for 72 hours at room temperature. The pouches were withdrawn and solvent completely squeezed out and the weight of the sample immediately measured to give an estimate of solvent uptake. The pouches were then dried in an oven at 80 °C till constant weight was reached. The gel content of the cured materials was determined from the difference in weight. The residual chloroform containing the soluble portion was allowed to evaporate at room temperature till a liquor was obtained. The liquor was then dried in a closed oven at 80 °C to obtain a solvent free extract, which was then used for NMR measurements, for determining the composition of the soluble portion.

7.4 RESULTS AND DISCUSSION

The fatty acid composition of the methyl oleate is listed in Table 7.1. It can be seen that the mixture, consists of mainly methyl oleate, with methyl linoleate being the other major fatty ester. Thus the products from the silylation would be representative of methyl oleate and as such mechanistic inferences drawn would be reflective of mono unsaturated fatty esters.

Table 7.1 Fatty acid composition of methyl oleate^{*}

Fatty Acid	Carbon	Weight %	FAME (Mol. Wt)
Myristic	14:0	2.83	242.38
Palmitic	16:0	4.37	270.43
Palmitoleic	16:1	4.64	268.42
Heptadecenoic	17:1	1.1	282.45
Stearic	18:0	0.86	298.49
Oleic	18:1	69.96	296.47
Linoleic	18:2	8.85	294.46
Other	-	7.39	-

* - samples analyzed on a Varian 3900 GC equipped with a WCOT fused silica column (100m X 0.25 mm) with a CP-Sil 88 (CP7489) coating. Injection temperature of 250 °C and isothermal run at 180 °C was used. An FID detector was employed at a flow rate of 1 mL/min.

7.4.1 Kinetics of silylation

As discussed in Chapter 6, the silylation proceeds in a manner similar to that of soybean oil. Eight samples were used to determine the conversion at different times and the results were fitted to a first order plot, following on the evidence from Chapter 6 that silane was essentially grafted to the fatty acid backbone, similar to what occurs in the manufacture of cross – linked polyethylene (1-3). The plot of conversion with time is provided in Figure 7.1. It should be noted only those samples at and beyond the set point temperature are used in the analysis.

It can be seen that the silylation, is similar to that observed for soybean oil. However, the overall conversion is higher than soybean oil. In this case also, silylation can be controlled by adjusting the time and temperature. Although, the added peroxide Luperox L101 is bound to decompose totally in a time of 6 minutes or less for the temperatures employed, it can be seen that silylation proceeds well beyond that time frame. Also contrary to what was observed in the case of soybean oil, the peroxide seems to play a role. The highest temperature run was replicated without the peroxide to yield a conversion which was half or lesser of what was obtained with the peroxide (Data provided in Table 7.2, entry 6).

Additionally, when methyl stearate (a saturated fatty acid ester) was used, the conversion of silane was the highest (260 °C, 1:5 ratio of methyl stearate: silane, 1 wt% L101) at 84% - determined gravimetrically.

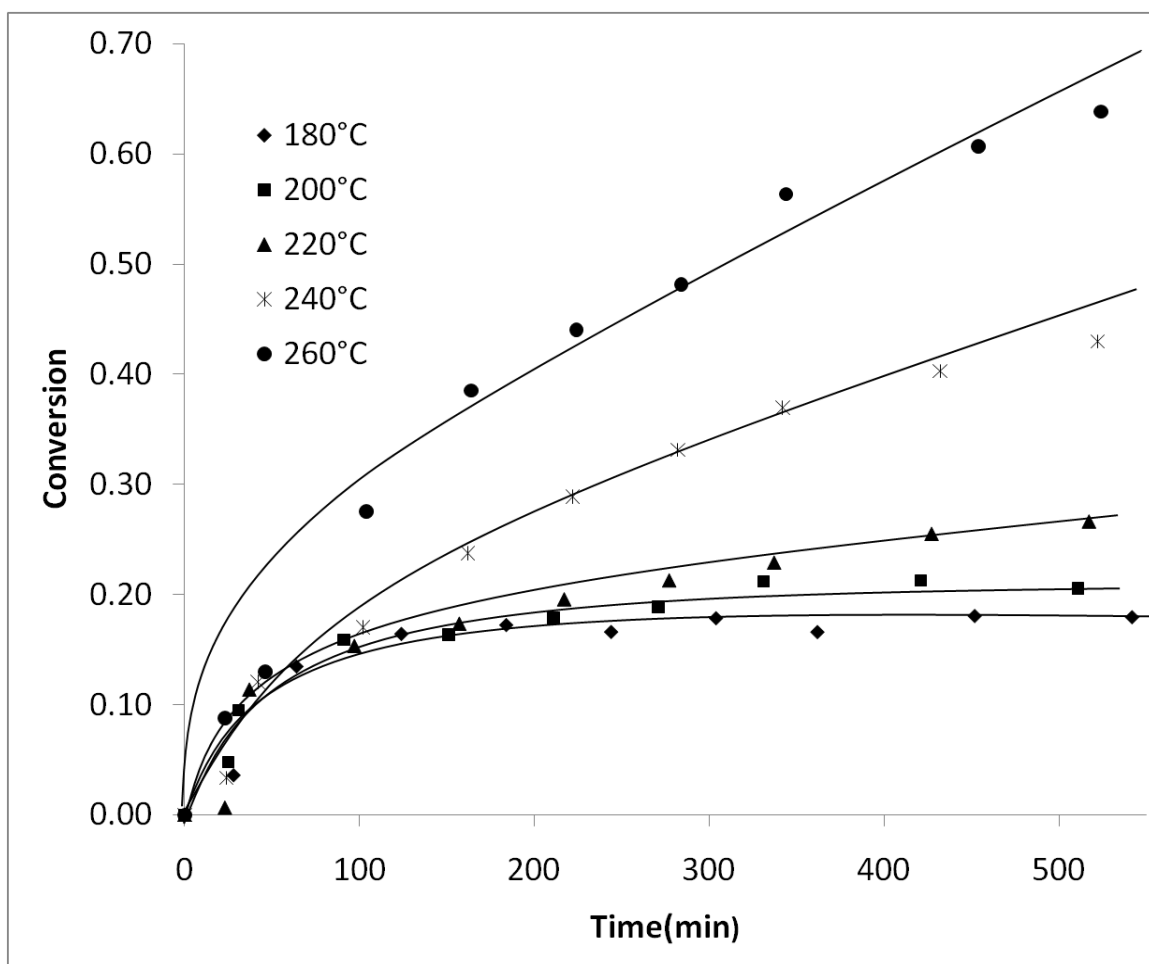


Figure 7.1 Conversion of silane with time - as determined by GC (methyl oleate: silane ratio = 1:5 mole, 1 wt% peroxide)

The first order fit to the data is shown in Figure 7.2. As in the case of soybean oil, the distinction between the 180 °C run and 200 °C run is not very clear in the initial phases. However, it is seen that beyond 220 °C, the data seem to fit the first order plot well. The lines have not been forced to touch the origin. The errors at the start of the reaction can be attributed to errors in measurement. From the first order plot, the rate constants were evaluated and their temperature dependence has been plotted in Figure

7.3. From the plot, an activation energy of 74.5 kJ/mol has been determined for the reaction.

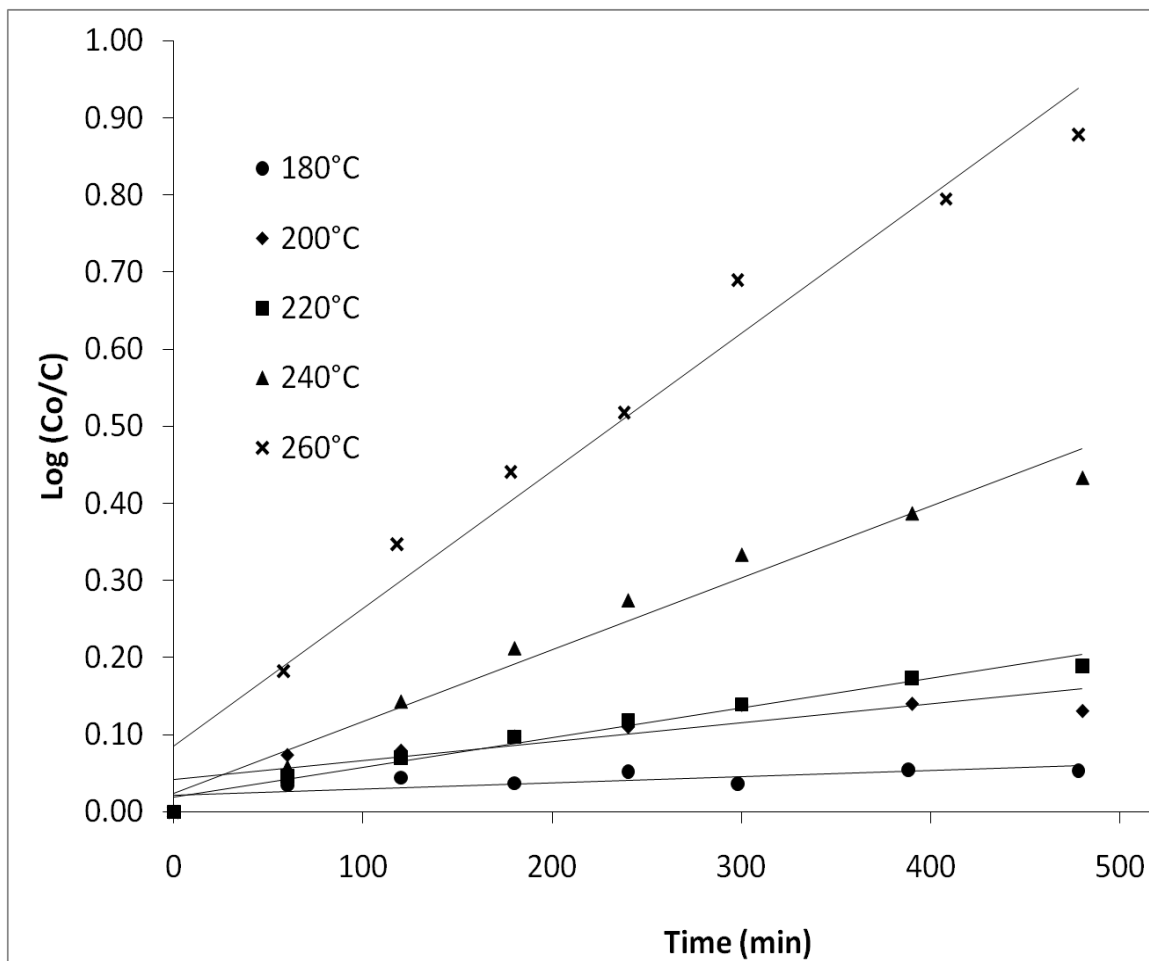


Figure 7.2 First order plot for the consumption of silane (methyl oleate: silane ratio = 1:5, 1 wt% peroxide)

The activation energy is about three times the value determined for soybean oil (see Chapter 6). The activation energy determined can be assumed to represent that of methyl oleate, since the starting methyl oleate is about 70% pure. Thus it can be inferred that, monounsaturated fatty acids undergo silylation slower than poly

unsaturated fatty acid residues. This could be due to the lesser proportion of active allylic and bis – allylic protons on these fatty acids. Also since soybean oil has close to 70% of polyunsaturated fats, the activation energy could be significantly low. However, what is common to both systems is that the silylation increases significantly at higher temperatures, probably corresponding to the thermal generation of radicals.

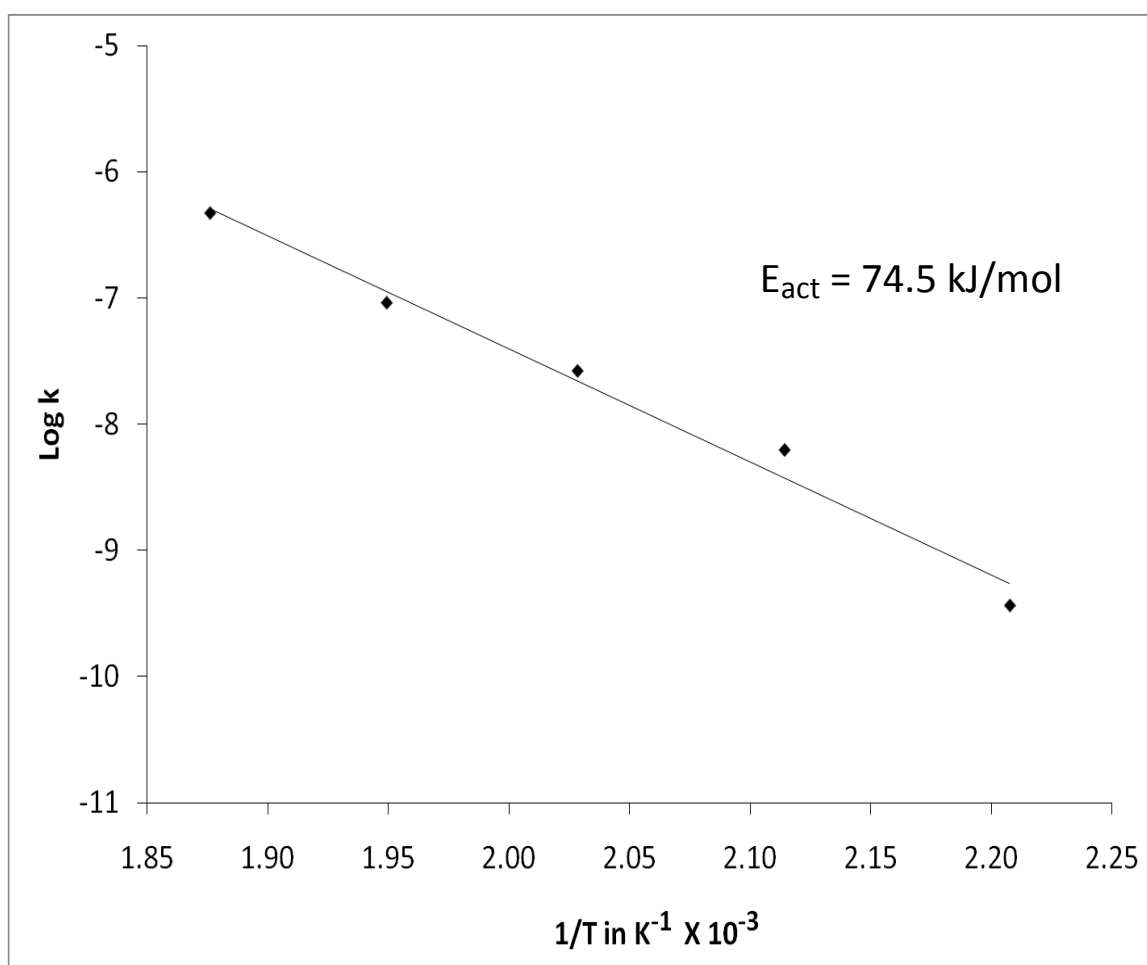


Figure7.3 Arrhenius plot of Log k Vs 1/T

The surprising result comes from methyl stearate (Table 7.2, entry 7), where the highest conversion is recorded. Saturated fats have no unsaturation and hence silylation would have to proceed by a purely radical grafting route as discussed in other works (1, 4). Although transesterification of the methyl ester to a silyl ester is possible, NMR spectra which are discussed subsequently do not support the hypothesis. It is also known that the extent of silylation is dependent on the concentration of peroxide for linear hydrocarbons (5), and independent of temperature. Thus even assuming a 100% efficient radical production from the decomposing Luperox 101 peroxide, approximately 36 mmol of radicals would be generated. Assuming a grafting efficiency of 22 silane units per radical, as determined by Parent et al. (5) for tetradecane, we would still be able to account for around 0.8 mol of silane grafting. The actual number is greater than 3, as determined by gravimetry. However, the gel content would give a clearer picture of the actual amount of grafting, since unreacted material can be removed. This is discussed subsequently.

The same argument would apply to the methyl oleate silylation case as well. However, the kinetics and activation energy discussed above is with respect to the silane being consumed in the reaction. The complete reaction of the methyl ester with the silane, would probably not affect the dynamics of the silane grafting reaction as such. Also the temperature sensitivity of the silylation process seems to be different than what is reported (5) for vinyltriethoxy silane.

7.4.2 Mechanism of silylation

Table 7.2 lists the relevant data from gravimetry, gas chromatography, and NMR and Iodine values for the different samples. It can be seen that the amount of double bonds in the starting material is not reduced significantly with increasing temperature compared with soybean oil. Thus, for the same ratio of silane employed, there is a 30% reduction in double bonds in the silylation of soy oil compared with only the 8% for the methyl oleate. This difference can be explained by the lower reactivity of the single olefinic bond in methyl oleate, which affects radical mediated reactions less than multiple olefinic bonds in the triglycerides (6-9). The polyunsaturated oils possess active methylenes that can effectively terminate any radical propagation.

In the case of oleate, such reactions are fewer and from the experiments above, even at elevated temperatures. Thus silylation if occurring on the backbone, would have to follow a peroxide grafting route. The other alternative explanation, for the diminishing residual silane, seen from distillation and GC would be a homopolymerization, which is not a common occurrence or a thermally driven condensation to form polysiloxanes, which is not supported by the NMR spectra, to be discussed later in this work.

From Table 7.2 it can also be seen that the conversions reported by the three methods are in good agreement with each other. The iodine values are seen to decrease with increasing silylation. This is due to small reduction in double bonds and the accompanying addition of silane, which dilutes the double bond concentration per unit

mass. Assuming an average mass for the fatty acid ester to be ~296.5 (mass of methyl oleate), and 1 double bond exists in the material, the theoretical iodine value would be given by $2 \times 126.9 / 296.5 = 0.855$ or 85.5 gm/100 gm of the sample.

If 1 mole of silane is added via peroxide grafting or an ENE mechanism, the double bond being intact (no polymerization etc.); the molecular weight of the fatty acid ester would increase by 148. Thus the new iodine value would be given by $2 \times 126.9 / 444.5 = 0.571$ or 57.1 gm/100 gm of the sample. This would however, not distinguish the ENE pathway from the radical pathway. From the iodine values listed it can be seen that the increasing silane addition is correlated to a good extent by the iodine values. Where there are discrepancies, it is mainly due to the fact that significant amounts of vinyl groups show up in the NMR spectra in the region corresponding to VTMOs vinyl protons. This residual silane could probably be the result of a condensation with a grafted silyl group. Thus distillation would not remove it and it adds to the iodine value.

It should also be noted that if there was no reaction with the ester and the silane polymerized via a radical route, the iodine values would still not be able to distinguish the product. However the sol content for such a material would clearly show the amount of fatty ester and the gel content would be indicative of the silane that has polymerized. The gel contents are given in Table 7.3. The percentage of methyl ester is calculated under the assumption, that complete cure of the material has taken place and that the methyl ester has not reacted with the silane. Based on the cure mechanism

proposed in Chapter 6, each vinyl silane unit, upon cure, would yield a structural unit of the formula $C_2H_3SiO_{1.5}$ (M.W 79). Thus a 1:1 mole mixture of the fatty ester and completely cured silane would have a fatty ester percentage of $296.5 / (296.5 + 79) = 79\%$. Additionally assuming that there is no polysiloxane in the extract, we can arrive at an estimate of how much fatty ester has reacted with the silane. Indeed NMR spectra reveal that the proportion of siloxanes in the extract is minimal.

Thus from the gel content it can be seen that increasing silylation is largely due to grafting on to the fatty ester backbone and not due to any polymerization/condensation of the silane. The striking difference is seen in the case of methyl stearate, where the gel content is low, considering that the conversion was around 84 %. The simplest explanation is that with the stearate, multiple grafts of the silane occurred on every stearate molecule that reacted and a lot of the stearate was unreacted, which then migrated to the solvent phase.

Table 7.2 Conversion, Iodine value and double bond reduction for silylated fatty acid methyl esters; methyl ester: silane molar ratio of 1:5, reaction time: 8 hours, 1 wt% L 101 used (except Entry 6)

Entry	Temperature	Silane grafted (mol silane/mol oil)			Area ratio ^d	Iodine value ^e
		GC ^a	Gravimetry ^b	NMR ^c		
1	180 °C	0.68	0.86	0.79	0.93	69
2	200 °C	1.04	1.04	0.91	0.89	63
3	220 °C	1.62	1.44	1.30	0.89	59
4	240 °C	2.03	2.16	2.02	0.89	52
5	260 °C	2.88	3.06	2.86	0.87	45
6 ^f	260 °C	1.04	1.53	1.39	0.85	58
7 ^g	260 °C	-	3.78	3.59	-	-

a – estimated by Gas chromatography on samples, for residual silane; b – Reduced pressure distillation of large sample (110 °C, 0.3 Torr); c – Ratio of $-\text{OCH}_3$ peak (3.55 ppm) to $-\text{CH}_2\text{C}(=\text{O})$ proton (1 mole silane/mole oil corresponds to a ratio 9:2); d – ratio of $-\text{CH}=\text{CH}-$ (5.4 ppm) to $-\text{CH}_2\text{C}(=\text{O})$ (Neat methyl oleate has a ratio 1.95:2 or 0.975); e – determined according to ASTM D1959 on vacuum distilled samples; methyl oleate has an iodine value ~86; f – no peroxide used; entries 1 – 5, 7 use 1 wt% Luperox 101; g – Methyl stearate run with 1 wt% L101 under the same conditions.

Table 7.3 Gel content and solvent uptake ratio for cured silylated methyl esters (Cure Temperature : 75 °C) after extraction with chloroform (72 hours); NMR data is for the extracted portion or “Sol”

Entry	Gel content (%)	Methyl ester content ^a (%)	Solvent uptake ratio	Area ratio	
				$\delta = 3.6 \text{ ppm}^b$	$\delta = 5.4 \text{ ppm}^c$
1	39 ± 1.3	81	3.3	1.04	0.11
2	39 ± 6.1	78	3.0	1.00	0.12
3	46 ± 1.2	72	2.4	1.15	0.06
4	62 ± 3.7	64	1.5	1.18	0.08
5	72 ± 0.3	55	1.1	1.25	0
6 ^d	50 ± 1.1	71	1.9	1.06	0.06
7 ^e	63 ± 0.6	50	1.6	0.98	-

a – theoretical content estimated from gravimetry assuming complete cure of material

b – ratio of multiplet at 3.6 ppm to the $-CH_3$ peak at 0.8 ppm

c – ratio of vinyl protons at 5.4 ppm to $-CH_3$ peak at 0.8 ppm (ratio in methyl oleate is 1.95:3 or 0.65)

d – sample synthesized with 1:5 methyl ester: silane ratio with no peroxide

e – Methyl stearate run – the NMR of the extract shows pure stearate.

7.4.2.1 NMR Spectra

NMR spectra give more insight into the nature of products formed with methyl oleate and methyl stearate. It should be noted that conversion based on NMR spectra relies on integrating the -OCH_3 peak ($\delta = 3.50$ ppm) of the silane without affecting the -OCH_3 peak of the methyl ester ($\delta = 3.58$ ppm). This was possible in all the spectra and thus the NMR results agree with conversions based on other methods. The ^1H NMR and ^{13}C NMR spectra for the methyl oleate and methyl stearate samples are given in Figures 7.4 & 7.5.

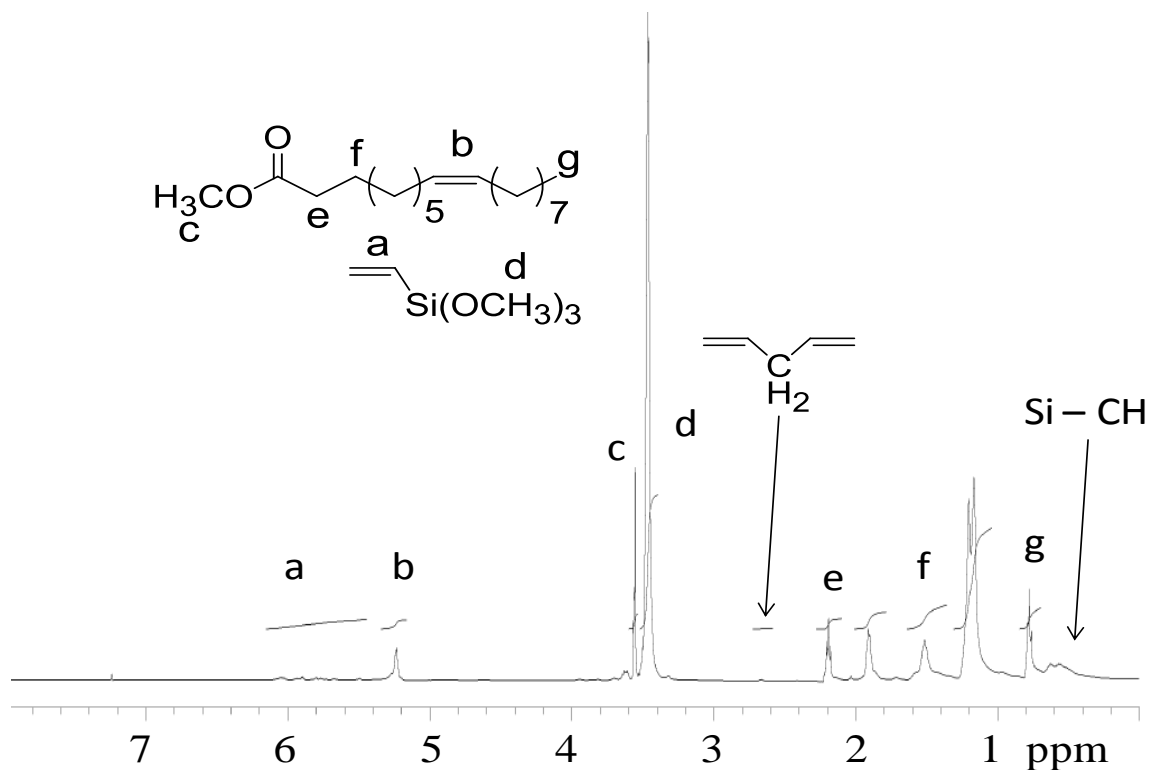


Figure 7.4 ^1H NMR spectrum of silylated methyl oleate with assignments (Table 7.2, Entry 5) – after distillation

From the NMR it can be seen that there is some residual vinyl groups from the silane. It can also be seen that the peaks corresponding the alkoxy group of the silane and the methyl ester are well resolved. The bis – allylic methylene of the linoleate fragment can also be seen. However its area is reduced from that of the starting methyl oleate (by $\sim 50\%$). Peaks corresponding to Si – CH protons can also be seen lower than 0.8 ppm at ~ 0.6 ppm. Ideally such protons would appear slightly more upfield as reported by Forsyth et al (4). This slight downfield shift observed in this case can be attributed to oligomerization of the vinyl silane and degradative chain transfer

(described in the same work) by a 1, 4 migration of the radical to the methoxy group of the silane. This can also be seen as a small peak adjacent to the methoxy of the ester at ~ 3.6 ppm. It can also be seen that the vinyl protons of the fatty ester are intact and their intensity is not significantly reduced.

The carbon NMR spectra also reveal information supportive of the peroxide mediated grafting process. New methines corresponding to graft points are clearly seen at ~ 38 ppm. Evidence of degradative chain transfer is seen from carbons at 64 ppm. The carbons attached to the "Si" atom have been broadly assigned as "d". However, it can be seen that the carbons of the silane attached to the deshielded methine would probably appear downfield (~ 10 -15 ppm) and the oligomerized siloxanes carbons would appear upfield (<10 ppm). Thus the carbon spectra also conclusively prove a radical mediated silylation occurring, without any radical abstraction by the double bond. This is seen from the vinyl carbons at 130 ppm very clearly.

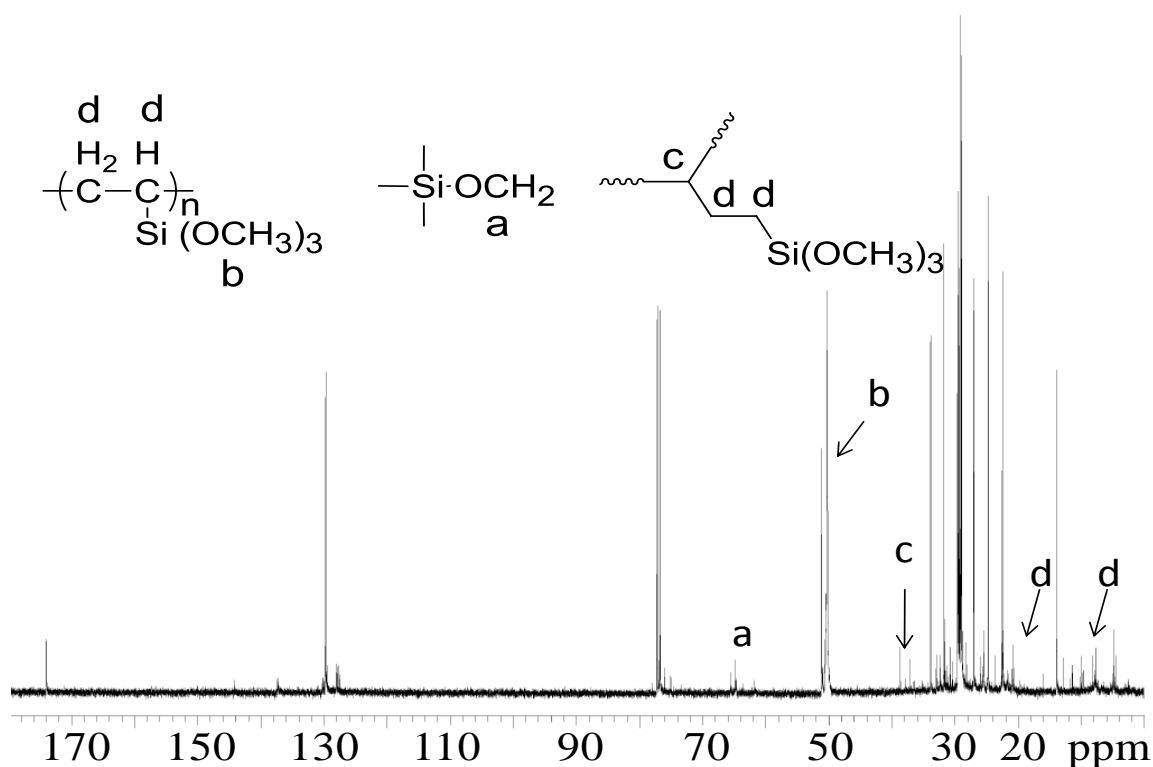


Figure 7.5 ^{13}C NMR of silylated methyl oleate with assignments (Table 2, Entry 5) after distillation.

The carbon NMR spectrum for methyl stearate also shows similar features as Figure 7.5. This shows that mechanistically, silane addition happens via the same pathway for both monounsaturated methyl oleate and the completely saturated methyl stearate. This is in agreement with work on free radical polymerizations conducted in fatty acid methyl esters as solvents (8-9). Thus from the above, it can be inferred that, the method can be used to functionalize both vegetable oils high in saturates as well as individual fatty acid methyl esters. However, it should be noted that while high conversions of silane are possible, total conversion of the fatty acid esters does not

necessarily occur. This is clear from Table 7.3 and from the NMR of the extracts of the cross – linked materials, which are given in Figures 7.6 – 7.8.

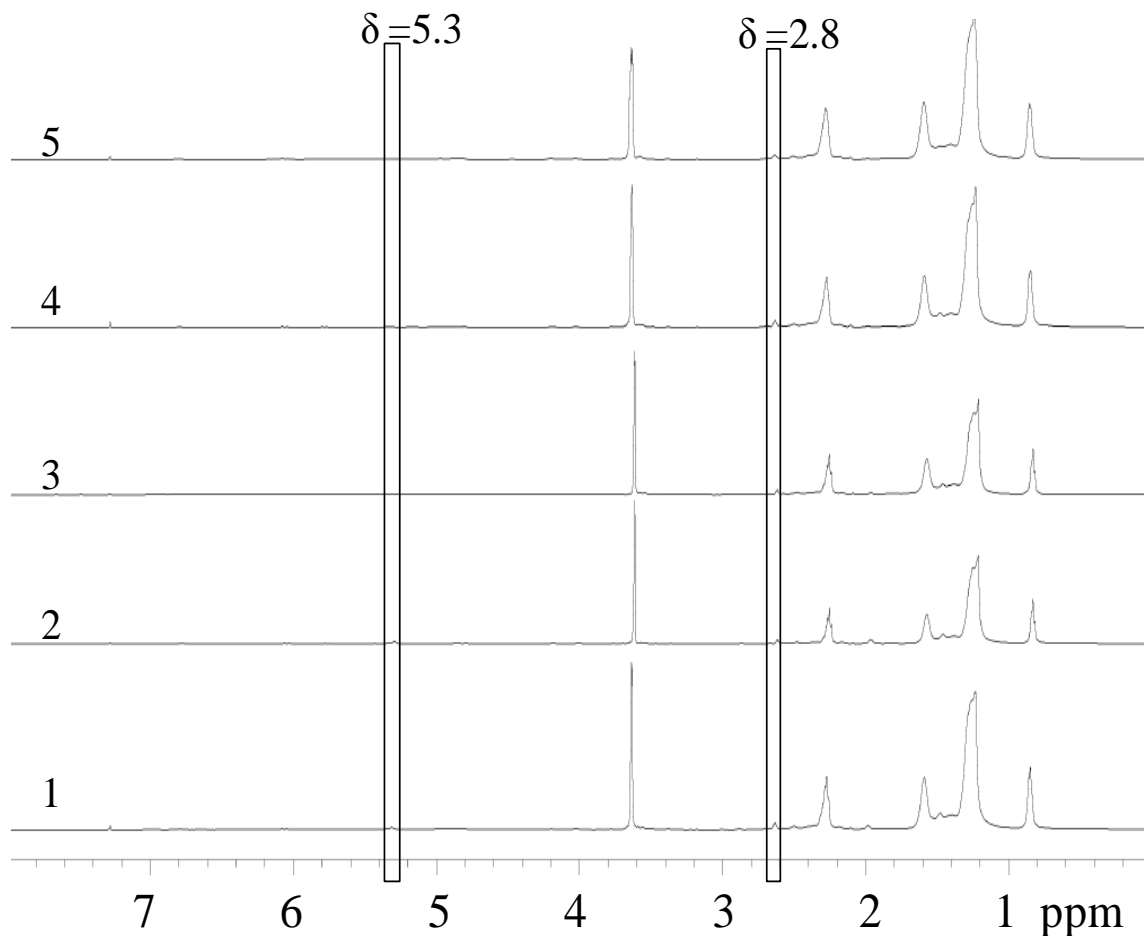


Figure 7.6 Stacked ^1H NMR spectra of soluble fractions (Table 7.2, Entries 1-5)

From the Figure 7.6 it can be seen that the extracted materials are all fatty acid esters. The peak at 3.6 ppm has been attributed to the methoxy peak of the ester. The peak is sharp, unlike the silane alkoxy groups which are broad. However, from the ratios provided in Table 7.3, it can also be seen that some siloxanes are also extracted out.

These could be products resulting from degradative transfer, which would create oligomers prone to hydrolysis. However from the spectra it is clear that the major component of the soluble fraction is unreacted fatty acid esters. The amount of methyl oleate seems to be minimal, as can be seen from the absence of significant peaks at 5.3 ppm. Thus the other fatty acid esters in the mixture, including the saturates, which are probably less reactive did not undergo silylation. Also their lower concentration in the mixture could contribute to their remaining unreacted.

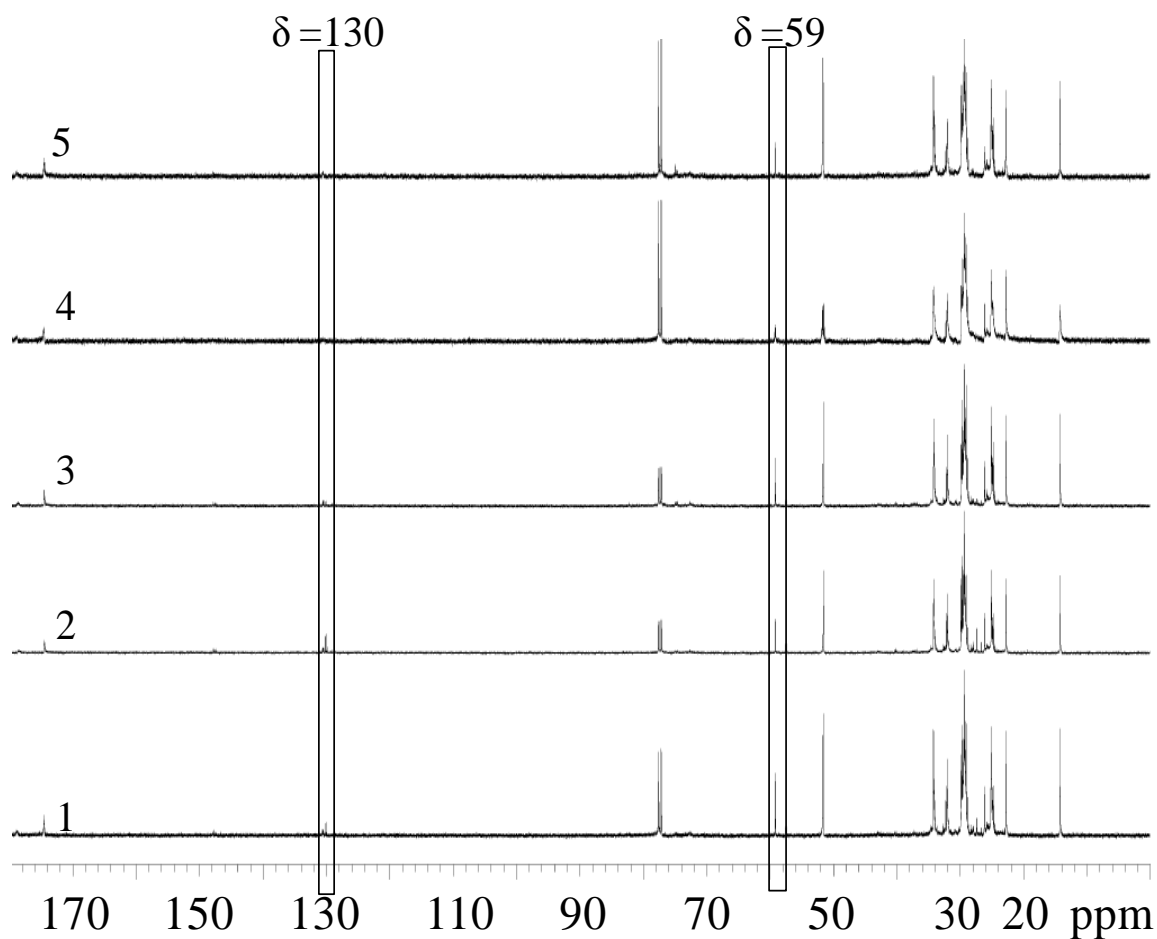


Figure 7.7 Stacked ^{13}C NMR spectra of soluble fractions (Table 7.2, Entries 1-5)

The carbon spectrum shows new peaks at 59 ppm. These peaks can be easily attributed to epoxidized derivatives of the fatty acid esters. It can be seen that the intensity is reduced with increasing silylation. This again establishes that since the gel content increases with silylation, the amount of free fatty acid ester in the extract are reduced (especially those with oxidizable unsaturation). This can explain the reduction in the intensity of the peaks at 59 ppm. This is further supported by the carbon spectra for the methyl stearate samples. Since the mechanism of silylation is similar for both methyl oleate and methyl stearate, and since the samples have been cured under identical conditions, they would be expected to have similar peaks in the soluble fractions. The carbon spectrum is provided in Figure 7.8.

It can be clearly seen that no such peaks are to be found, which then establishes that the peaks in the methyl oleate samples are a result of oxidation and thus do not introduce any new mechanistic aspects to the silylation. Interestingly, this is seen for methyl oleate only and not for soybean oil, which also has oxidizable fatty acids in its structure.

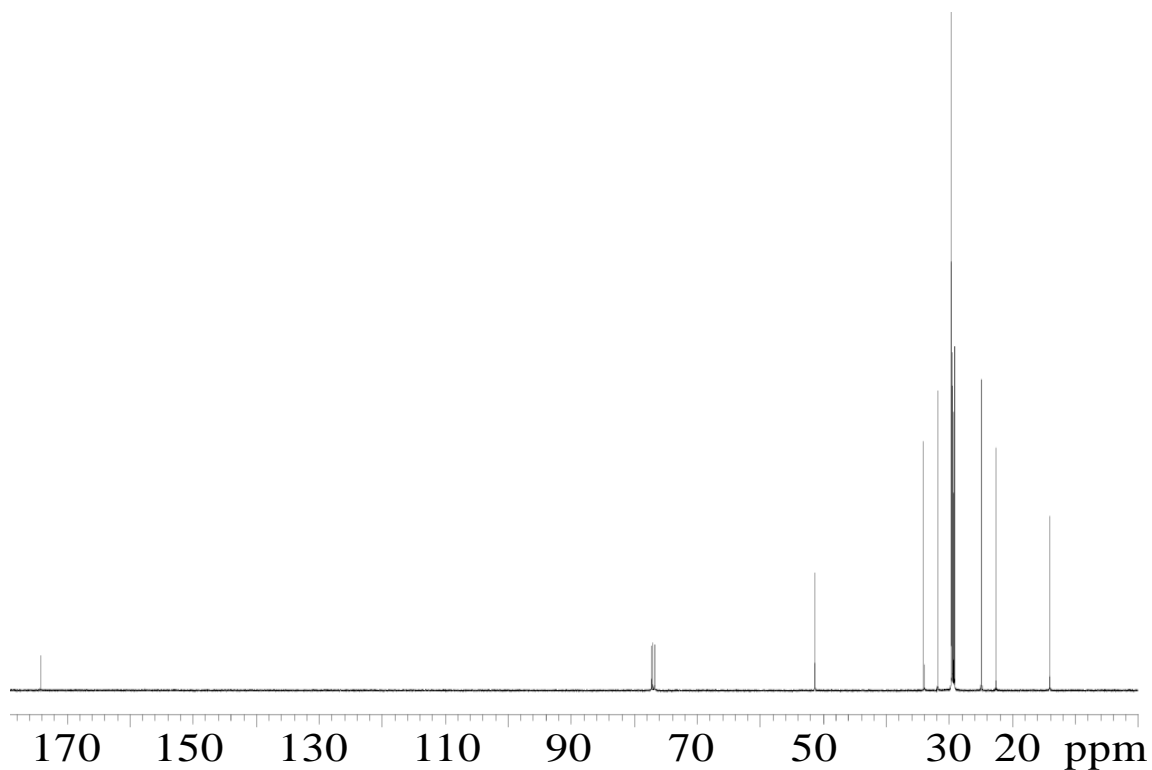


Figure 7.8 ^{13}C NMR spectrum of methyl stearate – soluble fraction

7.5 CONCLUSIONS

Silylation of methyl oleate as a model compound for fatty acid esters was carried out. This was done to extend the silylation method for soybean oil/vegetable oils to their fatty acid alkyl esters. The kinetics shows that the progress of silylation is similar for both the oil and the fatty acid methyl ester. However, the activation energy is 3 times that of soybean oil. It has been postulated that this increase is due to the non – reactive nature of the dominant fatty acid (oleic acid) in the mixture.

Unlike soybean oil, silylation proceeds solely via peroxide mediated grafting of the vinyl silane or its oligomers to the backbone. There is not a significant reduction in double bonds, suggesting that radical termination by double bonds is not dominant. The gel contents suggest that these materials are also curable like silylated soybean oil. However, the gel contents obtained are not as high as those with soybean oil. It has also been established that saturates can be functionalized this way. One thing common to both methyl oleate and methyl stearate is the fact that, although conversions are higher than soybean oil, the gel content is not commensurate. This has been attributed to the multiple single grafts that dominate these two systems, as opposed to the chain termination and grafting type mechanism involved in soybean oil.

However, increasing the peroxide concentration and reaction time might lead to better silylation of all the fatty acid esters and thus provide products with higher gel contents. Such silylated fatty acid esters may find use in coating applications, where lower viscosity might enable coatings to be developed without the need for vehicles to carry the coating material.

REFERENCES

7.6 REFERENCES

1. A. Sen, B. Mukherjee, A. Bhattacharyya, P. De, A. Bhowmick, *Journal of Applied Polymer Science* **44**, 1153 (1992).
2. M. Spencer, J. Parent, R. Whitney, *Polymer* **44**, 2015 (2003).
3. J. Weaver *et al.*, *Journal of Polymer Science Part A: Polymer Chemistry* **46**, 4542 (2008).
4. J. Forsyth, W. Baker, K. Russell, R. Whitney, *Journal of Polymer Science Part A: Polymer Chemistry* **35**, 3517 (1997).
5. J. Parent, R. Parodi, W. Wu, *Polymer Engineering & Science* **46**, 1754 (2006).
6. H. Teeter, M. Geerts, J. Cowan, *Journal of the American Oil Chemists' Society* **25**, 158 (1948).
7. H. Teeter, *Journal of the American Oil Chemists' Society* **40**, 143 (1963).
8. S. Harrison, W. Tolberg, *Journal of the American Oil Chemists' Society* **30**, 114 (1953).
9. S. Harrison, D. Wheeler, *Journal of the American Chemical Society* **73**, 839 (1951).

CHAPTER 8

RAPID RING-OPENING POLYMERIZATION OF 1, 4-DIOXAN-2-ONE INITIATED BY TITANIUM ALKOXIDES

The work presented below was done in collaboration with Dr. Jian-Bing Zeng¹ during his time as a visiting scholar at Michigan State University.

¹Center for Degradable and Flame-Retardant Polymeric Materials, College of Chemistry, State Key Laboratory of Polymer Materials Engineering, Sichuan University, Chengdu 610064, China.

ABSTRACT

Ring-opening polymerization of 1, 4-dioxan-2-one in bulk was initiated by three titanium alkoxides, titanium dichlorodiisopropoxide ($\text{TiCl}_2(\text{OiPr})_2$), titanium chlorotriisopropoxide ($\text{TiCl}(\text{OiPr})_3$), and titanium tetraisopropoxide ($\text{Ti}(\text{OiPr})_4$). The results indicate that the polymerization rate increased with number of OiPr groups in the initiator. High conversion of monomer (90%) and high molecular weight (11.9×10^4 g/mol) of resulting polymer can be achieved in only 5 minutes at 60 °C with $\text{Ti}(\text{OiPr})_4$ as an initiator. Analysis on nuclear magnetic resonance (NMR) spectra suggests the initiating sites for $\text{TiCl}_2(\text{OiPr})_2$, $\text{TiCl}(\text{OiPr})_3$, and $\text{Ti}(\text{OiPr})_4$ to be 1.9, 2.6, and 3.8, respectively. Coordination-insertion mechanism for the polymerization via cleavage of the acyl - oxygen bonds of the monomer was proved by NMR investigation. Kinetic studies indicate that polymerization initiated by $\text{Ti}(\text{OiPr})_4$ followed a first order kinetics, with an apparent activation energy of 33.7 kJ/mol. It is noteworthy that this value is significantly lower than earlier reported values with other catalysts, namely $\text{La}(\text{OiPr})_3$ (50.5 kJ/mol) and $\text{Sn}(\text{Oct})_2$ (71.8 kJ/mol), which makes it an attractive catalyst for reactive extrusion polymerization.

8.1 INTRODUCTION

Aliphatic polyesters, such as poly(L-lactide) (PLLA), poly(ϵ -caprolactone) (PCL), poly(1,4-dioxan-2-one) (PPDO) have gained increasing interest for their excellent biodegradability, biocompatibility, and bioabsorbability, and found applications in biomedical materials (1-10). Generally, these polyesters can be synthesized through ring-opening polymerization (ROP) of the corresponding cyclic ester monomers in the presence of initiators. Organometallic compounds are the most widely used initiators. Tin(II) bis(2-ethylhexanoate) ($\text{Sn}(\text{Oct})_2$) is one of the most frequently used initiators and it has been employed to initiate ROP of many cyclic ester monomers like lactide (11-13), ϵ -caprolactone (14-15) and 1,4-dioxan-2-one (16-17). In addition, aluminum alkoxides (8, 18-20), zinc derivatives (21-22), ferric alkoxides (23-25), titanium alkoxides (26-27), yttrium complexes (28-30) have also been utilized to initiate ROP of cyclic esters.

PPDO, with the existence of the ester and ether bonds in the repeat units of the polymer chain, is found to possess outstanding flexibility, biodegradability, and biocompatibility (2). It is usually synthesized through ROP of 1,4-dioxan-2-one (PDO) in the presence of initiators. The usually used initiators for the ROP of PDO are $\text{Sn}(\text{Oct})_2$, triethylaluminum ($\text{Al}(\text{Et})_3$) – not the actual initiator, and aluminum isopropoxide ($\text{Al}(\text{OiPr})_3$) (20). One advantage of $\text{Sn}(\text{Oct})_2$ as a catalyst is its approval by the FDA for biomedical applications. The efficiency however is very low when used to initiate the

ROP of PDO, and the polymerization rate is very slow. The maximum conversion of the monomer is 85.5% at 80 °C with a very long polymerization time of 20 hours (31). In the case of $\text{Al}(\text{Et})_3$, the polymerization is a little faster, high conversion of PDO of 93.5% is obtained in 6 hours at 60 °C (31). However, the catalyst is also extremely moisture sensitive and difficult to handle. $\text{Al}(\text{O}i\text{Pr})_3$ is a very effective initiator in the ROP of ϵ -caprolactone; the monomer conversion can reach more than 95% in several minutes, and the molecular weight of resulting PCL can reach several hundred thousand (32). But the catalyst does not offer the same efficacy when used to initiate the ROP of PDO. Raquez et al (20) have reported the application of $\text{Al}(\text{O}i\text{Pr})_3$ to initiate the ROP of PDO. The conversion of PDO reached 82% in 12 minutes only when the [monomer]:[initiator] ratio was very low (200:1). Ratios higher than 200:1, namely 400, 600 required times of 30 minutes or more. Thus the molecular weight of the resulting PPDO was only of the order of a few thousands. The difference can be attributed the structures of CL and PDO. CL is a seven-membered ring while PDO is a six-membered ring. In addition, zinc lactate ($\text{Zn}(\text{Lac})_2$) (21), enzymes (5), and lanthanum isopropoxide ($\text{La}(\text{O}i\text{Pr})_3$) (33) have also been reported to initiate the ROP of 1,4-dioxan-2-one. However, problems have been encountered when using these initiators, for example, low ultimate conversion of monomer (86%) with $\text{La}(\text{O}i\text{Pr})_3$ as a catalyst (33), low activity of $\text{Zn}(\text{Lac})_2$ and enzymes,

to mention a few. Thus new initiators with high activity and efficiency are still desirable for the efficient mass production of PPDO.

Titanium compounds (halides) are known to catalyze the polymerization of olefins in Ziegler – Natta polymerizations (34). Recently titanium complexes have been applied to initiate the ring-opening polymerization of some cyclic esters such as ϵ -caprolactone (35-36), lactide (37-38) and cyclic carbonates (39-40). Cayuela et al. (41) have reported the ROP of ϵ -caprolactone initiated by titanium alkoxides, the results indicated that the initiators were highly active for the ROP of ϵ -caprolactone, and very high conversion of monomer was achieved in several minutes when using titanium *n*-propoxide or titanium phenoxide as an initiator. In addition, the results for ROP of lactide initiated by titanium alkoxides suggested that these initiators showed remarkably high catalytic activity in bulk and solution polymerizations of LA, and very high conversion of LA (94%) was achieved rapidly in as little as 0.5 hours (37). Like some other metal alkoxides, for example $\text{Al}(\text{O}i\text{Pr})_3$ (8, 20, 42), the ROP of cyclic esters initiated by titanium alkoxides also follows a coordination-insertion mechanism (37). Furthermore, it is also a living polymerization (36, 39, 43), which enables the polymerization to be controlled and the molecular weight of the resulting polymer adjusted under certain conditions.

Although 1,4-dioxan-2-one has a similar structure to a lactide (both being six-membered rings), their polymerization behavior and kinetics are not always same. Since there are no reported works on the ROP of PDO initiated by titanium alkoxides at

present, it is necessary to study the mechanistic and kinetics aspects of polymerization in detail. So in this study, we have employed three titanium alkoxides $\text{TiCl}_2(\text{O}i\text{Pr})_2$, $\text{TiCl}(\text{O}i\text{Pr})_3$, and $\text{Ti}(\text{O}i\text{Pr})_4$ to initiate the ROP of PDO and postulated a mechanism for the polymerization and investigated the kinetics for the ROP of PDO initiated by $\text{Ti}(\text{O}i\text{Pr})_4$ in detail.

8.2 EXPERIMENTAL

8.2.1 Materials

The monomer 1, 4-dioxan-2-one (PDO) was provided by Department of Chemical Engineering and Materials Science, Michigan State University (East Lansing, United States). The PDO was dried for 48 hr over calcium hydride at room temperature under reduced pressure (100 Pa), and the water content was measured by an 831 KF Coulometer (Metrohm, Switzerland). It was distilled under reduced pressure before use (40 Pa, 70 °C). The moisture content of the purified PDO was estimated at about 100 ppm. $\text{Ti}(\text{O}i\text{Pr})_4$ of 97% purity obtained from Sigma Aldrich was dissolved in anhydrous toluene to prepare 0.25 mol/L solution before use. $\text{TiCl}(\text{O}i\text{Pr})_3$ with 1 mol/L in hexanes was purchased from Sigma Aldrich; it was diluted to 0.25 M solution by adding

anhydrous hexane (from Sigma Aldrich). $\text{TiCl}_2(\text{O}i\text{Pr})_2$ was synthesized via the procedures reported by Youngjo Kim (44). Calcium hydride, Phenol, 1,1,2,2-tetrachloroethane, and acetone (reagent grade) were procured from Sigma Aldrich and used without further purification.

8.2.2 Polymerization of PDO

The polymerization was carried out in a 7 mL vial with a magnetic stirrer and the vial was sealed with a rubber septum. Prior to its use in polymerization the vial was flame-dried, subjected to an alternating vacuum - nitrogen purge cycle for a minimum of 3 cycles then maintained under a nitrogen atmosphere. Then 0.012 mol PDO was introduced into the vial by a syringe. Thereafter the vial was immersed in a silicone oil bath maintained at a constant temperature for 5 minutes to attain set polymerization temperature. A predetermined amount of catalyst solution was then injected into the vial. The reaction vial was immersed in a cold alcohol ($-20\text{ }^{\circ}\text{C}$) bath after a predetermined amount of time to stop the reaction. The product was extracted with anhydrous acetone for 48 hours. The purified PPDO was then isolated and vacuum dried to constant weight at $40\text{ }^{\circ}\text{C}$.

8.2.3 Characterization and Measurement

^1H NMR spectra of the PPDO samples were recorded on a Varian Unity Plus 500 MHz spectrometer at $25\text{ }^{\circ}\text{C}$ with tetramethylsilane (TMS) as the internal reference in

CDCl₃. Intrinsic viscosities ($[\eta]$) were measured in phenol/1,1,2,2-tetrachloroethane (1:1, v/v) with $c=0.1$ g/dL at 25 °C using a Canon Ubbelohde viscometer. Viscosity-average molecular weights (M_v) of PPDO was calculated using the Mark-Houwink equation $[\eta]=KM^\alpha$ ($\alpha=0.63$, $K=7.9\times 10^{-4}\text{cm}^3\text{g}^{-1}$). (45)

8.3 RESULTS AND DISCUSSION

8.3.1 Polymerization of PDO initiated by Titanium Alkoxides

Three titanium compounds TiCl₂(O*i*Pr)₂, TiCl(O*i*Pr)₃, and Ti(O*i*Pr)₄ were used to initiate the ring-opening polymerization of PDO. To understand the effects of the different catalysts on the polymerization of PDO, comparative polymerization kinetics were recorded for the three catalysts under identical reaction conditions - temperature (60 °C), PDO to catalyst molar ratio (1200:1). The results are shown in Table 8.1. For the polymerization initiated by TiCl₂(O*i*Pr)₂, the conversion of PDO to PPDO increased very slowly with time, reaching 29.3% after four hours, and at 24 hours, the conversion was still less than 80%. The M_v of PPDO gradually increased from 2.3×10^4 to 8.1×10^4 g/mol during this time – a characteristic of living polymerization. In the case of TiCl(O*i*Pr)₃, the

conversion of PDO was high at the beginning of the reaction, exceeding 80% in half an hour, and increasing slowly thereafter. Similar to $\text{TiCl}_2(\text{O}i\text{Pr})_2$, the M_V of PPDO gradually increased with the conversion. In the case of $\text{Ti}(\text{O}i\text{Pr})_4$, the conversion of PDO increased the fastest, reaching 91.9% in 12 minutes, with an M_V of 11.1×10^4 g/mol for the resulting polymer. By comparing the structures of the three catalysts, it is evident that the number of *OiPr* group, of $\text{TiCl}_2(\text{O}i\text{Pr})_2$, $\text{TiCl}(\text{O}i\text{Pr})_3$, and $\text{Ti}(\text{O}i\text{Pr})_4$ is 2, 3, and 4, respectively. Since this group is the initiating site of the catalyst, it is reasonable to postulate that rates of initiation and propagation should increase as the increase in the number of the initiating sites. We have used $\text{Ti}(\text{O}i\text{Pr})_4$ as the initiator to investigate the polymerization of PDO in detail.

Table 8.1 Polymerization of PDO initiated by titanium alkoxides

Entry	Catalyst	Time (h)	Conversion ^a (%)	$[\eta]^b$ (dL/g)	$M_V \times 10^{-4}$ (g/mol)
1	TiCl ₂ (O <i>i</i> Pr) ₂	4	29.3	0.44	2.3
2	TiCl ₂ (O <i>i</i> Pr) ₂	8	57.5	0.82	6.1
3	TiCl ₂ (O <i>i</i> Pr) ₂	16	70.3	0.93	7.5
4	TiCl ₂ (O <i>i</i> Pr) ₂	24	74.5	0.98	8.1
5	TiCl(O <i>i</i> Pr) ₃	0.5	83.1	1.00	8.4
6	TiCl(O <i>i</i> Pr) ₃	2	84.0	1.03	8.8
7	TiCl(O <i>i</i> Pr) ₃	4	87.3	1.05	9.0
8	Ti(O <i>i</i> Pr) ₄	0.2	91.9	1.19	11.1
9	Ti(O <i>i</i> Pr) ₄	0.5	94.3	1.28	12.5
10	Ti(O <i>i</i> Pr) ₄	1	95.2	1.32	13.0

General reaction conditions: [PDO]/[I]=1200:1; reaction temperature=60 °C

^aConversion obtained by extraction using acetone as a solvent for 48 hours.

^bMeasured in phenol/1,1,2,2,-tetrachloroethane (1:1 V/V) at 25 °C.

8.3.2 Polymerization Mechanism

The ROP mechanisms of cyclic esters initiated by various initiators have been extensively studied. It has been revealed that the ROP of ϵ -caprolactone (35-36), lactide (38), and cyclic carbonates (39-40) initiated by titanium alkoxides occurs via the cleavage of acyl-oxygen bond. In addition, the ROP of 1,4-dioxan-2-one initiated by $\text{Al}(\text{O}i\text{Pr})_3$ (20) and $\text{La}(\text{O}i\text{Pr})_3$ (33) also occurs with cleavage of acyl-oxygen bonds.

To understand the mechanisms of ROP of PDO initiated by titanium alkoxides, three low molecular weight PPDOs were prepared using $\text{TiCl}_2(\text{O}i\text{Pr})_2$, $\text{TiCl}(\text{O}i\text{Pr})_3$, and $\text{Ti}(\text{O}i\text{Pr})_4$ as initiator with a low $[M]/[I]$ ratio of 100:1 at 60 °C for 1 hour in bulk. The products were purified by dissolving in chloroform and precipitated in excess of anhydrous methanol twice to remove unreacted PDO monomer before it was dried to a constant weight under vacuum at 40 °C. The three polymers were marked as PPDO2, PPDO3, and PPDO4, where 2, 3, and 4 represent the number of the $\text{O}i\text{Pr}$ groups of the corresponding initiator. The conversion for the three PPDOs was 71.2%, 78.0%, and 78.5%, respectively. The chemical structure of the three PPDOs was characterized by ^1H NMR as shown in Figure 8.1. The shifts of the three methylene protons of the repeat units were observed at 3.76($\delta\text{H}^{a+a'}$), 4.16($\delta\text{H}^{b+b'}$), and 4.34(δH^c) ppm respectively. The peaks at 1.22(δH^d) and 5.08(δH^e) ppm indicate the formation of the isopropyl end

group. In addition, $3.7(\delta H^c)$ a triplet was assigned to a methylene (CH_2) linked to hydroxyl (OH).

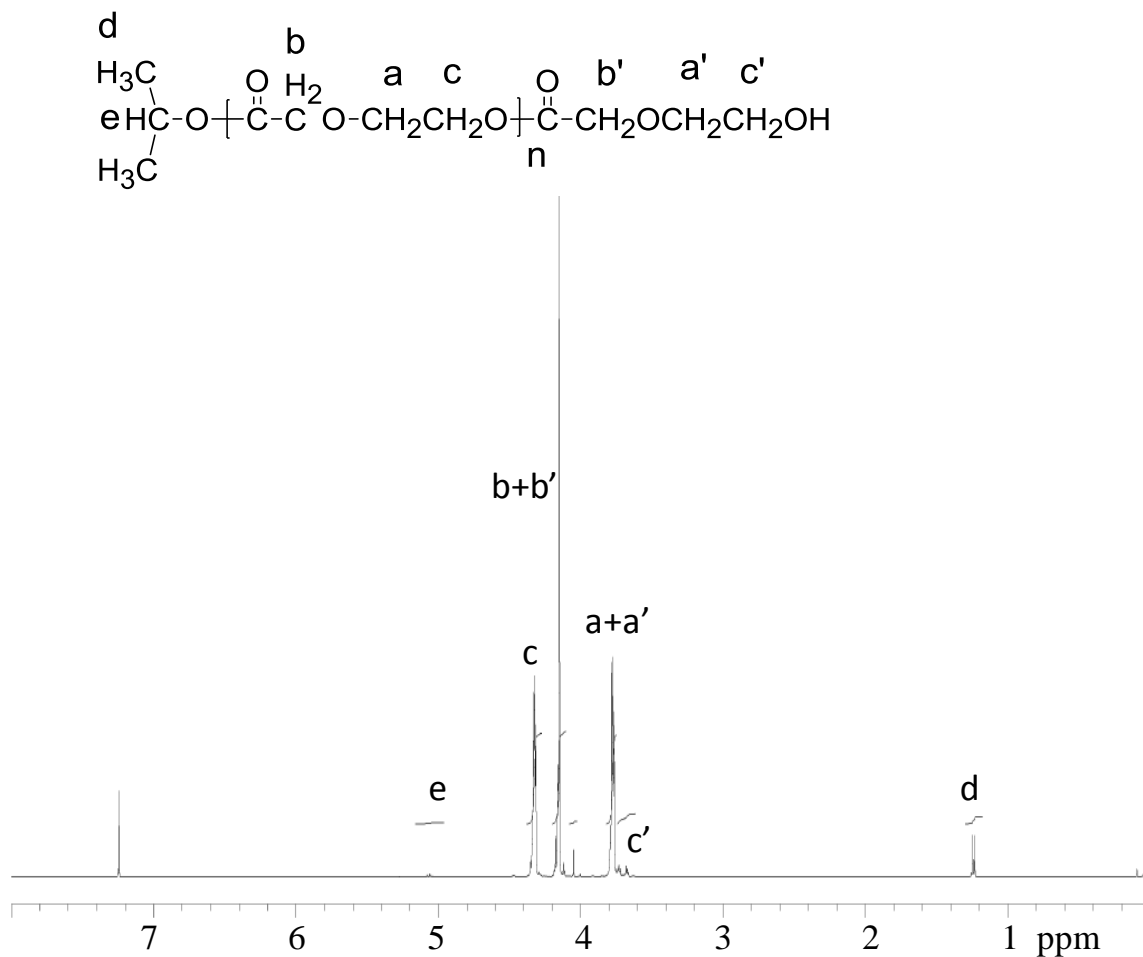


Figure 8.1 1H NMR of PPDO with titanium alkoxide initiators

Ring opening polymerizations of lactone (41) and lactide (37, 44), initiated by titanium alkoxides, occur via a coordination-insertion mechanism. This mechanism was proved to exist in the ROP of PDO initiated by $Al(OiPr)_3$ (20) and $La(OiPr)_3$ (33).

Therefore, it is reasonable to suppose that the coordination-insertion mechanism operates in the ROP of PDO initiated by titanium alkoxides in this study. The end groups of isopropyl ester and hydroxyl group generated by cleavage of metal-oxygen bond should therefore be present in the structure of the resulting PPDO. In agreement with the above hypothesis, the two end groups have been identified by ^1H NMR characterization of the resulting polymers.

When ROP of PDO was initiated by $\text{Al}(\text{O}i\text{Pr})_3$ (20) and $\text{La}(\text{O}i\text{Pr})_3$ (33) there were only 1.3 effective alkoxides in both cases, which indicated that not all the three $\text{O}i\text{Pr}$ groups are able to initiate the ring-opening polymerization of PDO. In this study, we have also estimated the effective alkoxide initiation sites of the individual titanium alkoxides. The chlorine group of titanium alkoxides is unable to initiate ring-opening polymerization (38). For the ROP of PDO initiated by $\text{TiCl}_2(\text{O}i\text{Pr})_2$, the theoretical average number of monomer (N_t) for each initiator molecule can be calculated from the initial ratio $[M]/[I]$ and the conversion percentage: $100 \times 71.2\% = 71.2$. If there were two $\text{O}i\text{Pr}$ groups per $\text{TiCl}_2(\text{O}i\text{Pr})_2$ that effectively initiated polymerization, the theoretical average degree of polymerization (DP_t) of each PPDO chain after cleavage of titanium-oxygen should be $71.2/2 = 35.6$. The experimental value (DP_e) was obtained as 37.8 from

the ratio of relative intensities of the methylene protons ($H^{a+a'}$) of the repeat units and the methyl protons of the isopropoxy group (H^d). The value of DP_e approaches DP_t , indicating that almost all OiPr groups are active sites able to initiate polymerization. The effective OiPr groups per $TiCl_2(OiPr)_2$ was thus calculated as $71.2/37.8=1.9$. In the case of $TiCl(OiPr)_3$, the N_t value was 78. If there were three OiPr groups per $TiCl(OiPr)_3$ effectively initiated polymerization, the value of DP_t would be 26 and the DP_e was determined to be 30 experimentally. The effective OiPr groups per $TiCl(OiPr)_3$ was calculated to be 2.6. When it comes to $Ti(OiPr)_4$, the N_t value was 78.5. If there were four OiPr groups per $Ti(OiPr)_4$ effectively initiated polymerization, the value of DP_t would be 17.1 and was experimentally determined to be 20.7. Thus the effective OiPr groups per $Ti(OiPr)_4$ was calculated as 3.8. It should be noted that similar findings have been made by Kricheldorf et al. (46) for the polymerization of lactide initiated by titanium alkoxides. This effectively implies, that unlike aluminium alkoxides, titanium alkoxides do not associate significantly in the polymerization of PDO. This has been reported at least for one catalyst employed in the study $Ti(OiPr)_4$ (47-48).

8.3.3 ROP of PDO initiated by $\text{Ti}(\text{O}i\text{Pr})_4$

To discuss the ROP of PDO initiated by $\text{Ti}(\text{O}i\text{Pr})_4$ in detail, the effects of molar ratio of PDO to initiator and reaction time on the polymerization of PDO were firstly studied, the reaction temperature was 60 °C for all the samples. The results are summarized in Table 8.2. It was found that the conversion of PDO to PPDO increased very fast in the first five minutes regardless of the $[M]/[I]$. When $[M]/[I]$ was 2400, the rate of increase in conversion was somewhat slower in comparison with the other ratios, due to the relatively lower concentration of initiator. When the ratio further increased to a higher value of 3600, the reaction was very slow, therefore the results have not been discussed here. For $[M]/[I]$ of 300, 600, 1200, as the polymerization time was extended, the conversion reached a maximum at 30 min, and then decreased very slowly. However for a ratio of 2400, longer time was needed to reach maximum attainable conversion. It is well known that the molecular weight of polymers in ROP of lactone and lactide initiated by metal alkoxides are controlled by adjusting the $[M]/[I]$ ratio because of the living characteristic of the polymerization. Similar results have been obtained in this system, with the M_v of PPDO increasing from 3.8×10^4 to 23.8×10^4 g/mol gradually when the $[M]/[I]$ ratio increased from 300 to 2400.

Table 8.2 Polymerization of 1,4-dioxan-2-one initiated by Ti(OiPr)₄

Entry	[M]/[I] (mol/mol)	Time (min)	Conversion ^a (%)	[η] ^b (dL/g)	$M_v \times 10^{-4}$ (g/mol)
14	300	5	84.9	0.58	3.5
15	300	30	91.3	0.61	3.8
16	300	120	90.6	0.60	3.7
17	600	5	91.3	0.86	6.6
18	600	30	93.6	0.88	6.9
19	600	120	90.8	0.83	6.3
20	1200	5	90.8	1.24	11.9
21	1200	30	94.3	1.30	12.8
22	1200	120	91.4	1.27	12.3
23	2400	5	75.6	1.67	18.5
24	2400	30	88.7	1.83	21.9
25	2400	120	93.6	1.92	23.8

General reaction conditions: Reaction temperature=60 °C

^aConversion obtained by extraction using acetone as a solvent for 48 hours.

^bMeasured in phenol/1,1,2,2-tetrachloroethane (1:1 V/V) at 25 °C.

The effect of reaction temperature on the ROP of PDO was studied by using [M]/[I] ratio of 2400 at which reaction was a little slow, which would make it easier to determine the effect of temperature on the polymerization. Four temperatures 40, 50,

60, and 70 °C were chosen in the study. The conversion versus time at different temperatures is shown graphically in Figure 8.2. It is clear that the conversion increases linearly with time at the beginning of polymerization irrespective of reaction temperature.

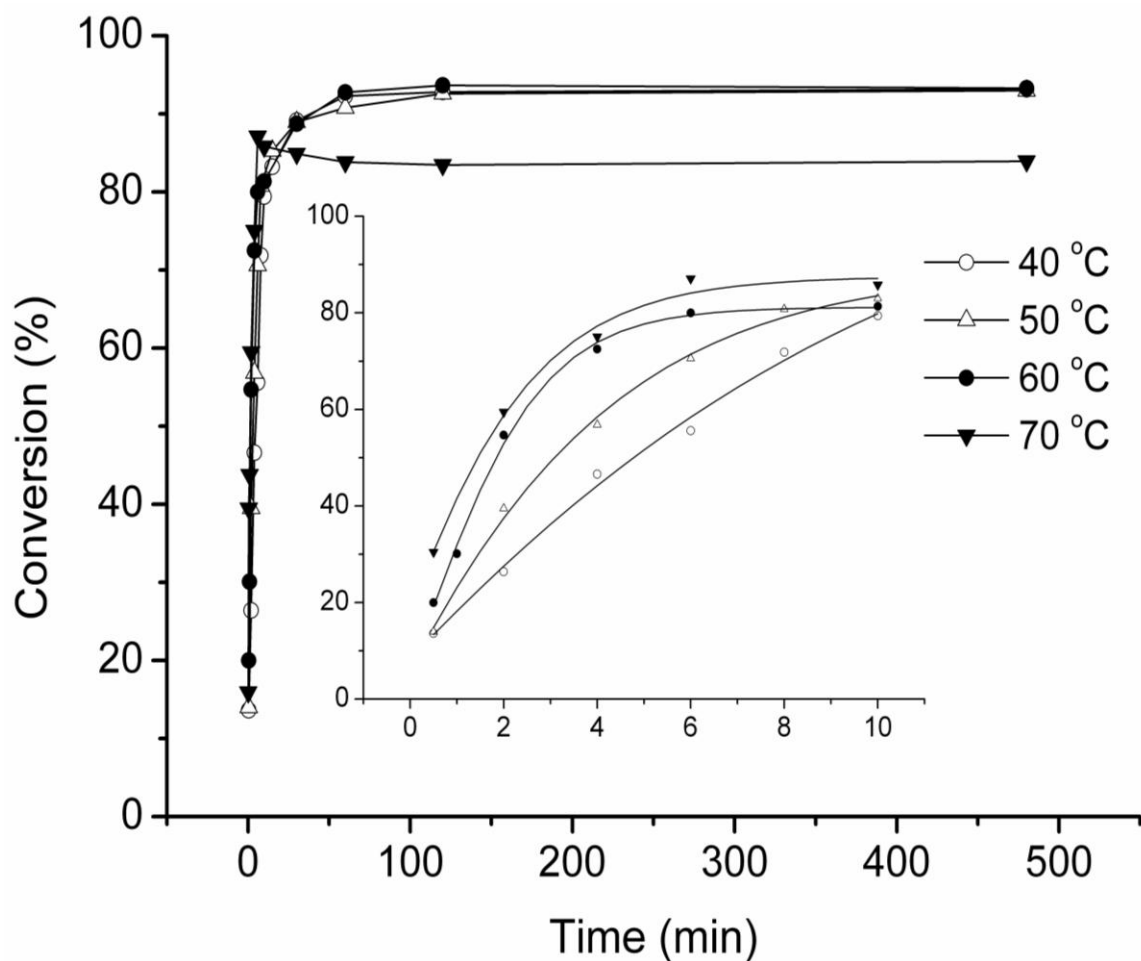


Figure 8.2 The effects of reaction time and temperature on the conversion of 1,4-dioxan-2-one, [M]/[I]=2400:1; initiator $\text{Ti}(\text{O}i\text{Pr})_4$

However, the slope of the straight-line increases as the temperature is increased, indicating increased polymerization rate with increase in reaction temperature. It is worth noting that the equilibrium conversions of PDO at 40, 50, and 60 °C were almost the same, around 93%. While at 70 °C, the value of equilibrium conversion decreased to 84%. The value of 93% is most likely the maximum attainable conversion of PDO in this system. This value corresponds well to the value of 94% reported by Nishida et al. with $\text{Al}(\text{Et})_3$ as the catalyst. There was little difference in the conversion of PDO in low temperature polymerizations (lower than 60 °C). When the temperature was increased to more than 60 °C, conversion of PDO gradually decreased with the increase of reaction temperature, a characteristic of equilibrium polymerizations.

To study the effect of reaction temperature on the conversion of PDO and M_v of PPDO, five PPDO samples were synthesized at 40, 50, 60, 70, and 80 °C for one hour. The results are listed in Table 8.3. The conversion of PDO is seen to decrease with increasing reaction temperatures.

Table 8.3 The effect of reaction temperature on the polymerization of 1,4-dioxan-2-one initiated by Ti(O*i*Pr)₄

Entry	Temp (°C)	Conversion ^a (%)	[η] ^b (dL/g)	$M_V \times 10^{-4}$ (g/mol)
26	40	93.2	1.98	24.9
27	50	93.0	1.86	22.6
28	60	92.7	1.85	22.3
29	70	84.9	1.60	17.8
30	80	81.9	1.58	17.5

General reaction conditions: [PDO]/[Ti(O*i*Pr)₄]=2400:1, Reaction time: 1hr.

8.3.4 Polymerization Kinetics

The bulk polymerization kinetics were investigated at 40-70 °C using Ti(O*i*Pr)₄ as an initiator. The ROP of PDO initiated by La(O*i*Pr)₃ (33) follows first order kinetics (reversible polymerization/depolymerization), so we can postulate that the ROP of PDO initiated by Ti(O*i*Pr)₄ also follows the same kinetics. Then, the rate equation can be expressed simply as:

$$\ln\{([M]_0 - [M]_e) / ([M]_t - [M]_e)\} = k_{app}t$$

where $[M]_0$ and $[M]_t$ are initial concentration of PDO and concentration at time t of PDO, respectively, $[M]_e$ is the equilibrium concentration of PDO, and k_{app} is the corresponding apparent rate constant. It is worth noting that, within a polymerization time lower than 13 min at the various temperatures involved in the study, the reaction medium remains homogeneous and that no crystallization happens. The values of $[M]_0$, $[M]_t$ and $[M]_e$ were calculated from the conversion of PDO and the densities of the monomers and molten polymers reported by Nishida et al. (31) The results obtained are plotted and shown in Figure 8.3. At any of the four temperatures, linear relationship between $\ln\{([M]_0 - [M]_e) / ([M]_t - [M]_e)\}$ and reaction time was observed at the $[M]/[I]$ of 2400 during 8 minutes. The results confirmed that the kinetics of ROP of PDO initiated by $Ti(OiPr)_4$ is first order in the full range of PDO conversions investigated. The plot was used to determine the apparent rate constant (k_{app}) of polymerization at each temperature from 40 to 70 °C as $0.171 \text{ L mol}^{-1} \text{ min}^{-1}$, $0.225 \text{ L mol}^{-1} \text{ min}^{-1}$, $0.335 \text{ L mol}^{-1} \text{ min}^{-1}$, and $0.529 \text{ L mol}^{-1} \text{ min}^{-1}$, respectively. The values are higher than those of the ROP of PDO initiated by $La(OiPr)_3$, (33) indicating that the polymerization rate of PDO initiated by $Ti(OiPr)_4$ is higher than $La(OiPr)_3$.

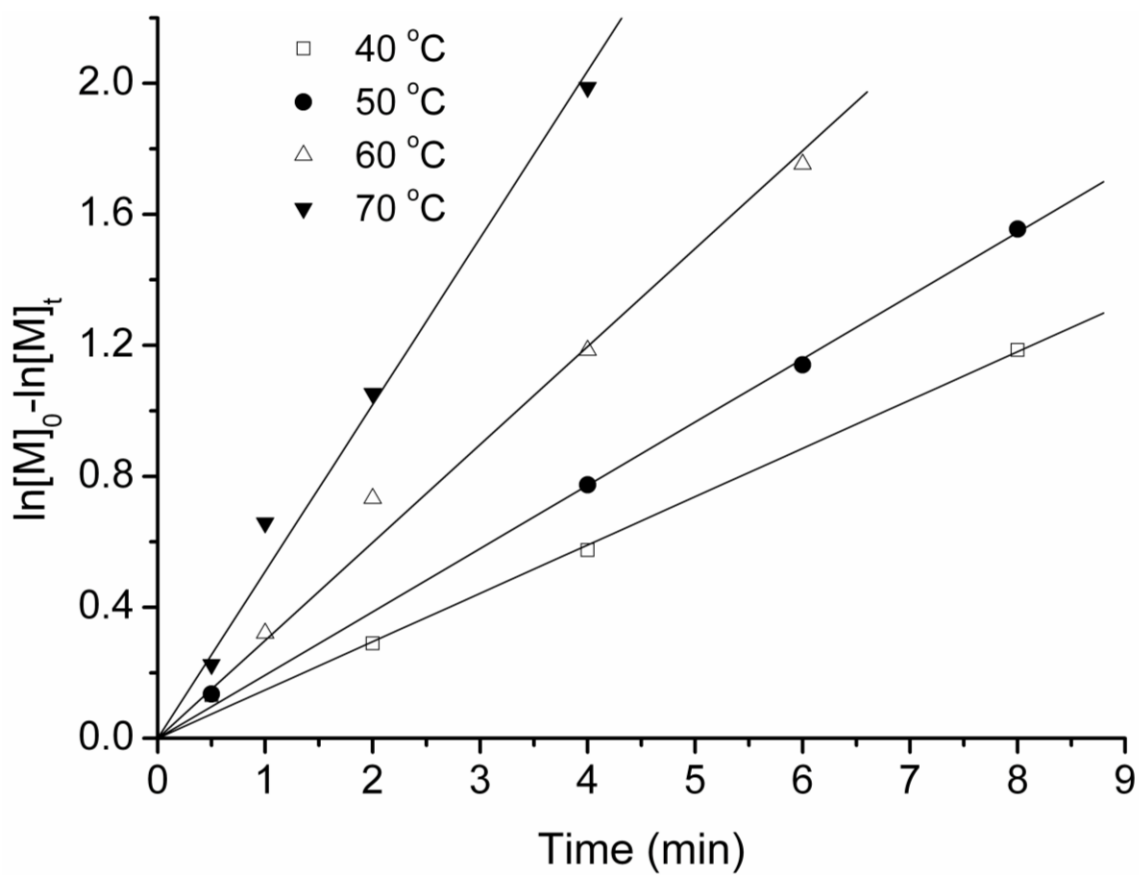


Figure 8.3 Plots of $\ln[M]_0 - \ln[M]_t$ versus time for different reaction temperatures

The temperature dependence of k_{app} is described with an Arrhenius plot in Figure 8.4. The apparent activation energy (E_{app}) was calculated as 33.7 kJ mol^{-1} by the slope of the plot, which is lower than that of PDO bulk polymerization using $\text{La}(\text{O}i\text{Pr})_3$ as a initiator ($E_{app} = 50.5 \text{ kJ/mol}$) determined by Zhu et al. (33) and using $\text{Sn}(\text{Oct})_2$ as a initiator ($E_{app} = 71.8 \text{ kJ/mol}$) calculated by Nishida et al. (31).

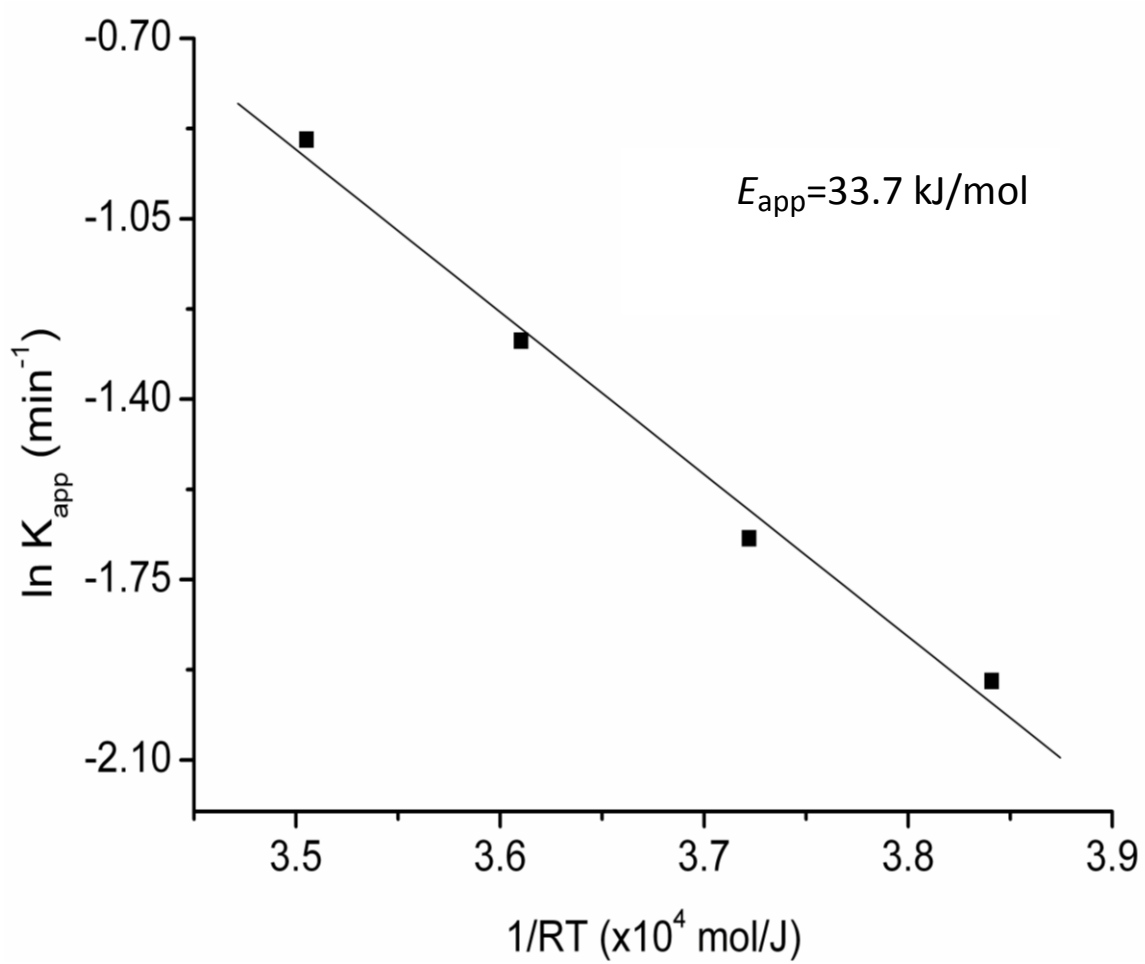


Figure 8.4 Plot of $\ln k_{\text{app}}$ versus $1/RT$

8.4 CONCLUSIONS

The ROP of 1,4-dioxan-2-one has been successfully initiated by $\text{TiCl}_2(\text{OiPr})_2$, $\text{TiCl}(\text{OiPr})_3$, and $\text{Ti}(\text{OiPr})_4$ in bulk. Conversion rate of PDO and structure of the resultant PPDO was different with different initiators. As with other cyclic esters, the ROP of PDO initiated by alkoxides follows the coordination-insertion mechanism with acyl-oxygen cleavage of the ester bond of PDO. This has been confirmed via NMR spectroscopy. The kinetic investigation of the polymerization also reveals the polymerization to be first-order with respect to the monomer concentration, and the apparent activation energy (E_{app}) was determined as 33.7 kJ/mol. From the values of activation energy determined, it is also seen that Titanium alkoxide catalysts are highly efficient and active in the polymerization of PDO. Polymerization times are in the order of minutes for conversions as high as 93 %. Thus these catalysts are attractive especially in processes like reactive extrusion polymerization of cyclic esters, where residence times are often small. The catalytic activity at low temperature is also likely to have implications, in post polymerization treatment to increase the degree of polymerization as demonstrated by Shinno et al. (49) for polylactide.

REFERENCES

8.5 REFERENCES

1. D. Garlotta, *Journal of Polymers and the Environment* **9**, 63 (Apr, 2001).
2. K. K. Yang, X. L. Wang, Y. Z. Wang, *Journal of Macromolecular Science-Polymer Reviews* **C42**, 373 (2002).
3. A. Duda, S. Penczek, *Polimery* **48**, 16 (2003).
4. H. Wang, J. H. Dong, K. Y. Qiu, Z. W. Gu, *Journal of Polymer Science Part a-Polymer Chemistry* **36**, 1301 (Jun, 1998).
5. H. Nishida, M. Yamashita, M. Nagashima, T. Endo, Y. Tokiwa, *Journal of Polymer Science Part a-Polymer Chemistry* **38**, 1560 (May, 2000).
6. S. W. Hong, K. H. Kim, J. Huh, C. H. Ahn, W. H. Jo, *Macromolecular Research* **13**, 397 (Oct, 2005).
7. M. A. R. Meier, U. S. Schubert, *E-Polymers*, (Dec, 2005).
8. P. Kurcok, P. Dubois, R. Jerome, *Polymer International* **41**, 479 (Dec, 1996).
9. H. D. She, X. F. Xiao, R. F. Liu, *Journal of Materials Science* **42**, 8113 (Oct, 2007).
10. Q. Zeng *et al.*, *European Polymer Journal* **44**, 465 (Feb, 2008).
11. A. Kowalski, A. Duda, S. Penczek, *Macromolecules* **33**, 7359 (Oct, 2000).
12. X. L. Hu *et al.*, *Biomacromolecules* **9**, 553 (Feb, 2008).
13. P. Degee, P. Dubois, S. Jacobsen, H. G. Fritz, R. Jerome, *Journal of Polymer Science Part a-Polymer Chemistry* **37**, 2413 (Jul, 1999).
14. P. Dubois, M. Krishnan, R. Narayan, *Polymer* **40**, 3091 (May, 1999).

15. D. Colak, I. Cianga, A. E. Muftuoglu, Y. Yagci, *Journal of Polymer Science Part a-Polymer Chemistry* **44**, 727 (Jan, 2006).
16. K. R. Yoon *et al.*, *Journal of Materials Chemistry* **13**, 2910 (2003).
17. S. C. Chen, X. L. Wang, K. K. Yang, G. Wu, Y. Z. Wang, *Journal of Polymer Science Part a-Polymer Chemistry* **44**, 3083 (May, 2006).
18. D. Tian, P. Dubois, R. Jerome, *Macromolecules* **30**, 2575 (May, 1997).
19. A. Duda, *Macromolecules* **29**, 1399 (Feb, 1996).
20. J. M. Raquez, P. Degée, R. Narayan, P. Dubois, *Macromolecules* **34**, 8419 (Nov, 2001).
21. H. R. Kricheldorf, D. O. Damrau, *Macromolecular Chemistry and Physics* **199**, 1089 (Jun, 1998).
22. B. M. Chamberlain *et al.*, *Journal of the American Chemical Society* **123**, 3229 (Apr, 2001).
23. B. J. O'Keefe, S. M. Monnier, M. A. Hillmyer, W. B. Tolman, *Journal of the American Chemical Society* **123**, 339 (Jan, 2001).
24. X. Y. Wang, K. R. Liao, D. P. Quan, Q. Wu, *Macromolecules* **38**, 4611 (May, 2005).
25. B. J. O'Keefe, L. E. Breyfogle, M. A. Hillmyer, W. B. Tolman, *Journal of the American Chemical Society* **124**, 4384 (Apr, 2002).
26. P. Albert, H. Warth, R. Mulhaupt, R. Janda, *Macromolecular Chemistry and Physics* **197**, 1633 (May, 1996).
27. C. S. Wu, *Journal of Applied Polymer Science* **92**, 1749 (May, 2004).

28. B. M. Chamberlain, B. A. Jazdzewski, M. Pink, M. A. Hillmyer, W. B. Tolman, *Macromolecules* **33**, 3970 (May, 2000).
29. E. Martin, P. Dubois, R. Jerome, *Macromolecules* **33**, 1530 (Mar, 2000).
30. K. B. Aubrecht, K. Chang, M. A. Hillmyer, W. B. Tolman, *Journal of Polymer Science Part a-Polymer Chemistry* **39**, 284 (Jan, 2001).
31. H. Nishida, M. Yamashita, T. Endo, Y. Tokiwa, *Macromolecules* **33**, 6982 (2000).
32. S. Balakrishnan, M. Krishnan, P. Dubois, R. Narayan, *Polymer Engineering & Science* **44**, 1491 (2004).
33. X. L. Zhu *et al.*, *Journal of Polymer Science Part a-Polymer Chemistry* **46**, 5214 (Aug, 2008).
34. J. A. Gladysz, *Chemical Reviews* **100**, 1167 (Apr, 2000).
35. D. Takeuchi, T. Nakamura, T. Aida, *Macromolecules* **33**, 725 (Feb, 2000).
36. A. D. Asandei, G. Saha, *Macromolecular Rapid Communications* **26**, 626 (Apr, 2005).
37. Y. J. Kim, J. G. Verkade, *Macromolecular Rapid Communications* **23**, 917 (Oct, 2002).
38. Y. Kim, G. K. Jnaneshwara, J. G. Verkade, *Inorganic Chemistry* **42**, 1437 (Mar, 2003).
39. D. Takeuchi, T. Aida, T. Endo, *Macromolecular Rapid Communications* **20**, 182 (Apr, 1999).
40. D. Takeuchi, T. Aida, T. Endo, *Macromolecular Chemistry and Physics* **201**, 2267 (Dec, 2000).

41. J. Cayuela, V. Bounor-Legare, P. Cassagnau, A. Michel, *Macromolecules* **39**, 1338 (Feb, 2006).
42. J. M. Raquez, P. Degée, R. Narayan, P. Dubois, *Macromolecular Rapid Communications* **21**, 1063 (Oct, 2000).
43. A. D. Asandei, Y. H. Chen, O. I. Adebolu, C. P. Simpson, *Journal of Polymer Science Part a-Polymer Chemistry* **46**, 2869 (Apr, 2008).
44. Y. Kim, J. G. Verkade, *Macromolecular Symposia* **224**, 105 (Apr, 2005).
45. M. A. Sabino, J. L. Feijoo, A. J. Muller, *Macromolecular Chemistry and Physics* **201**, 2687 (Dec, 2000).
46. H. Kricheldorf, M. Berl, N. Scharnagl, *Macromolecules* **21**, 286 (1988).
47. F. Babonneau *et al.*, *Inorganic Chemistry* **27**, 3166 (1988).
48. D. Bradley, C. Holloway, *Journal of the Chemical Society A: Inorganic, Physical, Theoretical* **1968**, 1316 (1968).
49. K. Shinno, M. Miyamoto, Y. Kimura, Y. Hirai, H. Yoshitome, *Macromolecules* **30**, 6438 (1997).

CONCLUSIONS AND FUTURE DIRECTION

9.1 OZONOLYSIS

Ozonolysis of a model compound (methyl oleate) and soybean oil was conducted in bulk in the presence of a solid heterogeneous catalyst. While double bonds were effectively oxidized, we were unable to direct the oxidation to the requisite products. This has been extensively discussed in the Chapter 3. The mixed products from ozonolysis were used in a polyester synthesis to determine their reactivity. The results are summarized in Chapter 4. Based on the conclusions drawn from Chapter 3, a two stage oxidation was proposed and the model compound methyl oleate was successfully transformed to hydroxyesters, using Ozone and Oxone.

Bulk ozonolysis has been seldom reported in literature and where it has, the purpose has been to determine products formed. Thus the interest has been academic. Much of ozonolysis is still conducted at low temperatures and in solvent, making the process unattractive from a scale up perspective. What has been demonstrated in Chapter 3 is that if the unsaturated compound and the reacting alcohol are brought into intimate contact, as they would be in solution, the ozonolysis can be redirected to some extent to provide the requisite products.

In this regard, there is a need to form fine emulsions of the oil or the methyl ester with the reacting alcohol. This can be accomplished, by the use of high speed mixing and injecting samples at a Venturi injector's throat. The high gas flow rate in our system should help in creating small particles, which should help in the trapping of reactive intermediates and help in product formation.

A key issue was not discussed in detail in Chapter 3, was the presence of exothermic decompositions. Samples which were deficient in base (especially NaOH) or were not water washed, tend to display an exotherm of around 90 °C when heated and held at 95 °C to 120 °C. The magnitude of this exotherm diminishes with water washing with either acidified water or alkaline water or just plain distilled water. The addition of base like NaOH also mitigates the issue. Also after the material returns to normal temperatures, the viscosity is markedly high. It would be of interest to see the products of such exotherms and also the cause for viscosity increase.

This would help gain insight into the decomposition of peroxygenic species in the ozonated products. It is known that, the decomposition pathway (pyrolysis) of ozonides and peroxygenic species is towards formation of aldehydes and acids. It would be worthwhile to explore if that decomposition itself can be re- routed to forming the hydroxy esters.

From Chapter 5, it is evident that Oxone is a good second stage oxidant for converting aldehydes and other intermediates into esters. However, the cost of Oxone might be a deterrent in its large scale use, since currently there are no known ways of

recycling the byproducts to Oxone. In such a case, it might be worthwhile to shift the focus away from the esters, to making the acids via ozonolysis. Separation would be the only challenge, since ozonolysis in water is well defined and ultimately acids are obtained in good yields. The acids can then be directly used in polymer synthesis.

9.2 Silylation of Soybean Oil/Fatty Acid Esters

Chapter 6 and 7 discuss some aspects of silylation of soybean oil and a fatty acid methyl ester to get room temperature curable products. The mechanism was shown to be a radical mediated grafting, with polyunsaturated fatty acids acting as chain terminators. Future work in this area should focus on mapping out completely, the dependence of silylation extent on the time, temperature, silane ratio and peroxide for a variety of oils and fatty acid esters.

The same could also be extended to cover other reactive silanes like vinyltriacetoxysilane and vinylmethyldimethoxysilane and divinyl silanes. The vinyl acetoxysilane derivative is more water sensitive and thus likely to hydrolyze quicker with shorter curing times. Also important is the use of divinyl silanes, to build up the molecular weight by radical mediated grafting.

Hydrosilylation of internal double bonds has been reported using a radical initiation sequence (RIS) for hydrosilanes containing halogen groups. It would be of interest to see if the high temperatures involved in the silylation of soybean oil can

provide a route for such hydrosilylation to happen on soybean oil. This would provide for an alternative method to functionalize the soybean oil with silicones.

Additional experiments were done which have not been reported to determine, if the reaction would happen in the presence of UV light and a photosensitizer, since the grafting was established to be radical mediated. So a simple trial run was set up with soybean oil: silane ratio (1:5) and 0.5 wt% of benzophenone. After 24 hours, it was seen that approximately 0.7 moles of the silane has been grafted to the oil. This result is interesting for the following reasons.

Although the process is simple, silylation is being done at high temperature, which would still make it energy intensive, especially because of the longer reaction times. The use of photosensitizer with UV light is attractive, since no heating then is required. The reaction times may also be reduced with the use of an appropriated wavelength lamp and of the proper intensity.

One aspect which has not been discussed in the work is the dependence of curing rate on the concentration (grafted amount) of silane. While it would appear, that the silane concentration would influence the rate of cure, it needs to verify experimentally to see the effect. Future experiments could be directed at using different silane grafted materials under identical conditions to determine the change in the curing rate.

The central theme of this work has been that the material is bio-based. It would also be interesting to see if the material is biodegradable. Preliminary studies seem to

suggest that one of the materials (soybean oil: silane of 1:7 ratio) after complete cure, biodegrades to 40% in a time of 15 days in an aqueous biodegradation set up. This would need to be expanded to cover different silane grafted products, to determine the effect of cross – link density on the biodegradability.

The physical properties of the coatings would need to be evaluated (hardness, gloss etc). Preliminary experiments on 2 mil thick coatings for water vapor transmission rate give a figure of $100 \text{ gm/m}^2 \cdot \text{day}$. This number is about three times the values reported for biodegradable polyesters like PLA as 20 mil coatings. Further work would need to be done in formulating the coatings with fillers (clays, silica etc) to determine the effect on barrier properties.

Also for large scale applications like paper coatings, where residence times are quite small, the cure process has to be optimized to fit the time frame of the manufacturing process. This can be done by a combination of adding filler to increase the viscosity of the coating material, pre – cure of the material to reach a certain viscosity and careful choice of temperature and catalyst concentrations for curing. It has already been established (not reported), that pre – curing the material with 20% or more water at 70°C aids in viscosity build up and provides for easy application to paper, without the oil being absorbed excessively by the paper. Such studies have to be systematized for future work.

9.3 TRANSESTERIFICATION CHEMISTRY

The work done has only been preliminary (Discussed in Chapter 10). However, the possibility of transesterification with a functional alcohol is interesting. Hydrosilylation has been proved at least for the allyl ester case. The propargyl ester has already been synthesized at around 70% purity (not reported) and work is on to synthesize the cinnamyl ester.

Future work would need to determine the physical properties of such products and then decide on the application areas. It has been previously stated that the propargyl group is amenable to radical polymerization. The allyl group itself may polymerize with metallocene type catalysts. It may polymerize better than in a radical system when cationic initiators are used.

Sulfitation of fatty acid esters has been reported in the past. It would be interesting to see how sulfonated derivatives of these products would behave as surfactants. The cinnamyl derivative can also be experimented with in different polymerization systems to see the type of products formed. It is easy to see that one of the potential drawbacks that these products may have is the ester nature, which might be susceptible to hydrolysis. Thus any potential use would probably be limited by this one aspect, in addition to their drawbacks in terms of required attributes.

9.4 RING OPENING POLYMERIZATION OF PDO

Titanium alkoxides were proved to be highly efficient and active catalysts for the ROP of PDO. Polymerization happened with reasonable conversion at temperatures as low as 40 °C. The activity has been ascribed to the Lewis acid character of titanium. Also since the titanium tetra isopropoxide, does not associated in dilute solutions, all four alkoxide sites are able to initiate polymerization, at least at low $[M]/[I]$ ratios. It is reasonable to assume that high shear conditions in reactive extrusion will enable this type of initiation, even at higher ratios leading multi – arm polyesters, with better melt strength.

It is also important to note that the alkoxide group is easy to manipulate. Thus instead isopropoxide, the end groups can be changed to allyl or acryl by choice of suitable alcohol, in synthesizing the catalyst. The allyl derivative has already been reported (Zerroukhi et al.(1)). These end functional PPDOs can then be suitably modified.

For example, an allyl functional PPDO, can then be hydrosilylated to yield different structures with silicones. The acryl group (from 2- hydroxyethyl methacrylate) can also be polymerized post extrusion, to yield new PPDOs with improved mechanical properties.

1. Z. Xia, A. Zerroukhi, Y. Chalamet, J. Chen, *Journal of Applied Polymer Science* **109**, 1772 (2008).

CHAPTER 10

OTHER PRELIMINARY STUDIES AND FUTURE RECOMMENDATIONS

ABSTRACT

The work outlines some preliminary work carried out with soybean oil using transesterification followed by hydrosilylation to yield different soybean oil – silicone hybrids which could find potential applications in cosmetics and lubricants. The procedure involves transesterification of the oil with olefinic alcohols (allyl alcohol, propargyl alcohol and cinnamyl alcohol) to yield fatty acid esters which act as pseudo alpha olefins. These esters, especially the ones with terminal unsaturation, can be reacted with either monomeric or polymeric hydrosilanes of different molecular structure, to yield a whole new family of fatty ester – silicone hybrids. In the following work, preliminary results on the above reactions feasibility have been reported with the allyl ester of soybean oil fatty acids and two different hydrosilanes.

The aromatic alcohol (cinnamyl alcohol) would yield a fatty ester with an aromatic ring in its structure. A sulfonation of such an ester would afford sulfonated derivatives of the esters, which could substitute LABS (linear alkyl benzene sulfonates) surfactants that are currently petroleum derived.

The second portion deals with a simple peroxide mediated silane grafting method, to improve compatibility of biodegradable polyesters with inorganic fillers, especially talc. The procedure is a direct application of the method used in the manufacture of XLPE (cross – linked polyethylene) for polyesters. The method can also be used to improve the mechanical properties of biodegradable polyesters in general (soft polyesters like PCL, PPDO).

SYNTHESIS OF ALPHA OLEFIN LIKE ESTERS FROM SOYBEAN OIL

10.1 INTRODUCTION

Alpha olefins are simple hydrocarbons having a double bond at one end of the molecule (1). Industrially, they are commonly manufactured by either oligomerization of ethylene, Fischer-Tropsch synthesis followed by purification or dehydration of high molecular weight alcohols. Prior to about 1970's linear alpha olefins were also manufactured by thermal cracking of waxes. Dehydration of alcohols to linear alpha olefins by passing alcohols in a vapor phase over acidic alumina catalyst has also been practiced. Normally, this process is not economical as the linear alcohols are more valuable than the corresponding linear alpha olefins.

Current applications of alpha olefins include chloroparaffins, synthetic drilling fluids, and paper sizing chemicals. They are also used in the manufacture of LABs (linear alkyl benzenes) for use in surfactants. They also find use in LLDPE (linear low density polyethylene) manufacture as co monomers with ethylene. Alpha olefins possess a terminal unsaturation which makes them very reactive. In vegetable oils however, unsaturations are internal. Creating terminal unsaturation would involve metathesis type chemistries. The simplest way to incorporate terminal olefin functionality to vegetable oils would be to transesterify the triglyceride, with an inexpensive alcohol,

like allyl alcohol. The resulting fatty acid allyl ester would have a terminal double bond, which could impart properties of an alpha olefin.

Other alcohols in this category can include propargyl and cinnamyl alcohol. The rationale for the choice of these alcohols is simple. Propargyl alcohol has acetylenic unsaturation and thus can have unique properties. The choice of cinnamyl alcohol is due to it being a styrenic alcohol and its availability as a natural product. Also valuable is the use of cinnamate esters in the perfumery industry. Cinnamyl alcohol can also be polymerized and thus could form a bio - based substitute for styrene or could be used as a co monomer in styrene polymerizations.

The aromatic core of the alcohol, could also serve as sites for sulfonation. Thus the cinnamyl ester would resemble linear alkyl benzene in structure. The advantage of transesterification is that, the functionalization happens at the acyl end of the fatty acid. Thus based on applications different oils can be used. For example, a lubricant application, could tap into oils with high saturates for thermal stability.

Also of interest in transesterification with unsaturated alcohols is the fact that these can be hydrosilylated, with a wide variety of hydrosilane polymers and monomers, leading to a new family of vegetable oil - silicone hybrids. These could find use in the personal care industry and in lubricants.

10.2 MATERIALS

Soybean oil (Select OilTM) was procured from Zeeland Farm Services (Zeeland, MI) and kept dried over molecular sieves. The oil had approximately 5 double bonds per mole (Iodine value ~ 148). Vegetable oil shortening (Crisco) was also used to make allyl esters of saturated fats. Three different hydrosilanes DMS H – 11 [CAS 70900-21-9], HMS – 082 [68037-59-2] and SIM – 6510.0 [68037-53-6] were procured from Gelest Inc. (Morrisville, PA). Allyl alcohol [CAS 107-18-6], chloroplatinic acid (H_2PtCl_6) hexahydrate [CAS 18497-13-7], anhydrous isopropanol [CAS 67-63-0] and anhydrous toluene [CAS 108-88-3] were procured from Sigma-Aldrich (St.Louis, MO) and used as received.

10.3 EXPERIMENTAL

10.3.1 Synthesis of allyl ester

A similar procedure described in US patent 2,536, 568 (2) was used using double the amount of the catalyst concentration described in this patent. About 215 gm of soybean oil (~0.25 mol) was heated to a reflux with 430 (~7.4 mol) gm of allyl alcohol and 2 gm of KOH as the catalyst for 3 hours. The reflux temperature for this particular composition was 108 °C. There was a slight yellowing of the product (relative to the soybean oil used).The catalyst was then discharged with about 3 gm of conc. HCl and

excess allyl alcohol removed by distillation. The product was then washed with warm distilled water to completely remove residual acid, salt (KCl), glycerol and excess allyl alcohol. The final product was obtained by distillation under reduced pressure at 90 °C (to remove traces of allyl alcohol). Allyl alcohol is sensitive to light and air and hence to prevent darkening of intermediates or final products, the reaction vessels were covered with aluminum foil. The system is held under a nitrogen blanket or just isolated from air using a mineral oil bubbler. A similar procedure was applied to the vegetable oil shortening also, but with triple the catalyst amount used in the patent, to account for the citric acid preservative in the shortening.

For larger batches (> 1Kg), the same procedure was employed, but only half the amount of allyl alcohol was used (1:15 mole ratio instead of 1:30). The product was subjected to the same procedure as before, except that the final distillation was done in a wiped film evaporator (Pope Scientific, Saukville, WI) at a temperature of 170 °C and pressure of 0.3 mTorr.

10.3.2 Hydrosilylation of allyl esters

Hydrosilylation was carried out using the hydrosilanes from Gelest Inc. A sample of allyl ester (~20 gm) was employed and the double bonds were estimated based on the NMR spectra and the iodine value. The quantity of hydrosilane was estimated based on the structure of the silane (37 gm DMS – H11, 10 gm of SIM – 6510.0 (referred to as MCSiH henceforth)).

The catalyst (chloroplatinic acid) was dissolved (0.586 gm) in 25 ml of dry isopropanol to give a solution which was then aged for a week shielded from light prior to use. For hydrosilylations, a 20 μ L volume of this solution was injected directly into the reaction mixture. 20 gm of allyl soyate (>90% pure) was dissolved in 30 ml of fresh dry toluene in a 3-necked flask. The DMS H-11 product (37 gm) and MCSiH (10 gm) were also dissolved in 30 ml of dry toluene in an addition funnel. The allyl soyate in the flask was heated to a steady temperature of 80 $^{\circ}$ C – 85 $^{\circ}$ C and then 0.4 mg of catalyst (20 μ L) was added. The siloxane was added in drops at a constant rate to this mixture. The heating was shut off to observe any exotherm resulting from the hydrosilylation. In the absence of observable exotherm – the solution was heated to a reflux for 2 hours (~115-120 $^{\circ}$ C). The set up is shown in Figure 10.1.

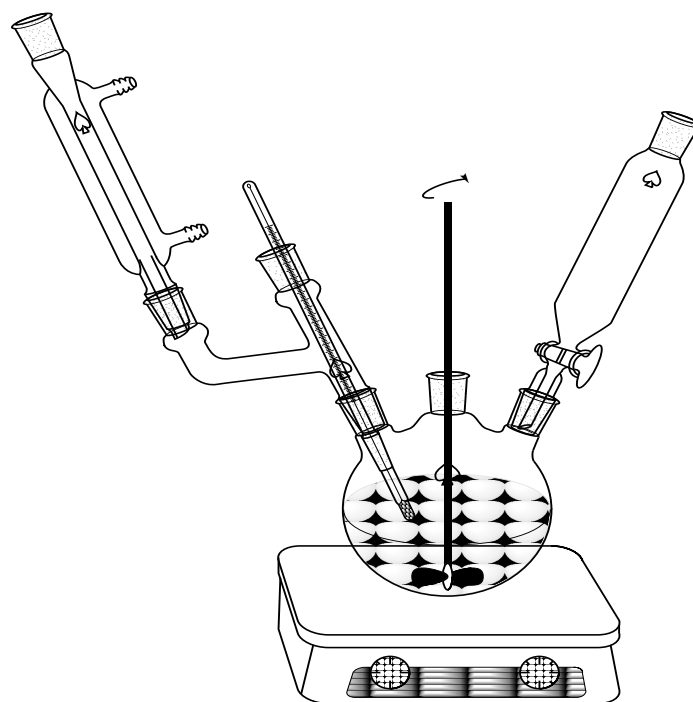


Figure 10.1 Reaction set up for hydrosilylation

10.4 CHARACTERIZATION

For allyl ester samples, samples were used in characterization after purification. For products of hydrosilylation, samples were used after complete removal of solvent. Iodine values were determined according to ASTM D1959 for both the starting soybean oil and the allyl ester product.

NMR spectra were recorded on a Varian Unity Plus spectrometer operating at 500 MHz. CDCl_3 was used as a solvent (^1H @ 7.24 ppm, ^{13}C @ 77 ppm) at a temperature of 25 °C for all experiments. Standard parameters were employed except for carbon spectra, where a recycle delay of 2 seconds was employed.

10.5 RESULTS AND DISCUSSION

The reaction scheme showing transesterification and hydrosilylation is shown in Figures 10.2 and 10.3 respectively. From Figure 10.3, it can be seen that hydrosilylation is simply a reduction of the double bond by the Si – H group. The hydrogen addition is typically at the carbon beta to the oxygen of the alcohol group (3-4) . Thus the products of hydrosilylation are linear and not branched i.e the derivative obtained with allyl alcohol is the n – propyl ester of the silyl carbinol and not the isopropyl ester This linear structure of the product is further confirmed by NMR as discussed below.

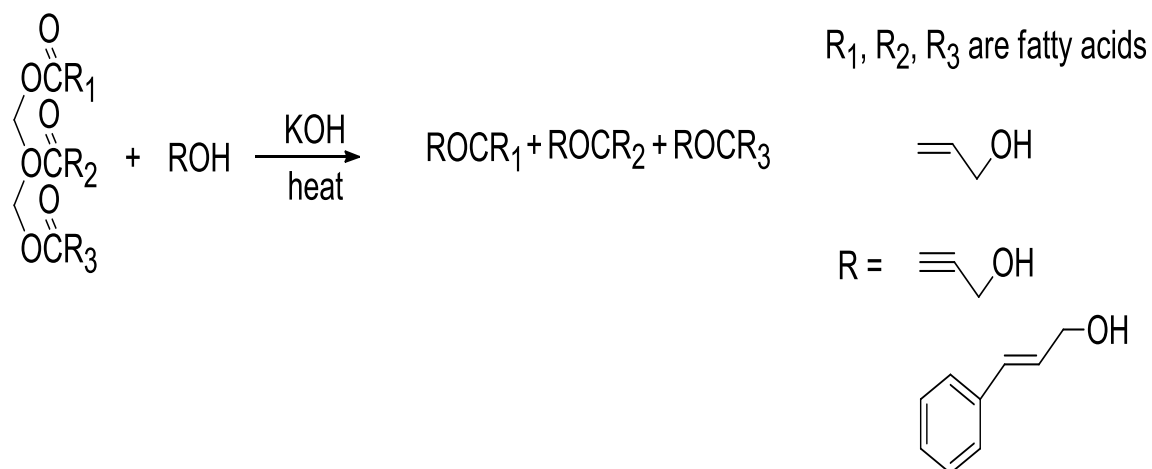


Figure 10.2 Transesterification of vegetable oil with different olefinic alcohols

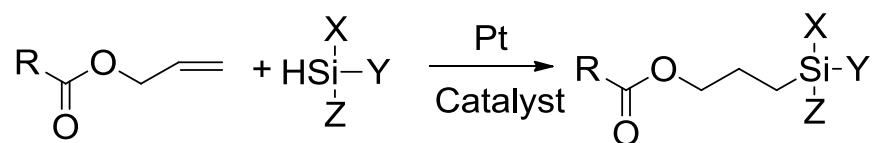


Figure 10.3 Hydrosilylation of a terminal olefin

From Figure 10.3 it can also be seen that the choice of silane is flexible. Both monomeric silanes and polymeric siloxanes can be employed to get a wide variety of products. However, it should be noted that hydrosilanes typically do not react with internal double bonds (exceptions are chlorosilanes and to some extent triethoxy hydrosilane). Thus the product from the cinnamyl alcohol is not likely to undergo hydrosilylation.

The NMR spectra of allyl ester of soybean oil and vegetable shortening are given in Figures 10.4, 10.5 and 10.6 respectively. From the integrals, a good estimate of the structure of the product can be obtained.

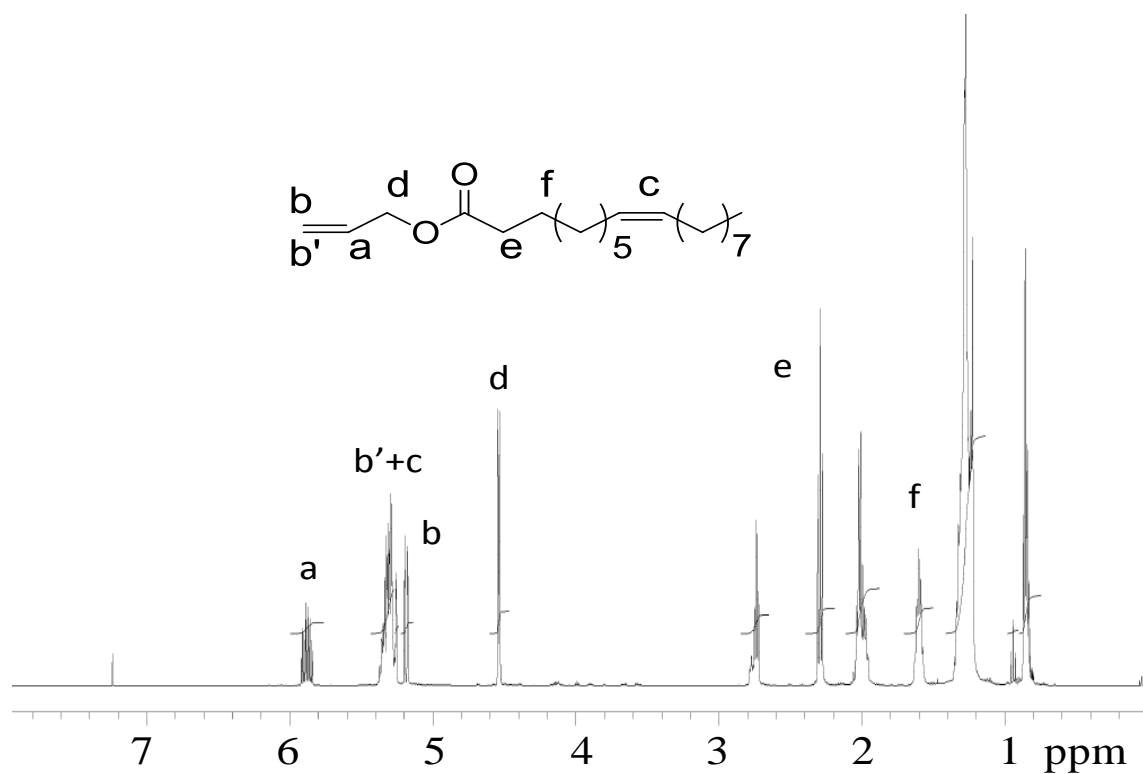


Figure 10.4 ^1H NMR spectrum of allyl fatty ester (from soybean oil) showing assignments

The NMR spectra for the allyl ester synthesized from the shortening is also similar except the level of unsaturation is lower due to hydrogenation.

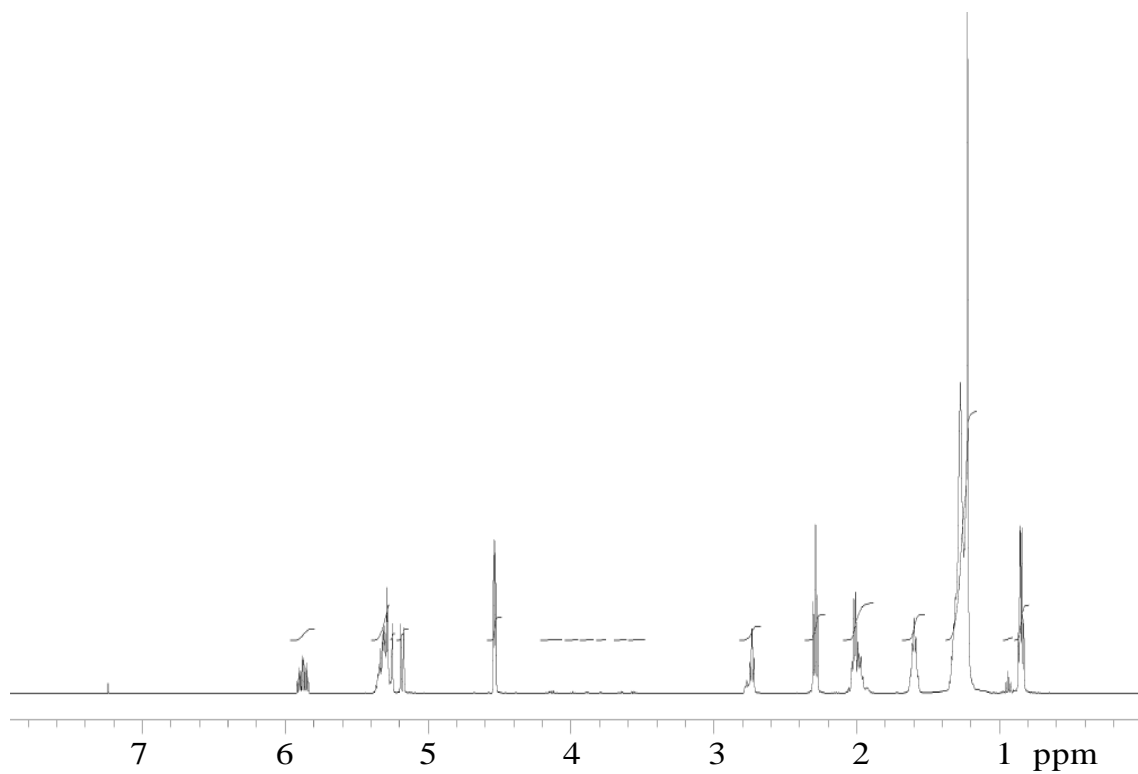


Figure 10.5 ^1H NMR spectrum of allyl ester from vegetable shortening

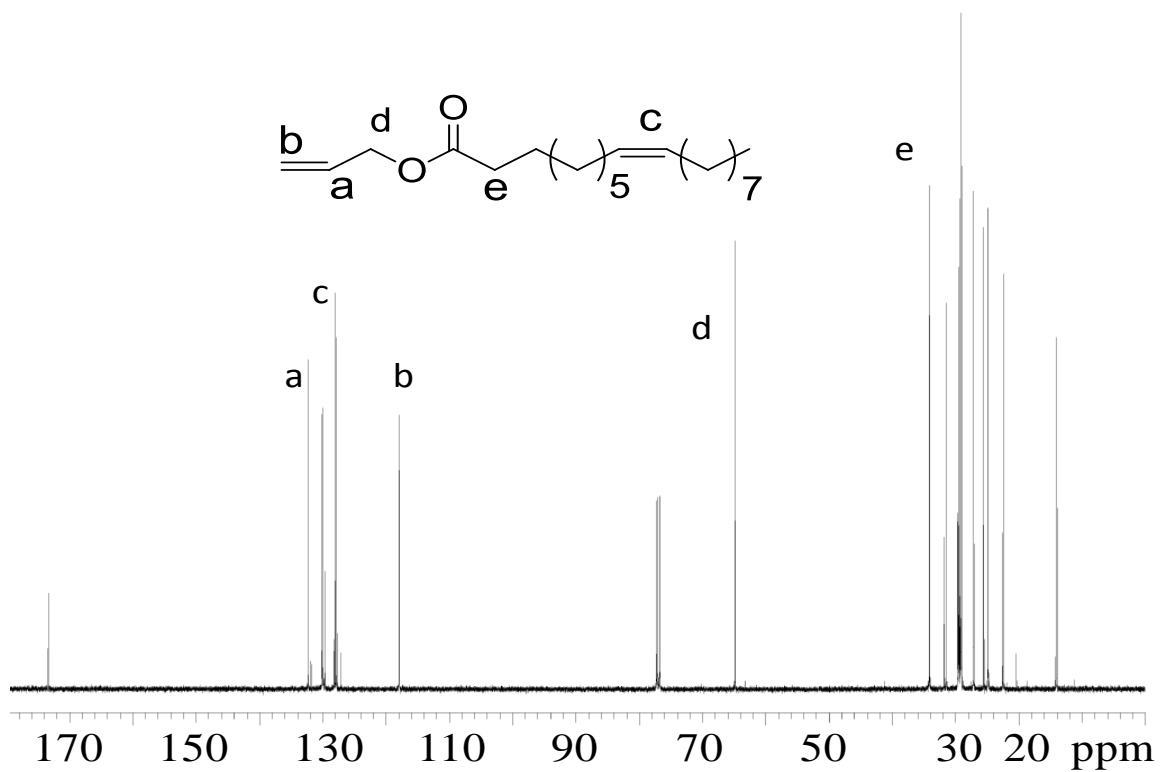


Figure 10.6 ^{13}C NMR of allyl fatty ester (from soybean oil) with assignments

It can be seen from the NMR assignments that based on the theoretical ratio of protons in the structure, an estimate of the purity of the allyl ester can be obtained. For integration purposes the protons alpha to oxygen of the alcohol are used to determine purity. For a 100% pure ester the ratio of the proton (d) at $\delta = 4.5$ ppm to the ratio of the proton (e) at $\delta = 2.3$ ppm (alpha to carbonyl) should be 1. For the allyl ester from soybean oil (Iodine value 148), this ratio was 0.88 (implying 88% allyl ester, Iodine value: 193) and for the vegetable shortening (Iodine value 130) this ratio was 0.90 (implying 90% allyl ester, Iodine value: 171) in product respectively. Thus the esters are obtained in good purity. For the larger batches which were purified by wiped film evaporation, the purity was > 98%, due to efficient removal of monoglycerides, glycerol water and any residual allyl alcohol.

The results of the hydrosilylation with the two hydrosilane containing materials with the two different allyl esters synthesized are given in Figures 10.7 and 10.8. For the products also, integration can be used to determine the reduction of the allyl group by hydrosilylation. From Figures 10.7 and 10.8, it can be seen that the ratio of proton (b) $\delta = 4$ ppm to the proton (c) $\delta = 2.3$ ppm is 0.35. For 100% conversion the peak at 4.5 should be absent and the above ratio should be 1 (for 100% pure allyl ester). From this it can be seen that for the DMS – H11 the conversion is 35% and for the MCSiH case it is about 60%. The small values of conversion for DMS – H11 can be due to the lower concentration of Si – H in it (DMS – H11 is oligomeric PDMS end capped by Si – H groups with a molecular weight of ~1200).

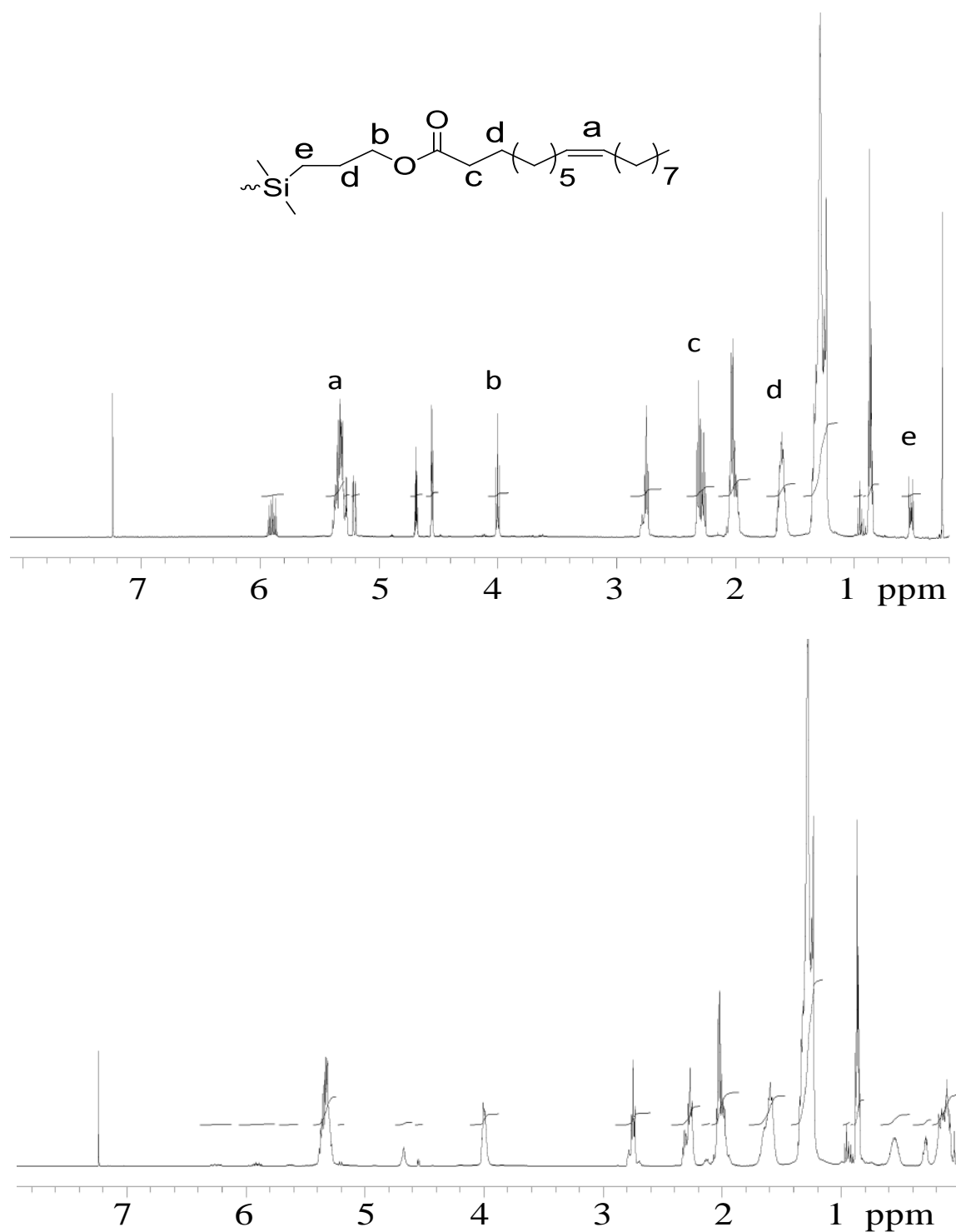


Figure 10.7 ^1H NMR of Hydrosilylated product (allyl soyate with DMS –H11) (Top); product with MCSiH (Bottom)

The carbon spectrum of the DMS – H11 product is shown in Figure 10.8. It can be seen that the peaks corresponding to the allyl group are reduced in intensity and there is a new peak at $\delta = 67$ ppm, which corresponds to the carbon alpha to the oxygen of the n – propyl group formed due to hydrosilylation.

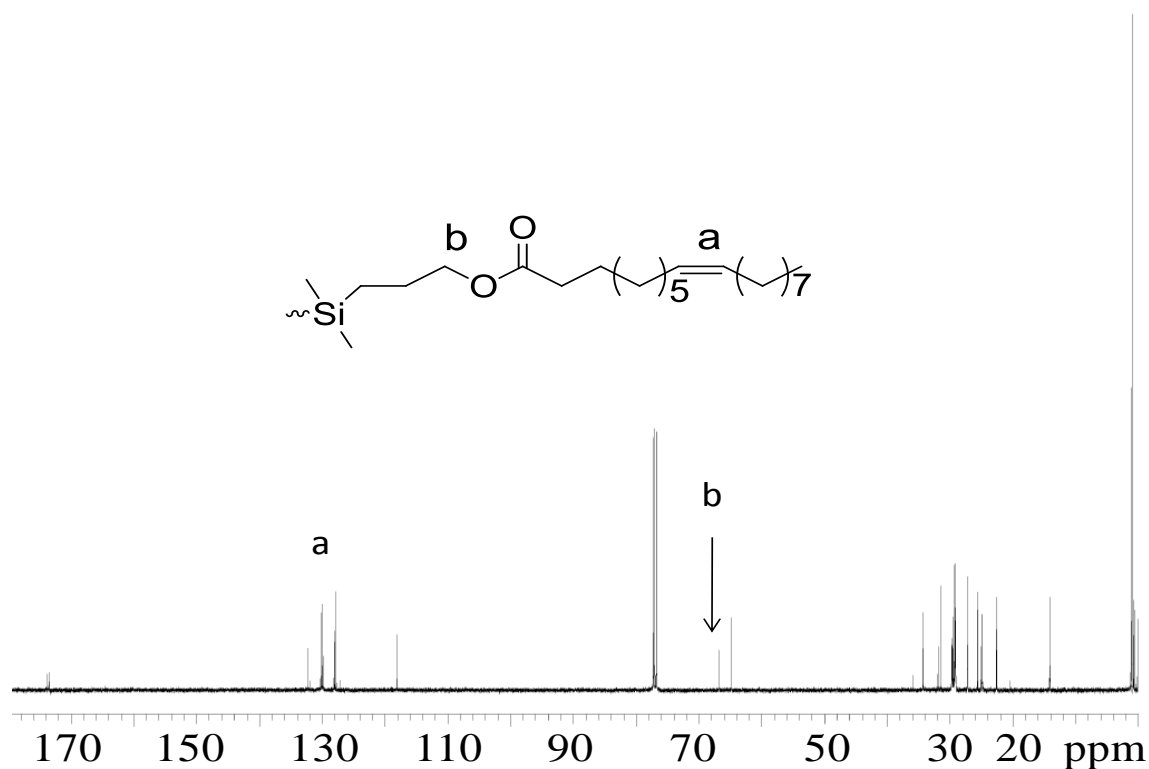


Figure 10.8 ^{13}C NMR of hydrosilylated product (allyl soyate with DMS – H11)

Subsequently, reactions run with higher purity allyl soyate ester and reduced solvent (10 mL instead of 30 mL) and higher temperatures (120 °C instead of 80 °C) gave higher conversions (60% for DMS – H11 and 90% for MCSiH). Reactions were also run without any solvent and with temperatures of 150 °C and comparable conversions could be achieved at lesser time (90 minutes). One of the problems with the catalyst used is

that it is susceptible to poisoning by elements like Sulfur and Phosphorous. So purity of the starting material is very important. Using a high purity starting material (easily obtained by wiped film evaporation) and minimizing the moisture content would lead to higher conversions, since the hydrosilane is also sensitive to moisture.

10.6 FUTURE WORK

The concept of transesterification with an olefinic alcohol with allyl soyate synthesis and subsequent hydrosilylation has been demonstrated. Unlike conventional hydrosilylation, the reaction is not exothermic, eliminating the need for a solvent in the reaction. The scale up of the transesterification should also be simple, since biodiesel is already manufactured via this route. However, the material would remain an object of curiosity until specific applications are better defined. It is recommended that the following characterizations will be done:

1. Determine the thermal properties of the material: DSC and TGA to determine crystallization, decomposition temperatures etc.
2. Run tests to determine application of the material as a lubricant
3. Tests to determine applicability of material in personal care products: gloss, tack etc.

Once some of the above properties are obtained, it would be easier to decide on an application area for the material. It should be noted that the hydrosilylation has not

affected the internal double bonds of the fatty acid. Thus, more functionalization of the oil is possible through these, for example: epoxidation (amphiphilic character), hydrosilylation by RIS (5) or by chlorosilanes (6-8).

Sulfonation can also be carried out on the derivative (Figure 10.9). Sulfonation has already been reported for such compounds, but it would be of interest to see the properties of the resulting sulfonates.

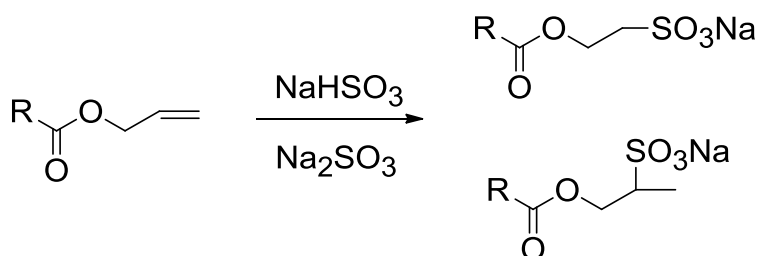


Figure 10.9 Sulfitation of alpha olefin from soybean oil

The procedure can also be extended to the earlier proposed cinnamyl derivative; however, the aromatic ring might require the use of stronger sulfonating agent like SO_3 (sulfur trioxide).

Copolymerization is also a possibility (Figure 10.10). However it should be noted that the allyl group is not a reactive monomer for polymerizations. Radical migration, often limits the molecular weight achievable in the polymerization. However, where such alpha olefins are not needed in high amounts, in the copolymer, these might be applicable. The propargyl group however is known to polymerize with ease even under

radical polymerization. It would be of interest to see, if metallocene type catalysts can be effectively employed to achieve high molecular weight polymers, especially from the allyl and cinnamyl derivatives.

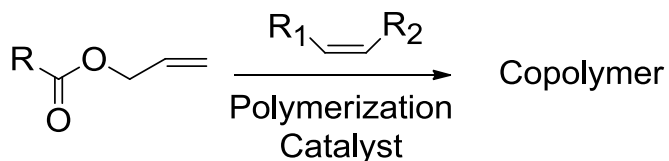


Figure 10.10 Copolymerization of alpha olefin with ethylenic monomer

Thus from the above it can be seen that transesterification, offers a viable route to creating new functional entities from soybean oil. Identification of key application areas would therefore be essential to pursue large scale production of these compounds. Although soybean oil is relatively inexpensive, the olefinic alcohols may not be. Hence the application would need to justify the cost of the material.

PBAT – VINYLSILANE– TALC BLENDS

(This work was carried out with Dr. Yogaraj Nabar(9) in May 2004)

10.7 INTRODUCTION

Biodegradable polyesters like PBAT are often expensive and thus fillers are commonly employed as a cost reduction measure. However, poor compatibility between the filler and matrix often leads to degradation of mechanical properties. One of the most common fillers used is talc. Being a silicate compound, compatibilization of talc would require that the matrix has polar groups. It is even better if silanes can be introduced as functional groups into the matrix; since the inorganic Si – OH groups in talc, can react with the organosilanes to give better interfacial adhesion. US Patent 3,646,155 issued to Scott (10) relates to the cross-linking of polyethylene materials using an organofunctional silane as a cross-linking agent, which is grafted on to the polymer using a peroxide catalyst. The process as described in the patent also leads to a reduction in melt flow of the polymer leading to difficulties in processability in normal equipment and significant reduction in elongation than the base material. Many other similar works (11-14) are reported.

US Patent 5,880,195 issued to Kalinowski et al. (15) relates to the preparation of addition curable high tensile strength compositions starting with hydrosilanes and alkenyl functional polymer backbones. The process, though efficient, involved the use of

very reactive hydrosilanes and use of polymers with unsaturations in their backbones, which are not very common. Also the hydrosilylation catalyst was very expensive, which required that extenders be added to the composition to reduce the cost, which in turn could lead to lesser property enhancements.

Thermoplastic polyurethanes have been modified using silane grafting agents (16). Their technique, however, was to use a condensation type reaction between an isocyanate grafting agent and an amino functional silane rather than a free radical peroxide induced grafting which was the aim of the present work. Similar work is reported in literature (17) where the authors have grafted a vinylsilane on to a silicone rubber using an organic peroxide catalyst to improve compatibility with polyurethane.

DE 10111992 discusses the use of silane grafting on polyolefins to make compatibilized blends with polyesters in the presence of a silane coupling agent- but in the invention, the focus was on grafting the polyolefin and not the polyester with the organosilane. Further the work did not mention about films, and is on manufacture of threads.

This present study deals with the improvement of the physico-mechanical properties of these silane-grafted filled polyester films by improving the compatibility between the filler and the polyester and chemical cross-linking between the silane groups. This graft co-polymer helps achieve the afore-mentioned objective by providing blends in a one-step extrusion process to give films with enhanced tensile strengths up

to 6000 psi. Preliminary results based on the mechanical properties of the blown films have been discussed in this chapter, and future recommendations have been provided.

10.8 MATERIALS

Poly (butylene–adipate-*co*-terephthalate) (PBAT) from BASF Corporation (Freeport, TX) , 2,5-dimethyl-2,5-di-(*tert*-butylperoxy) hexane (Luperox 101) from Sigma-Aldrich (St.Louis, MO) were procured and used as received. Talc having a particle size of ca. 6 μm under the trade name Luzenac 20M00S was provided by Luzenac Europe, and dried at 120 °C overnight before use. Vinyltrimethoxy silane (VTMOS) and Dimethoxy (methyl vinyl) silane (VMDMOS) were purchased from Gelest, Inc (Morrisville, PA).

10.9 EXPERIMENTAL

10.9.1 One-Step (*In Situ*) Reactive Extrusion Process

700g of PBAT was hand-mixed with 0.05/0.1/0.2 wt% (of PBAT) free radical initiator, 0.5/1/2 wt% (of PBAT) VTMOS/VMDMOS, and 300gm of talc, in that order, and fed together to a Century ZSK-30 co-rotating twin screw extruder at a feed rate of approximately 150 gm/min. The screw diameter was of 30 mm, and the length-to-diameter ratio of 42:1. Barrel and die temperatures were maintained by means of ten

electrical/cooling devices at 15/95/125/145/160/165/165/165/150/145 °C from the barrel section just after the feed throat to the die, with a melt temperature of 154 °C – 158 °C. The screw speed was 150 rpm resulting in a mean time residence of about 4-5 minutes. The strand was extruded through a mono-hole die having a nozzle opening of 2.7 mm in diameter, cooled down into a water-bath, and pelletized downstream.

The reactively modified PBAT-talc composites were extruded into films a Killion single-screw blown film unit. . The screw diameter was 25.4 mm with a length-to-diameter ratio of 25:1. The die inner diameter was 50.8 mm with a die gap size of 1.5 mm. The blown film processing conditions are shown in Table 10.1. The screw speed was maintained at 16 rpm. Blown films processing was carried out at a pressure of ~ 2000 psi, with a melt temperature of 150 °C -160 °C.

Table 10.1 Temperature profile used for blown films

Zone	1	2	3	Clamp Ring	Adaptor	Die1	Die 2	Die 3
T(°C)	150	150	150	135	130	125	125	25

10.10 RESULTS AND DISCUSSION

10.10.1 Mechanical properties of PBAT-silane-talc composites

Tables 10.2 and 10.3 report the tensile properties in the machine and transverse directions respectively, of blown films derived from the *in situ* silane-modified PBAT-talc composites, and the simple PBAT-talc melt-blend.

Using VTMOs (Entries 2 – 6, Table 10.2), it was observed that tensile strengths higher than 5000 psi in the machine direction could be achieved in some formulations (Entries 2 & 5, Table 10.2) with break elongations of 300 – 350%. Tensile strengths greater than 4000 psi and break elongations in the range of 150 – 300% were obtained from the remaining formulations (Entries 3, 4, & 6, Table 10.2). Thus, higher mechanical properties were obtained using lower contents of the free-radical initiator as well as of VTMOs. This was probably due to the fact that the low levels of branching would have occurred within the polyester chains due to the peroxide present. Also, the free-radically grafted silane would have induced low levels of branching. The branching in the polyester matrix due to the silane could be due to the curing of the methoxy groups with other methoxy groups from the grafted silane, as well as the curing of the grafted methoxy groups with the lateral hydroxyl groups possessed by the talc filler. This branching would effectively improve the tensile strength of the resulting composite, but result in a decrease in break elongations due to the formation of a network between the polyester and the filler (which would restrict the elongation of the polymer chains).

Higher levels of peroxide or VTMOs would lead to increased branching (or possibly cross-linking) restricting the break elongations to very low values of 150 – 300%.

VMDMOs were used with an intention to reduce the branching due to the silane within the polyester chains, and to form a more flexible network with improved tensile strengths as well as elongations. VMDMOs are, however, more expensive as compared to VTMOs, and, thus, not economically feasible. The tensile strengths of the composites obtained using VMDMOs were approximately 4300 psi, with break elongations in the range of 430 – 480% (Entries 7 – 8, Table 10.2).

The tensile properties of the films in the transverse direction displayed a similar trend to those in the machine direction (Table 10.3).

Table 10.2 Tensile Properties (Machine Direction) of blown films derived from the PBAT-silane-talc blends

Entry	% Free Radical Initiator	Type and (% Amount of Silane)	Young's modulus (psi)	Yield Stress (psi)	Tensile Stress (psi)	Break Elongation (%)
1	-	-	17004	1838.7	2058.9	600
2	0.1	VTMOs (0.5)	56850	5795	5809.31	300.38
3	0.1	VTMOs (1.0)	54862	4627.2	4698.6	230.5
4	0.1	VTMOs (2.0)	50840	4009.21	4339.33	156.73
5	0.05	VTMOs (1.0)	47033	5106.6	5116.9	340.52
6	0.2	VTMOs (1.0)	49257	4317.75	4334.5	270.22
7	0.1	VMDMOs (1.0)	48006	4246.2	4288.5	469.2
8	0.1	VMDMOs (2.0)	49710	4259.54	4306.8	423.8

Table 10.3 Tensile Properties (Transverse Direction) of blown films derived from the PBAT-silane-talc blends

Entry	% Free Radical Initiator	Type and (% Amount of Silane)	Young's modulus (psi)	Yield Stress (psi)	Tensile Stress (psi)	Break Elongation (%)
1	-	-	17225	1389.8	1528.2	300
2	0.1	VTMOS (0.5)	50743	3321	3343.51	269.9
3	0.1	VTMOS (1.0)	57262	3690	3819.14	196.85
4	0.1	VTMOS (2.0)	51593	3242	3329	161.15
5	0.05	VTMOS (1.0)	47641	2991.58	3005.95	173.27
6	0.2	VTMOS (1.0)	52217	3650	3971.02	283.06
7	0.1	VMDMOS (1.0)	51553	3482	3509	426.3
8	0.1	VMDMOS (2.0)	53618	3732	3799	391.5

10.11 RECOMMENDATIONS FOR THE PBAT-SILANE-TALC COMPOSITES

The results provided here are preliminary, and future work needs to be focused on the control of the grafting chemistry between the PBAT and the silanes. It is also necessary to characterize the reactive blends in the absence of the filler to determine the gel content in the branched/cross-linked polyester matrix. Luperox 101 used herein is a symmetric free-radical initiator, whose fragments are equally capable of creating radicals, thus leading to the formation of radicals in the vicinity of each other; leading to the formation of short cross-links and thus poor properties. An asymmetric organic

peroxide like tert-butyl perpivalate could be tried instead, which would improve the grafting of the silane onto the polyester backbone, and minimize the cross-linking of the polyester chains due to the radicals generated by the peroxide.

The study of the rheology of the resulting composites is also crucial, since the formation of gels (in cases when cross-linking dominates over the grafting reaction) within the polyester matrix affects its flow in the within the extrusion system, as well as affects the mechanical properties of the polyester films. Depending on the size of the gels formed, they can lead to the rupture of the films under strain/tension (large gel size), or they can function as reinforcing deformable fillers within the polyester matrix leading to enhanced mechanical properties (similar to reinforcing ethylene-propylene rubbers in the propylene matrix).

Also, condensation catalysts such as dibutyltin dilaurate (DBTDL) could be used for the curing of silanes, and its introduction through a “Masterbatch” is also worthwhile. This concept of the masterbatch could solve the problems with lower break elongations, while retaining the superior tensile strengths of the composites.

The procedure also can be extended to other polyesters like PCL or PPDO, which are often soft due to their low T_g . The cross – linking provided by moisture cure of the silanes can increase the mechanical properties. However it should be noted that the ultimate elongation will probably reduced at the cost of providing better mechanical properties.

REFERENCES

10.12 REFERENCES

1. G. Lappin, J. Sauer, *Alpha olefins applications handbook*. (CRC, 1989).
2. M. Pollack, N. Denville, US Patent 2,536,568 (1951).
3. B. Marciniec, *Hydrosilylation: A Comprehensive Review on Recent Advances*. (Springer Verlag, 2008).
4. B. Marciniec, *Comprehensive handbook on hydrosilylation*. (Pergamon Pr, 1992).
5. A. El Kadib, N. Katir, A. Castel, F. Delpech, P. Rivière, *Applied Organometallic Chemistry* **21**, 590 (2007).
6. A. Behr, F. Naendrup, D. Obst, *Advanced Synthesis & Catalysis* **344**, 1142 (2002).
7. A. Behr, F. Naendrup, D. Obst, *European Journal of Lipid Science and Technology* **104**, 161 (2002).
8. N. Saghian, D. Gertner, *Journal of the American Oil Chemists' Society* **51**, 363 (1974).
9. Y. U. Nabar, PhD Thesis, Michigan State University (2004).
10. H. Scott, US Patent 3,646,155 (1972).
11. G. Hattrich, S. Byron, US Patent 4,514,539 (1985).
12. T. Isaka, M. Ishioka, T. Shimada, T. Inoue, US Patent 4,413,066 (1983).
13. Y. Inoue, M. Kuno, T. Fukui, S. Ohsawa, US Patent 5,773,145 (1998).
14. P. Swarbrick, W. Green, C. Maillefer, US Patent 4,117,195 (1978).

15. R. Kalinowski, M. Tomalia, A. Wolf. US Patent 5,880,195 (1997).
16. S. Dassin, M. Dumon, F. Mechin, J. Pascault, *Polymer Engineering & Science* **42**, 1724 (2002).
17. M. Maity, B. Khatua, C. Das, *Journal of Elastomers and Plastics* **33**, 211 (2001).